

# THERMO2016

15th International Conference on ThermoChronology



September 18-23, 2016 - Maresias, Brazil

Supported by:



## ABSTRACTS

# THERMO2016

15th International Conference on Thermochemistry



September 18-23, 2016 - Maresias, Brazil

Supported by:

**unesp**

UNIVERSIDADE ESTADUAL PAULISTA  
"JULIO DE MESQUITA FILHO"



## ABSTRACTS

## Organizing Committee – 15<sup>th</sup> International Conference on Thermochronology (Thermo 2016)

Peter C. Hackspacher - UNESP, Brazil (Chair)  
Andrea R. Jelinek - UFRGS, Brazil  
Carlos H. Grohmann de Carvalho - USP, Brazil  
Carolina Doranti-Tiritan - UNESP, Brazil  
Daniel F. de Godoy - UNESP, Brazil  
Iata A. de Souza - UNESP, Brazil  
Marli Carina S. Ribeiro - UNESP, Brazil  
Miguel Tupinambá - UERJ, Brazil  
Sandro Guedes - UNICAMP, Brazil  
Ulrich A. Glasmacher - Heidelberg University, Germany

---

### Scientific Committee

Ana Olivia B. Franco Magalhães - UNIFAL, Brazil  
Andrea R. Jelinek - UFRGS, Brazil  
Andy Carter - Birkbeck University of London, UK  
Cecile Gautheron - University of Paris, France  
Finlay M. Stuart - Scottish Universities Environmental Research Centre, UK  
John O'Connor - VU University of Amsterdam, Netherlands  
Kerry Gallagher - University of Rennes, France  
Maria-Laura Balestrieri - National Research Council, Italy  
Marli Carina Siqueira Ribeiro - UNESP, Brazil  
Massimiliano Zattin - University of Padova, Italy  
Paul Fitzgerald - Syracuse University, USA  
Paul Green - Geotrack International, Australia  
Peter Zeitler - Lehigh University, USA  
Richard Ketcham - University of Texas, USA  
Roderick Brown - University of Glasgow, UK  
Silvio Hiruma - Instituto Geológico da Secretaria do Meio Ambiente, Brazil  
Takahiro Tagami - Kyoto University, Japan  
Ulrich A. Glasmacher - Heidelberg University, Germany

---

### Standing Committee

Peter Zeitler - Lehigh University, USA (Chair)  
Andrew Gleadow - University of Melbourne, Australia  
Anne Blythe - University of Southern California, USA  
Barry Kohn - University of Melbourne, Australia  
Cornelia Spiegel - Universität Bremen, Germany  
Finlay M. Stuart - Scottish Univ. Environmental Research Centre, UK  
Isabela Carmo - Petrobras, Brazil  
John Garver - Union College, USA  
Ken Farley - California Institute of Technology, USA  
Kerry Gallagher - University of Rennes, France  
Mark Harrison - University of California Los Angeles, USA  
Paul Andriessen - VU University of Amsterdam, Netherlands  
Paul Fitzgerald - Syracuse University, USA  
Peter Reiners - University of Arizona, USA  
Peter Van den Haute - Universiteit Gent, Belgium  
Peter van der Beek - Université Joseph Fourier, France  
Roderick Brown - University of Glasgow, UK  
Takahiro Tagami - Kyoto University, Japan  
Ulrich A. Glasmacher - Heidelberg University, Germany  
Wanming Yuan - China University of Geosciences, China

---

### Executive Board of the Brazilian Society of Geology (SBGeo)

Gilmar Vital Bueno – UFF (CEO)  
Luiz Carlos da Silva – CPRM (VP Director)  
Fábio Braz Machado – UNIFESP (Chief Secretary)  
Carlos Henrique Grohmann de Carvalho – USP (Chief Financial Officer)  
Julia Barbosa Curto Ma – UnB (Director of Communications and Publications)  
Rosemary Hoff – EMBRAPA (Program Director of Technical-Scientific)  
Rogério Cardoso Gontijo – PETROBRAS (Associate Director)

## **PREFACE**

For the first time in Brazil and South America, we have the honor on guesting the 15th edition of Thermo 2016 (International Conference on Thermochronology). Thermochronology scientific community has attended our abstract submission and participation call, which allows an information exchange between colleagues from institutions from all over the world, as universities, governmental institutions, public and private companies.

The 80 abstracts published on this volume, will be presented as talks and posters, distributed in 10 thematic sessions during the Thermo 2016. Apart the abstract contributions, the event counts with 8 keynote lectures that will be presented by experts of each session theme, all related to the new insights of thermochronology. Two excursions are programmed one pré-conference and a mid-conference and also a short course on thermochronology modelling.

We thank our Gold and Bronze level sponsors and Institutional Sponsors for their generous financial support to make this conference possible, as well as institution (SBGeo, UNESP, UERJ, UFRGS, USP, Unicamp, Univ. Heidelberg) for the efficient organization of the event. Finally the Organizing Committee thanks all the authors that contributed to this abstract book.

**Organizing Committee**

**Thermo 2016**

# CONTENTS

## **Keynotes Lectures**

GEOCHRON@HOME: A CROWDSOURCING APP FOR FISSION TRACK DATING.....	02
<i>Pieter Vermeesch, Jiangping He</i>	
APATITE (U-Th-Sm)/He AGE DISPERSION ARISING FROM ANALYSIS OF VARIABLE GRAIN SIZES AND BROKEN CRYSTALS.....	04
<i>Finlay M. Stuart, Katarzyna Łuszczak, Cristina Persano, Roderick Brown</i>	
(U-Th)/He METHOD: INSIGHT FROM ATOMIC TO MINERALOGICAL SCALE .....	06
<i>Cécile Gautheron, Laurent Tassan-Got, Jérôme Roques, Duval Mbongo-Djimbi, Chloé Gerin, Frédéric Garrido, Cyril Bachelet, Alice Recanatì, Rosella Pinna Jamme, Kerry Gallagher, Anne-Magali Seydoux-Guillaume</i>	
INTERPRETING AND INTEGRATING COMPLEX DATASETS WITH SIMPLE NUMERICAL MODELS.....	07
<i>Matthew Fox, Alka Tripathy-Lang, David L. Shuster</i>	
THERMAL HISTORY AND LONG-TERM CRUSTAL EVOLUTION IN RIFT AND PASSIVE CONTINENTAL MARGIN ENVIRONMENTS .....	08
<i>Ulrich A. Glasmacher, Peter C. Hackspacher</i>	
THE HUMAN ASPECTS BEHIND THE QUANTITATIVE THERMOCHRONOLOGY AND INTERDISCIPLINARY WORK (QTIW): A CONTINUOUS TIME-TEMPERATURE-PRESSURE-LEARNING PATH .....	11
<i>Mauricio A Bermúdez Cella</i>	
BASIN THERMAL HISTORY RECONSTRUCTION BASED ON MULTIPLE THERMOCHRONOMETERS: IMPROVING PETROLEUM SYSTEM MODELING .....	13
<i>Mauricio Parra, Andrés Mora, Richard A. Ketcham, Daniel F. Stockli</i>	
FISSION TRACK THERMOCHRONOLOGY APPLIED TO MINERALIZATION: EXAMPLE STUDIES.....	15
<i>Wanming Yuan</i>	

## **Session 01 - Ar/Ar Thermochronometry**

A CALEDONIAN CONUNDRUM: THERMOCHRONOLOGY OVER A VERY OLD SHEAR ZONE COMPLEX .....	17
<i>Ganerød, M., Henderson, I.H.C., Wilkinson, C.M., Redfield, T.F.</i>	
<sup>40</sup> Ar- <sup>39</sup> Ar AGES ON BIOTITE AND AMPHIBOLE FROM NEOPROTEROZOIC GRANITES FROM NORTHERN PART OF THE BORBOREMA PROVINCE: NEW EVIDENCES FOR COOLING HISTORIES .....	18
<i>Jaziel M. Sá, Antonio C. Galindo, Fernando C. Alves da Silva, Fernando A. P. L. Lins, Paulo M. Vasconcelos, David S. Thiede</i>	

## **Session 02 - Fission-Track System**

COMBINED APATITE FISSION TRACK DATING AND CHLORINE CONTENT ANALYSIS BY LA-ICP-MS.....	21
<i>Pang Jianzhang, Zheng Dewen, Wang Ying, Ma Yan, Wu Ying, Wang Yizhou</i>	
APPLICATION OF THREE-DIMENSIONAL MEASUREMENT OF FISSION-TRACK LENGTHS IN APATITE FISSION-TRACK ANALYSIS .....	22
<i>Qingyang Li, Andrew Gleadow, Barry Kohn, Christian Seiler, Pieter Vermeesch</i>	
METHODICAL ASPECTS ON FISSION TRACKS IN HYDROXYAPATITE .....	24
<i>Meinert Rahn, Ramon Schmid, Anette von der Handt, Cécile Gautheron, Leander Franz, Christian De Capitani</i>	

METHODOLOGICAL ADVANCES IN ZIRCON FISSION-TRACK AND U-Pb DATING .....	26
<i>Carlos Alberto Tello Sáenz, Rosana Silveira Resende, Elton Luiz Dantas</i>	
ON THE ETCHING PROCEDURE OF FISSION TRACKS IN APATITE .....	27
<i>Murat T. Tamer, Richard A. Ketcham, Raymond Jonckheere</i>	

### **Session 03 - U-Th-Sm-He System**

INVESTIGATION OF (U-Th)/He METHOD APPLICABILITY IN MAGNETITE AND SPINEL .....	30
<i>Stéphane Schwartz, Cécile Gautheron, Rosella Pinna-Jamme, Fabrice Brunet, Manuel Moreira</i>	
FORMATION AND THERMAL HISTORIES OF FRACTURE-FILLING HEMATITE IN PRECAMBRIAN BASEMENT FROM (U-Th)/He AND $^4\text{He}/^3\text{He}$ THERMOCHRONOLOGY .....	31
<i>Peter Reiners, David Shuster, Nathan Evenson</i>	
IMPACT OF THE ABRASION PATTERNS AND DRIVER TRANSPORT ON DETRITAL U-Th-Sm/He THERMOCHRONOLOGY: AN EXAMPLE FROM THE KALI GANDAKI VALLEY (CENTRAL NEPAL) .....	32
<i>Ruben Rosenkranz, Cornelia Spiegel, Mohammad S. Sohi</i>	
POTENTIAL INFLUENCE OF APATITE CHLORINE CONTENT ON (U-Th-Sm)/He THERMOCHRONOLOGY .....	34
<i>Cornelia Spiegel, Andreas Klügel, Patrick Monien, Vera Kolb</i>	
PERFORMANCE OF (U+Th)/He LABORATORY AT UNESP (RIO CLARO, BRAZIL) .....	36
<i>Marli Carina Siqueira-Ribeiro, Danieli Fernanda Canaver Marin, Peter C. Hackspacher, Finlay M. Stuart</i>	

### **Session 04 - Diffusion in minerals – What controls it and how to measure it**

INTERROGATING THE EFFECTS OF RADIATION DAMAGE ANNEALING ON HELIUM DIFFUSION KINETICS IN APATITE .....	39
<i>Chelsea D. Willett, Matthew Fox, David L. Shuster</i>	
A TEST OF THE INTERLAYER IONIC POROSITY AS A MEASURE OF ARGON DIFFUSIVITY IN MICAS .....	40
<i>A. Camacho, J.K.W. Lee, R. Armstrong, Y.A. Abdu, R.A. Creaser</i>	

### **Session 05 - Numerical methods - modelling of data (T-t extraction) and processes**

DEALING WITH DATA AND MODEL PARAMETER UNCERTAINTIES IN THERMAL HISTORY MODELLING .....	43
<i>Kerry Gallagher</i>	
MULTI-MINERAL FISSION-TRACK THERMOCHRONOLOGY SOFTWARE .....	44
<i>Arnaldo Luis Lixandrão Filho, Sandro Guedes, Julio Cesar Hadler Neto</i>	
DEFINING THE THERMAL EVOLUTION OF HYPEREXTENDED MAGMA-POOR RIFT MARGINS: CONSTRAINING A CONTINUOUS LITHOSPHERIC THERMAL HISTORY USING APATITE U-Pb THERMOCHRONOMETRY .....	46
<i>Patrick Boyd, Daniel F Stockli, Federico Galster</i>	
ANNEALING KINETICS OF $^{238}\text{U}$ ION TRACKS IN MUSCOVITE .....	48
<i>Sandro Guedes, Arnaldo L. Lixandrão Filho, Julio Cesar Hadler</i>	
TECTONO-THERMAL EVOLUTION OF THE REED BANK BASIN, SOUTHERN SOUTH CHINA SEA .....	50
<i>Shengbiao Hu, Xiaoyin Tang</i>	

NATURAL AGE DISPERSION ARISING FROM THE ANALYSIS OF BROKEN CRYSTALS: PART III. THE QTQT MODELLING APPROACH .....	51
<i>David M. Webster, Roderick W. Brown, Kerry Gallagher, Romain Beucher</i>	
USING THE GEOCHRON DATABASE FOR THERMOCHRONOLOGY DATA .....	53
<i>J. Douglas Walker, Noah M. McLean</i>	
TESTING THE REPRODUCIBILITY OF THERMAL HISTORY ANALYSIS .....	54
<i>Richard A. Ketcham, Matthias Bernet, Peter van der Beek</i>	

## **Session 06 - New developments, techniques, methods, what's in the pipeline**

IN SITU TEM OBSERVATION OF ION IRRADIATION INDUCED ANNEALING OF ALPHA-RECOIL TRACKS AND FISSION TRACKS IN APATITE.....	56
<i>Weixing Li, Rodney C. Ewing</i>	
MAPPING He DISTRIBUTION IN ZIRCON BY LASER ABLATION NOBLE GAS MASS-SPECTROMETRY: IMPLICATIONS FOR (U-Th)/He GEOCHRONOLOGY AND THERMOCHRONOLOGY .....	57
<i>Danišík, M., McInnes, B.I.A., Kirkland, C.L., McDonald, B.J., Evans, N.J., Becker, T.</i>	
OPTIMIZING WORKFLOW: AUTOMATED DATA COLLECTION OF APATITE IMAGES .....	59
<i>Ravi Kumar, Ray Donelick</i>	
EXTENDING THE RANGE OF U-Pb APATITE THERMOCHRONOLOGY USING SIMS ANALYSIS .....	60
<i>Peter Zeitler, Kalin McDannell, Mark Harrison, Blair Schoene</i>	
THE POTENTIAL OF SINTERED MUD TANK APATITE AS A MATRIX-MATCHED URANIUM REFERENCE MATERIAL FOR AFT LA-ICP-MS DATING .....	62
<i>Ling Chung, Andrew Gleadow, Hugh O'Neill, Barry, P. Kohn, Alan Greig</i>	
TEMPERATURE CONTROLLED LASER STEP-HEATING OF MONAZITE VIA OPTICAL PYROMETRY – TOWARDS ROUTINE APPLICATION OF MONAZITE (U-Th)/He THERMOCHRONOMETRY .....	64
<i>Nathan Niemi</i>	
LASER ABLATION U-Th-Sm/He DATING OF APATITE .....	66
<i>William Matthews, Julia Pickering, Brett Hamilton, Bernard Guest, Chris Sykes</i>	
THERMAL HISTORY RECOVERY FROM HIGH-RESOLUTION LASER-ABLATION ICP-MS U-Pb AND TRACE ELEMENT DEPTH PROFILING .....	68
<i>Lisa D. Stockli, Daniel F. Stockli, Andrew Smye, Nikki Seymour, Patrick Boyd</i>	
AN IMPROVED DETERMINATION OF ATMOSPHERIC $^{21}\text{Ne}/^{20}\text{Ne}$ .....	70
<i>John Saxton, Steven Edwards, David Rousell</i>	
SWIFT HEAVY ION INDUCED SURFACE MODIFICATION OF CALCITE ( $\text{CaCO}_3$ ) VISUALIZED BY VARIOUS TECHNIQUES.....	72
<i>Dedera, S., Glasmacher, U.A., Burchard, M., Trautmann, C.</i>	

## **Session 07 - “Post-orogenic” settings & long-term landscape evolution**

LATE CRETACEOUS TO CENOZOIC EXHUMATION OF THE FUPING METAMORPHIC CORE COMPLEX, CENTRAL NORTH CHINA CRATON: INSIGHTS FROM LOW-TEMPERATURE THERMOCHRONOLOGY .....	74
<i>Jian Chang, Nansheng Qiu, Chang'e Cai</i>	
THE LONG-TERM LANDSCAPE EVOLUTION OF ZIMBABWE: INSIGHTS FROM A MULTI-THERMOCHRONOMETER STUDY .....	75
<i>Vhairi Mackintosh, Barry Kohn, Andrew Gleadow</i>	

INTERPLAYS BETWEEN THE WEST AND THE EAST ANTARTICA ICE SHEETS: HINTS FROM BEDROCK AND DETRITAL THERMOCHRONOLOGY AND OTHER TECHNIQUES .....	77
<i>Balestrieri M.L., Olivetti V., Pace D., Rossetti F., Talarico F.M., Zattin M.</i>	
GEO-REFERENCED DATABASE OF BRAZILIAN THERMOCHRONOLOGICAL STUDIES .....	79
<i>Silvio Takashi Hiruma, Carlos Henrique Grohmann</i>	
THE TECTONIC AND GEOMORPHIC DEVELOPMENT OF SOUTHERN AFRICA AS REVEALED BY APATITE FISSION TRACK AND APATITE (U-Th-Sm)/He THERMOCHRONOLOGY .....	80
<i>Mark Wildman, Roderick Brown, Cristina Persano, Fin Stuart, Romain Beucher</i>	
THE ROLE OF THE BÜYÜK MENDERES DETACHMENT DURING LATE CENOZOIC EXHUMATION OF THE CENTRAL MENDERES MASSIF, SW TURKEY .....	82
<i>Nils-Peter Nilius, Andreas Wöflfler, Christoph Glotzbach, Caroline Heineke, Ralf Hetzel, Andrea Hampel, Cüneyt Akal, István Dunkl</i>	
CONSTRAINING THE EXTENT, THICKNESS AND EROSIONAL HISTORY OF THE JURASSIC CONTINENTAL FLOOD BASALTS OF WESTERN DRONNING MAUD LAND, EAST ANTARCTICA: EVIDENCE FROM LOW-T THERMOCHRONOLOGY .....	83
<i>Hallgeir Sirevaag, Joachim Jacobs, Anna K. Ksienzyk, István Dunkl</i>	
LARGE-SCALE RIFT TECTONICS ALONG THE PACIFIC MARGIN OF WEST ANTARCTICA: INSIGHTS FROM APATITE THERMOCHRONOLOGY .....	84
<i>Zundel Maximilian, Spiegel Cornelia, Lisker Frank</i>	
CENOZOIC DEVELOPMENT OF THE CENTRAL EUROPEAN EGER RIFT: FIRST LOW-T THERMOCHRONOLOGY RESULTS FROM BASEMENT BOREHOLE SAMPLES.....	85
<i>Annika Szameitat, Petra Štěpančíková, Ludwig Zöller, Jonas Kley, István Dunkl</i>	
THERMOCHRONOLOGY AND GEODYNAMICS OF CONTINENTAL EXTENSION ASSOCIATED WITH THE TURKANA DEPRESSION IN EAST AFRICA .....	86
<i>Andrew Gleadow, Samuel C Boone, Barry Kohn, Christian Seiler, David Foster</i>	
PALEOCENE-EARLY EOCENE UPLIFT OF THE ALTYN TAGH MOUNTAIN: EVIDENCE FROM DETRITAL ZIRCON FISSION TRACK ANALYSIS AND SEISMIC SECTIONS IN THE NORTHWESTERN QAIDAM BASIN .....	87
<i>Yadong Wang, Jianjing Zheng, Youwei Zheng, Xingwang Liu</i>	
DENUDATION HISTORY OF THE SE BRAZIL MARGIN FROM COMBINED LOW TEMPERATURE THERMOCHRONOLOGY AND <sup>40</sup> Ar/ <sup>39</sup> Ar WEATHERING GEOCHRONOLOGY: IMPLICATIONS FOR LANDSCAPE EVOLUTION .....	88
<i>B. P. Kohn, I. O. Carmo, P. M. Vasconcelos</i>	
CONTROLS OF DENUDATION IN CONTINENTAL MARGIN OF SOUTHEAST BRAZIL DEDUCTED BY ANALYSIS OF IN SITU PRODUCED <sup>10</sup> Be CONCENTRATION IN RIVER SEDIMENTS .....	90
<i>De Souza. D. H., Hackspacher. P. C., Stuart. F., Pupim. F. N.</i>	
LONG-TERM EVOLUTION OF THE WESTERN SOUTH ATLANTIC PASSIVE CONTINENTAL MARGIN IN A KEY AREA OF SE BRAZIL REVEALED BY THERMOKINEMATIC NUMERICAL MODELING.....	92
<i>Christian Stippich, Florian Krob, Ulrich A. Glasmacher, Peter C. Hackspacher</i>	
THE EVOLUTION OF BAFFIN ISLAND: AN INTEGRATED APATITE FISSION TRACK AND APATITE (U-Th)/He STUDY.....	93
<i>Scott Jess, Randell Stephenson, Roderick Brown</i>	
QUANTIFYING UPLIFT AND DENUDATION OF A HETEROGENEOUS CRUST; A DETAILED MULTI-THERMOCHRONOMETERIC STUDY OF CENTRAL WEST BRITAIN.....	95
<i>Katarzyna Łuszczak, Cristina Persano, Finlay M. Stuart</i>	



PRELIMINARY APATITE FISSION TRACK AGES FROM NW-MOZAMBIQUE PRECAMBRIAN SHIELD, AFRICA.....	97
<i>Marcos Müller Bicca, Andrea Ritter Jelinek, Ruy Paulo Philipp</i>	
PLATEAU EROSION AND RIDGE PRESERVATION: DIFFERENTIAL EROSION OR TECTONIC REACTIVATION IN THE MANTIQUEIRA RANGE, SE BRAZIL.....	98
<i>Leandro Duque, Miguel Tupinambá</i>	
EVALUATING POST-RIFT VERTICAL DISPLACEMENTS OF SOUTHEASTERN BRAZIL PASSIVE MARGIN USING GRANOPHYRIC DIABASE DYKES AS DEPTH INDICATOR.....	100
<i>Miguel Tupinambá, Monica Heilbron</i>	
LOW-TEMPERATURE THERMOCHRONOLOGY IN ALKALINE INTRUSIONS AREAS BRAZILIAN SOUTHEAST.....	102
<i>Carolina Doranti-Tiritan, Peter C. Hackspacher</i>	
TIMING AND PETROGENESIS OF THE MESOZOIC GRANITOIDS AT DUERJI AREAS, INNER MONGOLIA AND ITS TECTONIC IMPLICATIONS.....	104
<i>Su Zhou, Ruizhao Qiu, Guoqin Zhang, Cui Liu</i>	

## **Session 08 - Orogenesis & Long-term landscape evolution**

(U-Th)/He THERMOCHRONOMETRIC MAPPING OF NE JAPAN ARC: PRELIMINARY RESULTS.....	106
<i>Shigeru Sueoka, Takahiro Tagami, Barry P. Kohn, Shoma Fukuda</i>	
COOLING AND EXHUMATION HISTORY OF THE TIANFOZHISHAN, YANJI AREA, NE CHINA, REVEALED BY FISSION-TRACK THERMOCHRONOLOGY.....	108
<i>Xiaoming Li, Chuanjun Wu</i>	
THE APPLICATION OF LOW-TEMPERATURE THERMOCHRONOLOGY TO AN ACTIVE LOW ANGLE NORMAL FAULT, THE MAI'U FAULT IN PAPUA NEW GUINEA.....	110
<i>J. Oesterle, D. Seward, T. Little, K. Norton, D. Stockli</i>	
APATITE (U-Th)/He THERMOCHRONOMETRY IN THE NORTHERN PATAGONIAN ANDES: NEW INSIGHTS INTO THE EXHUMATION HISTORY OF THE THRUST BELT FORELAND SECTOR.....	112
<i>Elisa Savignano, Massimiliano Zattin, Stefano Mazzoli, Marta Franchini, Cécile Gautheron</i>	
THERMOCHRONOLOGIC PERSPECTIVES FOR THE CRUSTAL DYNAMICS OF THE JAPAN ARC.....	114
<i>Takahiro Tagami</i>	
LOW TEMPERATURE THERMOCHRONOMETRY REVEALS EARLY CENOZOIC DIFFERENTIAL EXHUMATION IN THE SOUTHERN ROCKY MOUNTAINS, COLORADO.....	115
<i>Alyssa Abbey, Nathan Niemi</i>	
RAPID PLIO-PLEISTOCENE EROSION OF THE CENTRAL COLORADO PLATEAU DOCUMENTED BY APATITE THERMOCHRONOLOGY FROM THE HENRY MOUNTAINS.....	117
<i>Kendra E Murray, Peter W Reiners, Stuart N Thomson</i>	
THERMOCHRONOLOGICAL CONSTRAINTS ON THE CENOZOIC ACCRETION AND DEFORMATION IN WESTERN COLOMBIA.....	119
<i>León, S., Parra, M., Cardona, A.</i>	
CONSTRAINTS ON THE MAGNITUDE AND LONGEVITY OF GEOTHERMAL AND METEORIC FLUID FLOW FROM (U-Th)/He THERMOCHRONOMETRY.....	121
<i>Daniel F. Stockli, Daniel Arnost, Alison MacNamee</i>	
POST-INCAIC PHASE SUPERGENE COPPER ENRICHMENT AND PEDIPLANATION, NORTHERN CHILE, CENTINELA DISTRICT.....	122
<i>Caroline Sanchez, Stéphanie Brichau, Rodrigo Riquelme, Sébastien Carretier, Cristopher Lopez, Eduardo Campos, Vincent Regard, Gérard Hérial, Carlos Marquardt, Constantino Mpodozis</i>	

LINKING LATE MIOCENE MAGMATISM AND EXHUMATION OF THE PAMIR-WEST KUNLUN MOUNTAINS TO LITHOSPHERIC THINNING ..... 123  
*Kai Cao, Guocan Wang, Zhongcheng Zeng, Anne Replumaz*

MULTI-STAGE COOLING EVENTS OF THE GANGDESE TERRANE DURING THE CENOZOIC: IMPLICATIONS FOR THE HIGH PLATEAU FORMING IN SOUTH TIBET ..... 124  
*Guocan Wang, Tianyi Shen, Peter van der Beek, Matthias Bernet, An Wang, Kexin Zhang*

CONSTRAINING UPLIFT AND EROSION IN THE WESTERN HIMALAYAN SYNTAXIS. A MULTIPLE THERMOCHRONOMETRIC STUDY FROM THE NEELUM RIVER REGION, NW HIMALAYAS, PAKISTAN ..... 126  
*Syed Ali Turab, Kurt Stüwe, Finlay M. Stuart, David M. Chew, Nathan Cogne*

PROVENANCE AND EXHUMATION HISTORY OF THE SIERRA NEVADA DE SANTA MARTA, COLOMBIAN CARIBBEAN: THE RELATIONSHIP BETWEEN OROGENIC PULSES AND THE CARIBBEAN - SOUTH AMERICA TECTONIC DURING THE CENOZOIC ..... 128  
*Sebastian Echeverri, Mauricio Parra*

UNRAVELLING THE LATE MIOCENE EXHUMATION IN THE WEST-CENTRAL PYRENEES ..... 130  
*Charlotte Fillon, Raphael Pik, Frédéric Mouthereau, Nicolas Bellahsen, C. Gautheron, Sylvain Calassou, Emmanuel Masini*

## **Session 09 - Basin evolution and thermal histories**

DETRITAL ZIRCON (U-Th)/He AND FISSION TRACK DATA OF NATURAL DEEP BOREHOLE SAMPLES AND ITS GEOLOGICAL SIGNIFICANCE ..... 133  
*Qiu Nansheng, Cai Change*

THERMAL HISTORY OF THE CAMPOS BASIN FROM APATITE FISSION TRACK THERMOCHRONOLOGY IN BOREHOLE SAMPLES ..... 134  
*Christie Helouise Engelmänn de Oliveira, Andréa Ritter Jelinek, Farid Chemale Jr.*

A TECTONICALLY UPLIFTED XICHANG BASIN AT THE SOUTHEASTERN TIBETAN PLATEAU, AS REVEALED BY STRUCTURAL GEOLOGY AND THERMOCHRONOLOGY DATA ..... 135  
*Bin Deng, Shugen Liu, Zhiwu Li, Gaoping Zhao, Lei Jiang, Luba Jansa*

THE TECTONIC AND DENUDATION HISTORY OF EAST GREENLAND: INSIGHTS FROM APATITE FT AND He DATA ..... 137  
*A.G. Szulc, T. Bernard, P. Steer, K. Gallagher, A. Carter, T. Kinnaird, A.G. Whitham, C. Johnson*

TRACKING LOW TEMPERATURE TECTONISM OF THE ST. LAWRENCE PLATFORM (CANADA) THROUGH APATITE AND ZIRCON (U-Th)/He THERMOCHRONOLOGY ..... 138  
*David Schneider, Rebecca Hardie, Justin Emberley, Jeremy Powell*

LOW-TEMPERATURE THERMOCHRONOLOGY OF THE TURKANA DEPRESSION, EAST AFRICAN RIFT SYSTEM: INSIGHT INTO THE LITHOSPHERIC RESPONSE TO RIFT SUPERPOSITION ..... 139  
*Samuel C. Boone, Andrew Gleadow, Barry Kohn, Christian Seiler, Ling Chung*

DISTINGUISHING THERMAL RIFT-RELATED INHERITANCE FROM SUBSEQUENT OROGENIC EXHUMATION IN THE PYRENEES ..... 140  
*Arnaud Vacherat, Frédéric Mouthereau, Raphaël Pik*

BURIAL AND EXHUMATION HISTORY OF THE MACKENZIE PLAIN, NWT, CANADA: INTEGRATION OF APATITE (U-Th)/He AND FISSION TRACK THERMOCHRONOMETRY ..... 141  
*Jeremy Powell, David Schneider, Dale Issler, Daniel Stockli*

LATE CENOZOIC EXHUMATION OF THE SOUTHERN PATAGONIAN ANDES (47°S) CONSTRAINED BY LOW-TEMPERATURE THERMOCHRONOLOGY AND INVERSE NUMERICAL MODELING ..... 143  
*Viktoria Georgieva, Edward R. Sobel, Artur Sobczyk, Kerry Gallagher, Taylor Schildgen, Todd A. Ehlers, Manfred R. Strecker*

EVOLUTION OF THE SOUTH ATLANTIC PASSIVE CONTINENTAL MARGIN AND LITHOSPHERE DYNAMIC MOVEMENT IN SOUTHERN BRAZIL DERIVED FROM ZIRCON AND APATITE (U-Th- Sm)/He AND FISSION-TRACK DATA.....145  
*Krob, F.C., Stippich, C., Glasmacher, U.A., Hackspacher, P.C.*

THE INFLUENCE OF INHERITED EXTENSIONAL STRUCTURES ON THE GROWTH OF BASEMENT-CORED RANGES AND THEIR FORELAND BASINS .....146  
*Sebastián Zapata, Edward Sobel, Cecilia del Papa*

## **Session 10 – Mineralizations**

POST-BATHOLITH MO(W) METALLOGENESIS FOLLOWING SUPER LARGE MAGMA ACTIVITY IN XIAO HINGGAN MOUNTAINS, NORTHEAST CHINA.....148  
*Liu C., Luo Z.H., Deng J.F., Zhang Y., Duan P.X., Zhao H.D., Tian S.P., Zhang L.L.*



**THERMO2016**

**KEYNOTES LECTURES**

## **geochron@home: a crowdsourcing app for fission track dating**

Pieter Vermeesch<sup>a</sup> and Jiangping He<sup>b</sup>

<sup>a</sup> *Department of Earth Sciences, University College London, London, United Kingdom*

<sup>b</sup> *Department of Geography, King's College London, London, United Kingdom*

In 1906, Sir Francis Galton visited a county fair in which a contest was held to guess the weight of an ox. 787 villagers participated in the event. Galton discovered that the average of all their estimates (1,197 lbs) was significantly closer to the true weight of the ox (1,198 lbs) than any of the individual estimates. Such is the wisdom of crowds [Galton, 1907]. Similar effects are seen in fission track geochronology. A 1984 interlaboratory comparison study showed that the average of several fission track age estimates is closer to the known age of mineral standards than the age obtained by any individual observer [Miller et al., 1985]. Unfortunately, routine measurement of samples by multiple analysts is prohibitively expensive in a normal laboratory environment. In contrast with other geochronological techniques, which rely on isotope geochemistry and mass spectrometry, fission track dating is still very much a manual process. However, during the past decade, spectacular advances in digital microscopy have allowed researchers at the University of Melbourne to develop software tools that: (a) acquire vertical stacks of digital images so that fission tracks can be counted on a computer screen, rather than by physically looking through the microscope; and (b) employ pattern recognition algorithms to automatically count the fission tracks on the digital imagery. These automated algorithms can be 'confused' by surface features produced by crystal defects or tiny polishing scratches. Pattern recognition is one aspect of intelligence in which humans still outperform computers. This is a classic example of a computational problem that can be solved by crowdsourcing. In an alternative approach to fully automated fission track dating, geochron@home implements a model in which the machine is put in charge of the image acquisition (step a above), while the actual counting (step b) is outsourced to humans. Taking fission track dating to a proverbial 'county fair' of citizen-scientists benefits the method in three ways: (1) it improves the accuracy of the ages by –based on the inter-laboratory comparison study– up to 25%; (2) having multiple estimates of the fission track density provides a treasure-trove of statistical data that can be used to better quantify the accuracy of legacy data; (3) it accelerates the analytical process and frees up precious time for academic users. At Thermo2016, we would like to officially launch geochron@home by inviting conference delegates to participate in a large scale fission track counting experiment. Please visit <http://geochron-at-home.london-geochron.com> and start counting!

## References

Galton, F. Vox populi. *Nature*, 75:450–451, 1907.

Miller, D.S. et al. Results of interlaboratory comparison of fission-track age standards: fission-track workshop – 1984. *Nuclear Tracks and Radiation Measurements*, 10(3):383–391, 1985.

# **Apatite (U-Th-Sm)/He age dispersion arising from analysis of variable grain sizes and broken crystals**

Finlay M. Stuart<sup>1</sup>, Katarzyna Łuszczak<sup>1,2</sup>, Cristina Persano<sup>2</sup>, Roderick Brown<sup>2</sup>

<sup>1</sup> *Isotope Geosciences Unit, Scottish Universities Environmental Research Centre, East Kilbride G75 0QF, UK*

<sup>2</sup> *School of Geographical & Earth Sciences, Glasgow University, Glasgow, G12 8QQ, UK*  
(*fin.stuart@glasgow.ac.uk*)

The apatite (U-Th-Sm)/He (AHe) thermochronometer is uniquely suited for deciphering the thermal history of the uppermost crust. Single grain ages from most samples are commonly more dispersed than expected from analytical uncertainties and analysis of the Durango apatite, and occasionally AHe ages are older than the fission track age of apatite from the same rock sample. Several processes have been posited to explain this phenomenon<sup>1</sup>. Grain size variation and radiation damage<sup>2</sup> can explain some of the age dispersion, however more often than not there is no clear correlation between grain age and grain diameter and radiation dose. It has been recently proposed the analysis of broken grains can generate much of the observed AHe age dispersion<sup>3,4</sup>. If the <sup>4</sup>He distribution within apatite grains is not uniform, for instance because of diffusive loss during cooling through the Partial Retention Zone, fragments will yield a range of He ages that are different from the whole grain age. The theory predicts that the He content of fragments can be modelled using finite cylinder approximation using the Helfrac code<sup>3</sup>. This is eminently testable and, if correct, means that the analysis of grains with one and two terminations and a range of diameters, should provide precise constraints on the thermal history. To date there has been no systematic test of the extent that fragmentation affects AHe ages. In order to address this we have initiated a programme of He age determinations of 20-25 apatites of variable size and fragment type, from samples with well-constrained thermal histories.

The thermal history of samples from the Scottish Southern Uplands differ principally in the amount (and rate?) of cooling at ~60 Ma. Apatite fission track ages across the region increase from ~60 Ma in the south to ~200 Ma in the north. As expected from the fragmentation model, AHe age dispersion increases with increasing AFT age (from 47% to 127%). AHe ages were modelled in Helfrac to test the extent that dispersion is due to fragmentation, and in QTQt using standard spherical approximation approach. In the case of the rapidly cooled sample, both models are similar. Helfrac models of the samples with complex thermal histories depends strongly on the fragment

type and size. For small grains Helfrag seems to simplify the thermal thermal histories, whereas for a wide range of grain size, including large grains (radius > 100  $\mu\text{m}$ ) the software was able to resolve high complexity of the thermal history. The resolved cooling and reheating events are in good agreement with independent geological constraints, although they were not resolved by corresponding QTQt model and only partially by model including AFT and AHe data. In all samples the age predictions for Helfrag models are slightly better, suggesting that in every case much of the age dispersion originates in the analysis of fragments.

The Helfrag results have been compared with models of AFT data and multiple sets of five randomly chosen AHe ages. In the case of complex thermal histories, the AFT and 5-sample AHe ages do not reproduce the cooling history complexity that is evident from the multi-grain analysis and geological evidence. We conclude that maximising the age dispersion and analysing multiple aliquots (>20) from selected samples provides better constraints on thermal histories than analysing many samples with 3-5 aliquots and attempting to minimise age dispersion. Because the amount of dispersion derived from fragmentation increases with grain size, to extract valuable information from fragmentation large grains ( $R > 50 \mu\text{m}$ ) should be picked and effort made to analyse short fragments with one termination plus some long fragments, as well as whole (2T) grains. The analysis of small 2T grains will add a dispersion component arising from the grain size variation.

## References

1. Fitzgerald, P.G., Baldwin, S.L. Webb, L.E. & O'Sullivan, P.B. Interpretation of (U-Th)/He single grain ages from slowly cooled crustal terranes: A case study from the Transantarctic Mountains of southern Victoria Land. *Chemical Geology*, 225, 91-120 (2006).
2. Flowers, R.M. & Kelley, S.A. Interpreting data dispersion and inverted dates in apatite (U-Th)/He and fission-track datasets: an example from the US midcontinent *Geochimica et Cosmochimica Acta* **75**, 5169–5186 (2011).
3. Brown, R.W., Beucher, R., Roper, S., Persano, C., Stuart, F.M. & Fitzgerald, P. Natural age dispersion arising from the analysis of broken crystals. Part I: Theoretical basis and implications for the apatite (U–Th)/He thermochronometer. *Geochimica et Cosmochimica Acta* **122**, 478–497 (2013).
4. Beucher, R., Brown, R.W., Roper, S., Stuart, F.M. & Persano, C. Natural age dispersion arising from the analysis of broken crystals: Part II. Practical application to apatite (U-Th)/He thermochronometry. *Geochimica et Cosmochimica Acta* **120**, 395–416 (2013).



## (U-Th)/He method: insight from atomic to mineralogical scale

Cécile Gautheron<sup>1</sup>, Laurent Tassan-Got<sup>2</sup>, Jérôme Roques<sup>2</sup>, Duval Mbongo-Djimbi<sup>2</sup>, Chloé Gerin<sup>1</sup>, Frédérico Garrido<sup>4</sup>, Cyril Bachelet<sup>4</sup>, Alice Recanati<sup>1</sup>, Rosella Pinna-Jamme<sup>1</sup>, Kerry Gallagher<sup>3</sup>, Anne-Magali Seydoux-Guillaume<sup>4</sup>  
1 GEOPS, Université Paris Sud, France  
2 IPN, in2p3, Université Paris Sud, France  
3 Geosciences Rennes, Rennes, France  
4 LMV, Université St Etienne, France  
([cecile.gautheron@u-psud.fr](mailto:cecile.gautheron@u-psud.fr))

The (U-Th)/He dating method can be applied to different minerals such as apatite, zircon, calcite, iron oxides, and age interpretation requires a good understanding of He retention through possible diffusion. Several parameters including damage, chemical composition and polycrystalline structure have been proposed to explain the range of He diffusion in crystals<sup>1,2,3</sup>. Debates are still ongoing about the blocking effect of damage on He diffusion in minerals, mostly due to their small sizes (nanometer scale).

In order to better characterize He diffusion in minerals, we propose a combination of methodologies from the atomic to mineralogical scales. At atomic scale, the Density Functional Theory (DSF) associated with Kinetic Monte Carlo (KMC) codes allows characterizing He diffusion in 3D in pure crystal lattice. At macroscopic scale, these methods permit to take care of helium diffusion in 3D for anisotropic crystals and for different chemical compositions<sup>4,5</sup>. The obtained He diffusion coefficients in apatite and hematite<sup>4,6</sup> demonstrate the robustness of these methods. In addition, the impact of damage on He diffusion can also be investigated by using DFT to calculate point-defect energetics, leading to a trapping phenomenon as in larger scale damage. Diffusion experiments on artificially damaged crystals using Elastic Recoil Diffusion Analysis (ERDA), can in addition illustrate the damage impact on diffusion. All these data allow to build a helium diffusion model taking into account the damage content, based on a physical model. Finally, the study of He diffusion at geological time and temperature scales enables to identify damage and annealing parameters and calibrate a realistic helium diffusion model.

### References

1. Shuster, D., Flowers, R., Farley, K.A., 2006. The influence of natural radiation damage on helium diffusion kinetics in apatite. *Earth Planet. Sci. Lett.* 249: 148-161.
2. Farley, K.A., Flowers, R., 2012. (U-Th)/Ne and multidomain (U-Th)/He systematics of a hydrothermal hematite from Eastern Grand Canyon. *Earth Planet. Sci. Lett.*, **359-360**: 131-140.
3. Gautheron, C. et al., 2013. Chemical influence on  $\alpha$ -recoil damage annealing in apatite: implications for (U-Th)/He dating. *Chem. Geol.*, **351**: 257-267.
4. Djimbi, D.M. et al., 2015. Impact of apatite chemical composition on (U-Th)/He thermochronometry: an atomistic point of view. *Geochim. Cosmoch. Acta*, **167**: 162-176.
5. Gautheron, C., Tassan-Got, L., 2010. A Monte Carlo approach of diffusion applied to noble gas/helium thermochronology. *Chemical Geology*, **273**: 212-224.
6. Balout, H., Roques, J., Gautheron, C., Tassan-Got, L., Mbongo-Djimbi, D., 2015. Helium diffusion in pure hematite ( $\alpha$ -Fe<sub>2</sub>O<sub>3</sub>) for thermochronometric applications: a theoretical multi-scale study. submitted to *Computational and Theoretical Chemistry*

# Interpreting and integrating complex datasets with simple numerical models

Matthew Fox, Alka Tripathy-Lang, David L. Shuster

Department of Earth and Planetary Science, University of California, Berkeley, CA, USA

Berkeley Geochronology Center, Berkeley, CA, USA

Interest in understanding near-surface processes and links between tectonics, erosion, and climate has motivated advances in the resolution and accuracy of thermochronometric methods. At the 10s of microns scale, we can constrain thermal histories from individual crystals using  $^4\text{He}/^3\text{He}$  data coupled with U and Th zonation maps combined with three dimensional models tracking the diffusion of  $^4\text{He}$  and the evolution of intra-crystal radiation damage. By analyzing these datasets simultaneously with crystals that share a same cooling history, but have different zonation patterns, it is possible to recover complex thermal histories and test key underlying assumptions about radiation damage and crystal geometry. At the 100s of kilometers scale, different thermochronometric systems with varying closure depths record mean exhumation rates over different, but overlapping, time spans. Using linear inverse methods, this redundant information can be exploited to extract temporal and spatial variations in exhumation rate at the scale of an entire orogen. Here, we will review approaches that provide new insights at such disparate scales with numerical and natural experiments. We will present new data from the Grand Canyon and Yosemite Valley where we have collected both  $^4\text{He}/^3\text{He}$  data and spatial distributions of U and Th from the same crystals. To accurately resolve spatial variations in U and Th concentrations, we have developed an approach to exploit redundant information. As the laser typically ablates material with a spot size of 20 microns diameter, several different overlapping spots will analyze the same part of the crystal. This leads to blurring of sharp variations in zonation and also a reduction in the range of U and Th concentrations. Our analytical and numerical approaches enable us to exploit intra-crystal variations in U and Th to further our understanding of radiation damage control on diffusivity, and should ultimately allow us to detect subtle differences in thermal histories to address new and challenging geomorphic and tectonic problems.

# Thermal history and long-term crustal evolution in Rift and Passive Continental Margin Environments

Ulrich A. Glasmacher<sup>a\*</sup>, Peter C. Hackspacher<sup>b</sup>

<sup>a</sup>Institute of Earth Sciences, Heidelberg University, Im Neuenheimer Feld 234, 69120 Heidelberg, Germany

<sup>b</sup>Departamento de Petrologia e Metalogenia, Instituto de Geociências e Ciências Exatas, Universidade Estadual Paulista, Av. 24-A, 1515, 13506-900, Rio Claro-SP, Brazil

“Rift” and “Passive” continental margin (PCM) environment are “first-order” archives of the Earth’s surface that store information from the interplay of endogeneous and exogenous forces related to continental rifting, breakup, sea-floor spreading, post-breakup, and climate changes during their living time. Along strike the recent elevation of Rifts and PCM’s vary from high elevations (> 1,000 m a.s.l.) parallel to the shore line to very low elevations (< 50 m a.s.l.). Causes of such strong variations in recent topography are still in debate (Bauer et al., 2010, 2013, 2015). From the coast to inland the topography of high elevated PCM’s is usually structured as described by Bishop (2007): “The classic morphology of high-elevation PCM’s consists of a coastal plain of varying width, backed by a steep, often wall-like escarpment and a low-relief plateau surface inland of the escarpment lip”. Traditionally, recent escarpments have been interpreted as formed by endogenous forces during the early rifting stage and, thereafter, steadily retreated landward into the upland plateau surface by exogenic forces (Ollier, 1985; Kooi and Beaumont, 1994, 1996; Gallagher et al., 1998; Summerfield, 2000; Braun and van der Beek, 2004; Braun et al., 2006; Cogné et al., 2012; Sacek et al., 2012). Initial tectonic and surface uplift of the rift shoulders was interpreted to be caused by mantle and asthenospheric driven processes such as plume activity, asthenosphere up-welling, and melt intrusion during rifting (McKenzie, 1978; Wernicke, 1985; Kusznir et al., 1987; Kusznir and Ziegler, 1992; Ziegler and Cloetingh, 2004). Numerical modelling by Huisman and Beaumont (2002, 2003, 2007, 2008) clearly indicated that the strength of the lithosphere is important to the height of the topography of the rift shoulder. Certain type of lithospheric strength will not generate high topography during the rifting stage Huisman and Beaumont (2011, 2014). Recently, the concept of dynamic topography evolution is supporting the mantle driven surface activities but clearly indicated that the process is ongoing and not only related to the rifting stage (Moucha and Forte 2011, Dávila and Lithgow-Bertelloni 2013).

The causes for the occurrence of high-elevated PCM’s (> 1,000 m) close to the recent coastline, e.g. in Brazil, long after ending of the active rifting stage (initial endogenous forces, Franco-Magalhães et al., 2010) is still a case of research (Bishop, 2007; Japsen, 2006; Hiruma et al., 2010; Cogné et al., 2012; Sacek et al., 2012; Karl et al., 2013; Green et al., 2013). In 2011, Osmundsen and Redfield (2011) published the hypothesis of a relationship between the gradient of crustal thinning and the evolution of the onshore seaward-facing escarpments. They showed that the highest recent escarpments and the most asymmetric recent margin morphology are located where the crystalline crust is tapering very sharply. In contrary, lower recent escarpments are situated on more gentle tapers (Osmundsen and Redfield, 2011).

Along the recent South Atlantic “passive” continental margin (SAPCM) the onshore topography varies significantly. Whereas the SAPCM’s in Brazil, Namibia, and South Africa are partly high-elevated margins (~2,000m a.s.l.), the SAPCM in Argentine and Uruguay is in general of low elevation. The onshore part of the SAPCM in Argentine is characterized by a very even topography with elevations of up to 50 m a.s.l., in general. Nevertheless, two NW-SE trending mountain ranges the Sierras Septentrionales and Sierras Australes, truncating the low elevation by reaching exceptionally elevations of more than 1.000 m a.s.l.. The trending direction is nearly perpendicular to the trending of the Argentine SAPCM and the recent offshore spreading ridge.

The presentation will focus on the following questions:

- What are the causes for the perpendicular trending of the mountain ranges in relation to the Argentine SAPCM?
- Why are differences in recent elevation of PCM's?
- Are all rifts surrounded by elevated shoulders?
- Is the pre-rift thermal and crustal history still accessible in surface rocks of rifts and PCM's?

Quantification of the rate at which landforms adapt to changing tectonic, and climate forces on a broad time scale uses data revealed by low-temperature thermochronology (LTT). LTT-dating techniques, such as fission-track (FT) and (U-Th-Sm)/He (He) dating of apatite and zircon provide information on the cooling and heating history of rocks. Using the geological published knowledge and the annealing and diffusion kinetics allows determining the t-T evolution of crustal segments by numerical modelling. Assumptions related to the geothermal gradient and the surface temperature over time provide the possibility to calculate the exhumation history of the crustal segments. Comparing the exhumation rates with the sedimentation rates of adjacent basins and assuming a lag time for the transportation of sediments from their source region to the basins allows judging the erosion rates. All this data and interpretation lead to answer the above described research questions.

## References:

- Bauer, F.U., Glasmacher, U.A., Malikwisha, M., Mambo, V.S., Mutete B.V., 2010. The Eastern Congo – a beauty spot, rediscovered from a geological point of view. *Geology Today*, Vol. 26, No. 2, March–April 2010
- Bauer, F.U., Glasmacher, U.A., Karl, M., Ring, U., Schumann, A., Nagudi, B, 2013. Tracing the exhumation history of the Rwenzori Mountains, Albertine Rift, Uganda, using low-temperature thermochronology. *Tectonophysics* 599, 8–28.
- Bauer, F.U., Glasmacher, U.A., Ring, U., **Grobe, R.W., Mambo, V.S., Starz, M.**, 2015. Outline on the cooling history of the Albertine Rift, new evidence from the western rift shoulder, D.R. Congo. *Int. J. of Earth Sciences*, DOI 10.1007/s00531-015-1146-6
- Bishop, P., 2007. Long-term landscape evolution: linking tectonics and surface processes. *Earth Surf. Process. Landforms* 32, 329–365.
- Braun, J., van der Beek, P., 2004. Evolution of passive margin escarpments: What can we learn from low-temperature thermochronology? *Journal of Geophysical Research: Earth Surface* (2003–2012) 109, Issue F4.
- Braun, J., van der Beek, P., Batt, Geoffrey, 2006. *Quantitative Thermochronology: Numerical Methods for the Interpretation of Thermochronological Data*. Cambridge University Press. ISBN-10: 0521830575
- Cogné, N., Gallagher, K., Cobbold, P.R., Riccomini, C., Gautheron, C., 2012. Post break-up tectonics in southeast Brazil from thermochronological data and combined inverse forward thermal history modeling. *Journal of Geophysical Research* 117, B11413.
- Dávila, F.M., Lithgow-Bertelloni, C., 2013. Dynamic topography in South America. *Journal of South American Earth Sciences* 43, 127–144.
- Franco-Magalhães, A.O.B., Hackspacher, P.C., Glasmacher, U.A., Saad, A.R., 2010. Rift to post-rift evolution of a —passive continental margin: The Ponta Grossa Arch, SE Brazil. *International Journal of Earth Sciences (Geologische Rundschau)* 99, 1599–1613.
- Gallagher, K., Brown, R.W., Johnson, C., 1998. Fission track analysis and its application to geological problems. *Annual Review of Earth and Planetary Science* 26, 519–572.
- Green, P.F., Lidmar-Bergström, K., Japsen, P., Bonow, J.M., Chalmers, J.A., 2013. Stratigraphic landscape analysis, thermochronology and the episodic development of elevated, passive continental margins. *Geological survey of Denmark and Greenland Bulletin* 30.
- Hiruma, S.T., Riccomini, C., Modenesi-Gauttieri, M.C., Hackspacher, P.C., Neto, J.C.H., Franco-Magalhaes, A.O.B., 2010. Denudation history of the Bocaina Plateau, Serra do Mar, southeastern Brazil: relationships to Gondwana breakup and passive margin development. *Gondwana Research* 18, 674–687.
- Huismans, R.S., Beaumont, C., 2002. Asymmetric lithospheric extension: the role of frictional-plastic strain softening inferred from numerical experiments, *Geology* 30, 211–214.
- Huismans, R.S., Beaumont, C., 2003. Symmetric and Asymmetric lithospheric extension: Relative effects of frictional-plastic and viscous strain softening, *Journal of Geophysical Research* 108, 2496, doi:10.1029/2002JB002026.
- Huismans, R.S., Beaumont, C., 2007. Roles of lithospheric strain softening and heterogeneity in determining the geometry of rifts and continental margins. *In: Karner, G.D., Manatschal, G., Pinheiro, L.M. (eds) Imaging, Mapping and Modelling Continental Lithosphere Extension and Breakup* 107–134. Geological Society, London, Special Publications, 282, DOI: 10.1144/SP282.6.
- Huismans, R.S., Beaumont, C., 2008. Complex rifted continental margins explained by dynamical models of depth-dependent lithospheric extension, *Geology* 36, 163–166, doi: 10.1130/G24231A.1.

- Huismans, R.S., Beaumont, C., 2011. Depth-dependent extension, two-stage breakup and cratonic underplating at rifted margins, *Nature* 473, doi: 10.1038/nature 09988
- Huismans, R.S., Beaumont, C., 2014. Contrasting Characteristics of Rifted Continental Margins Explained by Depth-Dependent Lithospheric Extension: Effects of Detachment and Strong and Weak Lower Crust, *Earth Planet. Sci. Lett.* **248**, 315-324.
- Japsen, P., Bonow, J.M., Green, P.F., Chalmers, J.A., Lidmar-Bergström, K., 2006. Elevated, passive continental margins: Long-term highs or Neogene uplifts? New evidence from West Greenland: *Earth Planet. Sci. Lett.* **248**, 315-324
- Karl, M., Glasmacher, U.A., Kollenz, S., Franco-Magalhaes, A.O.B., Stockli, D.F., Hackspacher, P. 2013. Evolution of the South Atlantic passive continental margin in southern Brazil derived from zircon and apatite (U–Th–Sm)/He and fission-track data. *Tectonophysics* 604, 224–244.
- Kooi, H., Beaumont, C., 1994. Escarpment evolution on high-elevation rifted margins: insights derived from a surface process model that combines diffusion, advection, and reaction. *JGR* 99, 12 191–12 209.
- Kooi, H., Beaumont, C., 1996. Large-scale geomorphology: classical concepts reconciled and integrated with contemporary ideas via a surface process model. *Journal of Geophysical Research* 101, 3361–3386.
- Kusznir, N.J., Karner, G.D. & Egan, S. 1987. Geometric, thermal and isostatic consequences of detachments in continental lithosphere extension and basin formation. In: *Sedimentary Basins and Basin Forming Mechanisms* (edited by Beaumont, C. & Tankard, A.J.). *Mem. Can. Soc. Petrol. Geol.* 12, 185-203.
- Kusznir, N.J., Ziegler, P.A. 1992. The mechanics of continental extension and sedimentary basin formation: a simple-shear/pure-shear flexural cantilever model. *Tectonophysics* 215 117-131.
- McKenzie, D.P. 1978. Some remarks on the development of sedimentary basins. *Earth and Planetary Science Letters* 40, 25-32.
- Moucha, R., Forte, A.M., 2011. Changes in African topography driven by mantle convection, *Nature Geos.*, doi: 10.1038/ngeo1235.
- Ollier, C. D., 1985. Morphotectonics of continental margins with great escarpments, in M. Morisawa, J. T. Hack (eds), *Tectonic Geomorphology* 3–25. Allen and Unwin, Boston.
- Osmundsen, P.T., Redfield, T.F., 2011. Crustal taper and topography at passive continental margins. *Terra Nova* 00, 1–13.
- Sacek, V., Braun, J., van der Beek, P., 2012. The influence of rifting on escarpment migration on high elevation passive continental margins. *Journal of Geophysical Research: Solid Earth* 117, Issue B4.
- Summerfield, M.A. (ed.), 2000. *Geomorphology and Global Tectonics*. Wiley: Chichester. 386 pp.
- Wernicke, B. 1985. Uniform-sense normal simple shear of the continental lithosphere. *Canadian Journal of Earth Sciences* 22, 108-125.
- Ziegler, P.A.; Cloetingh, S., 2004. "Dynamic processes controlling evolution of rifted basins". *Earth-Science Review* 64, 1–50.

# The human aspects behind the Quantitative Thermochronology and Interdisciplinary Work (QTIW): A continuous time-Temperature-Pressure-Learning path

Mauricio A Bermúdez Cella<sup>1,2,3,4</sup>

<sup>1</sup>Laboratorio de Termocronología, Universidad Central de Venezuela, Caracas-Venezuela

<sup>2</sup> Universidad de Ibagué, Ibagué-Tolima, Colombia

<sup>3</sup> Syracuse University, New York State

Applications of the Quantitative Thermochronology in conjunction with the Interdisciplinary Work (QTIW) are growing exponentially, mainly due to its importance to quantify processes, test hypotheses and validate them through the integration of data, field observations and simulations. In this talk I discuss two things: A) the main role of QT through the use of the 3D thermokinematic code 'PeCube' developed by Jean Braun (Braun, 2003, Braun et al., 2006, 2012), and B) the importance of interdisciplinary work and the role of different points of view in order to understand the problem to be studied, as basic inputs for numerical modeling.

The utility of using sophisticated clusters or high-performance computers in order to run 'PeCube' inversions of thermochronologic data is discussed, but also the role of forward models that can be done with a desktop computer is underlined. These applications allow: 1) To reconstruct the time-temperature history of different sectors; 2) To incorporate different fault geometries of across study areas; 3) To compare different scenarios: changes in exhumation rates, timing, relief amplification factors and 4) To predict long-term erosion rates from detrital synorogenic formations and modern river sediments, among others applications.

Different applications of QTIW across the world are highlighted. These areas generally exhibit high complexity (tectonic settings), but with the help of an interdisciplinary approach it is possible to obtain "*acceptable*" geo-"logic" results that reproduce efficiently field observations and the geological history. Through the use of QTIW, relationships between mantle, crustal, surface and climatic processes can be distinguished. Supported by the network of researchers with whom I collaborate, I will show examples of: Central Cordillera of Colombia, Papua New Guinea -the more exciting youngest world's rift-, Chiapas mountains, and of course our work throughout my home country Venezuela.

## References

Braun, J. (2003). Pecube: a new finite element code to solve the heat transport equation in three dimensions in the Earth's crust including the effects of a time varying, finite amplitude surface topography. *Computational Geosciences* 29, 787–794.

Braun, J., van der Beek, P., Batt, G. (2006). *Quantitative Thermochronology*. Cambridge University Press.

Braun, J., van der Beek, P., Valla, P., Robert, X., Herman, F., Glotzbach, C., Pedersen, V., Perry, C., Simon-Labric, T., and Prigent, C. (2012). Quantifying rates of landscape evolution and tectonic processes by thermochronology and numerical modeling of crustal heat transport using PECUBE: *Tectonophysics*, v. 524-525, p. 1-28

## **Basin thermal history reconstruction based on multiple thermochronometers: Improving petroleum system modeling**

Mauricio Parra<sup>1</sup>, Andrés Mora<sup>2</sup>, Richard A. Ketcham<sup>3</sup>, Daniel F. Stockli<sup>3</sup>

<sup>1</sup>Institute of Energy and Environment, University of Sao Paulo, Brazil <sup>2</sup>Ecopetrol, Exploration Division, Colombia <sup>3</sup>Department of Geological Sciences, The University of Texas at Austin, USA

([mparra@iee.usp.br](mailto:mparra@iee.usp.br))

Advances in technology and in the understanding of processes controlling the retentivity of radiogenic isotopes, specially noble gases, in a broader suite of minerals<sup>1</sup> have widened the spectra of available methods for quantifying rock cooling and prompted a boom in thermochronometry in the last decades. The resulting natural increase in the amounts of data available for particular regions along with the notion that thermochronometric information in minerals represents a continuum rather than discrete events have called for robustness in modeling strategies<sup>2</sup>. A successful industry-academy collaboration applied this concept to the study of the orogenic evolution of the northern Andes and the adjacent retro-arc foreland basin in eastern Colombia, with a particular emphasis in the understanding of the petroleum system of the Eastern Cordillera and the Llanos basin. The Eastern Cordillera is an inversion orogen located at the leading edge of the northern Andes<sup>3</sup>. Fault-limited syn-rift related strata, including km-thick organic matter rich shales, were accumulated in a back-arc basin in the early Cretaceous<sup>4</sup>. A subsequent, late Cretaceous phase of thermal subsidence favored accumulation of shallow marine sandstones and shales, the latter including the La Luna Formation, the world's most prolific hydrocarbon source-rock. Early Andean uplift since Paleocene<sup>5,6</sup> led to development of a flexural basin filled with mainly non-marine strata<sup>7</sup>. We have studied the Meso-Cenozoic thermal evolution of these basins through modeling of a large thermochronometric database including hundreds of apatite and zircon fission-track and (UTh)/He data, as well as paleothermometric information based on vitrinite reflectance and presentday temperatures measured in oil wells. We employed two main modeling strategies. First, onedimensional subsidence modeling in ~20 structural domains was used to invert the pre-extensional lithospheric thicknesses, the magnitude of stretching, and the resulting heat flow associated to extension. The amount of eroded section and the maximum temperatures for various stratigraphic units at each locality were calibrated with thermochronometry. Subsequently, two-dimensional thermal models were constructed using thermokinematic modeling of sequentially restored structural cross-sections, for which abundant thermochronometric data was inverse modeled using FETKIN<sup>8,9</sup>, a software developed within this collaborative project. The results



reveal that early Cretaceous back-arc development occurred along a pre-stretched, 90 km thick lithosphere with stretching factors of up to 1.8. Such conditions led to an early Cretaceous high heat flux which, along with rapid syn-rift subsidence, resulted in an early maturation of the potential early Cretaceous source rocks, limiting their ability to expulse hydrocarbons later on, during the petroleum system's critical moment. Our modeling approach also reveals that carbonate rich source rock of latest early Cretaceous age may have attained the maturation window when late Cretaceous reservoirs were in place, and likely constituted the source for some hydrocarbons currently produced in the Llanos basin. More importantly, our results illustrate that the Oligocene main inversion of the Eastern Cordillera was a key element for assessing the size of active hydrocarbon kitchens and is a decisive element to consider for volumetric calculations of yet-to find resources. Our work in the northern Andes demonstrated that thermal and structural kinematic modeling in thrust-belts is greatly improved by a careful usage of thermochronometric data, which involves robust modeling strategies.

## References

- <sup>1</sup>Reiners, P. W. & Brandon, M. T. Using thermochronology to understand orogenic erosion. *Annual Reviews of Earth and Planetary Sciences* 34, 419-466 (2006).
- <sup>2</sup>Braun, J. et al. Quantifying rates of landscape evolution and tectonic processes by thermochronology and numerical modeling of crustal heat transport using PECUBE. *Tectonophysics* 524–525, 1-28, doi:<http://dx.doi.org/10.1016/j.tecto.2011.12.035> (2012).
- <sup>3</sup>Mora, A. et al. Cenozoic contractional reactivation of Mesozoic extensional structures in the Eastern Cordillera of Colombia. *Tectonics* 25, n/a-n/a, doi:10.1029/2005tc001854 (2006).
- <sup>4</sup>Sarmiento-Rojas, L. F., Van Wess, J. D. & Cloetingh, S. Mesozoic transtensional basin history of the Eastern Cordillera, Colombian Andes: Inferences from tectonic models. *Journal of South American Earth Sciences* 21, 383-411 (2006).
- <sup>5</sup>Caballero, V. et al. Factors controlling selective abandonment and reactivation in thick-skin orogens: a case study in the Magdalena Valley, Colombia. *Geological Society, London, Special Publications* 377, doi:10.1144/sp377.4 (2013).
- <sup>6</sup>Parra, M., Mora, A., Lopez, C., Ernesto Rojas, L. & Horton, B. K. Detecting earliest shortening and deformation advance in thrust belt hinterlands: Example from the Colombian Andes. *Geology* 40, 175-178, doi:10.1130/g32519.1 (2012).
- <sup>7</sup>Gómez, E., Jordan, T. E., Allmendinger, R. W. & Cardozo, N. Development of the Colombian foreland-basin system as a consequence of diachronous exhumation of the northern Andes. *Geological Society of America Bulletin* 117, 1272-1292 (2005).
- <sup>8</sup>Almendral, A. et al. FetKin: Coupling kinematic restorations and temperature to predict thrusting, exhumation histories, and thermochronometric ages. *AAPG Bulletin* 99, 1557-1573 (2015).
- <sup>9</sup>Mora, A. et al. Kinematic restoration of contractional basement structures using thermokinematic models: A key tool for petroleum system modeling. *AAPG Bulletin* 99, 1575-1598 (2015).

# **Fission track thermochronology applied to mineralization: example studies**

Wanming Yuan

Institute of Earth Science, China University of Geosciences, Beijing 100083,  
China  
(*ywm010@yahoo.com*)

It is a new significant attempt to apply the fission track thermochronology to mineralization. The Jiapigou gold district is located in the northern margin of the North China Craton and auriferous quartz vein types of gold deposits dominantly exist besides a few disseminated types of ore deposits. The main thicknesses of the section removed by denudation of three phases are 3.71 km, 0 km, and 1.31km, respectively. Comparison of the total thickness of the rock column denudated since the time of mineralization with the depth of the gold deposit clearly indicates that it is well preserved being located beneath the surface.

The Dongyaozhuang metamorphic hydrothermal gold deposits is located in a shear zone of the Wutai Mountains. The NWW faults cut the ore district into 3 blocks. The apatite ages increase from NE to SW sections. The apatite age has a good correlation with sample elevation (Fig.1), presenting a consistent uplifting in single block.

Present gold ore mine and discovered ore deposits are all located at the northeastern block where a few of ore bodies outcropped. The reason why the ages are lower in the northeastern block is that this block experienced strong uplifting and denudation so that present surface rocks come from near annealing zone at the original deep. The higher age in the block mean a less uplifting and denudation than the northeastern block. The gold ore deposits were originally formed in deep and are found near surface after the block uplifting-denudation. It could exploit new gold ores in the two blocks of the mineralized area.

This work was supported by the National Basic Research Program of China (No.2015CB452606) and the Nature Science Foundation of China (Nos. 41172088 and 40872141).



**THERMO2016**

**SESSION 1**

**Ar/Ar THERMOCHRONOMETRY**

## **A Caledonian conundrum: Thermochronology over a very old shear zone complex**

Ganerød, M.<sup>1</sup>, Henderson, I.H.C.<sup>1</sup>, Wilkinson, C.M.<sup>1</sup>, Redfield, T.F.<sup>1</sup>  
*<sup>1</sup> Geological Survey of Norway, Norway  
(morgan.ganerod@ngu.no)*

The northern part of the Fennoscandian Shield in Norway, Sweden, Finland and Russia consists of several Archean and Paleoproterozoic exotic terranes that between 1.9 - 1.7 Ga were accreted onto Baltica during the Svecofennian orogeny. A combination of recently acquired high resolution aeromagnetic data, field structural and kinematic analysis within basement windows reveal prominent steep ductile transpressional shear zones. Elsewhere, these post-date (1.85 Ga) earlier formed flat-lying, orthogonal ductile thrust structures. These data indicate that below the later formed Caledonian nappes (~425 Ma), a swarm of ductile shear zone structures rampage through large parts of northern Norway.

Targeted Ar-Ar thermochronology within the basement windows in the Troms domain (Northern Norway) produced a series of ages that we expected would contain Caledonian signatures from the overlying nappe sequences, allowing us to impose some constraints regarding the dynamics of the Caledonian shearing and its impact on the Paleoproterozoic bedrock below. However, amphibole ages overlap with U-Pb results (1.85 Ga), even though they were exposed to upper greenschist to amphibolite facies conditions. Amphibole, muscovite and biotite data have a variety of spectrum qualities: Some show disturbance, but others exhibit statistically valid plateaus such that the data cannot be readily discarded. At the terrane level, some internal data consistency can be resolved. However, at the regional scale, the plateaus show a complex picture of muscovite and biotite ages that preclude a simple thermal history. Only the regional feldspar argon age pattern gives a Caledonian signature.

There is nothing either good or bad but thinking makes it so. Some obvious possibilities are that many of the samples have inherited or excess argon, not detected with the inverse isochron method. They may also have experienced potassium leaching, or other processes that resulted in elevated ages. However, to produce a plateau a uniform distribution of either of these processes would have been imparted. This is very unlikely. On the other hand, we recovered enough good quality plateaus that it is hard to escape the conclusion that some of the ages are meaningful. If we can accept these plateau data, we must begin to consider that in this region Caledonian thrusting was not accompanied by a temperature greater than isotopic closure in biotite. This conclusion has consequences for the post-Svecofennian and pre-Caledonian tectonics, and may be controversial.

# **<sup>40</sup>Ar-<sup>39</sup>Ar ages on biotite and amphibole from neoproterozoic granites from northern part of the Borborema Province: new evidences for cooling histories**

Jaziel M. Sá<sup>1</sup>, Antonio C. Galindo<sup>1,2</sup>, Fernando C. Alves da Silva<sup>1,2</sup>, Fernando A. P. L. Lins<sup>1</sup>, Paulo M. Vasconcelos<sup>3</sup>, David S. Thiede<sup>3</sup>

1 Departamento de Geologia, Universidade Federal do Rio Grande do Norte, Campus Central, 59078-970 Natal-RN

2 Programa de Pós-Graduação em Geodinâmica e Geofísica - PPGG

3 Department of Earth Sciences, University of Queensland, Brisbane, Australia  
(jaziel@ccet.ufrn.br)

This paper presents new <sup>40</sup>Ar-<sup>39</sup>Ar ages on biotite and amphibole from several Ediacaran granitic plutons intruded along an 800 Km ENE-WNW trending transect in northern part of the Borborema Province (BP), NE- Brazil (Figure 1). We integrated Ar-Ar results with previous U-Pb data to suggest a thermal evolution of this region. The studied plutons were selected in order to represent different tectonic Terranes separated by NNE trending shear zones.

Biotite and amphibole were manually separated from our crushed rock-samples and crystals were irradiated for 14 hours in the Oregon State University-USA. Aliquots of 2 to 4 grains were analysed at Ages Laboratory of the University of Queensland using step-heating procedures detailed in Vasconcelos *et al.* (2002). All analyzed samples contain the pair biotite-hornblende. Biotite (Ann<sub>40</sub> to Ann<sub>91</sub>) and amphibole (Mg-hornblende to Mg-hastingsite and hastingsite) presented K<sub>2</sub>O contents of 0.8% to 1.4%. <sup>40</sup>Ar-<sup>39</sup>Ar data for hornblende display a scattering plateau ages from 571 ± 5 Ma to 523 ± 8 Ma and biotite from 557 ± 4 to 490 ± 3 Ma. All plateau ages for hornblende are always higher than that for biotite. We realize that there are no remarkable differences between ages found on plutons from different Terranes and it is not possible delineate different cooling rates to establish a heating or cooling trend among them.

Previous U-Pb data on zircons (605 to 571 Ma, Nascimento *et al.* 2015) are interpreted as the plutons crystallization ages. Zircon crystallization temperatures, determined using parameters established by Watson & Harrison (1983) and Miller *et al.* (2003), indicate that they crystallized at about 821-874°C, at crustal depth between 16 to 21 Km (Campos *et al.* 2016). These values must represent the maximum closure temperature for U-Pb isotopic system for these granitic plutons. To calculate cooling rate we consider that the U-Pb system closure on zircon is about 850°C and that for K-Ar system is about 500°C for hornblende and 300°C for biotite (Harrison 1981; Harrison *et al.* 1985). Considering different ages obtained for each pluton individually, we realize that, in general, we have an expected faster cooling rate just after the crystallization of the rock, about 13°C/Ma to 16°C/Ma, and a moderate but variable cooling rate until the biotite closure system, about 3,7° to 5,9°C/Ma. Once these granites are interpreted as syn- or late tectonic in relation to Brasiliano orogeny, these data must represent the cooling rate of these orogenic Terranes on Ediacaran times for each pluton, until about 500 Ma ago, probably with no contribution of exhumation cooling. Even considering that different granitic plutons intruded into different Terranes have distinct sources, geochemistry and crustal depth crystallization, it is not possible to determine significant regional differences in terms of thermal flow histories, based on the presented <sup>40</sup>Ar-<sup>39</sup>Ar data, even coupled with available U-Pb data. However, we can point out that the different U-Pb and Ar-Ar ages certify different crystallization times and, at least during the Brasiliano/Pan-African orogeny, there were not significant differences on thermal histories among these different Terranes of the Borborema Province.

## **References**

Nascimento, M. A. L., Galindo, A. C. & Medeiros, V. C. Ediacaran to Cambrian magmatic suites in the Rio Grande do Norte domain, extreme Northeastern Borborema Province (NE of Brazil): Current knowledge. *Journal of South American Earth Sciences*: **58**, 281-299 (2015).

- Campos, C. S.C., Vilalva, F. C. J., Nascimento, M. A. & Galindo, A. C. Crystallization conditions of porphyritic high-K calc-alkaline granitoids in the extreme northeastern Borborema Province, NE Brazil, and geodynamic implications. *Journal of South American Earth Sciences*: **70**, 224-236 (2016). <http://dx.doi.org/10.1016/j.jsames.2016.05.010>
- Harrison, T.M., 1981. Diffusion of  $^{40}\text{Ar}$  in biotite. *Contributions to Mineralogy and Petrology*. **78**, 324–331.
- Harrison, M.T., Ducean, I. & MacDougall, I. Diffusion of  $^{40}\text{Ar}$  in biotite: temperature, pressure and compositional effects. *Geochimica and Cosmochimica Acta* **49**, 2461–2468 (1985).
- Miller, C.F., McDowell, S.M. & Mapes, R.W. Hot and cold granites? Implications of zircon saturation temperatures and preservation of inheritance. *Geology*, **31**, 529e532 (2003).
- Vasconcelos, P.M., Onoe, A.T., Kawashita, K., Soares A.J. & Teixeira W.  $^{40}\text{Ar}/^{39}\text{Ar}$  geochronology at the Instituto de Geociências, USP: instrumentation, analytical procedures, and calibration. *Annals of the Brazilian Academy of Sciences*, **74**, 297-342 (2002).
- Watson, E.B. & Harrison, T.M. Zircon saturation revisited: temperature and composition effects in a variety of crustal magma types. *Earth Planet. Sci. Lett.* **64**, 295e304 (1983).

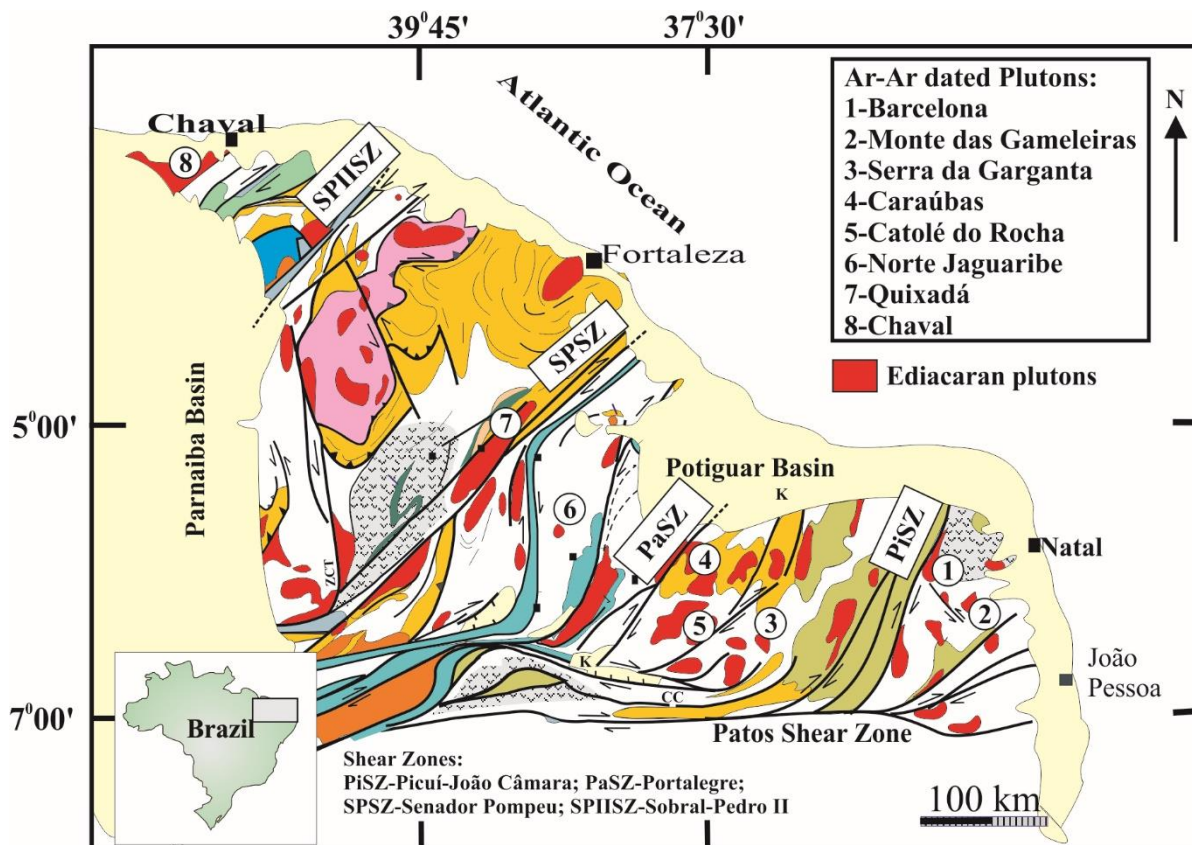


**Figure 1** – Sketch of geologic map of the Northern Domain of the Borborema Province showing the main shear zones and Ediacaran Granites. The analyzed plutons are numbered.



**THERMO2016**

**SESSION 2**

**FISSION-TRACK SYSTEM**

# Combined Apatite Fission track dating and chlorine content analysis by LA-ICP-MS

Pang Jianzhang<sup>1\*</sup>, Zheng Dewen<sup>1</sup>, Wang Ying<sup>1</sup>, Ma Yan<sup>1</sup>, Wu Ying<sup>1</sup>, Wang Yizhou<sup>1</sup>  
*1 State Key Laboratory of Earthquake Dynamics, Institute of Geology, China  
Earthquake Administration, Beijing 100029, China  
(Corresponding author: pangjzg@163.com)*

Fission track dating by Laser Ablation-Inductively Coupled Plasma-Mass Spectrometry (LA-ICP-MS) is a milestone of FT dating technology<sup>1</sup>. This method can help to not only avoid the error derived from poor thermalization and unevenly distributed thermal neutrons, but also improve the test efficiency greatly. Additionally, multi-elemental measurement also represents a significant advance for the FT dating method, such as chlorine analysis, which can promote the annealing mechanism study and improve the thermal modeling results<sup>2</sup>.

Here we present a study of analysis on both the FT ages and chlorine content simultaneously using LA-ICP-MS. Measurements were carried out using a resolution M-50 193 nm ArF Excimer laser (using a 22  $\mu$  m spot with an 10 Hz repetition rate and 4J/cm<sup>2</sup> energy) coupled with an Agilent 7900 quadrupole ICP-MS. Durango and Fish Canyon Tuff apatite standard samples were measured and the isotope of <sup>35</sup>Cl, <sup>37</sup>Cl, <sup>43</sup>Ca, <sup>232</sup>Th and <sup>238</sup>U were analyzed. The standard glasses NIST 610 were used as the out-standard and <sup>43</sup>Ca as the internal standard to calculate the uranium content. <sup>43</sup>Ca isotope was also used to correct instrument sensitivity and variations in ablation volume.

The ages obtained for Durango are 31.25  $\pm$  1.24 Ma and 33.2  $\pm$  1.57 Ma, for FCT are 29.81  $\pm$  2.13 Ma and 26.71  $\pm$  1.1 Ma. All the results agree well with their respected ages determined by other dating methods. For chlorine analysis, because of the poor ionization efficiency of chlorine, we managed to generate a relationship between the content and the signal of <sup>35</sup>Cl<sup>3</sup>. The well-constrained calibration relationship was yielded when plotting the <sup>35</sup>Cl/<sup>43</sup>Ca values against their published Cl concentrations, indicating that the analytical protocol is feasible and apatite Cl measurements by LA-ICP-MS are achievable.

## References

1. Hasebe, N., Barbarand, J., Jarvis, K., Carter, A. & Hurford, A. J. Apatite fission-track chronometry using laser ablation ICP-MS. *Chemical Geology* **207**, 135–145 (2004).
2. Barbarand, J., Carter, A., Wood, I. & Hurford, T. Compositional and structural control of fission-track annealing in apatite. *Chemical Geology* **198**, 107-137 (2003).
3. Chew, D. M., Donelick, R. A., Donelick, M. B., Kamber, B. S. & Stock, M. J. Apatite chlorine concentration measurements by LA-ICP-MS. *Geostandards & Geoanalytical Research* **38**, 23-35 (2014).



## Application of three-dimensional measurement of fission-track lengths in apatite fission-track analysis

Qingyang Li<sup>1</sup>, Andrew Gleadow<sup>1</sup>, Barry Kohn<sup>1</sup>, Christian Seiler<sup>1</sup>, Pieter Vermeesch<sup>2</sup>

*1 School of Earth Sciences, University of Melbourne, Melbourne, Australia*

*2 Department of Earth Sciences, University College London, London, UK*

*(q.li21@student.unimelb.edu.au)*

Apatite fission-track (AFT) lengths are a crucial component of the data required for modelling time-temperature histories<sup>1-3</sup>. AFT length data are traditionally measured on horizontal confined tracks (HCT), i.e., horizontal tracks that are fully enclosed within the interior of the crystal and horizontal to the observation surface. These tracks are revealed by a chemical etchant passing down suitable pathways such as surface-intersecting tracks or cleavage planes, and serve as the fundamental type of dataset for AFT annealing models. However, in some instances it becomes difficult to obtain a sufficient number of HCTs for carrying out robust track length modelling, for example in very young and/or uranium-poor apatites, or samples that are strongly annealed within boreholes.

In these cases, it may be necessary to enhance the number of fission-track lengths for modelling by measuring other types of track lengths. Two possible options are inclined confined tracks (ICT, i.e., confined tracks that are not horizontal) or semi-tracks (i.e., tracks exposed on and randomly truncated by the observation surface)<sup>4-6</sup>. In the past, it has been impractical to measure the true lengths of ICTs and semi-tracks due to the poor vertical resolution of microscope stage systems. As a result, few data are reported that evaluate the feasibility of measuring ICTs and semi-track lengths, and therefore no appropriate annealing models exist that are based on such data. This has changed with the latest generation of microscope stages have a sufficiently high precision that ICTs and semi-tracks can now be measured accurately in all three-dimensions (3D).

We carried out 3D measurements of induced and spontaneous confined fission tracks (both HCT and ICT, all using track-in-track features) on ten Fish Canyon Tuff (FCT) apatites and one Durango (DUR) apatite. FCT samples contain induced tracks that have been reheated to various degrees in the laboratory to represent different time-temperature histories. The DUR sample contains only spontaneous tracks. The data indicate that 3D measurements of random tracks are highly consistent with HCT-only results, as well as with HCT results measured independently at a different laboratory (Figure 1). Moreover, a comparison of DUR track lengths measured by different analysts using the 3D measurement approach produces more reproducible results between analysts compared to those observed in a previously published study on the same sample<sup>7</sup>.

We also measured semi-track lengths (N>1000 per sample) on the aforementioned FCT apatite samples. Our data reveal that length distributions of measured semi-tracks correlate well with the theoretically predicted patterns of a plateau that decays towards longer semi-track lengths, with two important differences. Firstly, there is a significant deficit of very short semi-tracks (<2-3 $\mu$ m) in each sample, and secondly, the longest semi-tracks measured are slightly shorter than expected from the confined track measurements. These discrepancies are probably due to difficulties in observing and measuring very short track lengths and the effect of surface etching in reducing the observed lengths of all the tracks. An improved understanding of these factors in evaluating the geometries of semi-track lengths invites further investigation.

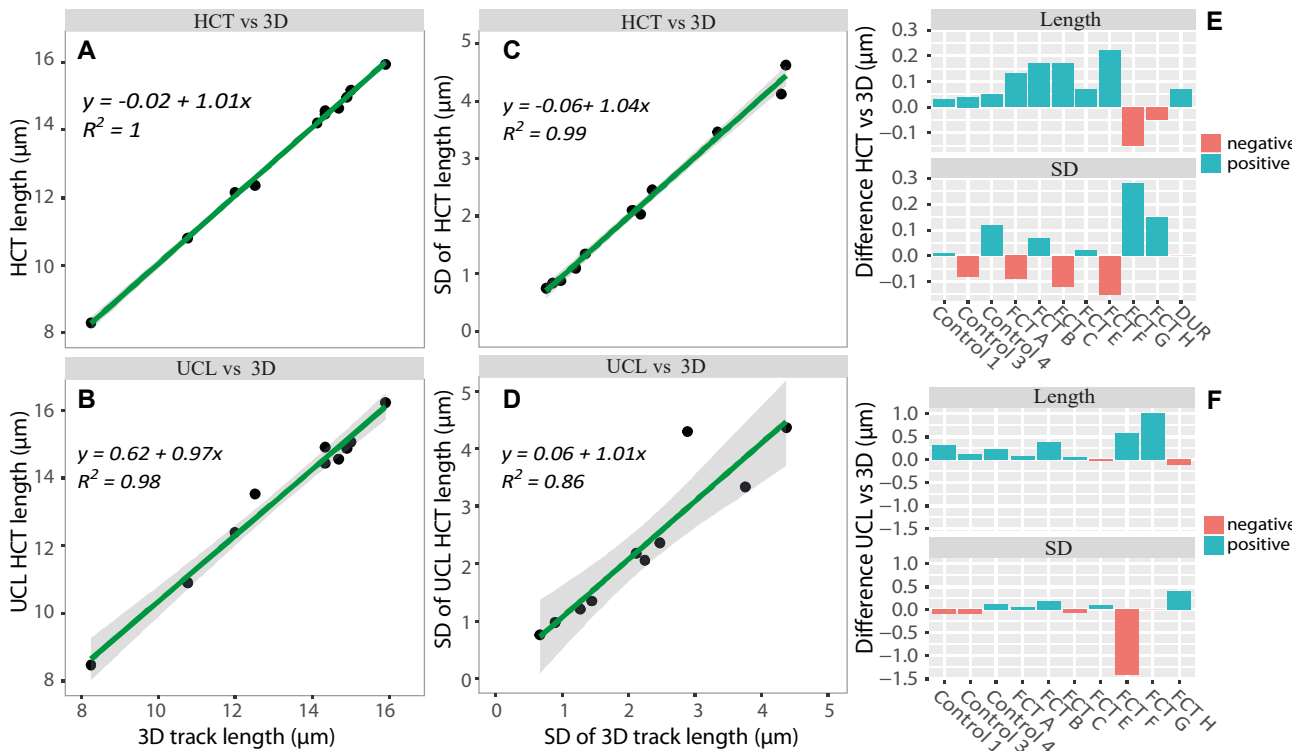


**Figure 1.** Comparison of mean track lengths and standard deviations (SD) between 3D results vs HCT-only results (A, C), and 3D results vs UCL HCT-only results (B, D). Shaded area is the 95% confidence interval. E, F) show absolute differences of length and SD between 3D results vs HCT-only results, and 3D results vs UCL HCT-only results.

## References

- Gleadow, A. J. W., Duddy, I. R., Green, P. F. & Lovering, J. F. Confined fission track lengths in apatite: a diagnostic tool for thermal history analysis. *Contributions to Mineralogy and Petrology* 94, 405-415 (1986).
- Laslett, G. M., Green, P. F., Duddy, I. R. & Gleadow, A. J. W. Thermal annealing of fission tracks in apatite 2. A quantitative analysis. *Chemical Geology: Isotope Geoscience section* 65, 1-13 (1987).
- Gleadow, A. J. W. & Brown, R. W. Fission track thermochronology and the long-term denudational response to tectonics. *Geomorphology and Global Tectonics* (Wiley, New York, 2000, p57-75).
- Laslett, G. M., Laslett, W. S., Kendall, A. J. W., Gleadow, I. R. & Duddy, I. R. Bias in measurement of fission-track length distributions. *Nuclear Tracks and Radiation Measurements* 6, 79-85 (1982).
- Laslett, G. M. & Galbraith, R. F. Statistical properties of semi-tracks in fission track analysis. *Radiation Measurements* 26, 565-576 (1996).
- Donelick, R. A., O'Sullivan, P. B. & Ketcham, R. A. Apatite Fission-Track Analysis. *Reviews in Mineralogy and Geochemistry* 58, 49-94, doi:10.2138/rmg.2005.58.3 (2005).
- Ketcham, R. A., Carter, A. & Hurford, A. J. Inter-laboratory comparison of fission track confined length and etch figure measurements in apatite. *American Mineralogist* 100, 1452-1468 (2015).

## Methodical aspects on fission tracks in hydroxyapatite

Meinert Rahn<sup>1</sup>, Ramon Schmid<sup>2</sup>, Anette von der Handt<sup>3</sup>, Cécile Gautheron<sup>4</sup>, Leander Franz<sup>5</sup>, Christian De Capitani<sup>5</sup>

<sup>1</sup> Swiss Federal Nuclear Safety Inspectorate ([meinert.rahn@ensi.ch](mailto:meinert.rahn@ensi.ch))

<sup>2</sup> Swiss Federal Laboratories for Materials Science and Technology

<sup>3</sup> Department of Earth Sciences, University of Minnesota, USA

<sup>4</sup> Département des Sciences de la Terre, Université Paris Sud, Orsay, France

<sup>5</sup> Institute of Mineralogy and Petrography, University of Basel, Switzerland

Apatites with variable portions of hydroxyl component from the Hegau volcanic field of southern Germany have been dated by the fission track method [1]. Despite their volcanic origin, apatites show complex chemical zonation patterns. Most striking is the observation that the Hegau apatite grains are mostly euhedral in shape, but show very large etch pits ( $D_{par} > 5 \mu\text{m}$  are common), leading to “bathtub”-shaped confined tracks, which makes these apatites very characteristic, e.g. when tracing them in detrital apatite series downstream or in surrounding sediment basins [2].

The counting of fission tracks is biased by the frequent presence of etched dislocation tubes, which may look similar to fission tracks (Fig. 1). Accordingly, dating requires that fission track data are cross-checked by e.g. accompanying (U-Th)/He dating on the same sample. Such control measurements have been done for the assumed youngest magmatic generation of the Hegau volcanoes (phonolites), as the obtained FT ages of around 11 Ma turn out to be distinctly younger than earlier K-Ar ages from the same rocks. The FT age was confirmed by the He ages.

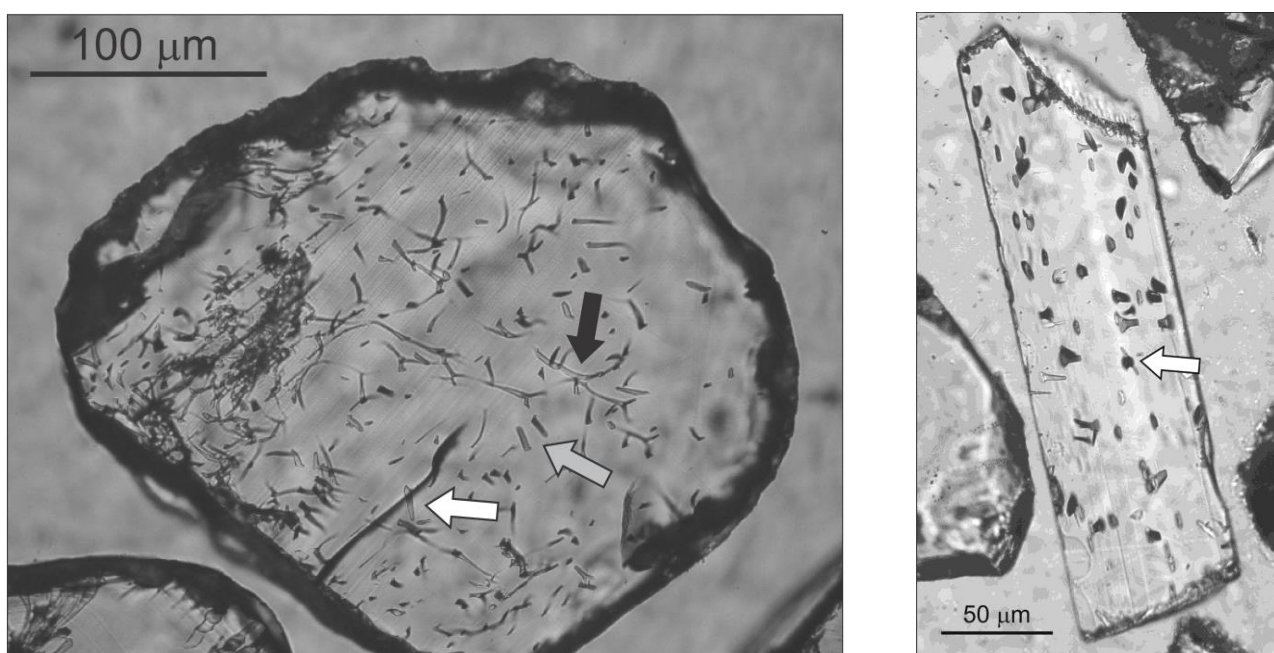


**Figure 1.** Representative apatite grains from the Hegau volcanic field, Southern Germany. Left: anhedral grain with many dislocation tubes (black arrow, result of fast cooling?), regular fission tracks (grey arrow) and a horizontal confined track (tintle). Right: long prismatic apatite with large  $D_{par}$  and one horizontal confined track (tint, note length of confined track with respect to average  $D_{par}$ ).

In line with their volcanic cooling history, the samples show very narrow track length distributions and long mean tracks. Different to regular volcanic samples (e.g. FCT), however, the number of tracks with lengths of more than 16, 17 or even 18  $\mu\text{m}$  is abnormally high. Based on the observed long  $D_{par}$ , we suggest that the long confined track lengths are influenced by fast etching along the c

axis. In addition, the “bathtub” shape of the tracks lead to erroneous length measurements, if not measured properly along the track axis.

Because the amount of hydroxy component cannot directly be determined by electron microprobe, Raman spectroscopy [3] was tested as an alternative. Due to the strong and irregular zoning of the Hegau apatites, an approach with artificially crystallized apatite material was used to test whether different peaks of the Raman spectrum may show diagnostic peak shifts and intensity changes with changing hydroxy content. A suite of samples from fluor to hydroxy endmember was crystallised and measured. The Raman peaks at 3572 and 332  $\text{cm}^{-1}$  show distinct changes in intensity and may be used to semi-quantitatively determine the hydroxyl content [4].

## References

1. Rahn, M. & Selbekk, R. (2007): Absolute age dating of the youngest Swiss Molasse sediments by apatite fission tracks. *Swiss Journal of Geosciences* 100, 10.1007/s00015-007-1234-0.
2. Rahn M.K. & Stumm F.G. (2011): Alter und Herkunft vulkanischer Apatite in der Molasse des Baselbieter und Aargauer Tafeljuras (NW-Schweiz). *Mitteilungen der Naturforschenden Gesellschaften beider Basel* 13, 129-142.
3. Zattin, M., Bersani, D. & Carter, A. (2007): Raman microspectroscopy: A non-destructive tool for routine calibration of apatite crystallographic structure for fission-track analyses. *Chemical Geology* 240, 197–204.
4. Schmid, R. (2015): Semi-quantitative Raman-Spektroskopie an Fluor-Hydroxyapatit-Mischungsreihen. Unpubl. Master thesis, University of Basel, 19pp.

## METHODOLOGICAL ADVANCES IN ZIRCON FISSION-TRACK AND U-Pb DATING

Carlos Alberto Tello Sáenz<sup>1</sup>, Rosana Silveira Resende<sup>1</sup>, Elton Luiz Dantas<sup>2</sup>

*1 Departamento de Física, UNESP – Universidade Estadual Paulista, Presidente Prudente, São Paulo – SP, Brazil*

*2 Instituto de Geociências, UnB – Universidade de Brasília, Brasília – DF, Brazil*

*E-mail of the corresponding author: tello@fct.unesp.br*

Studies using Zircon Fission-Track Method, ZFTM, showed that there is a strong etching variation from grain to grain of a same sample, even for igneous host rocks. There is significant fission-track density variation on different areas of the same zircon grain surface resulting in some small areas where the fission-track density is uniform and others where the crystal lattice was totally (or partially) damaged after etching processes. Several zircon grains belonging to igneous, sedimentary and metasedimentary samples, including the Fish Canyon Tuff, have been characterized through: optical microscopy; micro-Raman spectroscopy; cathodoluminescence (SEM-CL); electron microprobe analysis and LA-ICPMS, the last-mentioned is denominated *isotopic characterization*. These analyses were made before and after chemical etching processes to study the crystallographic structure and its likely relation with U-Pb and fission-track age obtained in the same grain. The U-Pb ages were obtained in different areas of the same grain and in some cases specifically at the same area from where the fission-track densities were determined. The results show that in some zircon grains the U-Pb ages are not similar which could be related to damage in its crystal lattice. On the other side, in areas where the fission-track density is uniform the isotopic system remains closed, which means that, in these cases, the ages are statistically compatibles.

## On the etching procedure of Fission Tracks in Apatite

Murat T. Tamer<sup>1</sup>, Richard A. Ketcham<sup>1</sup>, Raymond Jonckheere<sup>2</sup>  
1 The University of Texas at Austin, United States of America  
2 Technische Universitaet Bergakademie Freiberg, Germany  
(tamer@jsg.utexas.edu)

Track etching is a critical step of apatite fission-track dating and thermal history modeling. The current view assumes that the standard single-step etching procedures (e.g. 5.5M HNO<sub>3</sub> at 21 °C for 20s) reveal the full etchable track length at a track-etch rate ( $V_t$ ) and continued etching results in etching of the apatite crystal at the bulk etch rate ( $V_b$ ; Figure 1a)<sup>1-2</sup>. However, recent step-etch experiments performed on single confined tracks<sup>3-4</sup> show that neither the fossil nor the induced confined fission tracks in Durango apatite are etched to their full lengths with the standard protocols. Their lengths continue to increase at a reduced and decreasing rate past the break in slope in a mean-length versus etch-time plot, i.e. past the point at which they are considered to be fully etched. The lengths of the fossil and induced tracks increase at different rates but are projected to converge on a mean of ~18  $\mu\text{m}$  after ~180 s etching (5.5 M HNO<sub>3</sub>, 21 °C). The length increase within the range of our experiment is due to track etching, not bulk etching. Erratic length increments after 20 s etching are indicative of a discontinuous track structure, in agreement with recent experiments on latent ion and fission tracks in apatite<sup>5-6</sup>. The shortening of the fossil and induced tracks to their standard mean lengths (fossil: 14.47(5)  $\mu\text{m}$ ; induced: 15.67(6)  $\mu\text{m}$ ) is thus not the result of a shortening of the latent tracks but of a lowering of the average track-etch rate  $v_T$ . The rate of length increase of individual fossil confined tracks is correlated with their length; older (shorter) tracks experienced a greater reduction of the effective track-etch rate. Step-etching may thus allow us to distinguish between older and younger fossil tracks. Along-track  $v_T$ -measurements therefore have the potential of accessing additional thermal history information. In order to investigate this potential, we present a program of step-etch experiments on lab-annealed spontaneous and induced tracks in various apatites (Figure 1c).

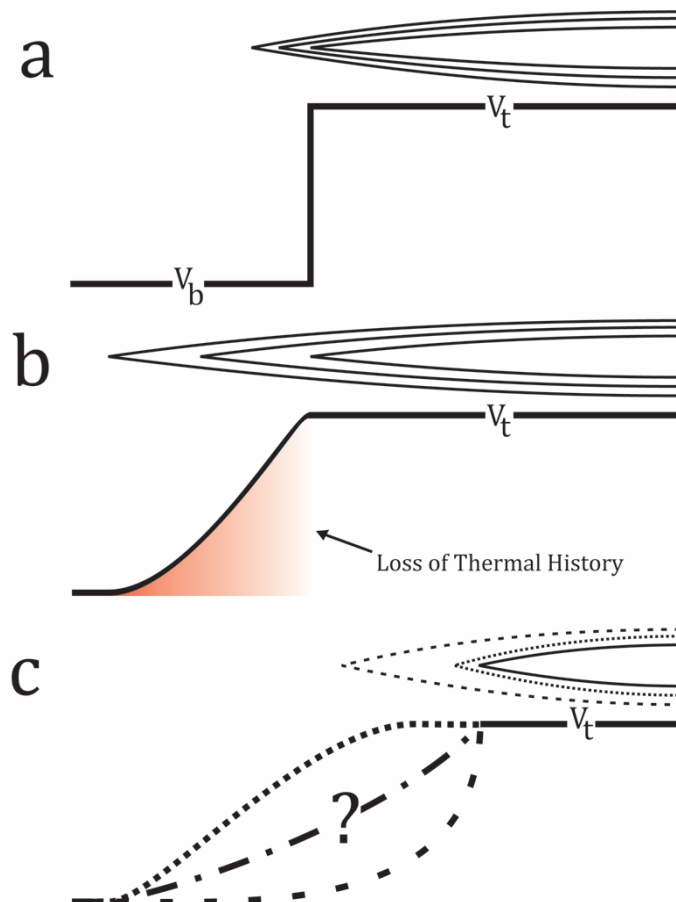


**Figure 1.** Track etching velocity models in Durango apatite. a) Traditional model, in which full etchable length is reached after 20 s at a constant rate ( $V_t$ ) and continued etching takes place at the bulk etching velocity ( $V_b$ ). b)  $V_t$  changes along the track near its etchable terminus, and the maximum etchable length is not reached. c) The etching behavior of annealed tracks under investigation.

## References

1. Laslett, G. M., Gleadow, A. J. W., Duddy, I. R.. The relationship between fission tracks length and track density in apatite Nuclear Tracks **9**, 29-38 (1984).
2. Tagami, T., O'Sullivan, P. B. Fundamentals of fission-track thermochronology.. Reviews in Mineralogy and Geochemistry **58**, 19-47 (2005).
3. Tamer, M.T. The lengths of fossil and induced fission tracks in Durango apatite. Technische Universitaet Bergakademie Freiberg, Master Thesis, 37p (2003).
4. Jonckheere, R., Tamer, M.T., Wauschkuhn, F., Wauschkuhn, B., Ratschbacher, L. "Vorsprung durch Technik": single-track length measurements of step-etched fission tracks in Durango apatite. (in review).
5. Li, W., Wang, L., Lang, M., Trautmann, C., Ewing, R.C., Thermal annealing mechanisms of latent fission tracks: Apatite vs. zircon Earth and Planetary Science Letters **302**: 227-235 (2011)
6. Lang, M., Davanathan, R., Toulemonde, M., Trautmann, C. Advances in understanding of swift heavy-ion tracks in complex ceramics. Current opinion in Solid State and Materials Science **19**: 39-48 (2015)



**THERMO2016**

**SESSION 3**

**U-Th-Sm/He SYSTEM**



## Investigation of (U-Th)/He method applicability in magnetite and spinel

Stéphane Schwartz<sup>1</sup>, Cécile Gautheron<sup>2</sup>, Rosella Pinna-Jamme<sup>2</sup>, Fabrice Brunet<sup>1</sup>, Manuel Moreira<sup>3</sup>

1 ISTERre, Université Grenoble-Alpes, France

2 GEOPS, Université Paris Sud, France

3 IPGP, Université Paris 7, France

(stephane.schwartz@ujf-grenoble-alpes.fr)

The (U-Th)/He dating method is currently performed in iron oxides such as hematite and goethite to date related ore mineralization or laterite formation (e.g., <sup>1, 2</sup>). We propose to test the methodology on other iron oxides such as spinel and magnetite. We investigate the potential of (U-Th)/He method in these minerals coming from magmatic and metamorphic ultra-mafic rocks, because they are frequent oxides in these lithologies. Published He diffusion data in magnetite from volcanic rocks<sup>3</sup> and from ore deposits<sup>4</sup> demonstrate that (U-Th)/He is retentive and that this method will give access to cooling and crystallization ages. However no He diffusion data exist for spinel.

The present study has been conducted on spinel and magnetite from ultra-mafic xenoliths sampled in the French Massif Central volcanic rocks and in serpentinized peridotite coming from the Alps. The crystals have been firstly characterized by SEM and electron microprobe analysis to determine their chemical purity. Grains were optically selected and packed for (U-Th)/He analysis. Age results are under investigation. In addition, the helium content and <sup>4</sup>He/<sup>3</sup>He isotopic ratio has been determined to investigate the impact of potential common He (i.e. mantle <sup>4</sup>He) in these samples. The first results indicate that no mantle helium is present in these samples. Finally, in order to characterize He retention in these oxide minerals, He diffusion experiments will be conducted on grains that have been saturated with He at high pressure and temperature.

With all the data, investigation of the (U-Th)/He method in magnetite and spinel will be done and the potential applicability of the method will be evaluated.

### References

1. Shuster, D.L., Vasconcelos, P.M., Heim, J.A., Farley, K.A., 2005. Weathering geochronology by (U-Th)/He dating of goethite. *Geochimica et Cosmochimica Acta*, **69**, 659-673.
2. Farley, K.A., Flowers, R., 2012. (U-Th)/Ne and multidomain (U-Th)/He systematics of a hydrothermal hematite from Eastern Grand Canyon. *Earth and Planetary Science Letters*, **359-360**, 131-140.
3. Blackburn, T.J., Stockli, D.F., Walker, J.D., 2007. Magnetite (U-Th)/He dating and its application to the geochronology of intermediate to mafic volcanic rocks. *Earth and Planetary Science Letters*, **259**, 360-371.
4. Fanale, F., Kulp, J.L., 1962. The helium method and the age of the Cornwall, Pennsylvania magnetite ore. *Economic Geology*, **57**, 735-756.

# Formation and thermal histories of fracture-filling hematite in Precambrian basement from (U-Th)/He and $^4\text{He}/^3\text{He}$ thermochronology

Peter Reiners<sup>1</sup>, David Shuster<sup>2</sup>, Nathan Evenson<sup>3</sup>

*1 Department of Geosciences, University of Arizona, Tucson, AZ, USA*

*2 Department of Earth & Planetary Sciences, University of California, Berkeley, Berkeley, CA, USA*

*3 Department of Geosciences, University of Arizona, Tucson, AZ, USA*

*reiners@email.arizona.edu*

Secondary Fe- and Mn-oxides in crystalline bedrock form from fluid flow representing regional tectonic, magmatic, or surficial events no longer preserved in stratigraphic records. Dating the timing of their formation is a critical first step in interpreting their geologic significance. The (U-Th)/He technique is well-suited for this due to low initial daughter to parent ratios, but the potential for post-formation He loss complicates simple geochronologic interpretations, especially for polycrystalline specimens. Understanding the He diffusion kinetics of dated samples, however, can help distinguish between formation and cooling ages and constrain bedrock thermal histories, as we show with a suite of He ages and  $^4\text{He}/^3\text{He}$  diffusion experiments from hematite (and one associated Mn-oxide) from several locations.

Proterozoic (1.6 Ga) volcanics in Aravaipa Canyon, southern Arizona, contain at least two distinct types of hematite, including specimens with ~1.4-1.6 Ga He ages in quartz veins, and another type precipitated on fracture planes with 1.0-1.1 Ga He ages, which are overlain by 20-30 Ma Mn-oxide, similar to apatite He ages from a few kilometers away. Hematite  $^4\text{He}/^3\text{He}$  age spectra and multi-domain (MD) diffusion models are consistent with a small proportion (4-10%) of domains between 1-500 nm, larger proportions (5-15%) of 1-10  $\mu\text{m}$  domains, and a majority (60-75%) of domains of 80-150  $\mu\text{m}$ . Although the smallest domains would have extremely low He retentivity, models predict bulk "closure temperatures" of 180-200 °C. The 1.4-1.6-Ga quartz-vein hematite likely formed soon after eruption of its host rock, and has not been hotter than ~250 °C for Ma durations. The 1.0-1.1 Ga age of the fracture-fill hematite likely also records the timing of precipitation, but from later fluids associated with a nearby diabase intrusion of the same age. In contrast, the  $^4\text{He}/^3\text{He}$  MD model of the 20-30-Ma Mn-oxide requires ~80% of 1-100 nm domains and 20% between 1-10  $\mu\text{m}$ . Although the Mn-oxide likely formed at the same time as the hematite it coats, its age records transient heating from overlying 28-Ma volcanics.

In all these cases, qualitative assessment of the distributions of approximate crystal sizes in SEM images are consistent with the predictions of the multi-domain modeling of the  $^3\text{He}$  diffusion data, and support the use of previous estimates for kinetics of He diffusion in hematite and Mn-oxide (~147-157 kJ/mol and  $\sim 2.2 \times 10^{-4}$  cm<sup>2</sup>/s for hematite, and ~134 kJ/mol and  $\sim 4 \times 10^{-3}$  cm<sup>2</sup>/s for Mn-oxide).

These results suggest that specular hematite can have, in at least some cases, bulk closure temperatures near ~200 °C, and may be a useful bedrock thermochronometer, and in some cases, geochronometer. We also present reproducible ages on fracture-filling specular hematite of 1.0-1.1 Ga from the Grand Canyon, Arizona and as old as 2.2 Ga from the Medicine Bow Mountains, Wyoming, suggesting the ability of relatively coarse-grained specularite to retain He over long time periods and metamorphic events.

# Impact of the abrasion patterns and river transport on detrital U-Th-Sm/He thermochronology: an example from the Kali Gandaki valley (central Nepal)

Ruben Rosenkranz<sup>1</sup>, Cornelia Spiegel<sup>1</sup>, Mohammad S. Sohi<sup>1</sup>

<sup>1</sup> *University of Bremen, Department 5 Geosciences, Geodynamics of Polar Regions, Klagenfurter Straße, 28359 Bremen, Germany*  
([ruben.rosenkranz@uni-bremen.de](mailto:ruben.rosenkranz@uni-bremen.de))

Detrital U-Th-Sm/He thermochronology has the potential to comprehensively characterize the exhumation history and erosion patterns over a whole catchment, complementing punctual bedrock sampling or substituting it where direct access to outcrops is unavailable (Tranel et al., 2011; Ehlers et al., 2015). The method is, however, not routinely carried out, which is partly due to complications that still need to be better constrained: (1) the distribution of the crystals in the river systems with respect to the source, (2) the abrasion dynamics of the single grains that relate with (3) how much alpha correction needs to be applied. However, measuring abraded grains in detrital samples has the advantage of mitigating the impact of He-ejection, implantation and zonation (Gautheron et al., 2012).

Most of the previous studies limited the sampling to small, uniform catchments and took a single river sample for each drainage system. We pursued a different approach: we collected several sand samples at regular intervals from the Kali Gandaki River in central Nepal, from the source to the mid-course, with the catchment size progressively increasing. The Kali Gandaki River drainage represents an ideal sample location to test our approach because it drains in the source area the present exposure of the Mustang granite, and then enters the syntectonic filling of the Takkhola graben. Furthermore, we sampled different stratigraphic levels of the Mio-Pliocene sedimentary rocks, i.e. from the Tetang and Takkahola formations deposited between 11 and 7 Ma, to test to which extent they contribute to the apatite content of the river.

To assess the level of abrasion of the various samples, as single grains or population of apatite grains, an imaging method was used in order to calculate the shape parameters of the grains. Our first results show that apatites are abraded due to river transport, and do so in a noticeable manner within the first 10-15 km of the river course. After this critical fluvial length, which coincides with the steepest part of the river channel, the population of crystals seems to reach an equilibrium between rounded and idiomorphic grains. We argue that lateral catchments may provide fresh euhedral grains, whereas the grain from distal places will mainly remain in the smaller, and rounded, fraction. Selecting just euhedral grains from a sample with this condition would lead to a significant bias towards the source of high-quality apatites.

From our preliminary analytical results, we can identify several grains that show a significant dispersion when the alpha correction is applied a priori. When the correction is applied selectively on the grains that conserve their pristine morphology, however, they cluster better and give more reliable ages in relation to the exhumation history of the Tethyan Himalaya.

## References

1. Tranel, L.M., Spotila, J.A., Kowalewski, M.J. and Waller, C.M. (2011). Spatial variation of erosion in a small, glaciated basin in the Teton Range, Wyoming, based on detrital apatite (U-Th)/He thermochronology. *Basin Research*, 23(5), pp.571-590.
2. Ehlers, T.A., Szameitat, A., Enkelmann, E., Yanites, B.J. and Woodsworth, G.J. (2015). Identifying spatial variations in glacial catchment erosion with detrital thermochronology. *Journal of Geophysical Research: Earth Surface*, 120(6), pp.1023-1039.
3. Gautheron, C., Tassan-Got, L., Ketcham, R.A. and Dobson, K.J. (2012). Accounting for long alpha-particle stopping distances in (U–Th–Sm)/He geochronology: 3D modeling of diffusion, zoning, implantation, and abrasion. *Geochimica et Cosmochimica Acta*, 96, pp.44-56.

# Potential influence of apatite chlorine content on (U-Th-Sm)/He thermochronology

Cornelia Spiegel<sup>1</sup>, Andreas Klügel<sup>1</sup>, Patrick Monien<sup>1</sup>, Vera Kolb<sup>1</sup>  
1 Department of Geosciences, University of Bremen, Germany  
(cornelia.spiegel@uni-bremen.de)

Apatite (U-Th-Sm)/He (AHe) dating often yields strong inter- and intra-sample dispersion, particularly when applied to samples from slowly cooled cratonic areas. Furthermore, these samples frequently show inverted age-relationships, with AHe dates older than apatite fission track (AFT) dates of the same sample. Various mechanisms were proposed for explaining age dispersion and inversion, including radiation damage [1] He implantation [2], and grain fragmentation [3], but none of these were able to fully explain the observed AHe age variations. Recently, it was proposed that the chemical composition of apatite, particularly its chlorine content, may influence He diffusion in apatite in that Cl substitution impedes He diffusion along the c-axis and additionally enhances He retentivity due to its influence on the damage annealing rate [4]. This study is based on calculated He diffusivity in response to different Cl-contents of apatite, and it predicts an increase of the closure temperature for apatite rich in Cl, as compared to F-apatite.

For natural samples, it is hard to test the influence of Cl, because routinely, Cl is measured by electron microprobe analysis. For AHe dating, apatite is dissolved prior to U, Th, and Sm analysis, excluding subsequent electron microprobe analysis of the same grain. For this study, we apply ICP-MS measurements for deriving Cl-contents from the same grain previously measured for U-Th-Sm contents. This allows to directly relate AHe age variations to potential variations of the Cl-content. We tested this approach on samples from the cratonic areas of northwest Greenland. These experienced protracted slow cooling (>100 Ma) through the He partial retention zone, and subsequent reheating into the He partial retention zone. For such a setting it is expected that even slight variations of He diffusion properties may have a strong effect on AHe age patterns.

He was extracted from apatite crystals by laser heating (5 min, 900°C) using a solid-state diode laser (970 nm wavelength). The extracted He was measured by the <sup>3</sup>He isotope dilution method using a PrismaPlus QMG 220 quadrupole mass spectrometer. The element contents of apatites were determined by ICP-MS in low (U, Th, Sm) and medium resolution mode (Cl) using a Thermo Element2. Single apatite grains with enclosing Pt tubes were placed in Savillex beakers and dissolved in HNO<sub>3</sub> on a hot plate. The instrument was calibrated using high-purity single element standard solutions. As expected, AHe thermochronology yielded strong inter- and intra-sample age dispersion, with AHe dates ranging from 24 to 378 Ma. Effective U-concentrations, used as a measure for radiation damage, also showed strong variations, ranging from 45 to <1 ppm. Cl-contents ranged from 0.3 to 2.0 wt-%. While we could find no correlation between AHe dates and effective U-concentrations, a slight correlation between AHe dates and apatite grain sizes ( $r^2=0.24$ ), and a fairly good correlation between AHe dates and Cl-content ( $r^2=0.35$ ) was observed. Surprisingly, the observed age-Cl-relationship is exactly opposite to what was expected, with AHe dates becoming younger with increasing Cl-content of apatite. Also, apatites with high Cl-contents show normal age-relationships with their corresponding AFT dates, whereas low-Cl apatites show inverted age-relationships. However, these first results should be viewed with caution, as the number of analyses is still low, and the blank levels for the Cl-measurements are still relatively high. For further analyses, we plan to replace the Savillex beakers by materials that do not contain halogenides, which may further reduce Cl-blank levels.

## References

1. Schuster, D., Flowers, R. & Farley, K.. The influence of natural radiation damage on helium diffusion kinetics in apatite. *Earth and Planetary Science Letter* **249**, 148-161 (2006).

2. Spiegel, C., Kohn, B., Belton, D., Berner, Z., & Gleadow, A. Apatite (U-Th-Sm)/He thermochronology of rapidly cooled samples: the effect of He implantation. *Earth and Planetary Science Letters* **285**, 105-114 (2009).
3. Brown, R., Beucher, R., Roper, S., Persano, C., Stuart, F. & Fitzgerald, P. Natural age dispersion arising from the analysis of broken crystals: Part I. Theoretical basis and implications for the apatite (U-Th)/He thermochronometer. *Geochimica et Cosmochimica Acta*, **122**, 478-497 (2013).
4. Mbongo Djimbi, D., Gautheron, C., Roques, J., Tassan-Got, L., Gerin, C. & Simoni, E. Impact of apatite chemical composition on (U-Th)/He thermochronometry: an atomistic point of view. *Geochimica et Cosmochimica Acta* **167**, 162-176 (2015).

## Performance of (U+Th)/He laboratory at UNESP (Rio Claro, Brazil)

Marli Carina Siqueira-Ribeiro<sup>1</sup>, Danieli Fernanda Canaver Marin<sup>1</sup>, Peter C. Hackspacher<sup>1</sup>,  
Finlay M. Stuart<sup>2</sup>

<sup>1</sup>*Department of Petrology and Metallogeny, São Paulo State University, Rio Claro (SP),  
Brazil*

<sup>2</sup>*Isotope Geosciences Unit, SUERC, East Kilbride, G75 0QF, UK  
([carinasr@rc.unesp.br](mailto:carinasr@rc.unesp.br))*

Combining apatite fission track and apatite (U+Th)/He thermochronometers provides unrivalled ability to quantify the denudation of shallow crust. These low temperature thermochronological techniques are now routinely applied to the reconstruction of geodynamic. The fission track laboratory at UNESP Rio Claro has been routinely performing analysis of apatite and zircon for many years. This has recently been complemented with a new laboratory for apatite (U+Th)/He thermochronology with the aim of combining both techniques to unravelling the complex pre- and post-break up tectonic evolution of the Atlantic Ocean margin of Brazil, and the conjugate margin in Africa.

<sup>4</sup>He is measured on a Faraday detector in a GVI Helix-SFT mass spectrometer. Absolute amounts are determined by peak height comparison to <sup>4</sup>He from a reservoir that has been calibrated in the SUERC He thermochronology laboratory. Repeated determinations of the He standard (n ~120) yields a long-term reproducibility of 0.8%. The instrumental sensitivity is linear over the range of He we expect in samples. Helium is extracted from apatites by heating with an infrared (970 nm) diode laser with optics and stage automation by Photon Machines to approximately 650°C for 60 seconds. Laser heating of empty Pt tubes yields <sup>4</sup>He blank levels that are at system background levels (< 6 x 10<sup>-12</sup> ccSTP, n=30). U, Th and Sm measurements are carried out using a Thermo Scientific ELEMENT2 single collector double-focusing ICP-MS. <sup>238</sup>U, <sup>232</sup>Th and <sup>147</sup>Sm are determined by isotopic dilution analysis with calibrated <sup>235</sup>U, <sup>230</sup>Th and <sup>149</sup>Sm spikes. Fractionation in the mass spectrometer (mass bias correction) is monitored using CRM U500 and a Sm standard interspersed every 3 samples. Reproducibility of the U500 and Sm solution in 100 measurements was ~ 0.2% and 0.1% respectively.

The U, Th and He data of Durango apatites are plotted in Figure 1. Seven fragments of Durango apatite crystals (EK) supplied by SUERC and sixty fragments from UNESP (RC) have been analyzed over the last 12 months. The average age (31.3 ± 1.8 Ma n = 63) overlaps the long-term average of Durango apatite measured in other laboratories. These calibration and standardization procedures ensure that the analysis carried out in our laboratories will gain international credibility, enabling Brazilian students and scientists to conduct research in geosciences using (U-Th-Sm)/He thermochronology.

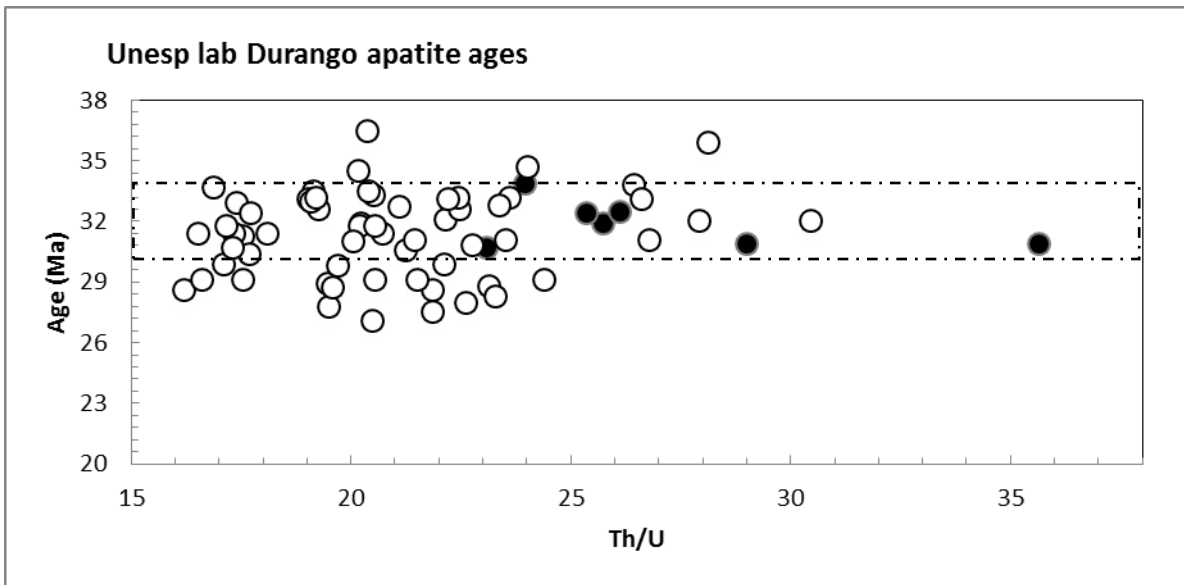


Fig. 1. He ages versus Th/U for Durango Apatite. Open circles represent UNESP RC Durango; black circles are EK Durango.





**THERMO2016**

**SESSION 4**

**DIFFUSION IN MINERALS:  
WHAT CONTROLS IT AND HOW TO MEASURE IT**

# Interrogating the Effects of Radiation Damage Annealing on Helium Diffusion Kinetics in Apatite

Chelsea D. Willett<sup>1,2</sup>, Matthew Fox<sup>1,2</sup>, David L. Shuster<sup>1,2</sup>

<sup>1</sup> *University of California, Berkeley, USA*

<sup>2</sup> *Berkeley Geochronology Center, USA*  
(*cwillett@berkeley.edu*)

Apatite (U-Th)/He thermochronology is commonly used to study landscape evolution and the potential links between climate, erosion and tectonics. The technique relies on a quantitative understanding of (i) helium diffusion kinetics in apatite, (ii) an evolving <sup>4</sup>He concentration, (iii) accumulating damage to the crystal lattice caused by the processes of radioactive decay<sup>[1]</sup>, and (iv) the thermal annealing of such damage<sup>[2],[3]</sup>, which are each functions of both time and temperature. Uncertainty in existing models of helium diffusion kinetics has resulted in conflicting conclusions, especially in settings involving burial heating through geologic time<sup>[4,5]</sup>. The effects of alpha recoil damage annealing are currently assumed to follow the kinetics of fission track annealing (e.g., Ref. 3), although this assumption is difficult to fully validate. Here, we present results of a new empirical model and a set of experiments designed to interrogate the effects of damage annealing on He diffusivity in apatite that are independent of calibrations of fission track annealing. We use the existing experimental results for the diffusion kinetics parameters measured in Durango apatite<sup>[2]</sup> to develop and calibrate a new function that predicts the effects of annealing temperature and duration on measured activation energy and frequency factor. We also present results from two suites of experiments conducted on Durango apatite and apatite from Sierra Nevada, CA granite to establish whether apatites with different chemical compositions exhibit the same response to annealing treatment. Crystals were heated under vacuum to temperatures between 250 and 500°C for 1, 10, or 100 hours. The samples were then irradiated with ~220 MeV protons to produce spallogenic <sup>3</sup>He, the diffusant then used in step-heating diffusion experiments. We compare the results of these experiments and new model to existing models<sup>[3]</sup>.

## References

1. Shuster, D.L., R.M. Flowers, and K.A. Farley. The influence of natural radiation damage on helium diffusion kinetics in apatite. *Earth Planet. Sci. Lett.* **249(3-4)**, 148-161, (2006).
2. Shuster, D.L. and K.A. Farley. The influence of artificial radiation damage and thermal annealing on helium diffusion kinetics in apatite. *Geochim. Cosmochim. Acta* **73 (1)**, 6183-6196, (2009).
3. Flowers, R. M., R.A. Ketcham, D.L. Shuster and K.A. Farley. Apatite (U-Th)/He thermochronometry using a radiation damage accumulation and annealing model. *Geochim. Cosmochim. Acta* **73**, 2347-2365, (2009).
4. Flowers, R.M. and K.A. Farley. Apatite 4He/3He and (U-Th)/helium evidence for an ancient Grand Canyon. *Science* **338 (6114)**, 1616–1619, (2012).
5. Fox, M., and D.L. Shuster. The influence of burial heating on the (U-Th)/He system in apatite: Grand Canyon case study. *Earth Planet. Sci. Lett.* **397**, 174-183, (2014).

## A test of the interlayer ionic porosity as a measure of argon diffusivity in micas

A. Camacho<sup>1</sup>, J.K.W. Lee<sup>2</sup>, R. Armstrong<sup>3</sup>, Y.A. Abdu<sup>1</sup>, R.A. Creaser<sup>4</sup>

<sup>1</sup> Dept of Geological Sci., Univ. of Manitoba, MB, R3T 2N2, Canada

<sup>2</sup> Dept of Geological Sci. and Geological Eng., Queen's University, ON K7L 3N6, Canada

<sup>3</sup> Research School of Earth Sci., The Australian National University, ACT 0200, Australia

<sup>4</sup> Dept of Earth and Atmospheric Sciences, University of Alberta, AB T6G 2E3, Canada

(camacho@umanitoba.ca)

Understanding the mechanisms that govern the mobility of elements in rocks and minerals is critical to deciphering the tectonothermal evolution of orogenic belts. The redistribution by diffusion of elements in a system is considered to be extremely sluggish under dry, static conditions, such that reequilibration will not take place even though temperatures far exceed commonly assumed closure temperatures over long periods of time. Consequently, there is a school of thought that believes that thermochronological information can only be extracted from systems where considerable amounts of fluid are involved.

The ionic porosity (Z) model of Fortier and Giletti (1989)<sup>1</sup> originated from the concept introduced by Dowty (1980)<sup>2</sup> of the anion porosity of a crystal structure (the percentage of unit-cell volume not occupied by anions). Dahl (1996)<sup>3</sup> refined this model for micas by focusing on the ionic porosity of the interlayer site (Zi). This model assumes that the large interlayer site, in comparison to the small dimension of the c axis, is the primary site in the mica structure for the atomic transport of argon (i.e. diffusion occurs preferentially parallel to the T-O-T layer rather than perpendicular to the layer). Dahl (1996) suggested that since Zi is, in general, inversely correlated with interlayer-bond strength, it can thus be regarded as a major controlling factor of argon mobility in micas.

We tested this model by dating micas from several outcrops using the <sup>40</sup>Ar/<sup>39</sup>Ar, and Rb/Sr techniques along a ~ 5.2 km transect in the Frontenac terrane, Grenville Province, Ontario. This transect is ideal because: (a) the rocks in this small area experienced the same geologic history, and (b) there are a variety of lithologies (marble, pyroxenite, granitoid and pegmatite) containing trioctahedral and dioctahedral micas of different chemical compositions. The micas crystallized during amphibolite-facies metamorphism and in granitic melts at ~1170 Ma, and experienced a thermal pulse ~100 Ma later at shallow crustal levels associated with the emplacement of plutons. Surprisingly, our results showed that coexisting trioctahedral and dioctahedral micas yielded <sup>40</sup>Ar/<sup>39</sup>Ar plateau ages that differ by >100 Ma.

From chemical and X-ray data, the interlayer ionic porosity of the micas varies by as much as ~3.3%. Significantly, however, our Ar data show that there is no correlation between interlayer ionic porosity and <sup>40</sup>Ar/<sup>39</sup>Ar age. Instead, we propose that defect structures enclosed entirely within a coherent crystal lattice may serve as Ar traps, effectively increasing the Ar retentivity of the mineral<sup>4</sup> and thus becoming the dominant control on Ar mobility in the crystal. This model is being continuously tested.

### References

1. Fortier, S.M. & Giletti, B.J. An empirical model for predicting diffusion coefficients in silicate minerals. *Science* **245**, 1481-1484 (1989).
2. Dowty, E. Crystal-chemical factors affecting the mobility of ions in minerals. *American Mineralogist* **65**, 174-182 (1980).

3. Dahl, P.S. The crystal-chemical basis for Ar retention in mica: Inference from interlayer partition and implications for geochronology. *Contributions to Mineralogy and Petrology* **123**, 22-39 (1996).
4. Camacho, A., Lee, J.K.W., Fitz Gerald, J.D., Zhao, J., Abdu, Y.A., Jenkins, D.M., Hawthorne, F.C., Kyser, T.K., Creaser, R.A., Armstrong, R., & Heaman, L.W. Planar defects as Ar traps in trioctahedral micas: a mechanism for increased Ar retentivity in phlogopite. *Earth and Planetary Science Letters*, **341**, 255-267 (2012)



**THERMO2016**

**SESSION 5**

**NUMERICAL METHODS:  
MODELLING OF DATA (T-t EXTRACTION)  
AND PROCESSES**

# Dealing with data and model parameter uncertainties in thermal history modelling

*Kerry Gallagher*

*University of Rennes 1, Rennes, France*

Since the publication of Dodson (1973) quantifying the relationship between geochronological ages and closure temperatures, an ongoing concern in thermochronology is reconstruction of thermal histories consistent with the measured data. Extracting this thermal history information is best treated as an inverse problem, given the complex relationship between the observations and the thermal history. When solving the inverse problem (i.e. finding thermal acceptable thermal histories), stochastic sampling methods have often been used, as these are relatively global when searching the model space. However, the issue remains how best to estimate those parts of the thermal history unconstrained by independent information, i.e. what is required to fit the data ? To solve this general problem, we use a Bayesian transdimensional Markov Chain Monte Carlo method. The Bayesian approach allows us to consider a wide range of possible thermal history as general prior information on time, temperature (and temperature offset for multiple samples in a vertical profile). We can also incorporate more focused geological constraints in terms of more specific priors. In this framework, it is the data themselves (and their errors) that determine the complexity of the thermal history solutions. For example, more precise data will justify a more complex solution, while more noisy data will be happy with simpler solutions.

Another useful feature of this method is that we can easily deal with imprecise parameter values by drawing samples from a user specified probability distribution, rather than using a single value. This is often referred to as hierarchical Bayes. The resampling approach can be applied to uncertain parameters required for modeling the data, such as the kinetic parameter for fission track annealing, or the eU value or zoning for AHe and ZHe data. This can be justified as the models can not capture all the underlying physical processes, and so relying on fully deterministic models can lead to difficulties in finding thermal history models consistent with multiple data and multiple samples. The resampling approach gives a bit of flexibility in the forward model parameterization. We can also apply a resampling approach to the data themselves or the errors on the data. This can allow us to deal with outliers in a flexible way, and also to assess which data are more dominant in the inference of the thermal history solutions. Resampling the data or data errors can be justified intuitively as we accept the data are noisy (i.e. not perfect) and geological complexity will generally increase the noise relative to the analytical error. Again, this approach is useful for finding thermal history solutions compatible with multiple data from single samples and multiple samples.

To demonstrate the features and implementation of the resampling approach, examples will be presented using both synthetic and real data.

# Multi-Mineral Fission-Track Thermochronology Software

Arnaldo Luis Lixandrão Filho, Sandro Guedes, Julio Cesar Hadler Neto  
"Gleb Wataghin" Physics Institute, University of Campinas, Brazil  
allfilho@ifi.unicamp.br

We present a new Multi-Mineral Fission-Track Thermochronology Software (MMFTTS) developed in R language. MMFTTS uses the inverse method [2] proposed by Lutz & Omar for thermal history search. It is possible to use any annealing model as basis for inverse method. MMFTTS also calculates Partial Annealing Zone (PAZ) and Closure Temperature (CT) for a given annealing equation. We also present a new length reduction model with only 3 parameters. PAZ and CT for this model are similar to those calculated by other computational tools [3] or published by other researchers [4,5]. MMFTTS uses it as default and can, automatically fit any mineral experimental annealing data, ie: Apatite, Zircon or, more recently, Epidote. The general equation is:

$$\frac{L}{L_0} = 1 + A \cdot e^{\frac{T}{B-C \cdot \ln(t)}}$$

A, B e C are fit parameters from experimental data. This is a mathematical model with no physical basis, but represents laboratory and geological data very well. The default age reduction equation that MMFTTS uses is:

$$(\rho / \rho_0) = (l / l_0) \{1 - [1 + (kl_0(l / l_0))^n]^{-2}\} / \{1 - [1 + (kl_0)^n]^{-2}\},$$

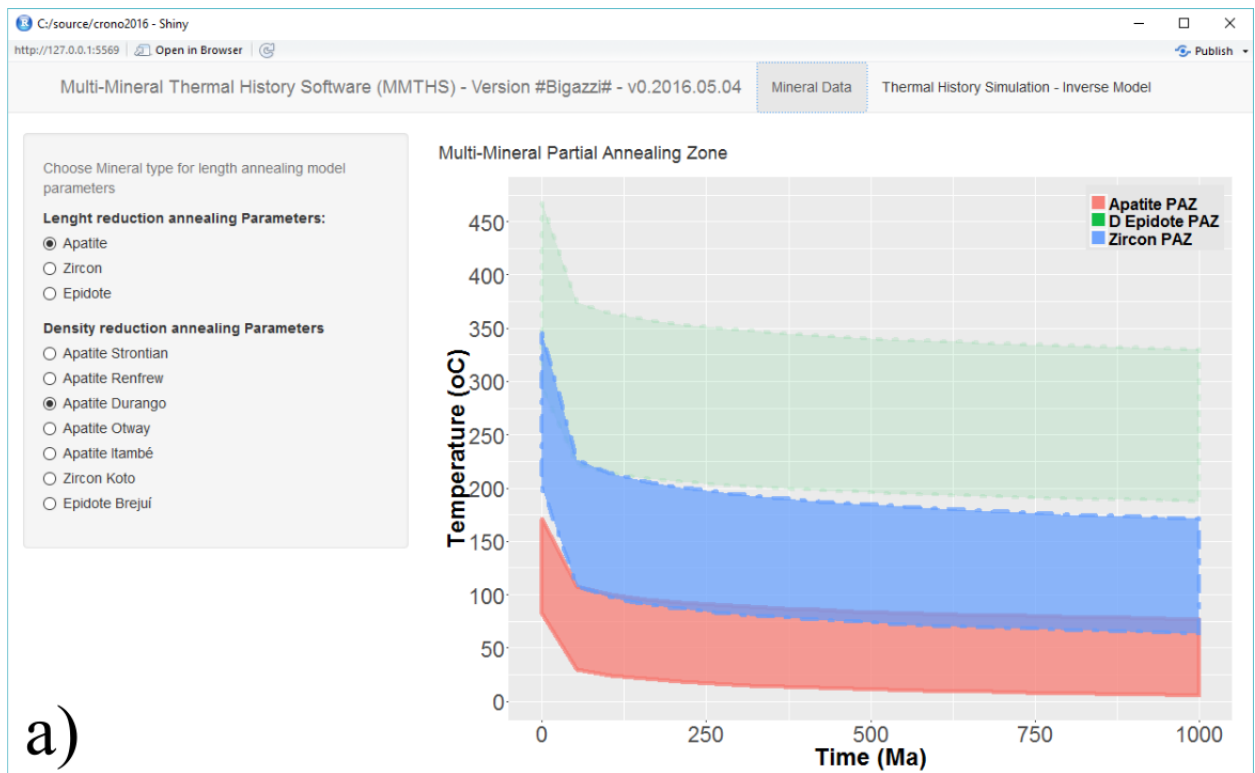
proposed by Guedes and coworkers [1]. In Figure 1a) (left side) shows all the multi-mineral parameters fitted from data. In the right side the PAZ for Apatite, Zircon and Epidote in one graph showing complementarity among them. Using other minerals than apatite it is possible to expand the range of time and temperature studied, obtaining different information about thermal evolution of study regions. It will be also possible to include other experimental data sets to increase the software database to work with even more minerals.

Figure 1b illustrates the thermal evolution tab interface. The user load confined tracks list, set the age calculated by fission track with uncertain and finally set up some geological constraints. The software searches for a thermal path following all the constraints and check the compatibility of the generated list of reduced confined tracks with the input list of experimental measured tracks. It is used the Kolmogorov-Smirnov test since confined track lists are a continuous distribution. The user also can change the minimum p-value. This is a fine tuning that should be used with caution since it depends on firm knowledge of statistics.

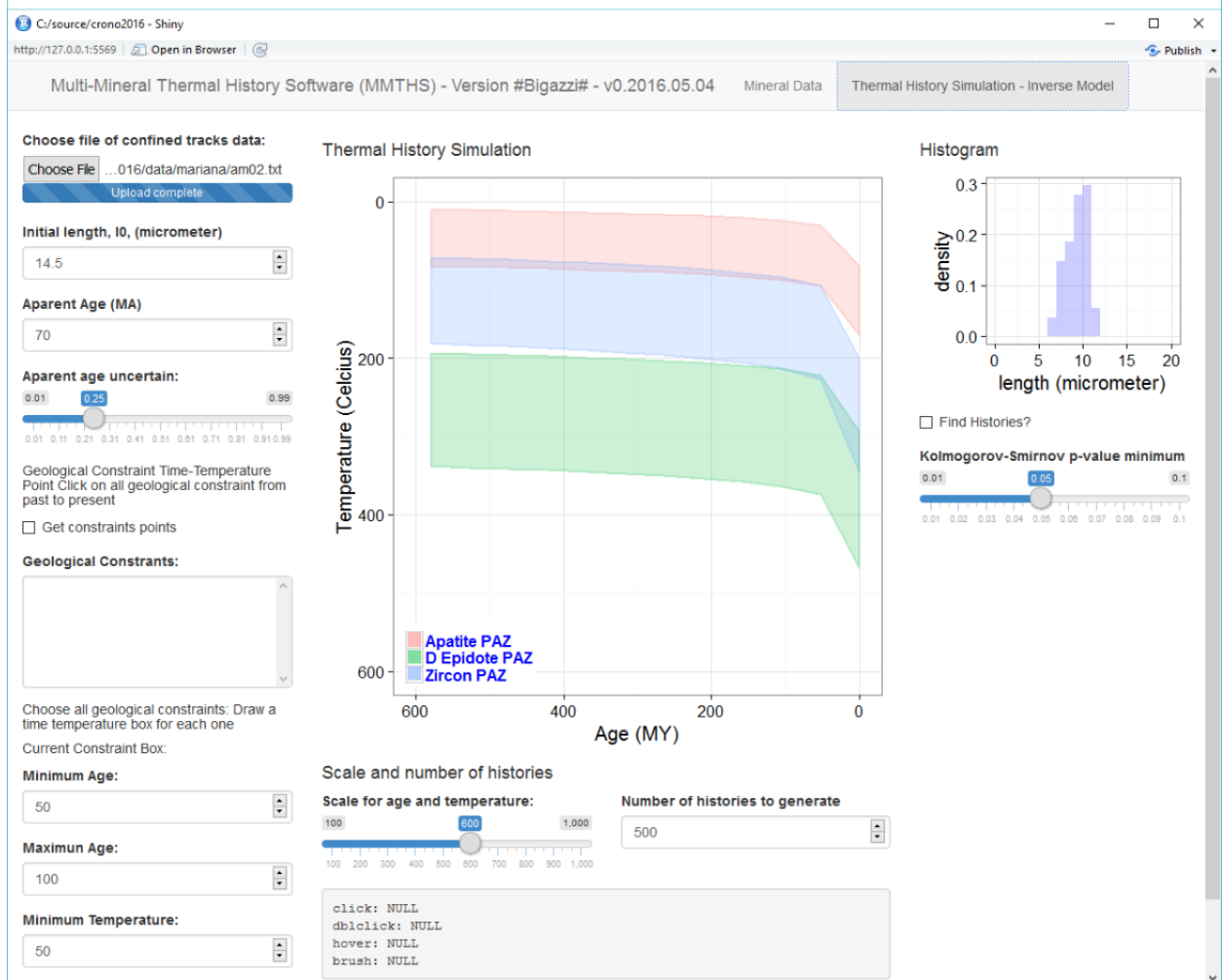
The approach proposed in MMFTTS is innovative since users can track each step in thermal evolution prediction, from fitting annealing models to fine tuning statistics criteria. This improves the research integrity in fission-track thermochronology as proposed by Flowers and coworkers [6].

## References

1. Guedes, S., Hadler Neto, J. C., Iunes, P. J., Saenz, C. A. T., Nuclear Instruments and Methods in Physics Research Section B: Beam Interactions with Materials and Atoms, **217** 627-636 (2004);
2. Lutz, M. T. & Omar, G. *Earth Planetary Science Letters*, **104** 181-195 (1991);
3. Todd A. Ehlers, Tehmasp Chaudhri, Santosh Kumar, Chris W. Fuller, Sean D. Willett, Richard A. Ketcham, Mark T. Brandon, David X. Belton, Barry P. Kohn, Andrew J.W. Gleadow, Tibor J. Dunai, and Frank Q. Fu, *Reviews in Mineralogy and Geochemistry*, **58** 589-622 (2005);
4. Meinert K. Rahn, Mark T. Brandon, Geoffrey E. Batt, and John I. Garver, *American Mineralogist*, **89** 473-484 (2004);
5. S. Guedes, P. A. F. P. Moreira, R. Devanathan, W. J. Weber, J. C. Hadler, *Physics and Chemistry of Minerals*, **40** 93-106 (2012).
6. R. M. Flowers, K. A. Farley, R. A. Ketcham, *Earth and Planetary Science Letters*, **432** 425-435 (2015)



a)



b)

Figure 1. Software screen shoot shows the capability multi-mineral choices and partial annealing zone for Apatite, Zircon and Epidote.



# **Defining the thermal evolution of hyperextended magma-poor rift margins: Constraining a continuous lithospheric thermal history using apatite U-Pb thermochronometry**

Patrick Boyd<sup>1</sup> Daniel F Stockli<sup>1</sup> Federico Galster<sup>1</sup>

*1 Department of Geologic Sciences, University of Texas at Austin, USA*

Lithospheric thermal history is kept within key accessory mineral grains in the form of diffusive loss and retention of radiogenic daughter products. While thermal histories have been traditionally recovered through bulk thermochronometry (e.g. K-Ar or (U-Th)/He), using the estimation of mineral closure temperatures ( $T_c$ ) and volume-averaged total gas radiometric ages, the utility of total-gas mineral thermochronometry is often limited and does not take advantage of the spatial distribution of the radiogenic diffusant as a more powerful thermochronometric tool. Novel in-situ laser ablation techniques have been pioneered in recent years to directly measure the parent and diffusive daughter concentration ratios as a function of radial position within a grain. These new methods are revolutionizing high-temperature U-Pb thermochronometry and trace element diffusion speedometry and allow for the investigation of timing and rates of middle and lower crustal tectonic processes.

In particular, apatite and rutile U-Pb high-temperature thermochronometry has been recognized as a novel and powerful tool for reconstructing nearly continuous temperature histories from  $\sim 600\text{-}350^\circ\text{C}$ <sup>2</sup>. Depth-Profile Laser Ablation Split-Stream Inductively Coupled Plasma Mass Spectrometry (DP-LASS-ICP-MS) analysis has the ability to measure diffusive concentration gradients of radiogenic daughter products and trace elements simultaneous at 1-2 micron resolution, something that was technologically not feasible until very recently. The variable isotope concentration within a single grain can then be extrapolated to quantify the continuous thermal history a grain has experienced through time.

With estimates of the thermal signature caused by hyperextension and mantle upwelling in hyperextended margins overlapping with the closure temperature for Pb diffusion in apatite and rutile ( $\sim 350\text{-}600^\circ\text{C}$ ) the minerals are ideal high temperature thermochronometers to measure and provide a better understanding of the lithospheric thermal evolution through hyperextension. The Alpine Tethyan magma-poor hyperextended rift margin is currently preserved in the Austroalpine and Penninic nappes of Eastern Switzerland<sup>3</sup> and has contributed to the development of tectonic models for magma-poor rift margins. By performing DP-LASS-ICP-MS techniques on apatite and rutile from the preserved Alpine Tethyan margin it is possible to construct a continuous thermal history and constrain the evolution of the lower to middle-crust of rift margins as it undergoes hyperextension.

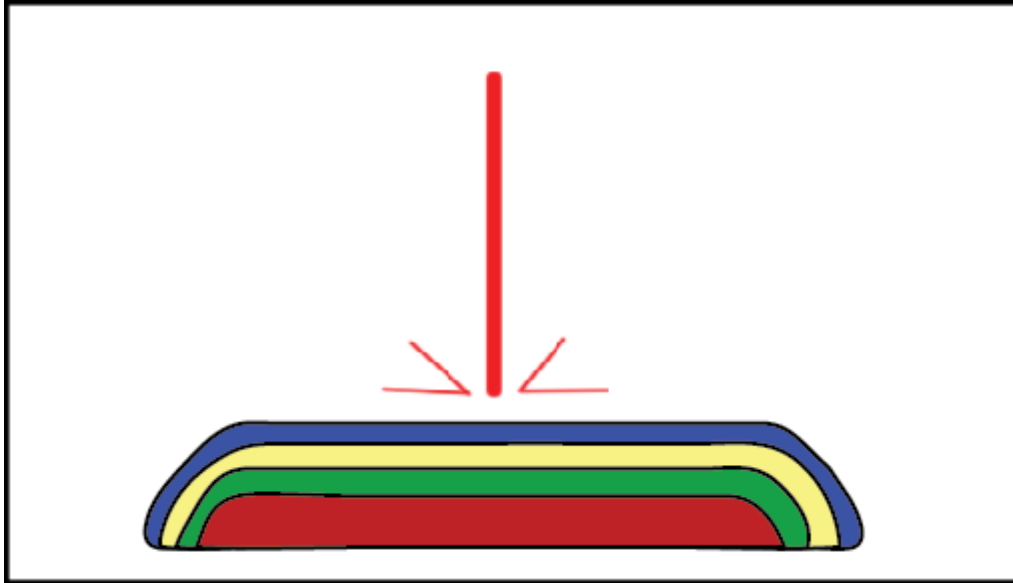


**Figure 1.** Apatite with different parent/daughter isotope concentrations at different depths within the grain. DP-LASS-ICP-MS analysis has the ability to measure diffusive isotope concentration gradients within a single grain to model a continuous thermal history.

### References

1. Cherniak, D. J., Lanford, W. A., & Ryerson, F. J. Lead diffusion in apatite and zircon using ion implantation and Rutherford backscattering techniques. *Geochimica et Cosmochimica Acta*. **55**. 1663-1673. (1991).
2. Smye, A.J., & Stockli, D.F. Rutile U-Pb age depth profiling: A continuous record of lithospheric thermal evolution. *Earth and Planetary Science Letters*. **408**. 171-182. (2014).
3. Manatschal, G., & Nievergelt, P. A continent-ocean transition recorded in the Err and Platta nappes (Eastern Switzerland). *Eclogae Geologicae Helvetiae*. **90**. 3-27. (1997).

## Annealing kinetics of $^{238}\text{U}$ ion tracks in muscovite

Sandro Guedes, Arnaldo L. Lixandrão Filho, Julio Cesar Hadler  
"Gleb Wataghin" Physics Institute, University of Campinas, Brazil  
(sguedes@ifp.unicamp.br)

Even though muscovite was one of the first minerals in which the annealing of fission tracks was recognized<sup>1</sup>, its low uranium content precluded the application of muscovite for Fission-Track Thermochronology (FTT). In the last decade, researchers realized that ion bombardment of minerals could be used to create artificial channels through which confined fission tracks could be etched<sup>2</sup>, increasing the probability finding confined fission tracks even in low uranium content mineral samples. This new development made Muscovite FTT viable. A preliminary laboratory study<sup>3</sup> showed that the closure temperature of tracks in muscovite lies between the closure temperatures of tracks in apatite and zircon. Ion bombardment has also been used to study track annealing in controlled conditions<sup>4,5</sup>, as a proxy to the understanding of annealing characteristics. We used this method to study the track annealing kinetics in muscovite.

Muscovite plates were irradiated with  $^{238}\text{U}$  ions, with a fluence of  $1.4 \times 10^5$  ions/cm<sup>2</sup>, in the Gesellschaft für Schwerionenforschung, GSI (Germany). The  $^{238}\text{U}$  ions were accelerated to 2.54 GeV. Muscovite plates were covered with aluminum foils of different thicknesses to reduce ion energies and obtain different incidence energies. Each plate was irradiated in three different angles (30, 45 and 60°) from surface. After irradiation with each angle the plates were turned of 90° to facilitate the recognition of the tracks with specific incidence angle. Incidence energies varied from 151 to 1917 MeV, calculated with SRIM<sup>6</sup>. Each plate was divided in smaller pieces for the annealing experiments. Temperatures and durations of the annealing experiments were chosen using D-optimal design<sup>7</sup> using information collected in a preliminary experiment<sup>3</sup>. Annealing experiments were carried out in tube furnaces. Temperatures were registered by thermocouples type K, placed in contact with the samples and connected to a datalogger. After heating, samples were etched with HF 40%, at 15°C, for 40 minutes. Track lengths were measured using a microscope Zeiss Axioplan with nominal magnifications of 1000x coupled with a graphic capture tablet.

Results are shown in Fig. 1. Experimental data have been fitted with the following annealing equation<sup>8</sup>:

$$L = L_0 + A \times \text{energy} - e^{\frac{T}{B+C \log t}} \quad (1)$$

A, B e C are fit parameters obtained from experimental data,  $T$  is the temperature and  $t$  is the duration of annealing.  $L$  is the track length after annealing and  $L_0$  is length of the unannealed tracks. Although it has been suggested that surface tracks (the ones in this study) are more resistant to annealing than confined tracks (the ones used in thermochronology)<sup>9</sup>, this study furnishes a first insight on the annealing of fission tracks in muscovite. We did not observe an obvious dependence of annealing in the ion incidence angle. Also, as it can be seen in Fig.1, curves for the different incidence energies follow the same trend, indicating total annealing at the same temperatures. This is compatible with a mechanism of axial shortening, like the one observed for zircon fission tracks. Apatite anneals through a different mechanism<sup>10</sup>. This study also serves to plan annealing experiments in muscovite confined fission tracks.

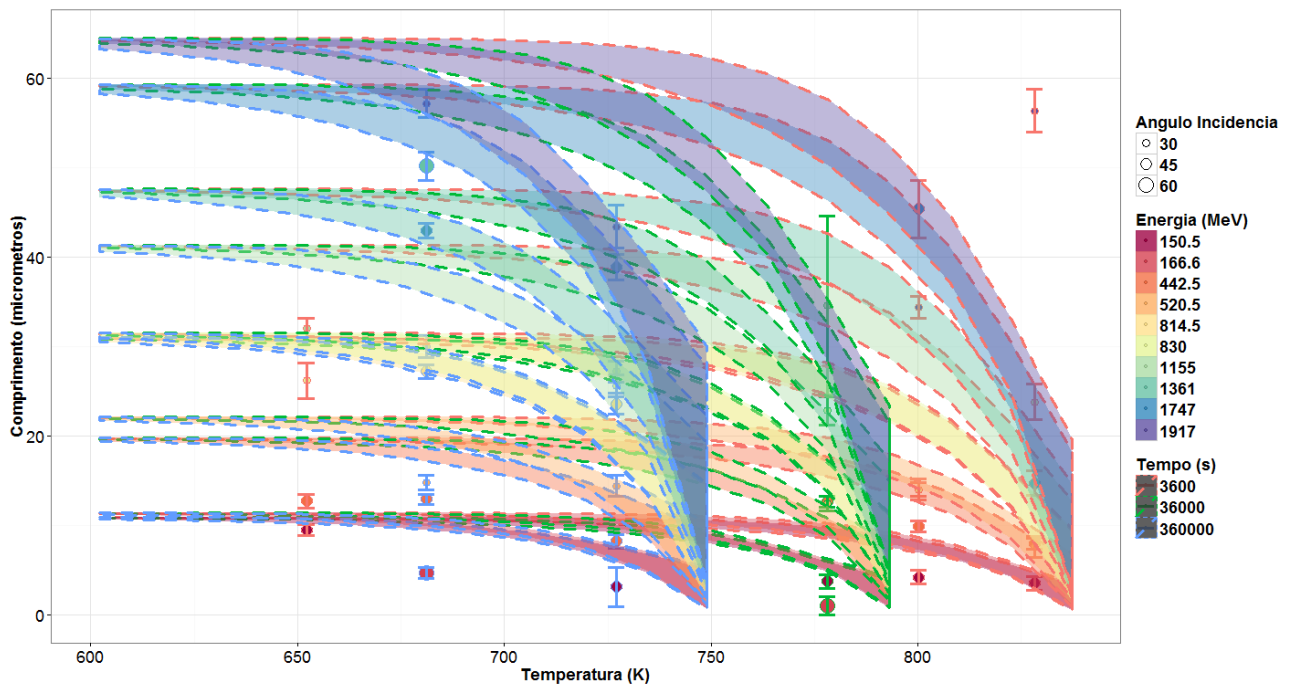


**Figure 1.** Annealing data. Experimental data are represented by circles. Annealing curves are depicted with ranges obtained from the propagation of parameter deviations.

## References

1. Bigazzi, G. Length of fission tracks and age of muscovite samples *Earth Planet. Sci. Lett.* **3**, 434-438 (1967).
2. Jonckheere, R., Enkelmann, E., Min, M., Trutmann, C. & Ratschbacher, L. Confined fission tracks in ion-irradiated and step-etched prismatic sections of Durango apatite *Chem. Geol.* **242**, 202-217 (2007).
3. Guedes, S., Maino, L.M., Jonckheere, R., Ratschbacher, L., Trautmann, C., Iunes, P.J. & Hadler, J.C. Ion-track annealing studies in muscovite *12<sup>th</sup> International Conference on Thermochronology – Book of abstracts*, p. 122 (2010).
4. Alencar, I., Guedes S., Jonckheere, R., Trautmann, C., Nakasuga, W.M., Dias, A.N.C. & Hadler, J.C. Projected length annealing of etched Sm-152 ion tracks in apatite *Nucl. Instrum. Meth. Phys. Res. B* **288**, 48-52 (2012).
5. Weise, C., van den Boogaart, K. G., Jonckheere, R. & Ratschbacher, L. Annealing kinetics of Kr-tracks in monazite: Implications for fission-track modeling *Chem. Geol.* **260**, 129-137 (2009).
6. Ziegler, J.F. SRIM-2003 *Nucl. Instrum. Meth. Phys. Res. B* **219-220**, 1027-1036 (2004).
7. Moreira, P.A.F.P., Guedes, S., Iunes, P.J. & Hadler, J.C. D-optimal design of fission-track annealing experiments *Nucl. Instrum. Meth. Phys. Res. B* **240**, 881-887 (2005).
8. Lixandrão Filho, A.L.L. Estudos de “annealing” de traços de fissão em muscovita *Master dissertation in preparation*.
9. Xe- and U-tracks in apatite and muscovite near the etching threshold *Nucl. Instrum. Meth. Phys. Res. B* **343**, 146-152 (2015).
10. Li, W., wang, L., Lang, M., Trautmann, C. & Ewing, R.C. Thermal annealing mechanisms of latent fission tracks: Apatite vs zircon *Earth Planet. Sci. Lett.* **302**, 227-235 (2011).

## Acknowledgements

Authors are grateful to Raymond Jonckheere and Christina Trautmann for all the help with sample irradiation.

# Tectono-thermal evolution of the Reed Bank Basin, Southern South China Sea

Shengbiao Hu<sup>1</sup> and Xiaoyin Tang<sup>1</sup>

1. *Institute of Geology & Geophysics, Chinese academy of Sciences*

The Reed Bank Basin in the southern margin of the South China Sea is considered to be a Cenozoic rifted basin. Tectono-thermal history is widely thought to be important to understand tectonics as well as oil and gas potential of basin. In order to investigate the Cenozoic tectono-thermal history of the Reed Bank Basin, we carried out thermal modeling on one drill well and 22 pseudo-wells using the multi-stage finite stretching model. Two stages of rifting during the time periods of 65.5–40.4 Ma and 40.4–28.4 Ma can be recognized from the tectonic subsidence rates, and there are two phases of heating corresponding to the rifting. The reconstructed average basal paleo-heat flow values at the end of the rifting events are 60 and 66.3 mW/m<sup>2</sup>, respectively. Following the heating periods, this basin has undergone a persistent thermal attenuation phase since 28.4 Ma and the basal heat flow cooled down to 57.8–63.5 mW/m<sup>2</sup> at present. In combination with the radiogenic heat production of the sedimentary sequences, the surface heat flow of the Reed Bank Basin ranges from 60.4 to 69.9 mW/m<sup>2</sup>.

## References

1. Barckhausen, U., Roeser, H.A., 2004. Seafloor spreading anomalies in the South China Sea revisited. In: Clift, P., Kuhnt, W., Wang, P., Hayes, D.E. (Eds.), *Continent–Ocean Interactions in the East Asian Marginal Seas*. American Geophysical Union, Geophys. Monograph Series, pp. 121–125.
2. Briais, A., Patriat, P., Tapponier, P., 1993. Updated interpretation of magnetic anomalies and sea floor spreading stages in the South China Sea: implications for the Tertiary tectonics of Southeast Asia. *J. Geophys. Res.* 98, 6299–6328.
3. Chen, L., 2009. Numerical Modeling Study of the Rifted Continental Margin of the South China Sea. Ph.D. Dissertation, Institute of Geology and Geophysics, Chinese Academy of Sciences, Beijing, China, 165pp (in Chinese with English abstract).

# Natural age dispersion arising from the analysis of broken crystals: Part III. The QTQt modelling approach.

David M. Webster<sup>1</sup>, Roderick W. Brown<sup>1</sup>, Kerry Gallagher<sup>2</sup>, Romain Beucher<sup>3</sup>.

<sup>1</sup> *School of Geographical and Earth Sciences, College of Science and Engineering,  
University of Glasgow, United Kingdom*

<sup>2</sup> *Géosciences Rennes, Université de Rennes 1, France*

<sup>3</sup> *Department of Earth Science, University of Bergen, Bergen, Norway*

*(d.webster.2@research.gla.ac.uk)*

**Abstract:** Over the last decade or so major progress has been made in developing both the theoretical and practical aspects of apatite (U-Th)/He thermochronology<sup>1-2</sup>. However, a persistent problem of excessive age dispersion, especially from samples from slowly cooled terranes such as cratons, has not yet been satisfactorily explained<sup>3</sup>. This often undermines the routine application of the methodology.

In seeking to address this, Brown, Beucher and co-workers<sup>4-5</sup> proposed a new modelling approach to account for the common occurrence of broken crystals in apatite separates, demonstrating that the additional ‘inherent natural age dispersion’ arising from analysing fragments can be exploited when reconstructing thermal histories. This was implemented through the new HelFRAG inversion technique, based on a finite length cylinder diffusion model. This model is computationally demanding, and so sampling based inversion methods requiring many forward model simulations become less practical. Consequently, we have looked at approximations to the finite cylinder model, one of which has been implemented into the QTQt modelling software<sup>6</sup>.

Here we aim to use the synthetic experiments of Brown, Beucher and co-workers<sup>4-5</sup> to assess the effectiveness of this approximation in the QTQt software<sup>6</sup> for modelling broken apatite grains. The five synthetic Wolf<sup>7</sup> thermal histories are successfully recovered when treating fragments explicitly as fragments of whole grains of unknown original lengths, whereas assuming the fragments are whole crystals and modelling them in the conventional manner using a spherical model yields perfectly sensible looking yet ultimately incorrect thermal histories.

The QTQt approach offers a computationally faster approximation of HelFRAG that effectively deals with broken grains and enables the fragment effect to be routinely and explicitly included in thermal history modelling.

## References

1. Farley, K. A. (U-Th)/He dating: techniques, calibrations and applications. *Rev. Min. Geochem.* **47**, 819-844 (2002)
2. Shuster, D. L. & Farley, K. A., 4He/3He thermochronometry: theory, practice and potential applications. *Rev. Min. Geochem.* **58**, 181-203 (2005)

3. Fitzgerald P. G. *et al.* Interpretation of (U–Th)/He single grain ages from slowly cooled crustal terranes: A case study from the Transantarctic Mountains of southern Victoria Land. *Chem. Geol.* **225**, 91-120 (2006)
4. Brown, W. R. *et al.* Natural age dispersion arising from the analysis of broken crystals. Part I: Theoretical basis and implications for the apatite (U-Th)/He thermochronometer. *Geochem. Cosmo. Acta.* **122**, 478-497 (2013)
5. Beucher, R. *et al.* Natural age dispersion arising from the analysis of broken crystals. Part II: Practical application to apatite (U-Th)/He thermochronometry. *Geochem. Cosmo. Acta.* **102**, 395-416 (2013)
6. Gallagher, K. Transdimensional inverse thermal history modelling for quantitative thermochronology. *J. Geophys. Res.* **117**, (2012)
7. Wolf, R., Farley, K. and Kass, D. Modelling of the temperature sensitivity of the apatite (U–Th)/He thermochronometer. *Chem. Geol.* **148 (1-2)**, 105-114 (1998)

## Using the Geochron Database for Thermochronology Data

J. Douglas Walker<sup>1</sup>, Noah M. McLean<sup>1</sup>

*1 Department of Geology, University of Kansas, Lawrence, KS, USA  
(jdwalker@ku.edu)*

We report on efforts to build a database for thermochronology and geochronology data. The data system, Geochron ([geochron.org](http://geochron.org)), is an outgrowth of the EarthChem effort and operates under the IEDA (Interdisciplinary Earth Data Alliance) project. The main aim of Geochron is to work with community experts in geochronology and thermochronology (e.g., EARTHTIME) to best capture and archive the data and metadata these groups generate. We have worked extensively on two fronts. The first is to help research groups understand or implement community-defined data reporting standards. This includes all measured data as well as supplying critical metadata for understanding published dates and the way these dates are interpreted. The second is to fit data submission operations as closely as possible into existing scientific workflows, so that data collection does not represent an additional burden on already-busy researchers.

For thermochronology in particular, modelled temperature-time paths and the tectonic or landscape evolution models they inform depend not just on measured data like isotope ratios, grain sizes, and fission track length distributions, but on assumed or calculated diffusion kinetics, isotope decay constants, and a range of statistical software packages that invert all of this information. Although the underlying measured datasets should never change, the rest of the model parameters may, resulting in new interpretations of the same measured data. It is highly important, therefore, to archive the measured data in a systematic, accessible way that will let current and future research projects access the data and integrate them into the next generation of thermochronological models. Formats should be flexible, but complete, for both data entry and retrieval. Likewise, they should correspond to user needs in both data reporting and modeling.



## Testing the Reproducibility of Thermal History Analysis

Richard A. Ketcham<sup>1</sup>, Matthias Bernet<sup>2</sup>, Peter van der Beek<sup>3</sup>

<sup>1</sup> Jackson School of Geosciences, University of Texas at Austin, Austin, TX, USA

<sup>2</sup> Institut des Sciences de la Terre, Université Grenoble Alpes, Grenoble, France

<sup>3</sup> Institut des Sciences de la Terre, Université Joseph Fourier, Grenoble, France  
ketcham@jsg.utexas.edu

Inter-laboratory exercises provide an important means of gauging the robustness of a range of geoscientific analytical methods, providing results that are sometimes uncomfortable but often necessary. This principle was recently exemplified by a study of the reproducibility of fission-track length measurements<sup>1,2</sup>, in which considerable variation among lab groups was observed, and the compensatory effects of normalizing for track angle and unannealed track length, and the importance of training, were clearly recognizable. As a follow-up to that study, a new experiment was organized in association with the Thermo2014 meeting in Chamonix, France, which was designed to investigate the reproducibility of not only the data, but the derivative product of thermal history reconstruction. Aliquots of apatite from two natural samples were distributed to 30 lab groups, with the instructions of measuring whatever thermochronometer the group had access to (typically fission-track and/or (U-Th)/He, with some adding U/Pb), and also conducting thermal history modeling using the software of choice such as HeFTy<sup>3</sup> or QTQt<sup>4</sup>. Both samples were granites that had been analyzed in previous studies. Limited contextual information was also provided: present-day surface temperature for both, and for one that the sample was unconformably overlain by 195-200 Ma strata. Each lab group was also asked to fill out a questionnaire to report on calibration, measurement, and modeling procedures. As of the writing of this abstract seven laboratory groups had responded, and several more reported their analyses were nearing completion, and should be completed in summer 2016.

Results among the data and models submitted thus far show broad agreement, but also discrepancies that would likely lead to variation in geological interpretations. Overall, HeFTy and QTQt results were generally congruent, with the primary exceptions being where the model was probably set up incorrectly. Among models with no obvious evidence of set-up error, divergent results are most probably attributable to differences in the fission-track length data, although one lab noted a distinct change in results when AHe data were included with or without single-terminated grains. Among six labs providing fission-track length data, only one reported using a length calibration. For the unconformably overlain sample, some data sets allow for two different extents of burial, either fully reset or only partially reset, whereas other analyses seem to only allow one of these two possibilities. Taken together, results thus far reinforce the importance of calibration and careful setup of thermal history inverse modeling to maximize inter-laboratory reproducibility.

### References

- 1 Hurford, A. J., Carter, A. & Ketcham, R. A. in *11th International Conference on Thermochronometry*. (ed J.I. Garver) 128.
- 2 Ketcham, R. A., Carter, A. & Hurford, A. J. Inter-laboratory comparison of fission track confined length and etch figure measurements in apatite. *Am. Mineral.* **100**, 1452-1468, doi:10.2138/am-2015-5167 (2015).
- 3 Ketcham, R. A. in *Low-Temperature Thermochronology Vol. 58 Reviews in Mineralogy and Geochemistry* (eds P.W. Reiners & T.A. Ehlers) 275-314 (Mineralogical Society of America, 2005).
- 4 Gallagher, K. Transdimensional inverse thermal history modeling for quantitative thermochronology. *J. Geophys. Res.* **117**, B02408, doi:10.1029/2011JB008825 (2012).



**THERMO2016**

**SESSION 6**

**NEW DEVELOPMENTS, TECHNIQUES,  
METHODS, WHAT'S IN THE PIPELINE**

# ***In situ* TEM observation of ion irradiation induced annealing of alpha-recoil tracks and fission tracks in apatite**

Weixing Li<sup>1,2,\*</sup>, Rodney C. Ewing<sup>2</sup>

1 CAS Center for Excellence in Tibetan Plateau Earth Sciences and Key Laboratory of Continental Collision and Plateau Uplift, Institute of Tibetan Plateau Research, Chinese Academy of Sciences, Beijing 100101, China

2 Department of Geological Sciences, Stanford University, Stanford, CA 94305, USA  
(\* wxli@itpcas.ac.cn)

Thermal events are considered as the sole source for the recovery of radiation damage, and that is the basis for extrapolating the thermal history of rocks in both fission track and (U,Th)/He thermochronology. In contrast, the recovery of the damage microstructure in nuclear materials science is believed to be caused not only by thermal source but also by internal irradiation in solids<sup>1</sup>. As most of the thermochronological techniques are limited to the micrometer scale, the important information on the damage microstructure, i.e., the nano-sized  $\alpha$ -recoil tracks (ARTs) and fission tracks (FTs) in minerals, is lost. Without the atomic scale evidence, the hypothesis of  $\alpha$ -induced annealing of the preexisted fission tracks<sup>2</sup>, in addition to thermal annealing, has not been accepted<sup>3</sup>.

In this study, we have combined transmission electron microscopy (TEM) with ion beam techniques to simulate  $\alpha$ -induced annealing of the preexisted ARTs or FTs in Durango apatite at the nano or even atomic level. The  $\alpha$ -particle annealing experiments of the preexisted ARTs were conducted via *in situ* TEM observation of consecutive ion-irradiations: i.) 1 MeV Kr<sup>2+</sup> (simulating the ARTs created by 70 keV  $\alpha$ -recoils), ii.) followed by 400 keV He<sup>+</sup> (simulating the radiation-induced annealing by 4.5 MeV  $\alpha$ -particles). The two-step irradiations were monitored by observing the gradual change in both morphology and diffraction pattern of electron-transparent slices, which were prepared by the diamond microtome method<sup>4</sup>. This method ensures uniform sample thickness (~70 nm) and irradiation in the same crystallographic orientation, that is the [0001] of apatite. Partial recrystallization of the original, fully-amorphous apatite pre-damaged by Kr<sup>2+</sup> ions was evidenced by the gradual appearance of new crystals and new diffraction maxima upon the additional irradiation of He<sup>+</sup> ions. In addition, the  $\alpha$ -recoil induced annealing experiments of FTs were simulated by the irradiation of 1 MeV Kr<sup>2+</sup> ions (simulating  $\alpha$ -recoils) on the preexisted tracks implanted by 80 MeV Xe ions (simulating fission tracks) in apatite. The microtome cutting method was used to prepare cross-sectional TEM specimens containing parallel ion tracks, allowing for the observation of radiation damage at each point along the length of a latent track and how each section of the track responds to  $\alpha$ -recoil induced annealing. Upon the irradiation of 1 MeV Kr<sup>2+</sup> ions, latent 80 MeV Xe ion tracks break up into smaller fragments and eventually disappear. The rate of  $\alpha$ -recoil induced track annealing significantly increases as the track diameter decreases along the ion trajectory, which is similar to thermally-induced track annealing<sup>4</sup>.

In summary, the atomic scale study of radiation damage is critical for better understanding the mechanisms of ART and FT annealing, and placing thermochronology on a firmer theoretical basis.

## **References**

1. Weber, W. J., Ewing, R. C. & Meldrum, A. The kinetics of alpha-decay-induced amorphization in zircon and apatite containing weapons-grade plutonium or other actinides. *Journal of Nuclear Materials* **250**, 147-155 (1997).
2. Hendriks, B. W. H. & Redfield, T. F. Apatite fission track and (U-Th)/He data from Fennoscandia: An example of underestimation of fission track annealing in apatite. *Earth and Planetary Science Letters* **236**, 443-458 (2005).
3. Green, P. F., Crowhurst, P. V., Duddy, I. R., Japsen, P. & Holford, S. P. Conflicting (U-Th)/He and fission track ages in apatite: Enhanced He retention, not anomalous annealing behaviour. *Earth Planet. Sci. Lett.* **250**, 407-427, (2006).
4. Li, W. X., Lang, M., Gleadow, A. J. W., Zdorovets, M. V. & Ewing, R. C. Thermal annealing of unetched fission tracks in apatite. *Earth and Planetary Science Letters* **321**, 121-127 (2012).

# Mapping He distribution in zircon by laser ablation noble gas mass-spectrometry: Implications for (U-Th)/He geochronology and thermochronology

Danišik, M.<sup>1</sup>, McInnes, B.I.A.<sup>1</sup>, Kirkland, C.L.<sup>1,2</sup>, McDonald, B.J.<sup>1</sup>, Evans, N.J.<sup>1</sup>, Becker, T.<sup>3</sup>

<sup>1</sup> Auscope AGOS GeoHistory Facility, John de Laeter Centre, TIGeR, Applied Geology/Applied Physics, Curtin University, Perth, Australia

<sup>2</sup> Centre for Exploration Targeting – Curtin, Department of Applied Geology, Western Australian School of Mines, Curtin University, Australia

<sup>3</sup> Nanochemistry Research Institute, Department of Chemistry, Curtin University, Perth, WA Australia

(m.danisik@curtin.edu.au)

Conventional (U-Th)/He dating of zircon is traditionally undertaken by measuring bulk He, U and Th abundances in single zircon crystals, and by applying an alpha ejection correction<sup>1</sup>. The homogeneity of U-Th in dated crystals is commonly assumed but is clearly not always valid<sup>2-4</sup>, which may result in ages that are not concordant with the ages obtained from other techniques. It has been demonstrated that age discrepancies may arise from intra-grain variations in isotopic and/or structural composition in dated zircon crystals<sup>2-7</sup>, however these are difficult to quantify given the lack of suitable analytical instrumentation.

In this paper we will present a new methodology, based on integrated *in situ* laser ablation micro-sampling and noble-gas mass-spectrometry, that allows the 2-dimensional visualization and quantification of He distribution in zircon (and possibly other minerals) at a micrometer scale. This approach provides the first opportunity to examine intra-grain distribution of He and allows us to investigate and visualize the impact of the several underlying reasons for problematic zircon (U-Th)/He ages. Using this methodology, we constructed high-resolution He “maps” for a set of zircon crystals in order to investigate the impact of U-Th zoning, radiation damage and inclusions on He distribution. The He maps, in combination with characterization information from other imaging techniques (i.e., cathodoluminescence, confocal Raman microscopy and LA-ICPMS elemental maps) allow us to visualize the impact of these commonly ignored grain features to the fundamental principles and assumptions of (U-Th)/He geochronology. Based on the outcomes of this work, we suggest refinements to analytical protocols currently used for conventional as well as *in situ* (U-Th)/He dating, <sup>4</sup>He/<sup>3</sup>He thermochronometry and diffusion experiments. Finally, we will illustrate how He mapping may potentially provide a new means for thermal history reconstructions by allowing direct measurement of He diffusional profiles.

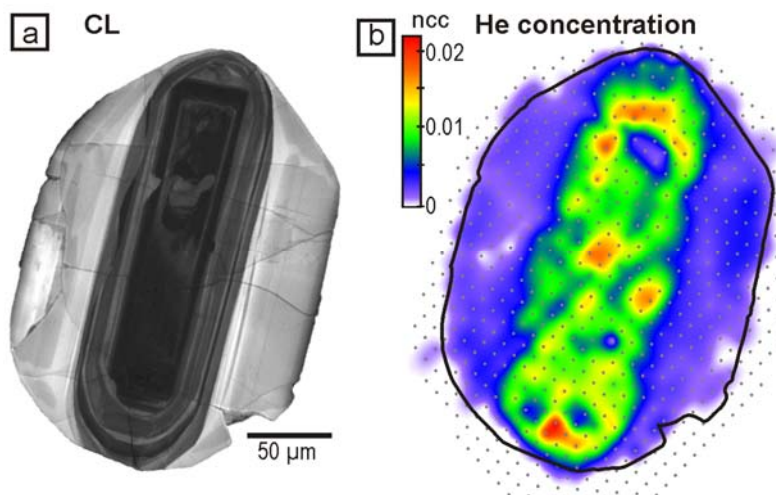


**Figure 1.** CL image (a) and He concentration map (b) of a zircon with U-rich core and U-depleted rims generated by SEM and RESOchron<sup>TM</sup> instruments, respectively. Note that He distribution correlates well with CL intensity and therefore with U distribution. Understanding the intra-grain distribution of He, U and Th is essential for correct interpretation of (U-Th)/He results.

## References

1. Farley, K. A., Wolf, R. A. & Silver, L. T. The effects of long alpha-stopping distances on (U–Th)/He ages. *Geochim. Cosmochim. Acta* 60, 4223–4229 (1996).
2. Meesters, A. G. C. A. & Dunai, T. J. Solving the production–diffusion equation for finite diffusion domains of various shapes part 2, Application to cases with Alpha ejection and non-homogeneous distribution of the source. *Chem. Geol.* 186, 345–363 (2002b).
3. Dobson, K. H., Stuart, F. M., Dempster, T. J. & EIMF. U and Th zonation in Fish Canyon Tuff zircons: implications for a zircon (U–Th)/He standard. *Geochim. Cosmochim. Acta* 72, 4545–4755 (2008).
4. Hourigan, J. K., Reiners, P. W. & Brandon, M. T. U-Th zonation-dependent alpha-ejection in (U–Th)/He chronometry. *Geochim. Cosmochim. Acta* 69, 3349–3365 (2005).
5. Hurley, P. M. Alpha ionization damage as a cause of low He ratios. *EOS Trans. Am. Geophys. Union* 33, 174-183 (1952).
6. Shuster, D. L., Flowers, R. M. & Farley, K. A. The influence of natural radiation damage on helium diffusion kinetics in apatite. *Earth Planet. Sci. Lett.* 249, 148–161 (2006).
7. Stockli, D. F., Farley, K. A. & Dumitru, T. Calibration of the (U-Th)/He thermochronometer on an exhumed fault block, White Mountains, California. *Geology* 28, 983–986 (2000).

# Optimizing Workflow: Automated Data Collection of Apatite Images

Ravi Kumar<sup>1</sup>, Ray Donelick<sup>2</sup>  
8304 Triplecrown Road Bowie, MD, 20715, USA  
1075 Matson Road, Viola, Idaho, 83872-9709, USA  
rkumar@g.hmc.edu, donelick@apatite.com

The goal of this project was to create a simple, user-friendly application that could automate microscopy image collection tasks. It achieves this goal by moving in a grid pattern across a specified area of a slide, taking images of each location at any desired magnification. Once acquired, this set of images is then combined to form a single larger image of the entire area, which is accessible to the user through an image viewer program. This enables easy visual access to the entire data set, as the user can zoom out to find regions of interest and zoom in on them to look at the details.

This data collection software was designed largely to support thermochronology research. It supports taking images at multiple Z-levels per scan, enabling identification of fission tracks at different focal depths. It also supports reimaging an area at a higher magnification, so that users can identify features of interest (such as apatite grains or fission tracks) at a low magnification and later measure them precisely at a higher magnification. In addition, the software supports almost all commonly used stage and camera interfaces, and does not require any special hardware to function.

The data collected by this software enables many more interesting automation problems to be approached. Having a large body of image data is useful for developing image processing algorithms to identify features such as apatite crystals, or select promising crystals for geological analysis. Such image data would also enable more advanced computer science techniques to be used, such as training machine learning systems to identify fission tracks or other structures of interest. Prototypes for these tasks have already been created and produced promising results<sup>1,2</sup>.

## References

1. Donelick, A. & Donelick, R. Machine learning applied to finding and characterizing the tips of etched fission tracks. *Goldschmidt Abstracts* 759 (2015)
2. Kumar, R. Machine learning applied to autonomous identification of fission tracks in apatite. *Goldschmidt Abstracts* 1712 (2015)

# Extending the range of U-Pb apatite thermochronology using SIMS analysis

Peter Zeitler<sup>1</sup>, Kalin McDannell<sup>1</sup>, Mark Harrison<sup>2</sup>, Blair Schoene<sup>3</sup>

<sup>1</sup> Earth and Environmental Sciences, Lehigh University, Bethlehem, PA, USA

<sup>2</sup> Earth, Planetary, and Space Sciences, UCLA, Los Angeles, CA, USA

<sup>3</sup> Geosciences, Princeton University, Princeton, NJ, USA

(peter.zeitler@lehigh.edu)

A fundamental principle of thermochronology is that diffusion profiles in minerals provide a wealth of time-temperature information. This information has mostly been exploited in lower-temperature noble-gas systems through step-heating analysis of helium in apatite and argon in K-feldspars, and less commonly in higher-temperature systems like monazite, through depth profiling of lead concentrations (e.g. Harrison et al., 2005). Here we assess the potential of using SIMS analysis to reveal the fine details of lead diffusion profiles at apatite grain margins. Such profiles could provide continuous thermal-history information across an intermediate temperature range that would be important in connecting higher- and lower-temperature thermochronological data.

Conventional U-Pb analysis of apatites (e.g. Schoene and Bowring, 2007) demonstrates that the system has an intermediate to higher closure temperature and that apatite shows the expected grain-size dependence that emerges from the presence of closure profiles (Figure 1, left). However, in apatite as in all minerals, the zero-concentration boundary condition at grain margins is clearly independent of grain size and the diffusion geometry approaches that of a half-space. As a result, in their outer few microns, apatite grains of a great range of sizes will share nearly identical closure profiles (Figure 1, right).

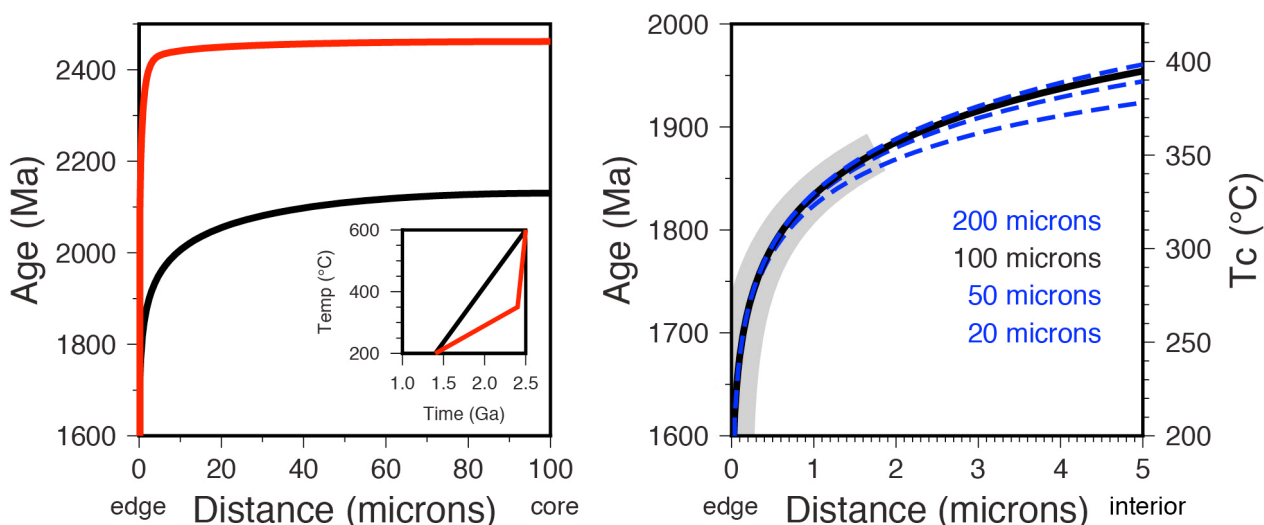


**Figure 1.** Modeled U-Pb age profiles across a 100  $\mu\text{m}$  apatite grain cooled slowly with thermal histories show in inset, using kinetic data from Cherniak et al. (1991). **Left:** Predicted age profiles for two thermal histories sharing starting and ending points, showing how apatite depth profiling can clearly distinguish the two histories. **Right:** Age profiles near grain edge as a function of grain size for linear slow cooling at 0.36°C/m.y. (thermal shown in black in inset). Note how for very different grain sizes, diffusion geometry near the grain boundary causes convergence to similar low closure temperatures in the outer few microns. The gray band shows overlap with the typical temperature sensitivity for the <sup>40</sup>Ar/<sup>39</sup>Ar K-feldspar system.

This observation has several important practical implications for apatite U-Pb thermochronology. First, apatite grains of virtually any size can be used to obtain consistent thermal-history information. Second, the large gradients near grain margins will address much lower closure

temperatures than bulk values obtained from even very small grains – using the Cherniak et al. (1991) kinetic data, modeling shows that it might be possible to record thermal histories extending to below 250 °C (Figure 1, right). Finally, analysis of a several-micron grain-margin profile could reveal some 150°C of continuous thermal history that overlaps information obtainable from helium diffusion in zircon and argon diffusion in K-feldspar.

The key to realizing the potential of this approach is the use of SIMS analysis to carefully sample the delicate grain-margin diffusion profile through progressive drilling across this region. For apatite, one limitation will be the presence of sufficient quantities of radiogenic  $^{206}\text{Pb}$ , and currently this means that the approach will be limited to older samples. We report on a set of trial samples from the Superior Province in Canada that experienced very slow cooling across the Proterozoic. Preliminary analyses reveal grain-margin gradients in  $^{206}\text{Pb}^*/^{238}\text{U}$  that vary by over a factor of two, consistent with the very slow cooling experienced by the samples.

## References

1. Harrison, T. M., Grove, M., Lovera, O. M., & Zeitler, P. K., 2005. Continuous thermal histories from inversion of closure profiles, in *Low-temperature Thermochronology: Techniques, Interpretations, and Applications* (eds. Reiners, P. W. & Ehlers, T. A.) 123-149 (Mineralogical Society of America/Geochemical Society Reviews in Mineralogy and Geochemistry, Chantilly, Virginia, 2005).
2. Schoene, B., & Bowring, S. A. Determining accurate temperature-time paths in U-Pb thermochronology: an example from the SE Kaapvaal craton, southern Africa, *Geochim. Cosmochim. Acta*, **71**, 165-185 (2007).
3. Cherniak, D., W. Lanford, W., & Ryerson, F. Lead diffusion in apatite and zircon using ion implantation and Rutherford backscattering techniques. *Geochimica et Cosmochimica Acta*, **55(6)**, 1663-1673 (1991).



## The potential of sintered Mud Tank apatite as a matrix-matched uranium reference material for AFT LA-ICP-MS dating

Ling Chung<sup>1</sup>, Andrew Gleadow<sup>1</sup>, Hugh O'Neill<sup>2</sup>, Barry, P. Kohn<sup>1</sup>, and Alan Greig<sup>1</sup>

1. School of Earth Sciences, University of Melbourne

2. Research School of Earth Sciences, Australian National University  
(lchung1@unimelb.edu.au)

Using laser ablation (LA)-ICP-MS to determine  $^{238}\text{U}$  concentrations directly for apatite fission-track (AFT) dating eliminates the handling of radioactive material, allows more rapid data acquisition and simultaneous dating of the same grains. As for other LA applications, a well-characterised matrix-matched standard with a homogeneous composition is desirable for monitoring elemental fractionation and for accurate calibration<sup>1</sup>. However, such standards are still not available for apatite LA-ICP-MS dating<sup>1,2</sup>. Here we report preliminary composition and homogeneity results on sintered<sup>3,4</sup> polycrystalline samples of Mud Tank (MT) apatite to evaluate the potential of using such material as a matrix-matched U reference for AFT LA-ICP-MS dating.

We used the ca. 730 Ma apatite from the Mud Tank Carbonatite complex in the Harts Range, central Australia. Within this complex, individual apatite crystals of > 2 cm and massive aggregates up to 60 cm across are common<sup>5,6</sup>. Some compositional heterogeneity is expected in these natural crystals, although analyses show these to be generally < 10%<sup>2</sup>. To further optimise the homogeneity, apatite was pulverised in a hand mortar and pestle to reduce the grain size to < 20  $\mu\text{m}$ . The fine powder was then sintered under different time-temperature-pressure conditions in a graphite capsule in a high pressure piston cylinder rig at the Australian National University (MT7: at 700°C for 30 minutes at 15 kb, and MT9: at 900°C for 4 hours at 15 kb). This produced a dense compact material with minimal remaining porosity, suitable for laser-ablation studies.

X-ray diffraction analysis of the sintered material showed that only apatite was present demonstrating that no mineral breakdown had occurred. Observations from scanning electron microscope (SEM) images suggested MT9 (Fig. 1A) has a relatively higher degree of recrystallisation and coarser grain size in the fine matrix, whereas in MT7 angular fragments of the crushed material in a fine sintered matrix were still visible. Analysis of both non-sintered powder and the sintered material by solution nebulisation (SN)-ICP-MS showed essentially identical compositions. We also examined the compositional stability in response to different laser beam size (Fig. 1B). Observations from this test (> 60 analysis per size) suggest that the U content was highly uniform but the RSD significantly decreased when using laser beam size > 30  $\mu\text{m}$  due to higher U count rates and the inclusion of more grains in each analysis.

We used the SRM NIST612 glass to calibrate U in LA experiments, and MT9 as a secondary reference material during our routine SN and LA experiments. Over the past three years, MT9 has yielded an average U of  $3.04 \pm 0.012$  ppm (RSD = 0.39%) from ~100 SN analyses and  $3.03 \pm 0.12$  ppm (RSD = 4.0%) from > 250 spot-analyses over an area of  $0.5 \times 0.4$  cm<sup>2</sup> (polished twice for repeated use) (Fig. 1C). This result indicates that this polycrystalline sintered apatite material has a homogeneous U content and consistent ablation characteristics. The sintering approach may also provide a solution towards preparing various ranges of U content matrix-matched standards for other LA applications (eg. by sintering mixtures of different apatites/minerals).

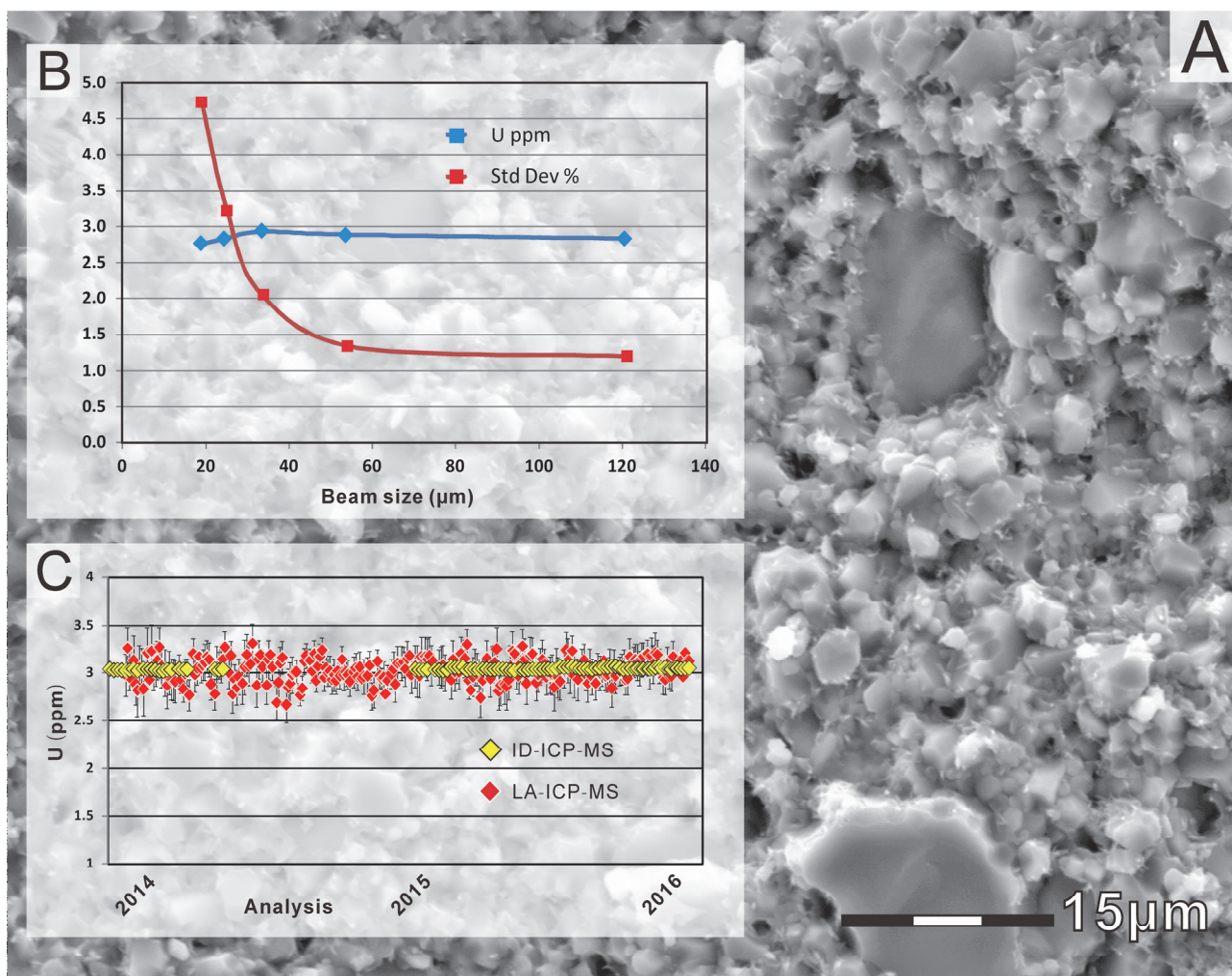


**Figure 1** (A) SEM image of MT9 showing recrystallised apatite almost zero matrix porosity. (B) U concentration and standard deviation from a New Wave UP213 laser analysis for 19, 25, 33, 55 and 121 µm beam-size test over 60 ablations for each size. (C) U concentrations from ~100 SN analyses and ~ 250 LA analyses of MT9 over the past 3 years.

## References

- 1 Chew, D. M., Sylvester, P. J. & Tubrett, M. N. U–Pb and Th–Pb dating of apatite by LA-ICPMS. *Chemical Geology* **280**, 200-216 (2011).
- 2 Soares, C. J., Mertz-Kraus, R., Guedes, S., Stockli, D. F. & Zack, T. Characterisation of Apatites as Potential Uranium Reference Materials for Fission-track Dating by LA-ICP-MS. *Geostandards and Geoanalytical Research* **39**, 305-313 (2015).
- 3 Boyce, J. W. *The development and application of microanalytical (U-Th)/He Thermochronology* PhD thesis, Massachusetts Institute of Technology, (2006).
- 4 Garbe-Schonberg, D. & Muller, S. Nano-particulate pressed powder tablets for LA-ICP-MS. *Journal of Analytical Atomic Spectrometry* **29**, 990-1000 (2014).
- 5 Black, L. P. & Gulson, B. L. The age of the Mud Tank Carbonatite, Strangways Range, Northern Territory. *BMR Journal of Australian Geology and Geophysics* **3**, 227-232 (1978).
- 6 Currie, K. L., Knutson, J. & Temby, P. A. The Mud Tank carbonatite complex, central Australia —an example of metasomatism at mid-crustal levels. *Contributions to Mineralogy and Petrology* **109**, 326-339 (1992).

# Temperature controlled laser step-heating of monazite via optical pyrometry – towards routine application of monazite (U-Th)/He thermochronometry

Nathan Niemi  
University of Michigan, USA  
(naniemi@umich.edu)

Monazite is a common accessory mineral in both igneous and metamorphic rocks, with recognized potential as a target for (U-Th-Sm)/He thermochronology<sup>1,2</sup>. Despite this potential, routine application of monazite thermochronology has not been established. A significant challenge to developing routine methods for thermochronologic applications for this mineral is the diverse range of He diffusion behavior in monazite<sup>3-5</sup>. The variability of He diffusion behavior in natural monazite is thought to arise principally from grain-to-grain differences in rare earth element compositions and concentrations<sup>1,3,5</sup>, with intra-sample variations in He diffusion characteristics large enough that step-heating experiments on individual monazite grains are presumed necessary for thermochronologic applications<sup>1,3</sup>. Here we assess the viability of using optical pyrometry as a method to perform temperature-controlled laser step-heating experiments on monazite grains encapsulated in Pt microfurnaces as a routine method to derive He diffusion parameters and closure temperatures of individual monazite grains.

We undertook a preliminary experiment on Monazite Standard 554 from the Catnip Sill in Arizona, well characterized for other geochemical and geochronological purposes, and performed heating experiments on 10 individual grains to determine their closure temperatures. The experiments were undertaken using an Alphachron Helium Instrument. Monazite grains were heated in Pt microfurnaces with a CO<sub>2</sub> laser, and laser power was modulated to maintain constant temperature via feedback from an Impac 4-color optical pyrometer that monitored emittance from the Pt tube (Fig. 1D). Arrhenius relationships were derived for each individual grain analyzed (Fig. 1A), with generally reproducible results (Fig. 1B). Our preliminary data agree with previous studies in suggesting that monazite grains from the Catnip Sill may have closure temperatures that span ~100°C<sup>1</sup> (Fig. 1C), well beyond the 20-40°C range of most thermochronometers. Furthermore, several of the monazite grains have closure temperatures that extend above 200°C, potentially providing insight into higher temperature processes than are currently sampled by other helium thermochronometers.

Our results suggest that a robust thermochronologic method may be developed around the monazite (U-Th-Sm)/He system that may offer advantages over existing thermochronometric systems. Optical pyrometry laser step heating may be one approach to overcoming the challenges of determining monazite He diffusion behavior needed for routine application of this method. Accurate measurement of Th at wt. % concentrations in many monazite grains presently appears to be the next challenge to solve.

## References

1. Peterman, E. et al. Experimental and geologic evaluation of monazite (U-Th)/He thermochronometry: Catnip Sill, Catalina Core Complex, Tucson, AZ. *Earth Planet. Sci Lett.* **403**, 48-55 (2014).
2. Farley, K. A. & Stockli, D. in Phosphates (eds. Kohn, M. L., Rakovan, J., & Hughes, J. M.) 559-578 (Mineralogical Society of America/Geochemical Society Reviews in Mineralogy and Geochemistry, Chantilly, Virginia, 2005).
3. Boyce, J. W., et al. He diffusion in monazite: Implications for (U-Th)/He thermochronometry. *G-Cubed*. **6**, Q12004 (2005).
4. Farley, K. He diffusion systematics in minerals: Evidence from synthetic monazite and zircon structure phosphates. *Geochem. Cosmochim. Acta.* **71**, 4015-4024 (2007).
5. Cherniak, D. J. & Watson, E. B. Diffusion of helium in natural monazite and preliminary results on He diffusion in synthetic light rare earth phosphates. *Am. Mineral.* **98**, 1407-1420 (2013).

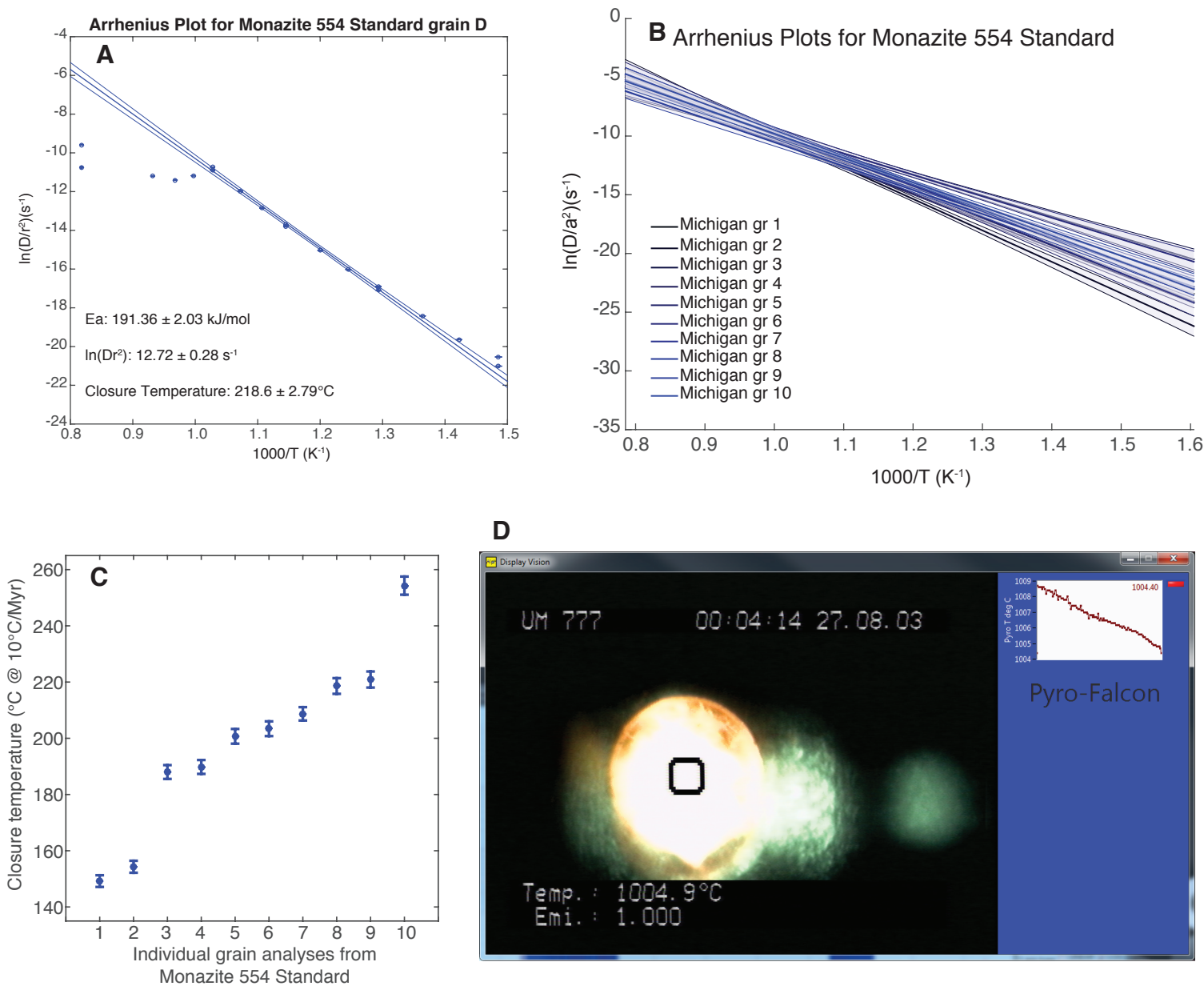


**Figure 1.** Results from laser step heating experiments of monazite in an Alphachron Helium Instrument, with temperature controlled by optical pyrometry. (A) Arrhenius plot for a single monazite grain (grain D) from the Monazite 554 Standard, collected from the Catnip Sill in Arizona. The Arrhenius relationship is fit for individual analyses conducted at temperatures lower than  $700^\circ C$ . A best fit linear regression was performed using the York method. Sample heating steps were  $400^\circ C$ ,  $430^\circ C$ ,  $460^\circ C$ ,  $500^\circ C$ ,  $530^\circ C$ , etc. with each step held for 20 min. Each step at an even 100 degree increment was repeated for an additional 40 min. After the  $800^\circ C$  step was completed, the sample was heated to  $950^\circ C$  for 60 min and then 30 min to assure complete outgassing of He. (B) Best fit Arrhenius relationships for all Monazite 554 Standard grains analyzed at Michigan. (C) Closure temperatures calculated for all Monazite 554 Standard grains analyzed at Michigan, assuming a cooling rate of  $10^\circ C/Myr$ . The closure temperatures span over  $100^\circ C$ , although most cluster around  $190$ - $220^\circ C$ . (D) Screen capture of sample in Pt microfurnace undergoing laser heating in the sample chamber of the Alphachron Helium Instrument. The sample temperature, based on 4-color optical pyrometry, is shown below the sample image. A short temperature history of the sample is shown at the upper right. Laser output power is adjusted to maintain a constant temperature based on feedback from the optical pyrometer.

## Laser ablation U-Th-Sm/He dating of apatite

William Matthews<sup>1</sup>, Julia Pickering<sup>1</sup>, Brett Hamilton<sup>1</sup>, Bernard Guest<sup>1</sup>, Chris Sykes<sup>1</sup>

*1 University of Calgary, 2500 University Drive, NW, Calgary, AB, T2N 1N4, Canada  
(wamatthe@ucalgary.ca)*

Laser ablation U-Th-Sm/He dating is an emerging technique in thermochronology that has been proven as a means to date monazite, zircon and titanite (Boyce et.al., 2006; Tripathy-Lang, et.al., 2013; Evans et.al., 2015; Horne et.al., 2016). Laser ablation U-Th-Sm/He thermochronology eliminates many of the problems and inconveniences associated with conventional, whole grain methods, including; reducing grain selection bias based on size, shape, clarity, broken grains and grains with inclusions; avoiding bad neighbour effects; eliminating dissolution safety hazards; and improving analytical efficiency. Laser ablation apatite U-Th/He thermochronology is challenging due to apatite's typically low concentrations of U and Th and therefore <sup>4</sup>He. We present a new analytical procedure for U-Th/He dating of apatite that relies on low-blank composite sample mounts, a two-step ablation protocol, and an automated ablation pit measurement routine. This procedure provides accurate, and reproducible apatite U-Th/He dates while simultaneously improving analytical efficiency and preserving the grains for further analyses.

Our mounting process uses a heated platen press, to press samples into fluorinated ethylene propylene Teflon™ bonded to an aluminum backing plate. Samples are ablated using a Resonetics 193 nm excimer laser and the liberated He is measured using a quadrupole mass spectrometer on an Australian Scientific Instruments Alphachron quadrupole helium mass spectrometer; collectively this system is known as a Resochron™. The ablated sites are imaged using a Zygo Zscope™ optical profilometer and ablated pit volumes measured using PitVol, a custom MatLab™ algorithm.

We use a well-characterized Durango apatite reference material along with a Fish Canyon Tuff (FCT) apatite secondary reference material to demonstrate the accuracy and precision of this method. <sup>4</sup>He liberated by laser ablation in a Lauren Technic™ ultra high vacuum static cell was measured for 115 grains using the Resochron. After measuring pit volumes, U, Th and Sm concentrations were obtained by over-ablating the helium pits in a Lauren Technic™ M50 Helium flow-through cell. U-Th-Sm/He dates were calculated using the standard age equation. The weighted average of our laser ablation Durango dates (30.5±0.35 Ma) compares well with conventional whole grain degassing and dissolution U-Th/He methods (32.56±0.43 Ma) for chips derived from the same Durango crystal (Jonckheere et.al., 1993; Farley, 2000; McDowell et.al., 2005). These Durango primary standard dates were used to produce a  $\kappa$ -value to correct the secondary references and unknown samples. After correction, FCT apatite has a weighted average of 28.37 ± 0.96 Ma, which agrees well with published ages. Further dating of other well characterized apatite crystals will be used to test the robustness of the method.

### References

1. Boyce, J. W., Hodges, K. V., Olszewski, W. J., Jercinovic, M. J., Carpenter, B. D., & Reiners, P. W. (2006) Laser microprobe (U–Th)/He geochronology. *Geochimica et cosmochimica acta*, 70(12), 3031–3039
2. Evans, N. J., McInnes, B. I. A., McDonald, B., Danišik, M., Becker, T., Vermeesch, P., & Patterson, D. B. (2015) An in situ technique for (U–Th–Sm)/He and U–Pb double dating. *Journal of Analytical Atomic Spectrometry*, 30(7), 1636–1645.
3. Farley, K. A. (2000) Helium diffusion from apatite: General behavior as illustrated by Durango fluorapatite. *Journal of Geophysical Research: Solid Earth*, 105(B2), 2903–2914.
4. Horne, A. M., van Soest, M. C., Hodges, K. V., Tripathy-Lang, A., & Hourigan, J. K. (2016) Integrated single crystal laser ablation U/Pb and (U–Th)/He dating of detrital accessory minerals—Proof-of-concept studies of titanites and zircons from the Fish Canyon tuff. *Geochimica et Cosmochimica Acta*, 178, 106–123.
5. Jonckheere, R., Mars, M., Rebetez, M., & Chambaudet, A. (1993) L'apatite de Durango (Mexique): Analyse d'un minéral standard pour la datation par traces de fission. *Chemical geology*, 103(1), 141–154.

6. McDowell, F. W., McIntosh, W. C., & Farley, K. A. (2005) A precise  $^{40}\text{Ar}$ – $^{39}\text{Ar}$  reference age for the Durango apatite (U–Th)/He and fission-track dating standard. *Chemical Geology*, 214(3), 249-263.
7. Tripathy-Lang, A., Hodges, K. V., Monteleone, B. D., & Soest, M. C. (2013) Laser (U-Th)/He thermochronology of detrital zircons as a tool for studying surface processes in modern catchments. *Journal of Geophysical Research: Earth Surface*, 118(3), 1333-1341.

## Thermal history recovery from high-resolution laser-ablation ICP-MS U-Pb and trace element depth profiling

Lisa D. Stockli<sup>1</sup>, Daniel F. Stockli<sup>1</sup>, Andrew Smye<sup>1,2</sup>, Nikki Seymour<sup>1,3</sup>, Patrick Boyd<sup>1</sup>

*1 Dept. of Geological Sciences, University of Texas at Austin, USA*

*2 Dept. of Geosciences, Penn State, USA*

*3 College of Natural Sciences, Colorado State University, USA*

*(lstockli@jsg.utexas.edu)*

The concentration profiles of the daughter isotope - the radial spatial distribution of a diffusant - within a mineral is extremely sensitive to the rock's thermal history and has been used for both <sup>40</sup>Ar/<sup>39</sup>Ar thermochronometry and trace element speedometry. In contrast to bulk thermochronometry, requiring analysis of multiple thermochronometric systems from different samples or single thermochronometry sample arrays (e.g., elevation transects or boreholes), quantitative recovery of concentration profiles of the radiogenic daughter from a single grain has the potential to reconstruct a continuous, high-resolution thermal history through the specific thermochronometers thermal sensitivity window. While this methodology has been applied successfully for both <sup>40</sup>Ar/<sup>39</sup>Ar and <sup>4</sup>He/<sup>3</sup>He thermochronometry through fractional loss, step-heating experiments to recover concentration profiles and invert for thermal history<sup>1,2</sup>, laser ablation techniques have the ability to measure and recover concentration profiles directly and without step-heat degassing of samples. Laser ablation depth profiling has the advantage that (1) sample are not subjected to heating and potential prograde annealing or mineralogical modifications and (2) concentration profile recovery and continuous thermal history recovery is not limited to noble gas daughter products, opening the door for detailed U-Pb thermochronometry.

Apatite and rutile U-Pb laser ablation depth-profile thermochronometry allows for recovery of moderate temperature thermal history information from the middle and lower crust – a critical part of the crust that has often been inaccessible to thermal history reconstructions. Furthermore, the development and application of rutile and apatite laser-ablation depth-profile thermochronometry can be combined with laser ablation depth-profile information of minor and trace element diffusion profiles (e.g., Sr in apatite or Hf in rutile) to reconstruct detailed and semi-continuous, high-resolution thermal histories. This study presents laser-ablation depth-profile ICP-MS methodology from exhumed middle and lower crustal rocks in the Alps and Pyrenees recovering high spatial resolution (<1/2 μm depth) U-Pb age and Pb and trace element concentration profile data to reconstruct thermal histories. Rutile and apatite grains were mounted on double-sided tape on epoxy discs parallel to the c-axis. Unpolished grains were ablated using an Excimer laser (192 nm) and the aerosol simultaneously analyzed for U-Pb and trace element concentrations by split-streaming on two magnetic sector ICP-MS instruments. A large-volume Helex cell achieves <1s washout times correlating to 0.5 μm vertical resolution, critical for high-resolution depth profiles<sup>3</sup>. Ablation rates and pit depths were measured and calibrated using a 3D laser interferometric microscope. For rutile, 65-μm diameter spots were ablated for 30 sec to a depth of ~35 μm and signals calibrated against primary U-Pb age standard R10 and trace elements against USGS basalt glasses. Terra-Wasserburg concordia data for whole-grain data are used to constrain the radiogenic Pb composition. For apatite, 40-μm diameter spots were ablated for 30 sec to pit depth of ~30 μm and calibrated against primary U-Pb standard UWA-1 and synthetic glass trace element standard NIST 612. Single-grain ablation volumes were divided into 2 s (1.5-2 μm) increments and corrected for common Pb using the model-Pb composition. Ages were plotted by increasing distance from the grain rim in order to ascertain the topology of the <sup>238</sup>U/<sup>206</sup>Pb age profile and fitted with a power-law curve and 95% confidence bands. Rutile and apatite depth-interval U-Pb profiles were inverted using MATLAB®, which predicts the radial concentration profile of radiogenic <sup>206</sup>Pb based on a specified thermal history<sup>3</sup>. 10,000 randomly-generated monotonic cooling *T-t* paths were forward modeled and produced synthetic age depth profiles. 95% confidence bands were used to determine the goodness of fit and identify the best-fit t-T path. Modeled jointly, such rutile and apatite U-Pb depth-profile

thermochronometry provides continuous thermal history from ~620 to 450°C.

## References

1. Shuster, D. L., and Farley, K. A., (2005),  $^4\text{He}/^3\text{He}$  Thermochronometry: Theory, Practice, and Potential Complications: *Reviews in Mineralogy and Geochemistry*, v. 58, no. 1, p. 181-203.
2. McDougall, I. and Harrison, T.M. (1999). *Geochronology and thermochronology by the  $^{40}\text{Ar}/^{39}\text{Ar}$  method*. Oxford Press.
3. Smye, AJ and Stockli, DF (2014) , Rutile U-Pb age depth profiling: A continuous record of lithospheric thermal evolution. *Earth and Planetary Science Letters* **408**: 171-182.



# An improved determination of atmospheric $^{21}\text{Ne}/^{20}\text{Ne}$

John Saxton, Steven Edwards, David Rousell  
Nu Instruments Ltd, Wrexham, LL13 9XS, UK  
(john.saxton@nu-ins.com)

The rare isotope  $^{21}\text{Ne}$  is used in geochronology but it has recently been claimed<sup>1</sup> that previous determinations of atmospheric  $^{21}\text{Ne}/^{20}\text{Ne}$  were significantly in error due to unrecognised  $^{20}\text{NeH}$  interference at mass 21. We have continued our efforts to accurately measure  $^{21}\text{Ne}/^{20}\text{Ne}$  in a sample of commercial Ne (but of atmospheric origin) using the *Noblesse* mass spectrometer. Experiment design differs from usual Ne isotope measurements, in that assumption of mass dependent fractionation is critical; for this reason measurements were made by peak jumping on a single electron multiplier, with all peaks measured at the same relative position at the high mass side of the peak top.  $^{40}\text{Ar}^{2+}$ ,  $^{63}\text{Cu}^{3+}$  and  $^{66}\text{Zn}^{3+}$  are then edge resolved; corrections are necessary for  $\text{CO}_2^{2+}$ ,  $\text{H}_2^{18}\text{O}$  and HF, but these make negligible contribution to the overall uncertainty budget. Individual measurements of  $^{21}\text{Ne}/^{20}\text{Ne}$  were corrected to  $^{22}\text{Ne}/^{20}\text{Ne}=0.102$  assuming mass dependent fractionation<sup>2</sup>.

Measurements have now been made on three different Noblesse instruments, all with MRP >5000. In principle this allows edge resolution of  $^{20}\text{NeH}$  from  $^{21}\text{Ne}$  ( $m/\Delta m=3271$ ), but in view of the requirement that all peaks be measured at the same relative position, most measurements have been of the combined [ $^{21}\text{Ne}+^{20}\text{NeH}$ ] signal at the high mass side of the peak. This requires a small correction for  $^{20}\text{NeH}$  (described below). A few initial measurements were made with  $^{21}\text{Ne}$  edge resolved from  $^{20}\text{NeH}$  near the low mass shoulder; although reproducible, this method was rapidly found to be less satisfactory (for the present experiment) owing to the complication of considering any deviations from peak flat over the full width of the mass 21 peak. Some measurements were also made on a Nu Instruments Evolution, which is a high resolution gas source instrument.

Initial results<sup>3</sup> showed that uncertainty was dominated by non-statistical effects, in particular the NeH correction itself and electron multiplier effects (e.g. deadtime). In that study (Noblesse #1 and #2) a very simple method of estimating  $^{20}\text{NeH}/^{21}\text{Ne}$  was used, which suggested  $^{20}\text{NeH}/^{21}\text{Ne} = 0.001$  to 0.002, albeit with an assigned uncertainty of  $\pm 100\%$ . An improved method of determining  $^{20}\text{NeH}/^{21}\text{Ne}$  has now been developed. The shapes of the high mass sides of the mass 20 and 22 peaks were found to be in excellent agreement with each other, and can be subtracted from mass 21 to clearly reveal the  $^{20}\text{NeH}$  contribution. On Noblesse #3,  $^{20}\text{NeH}/^{21}\text{Ne}$  was then found to be  $0.0022 \pm 0.0005$ , which is an order of magnitude lower than found by [1]. Results so far are good agreement with the values reported by [4] and [5].

In the course of this work we also made some experiments with a source getter of lower volume, but also giving lower conductance between source and getter. The smaller getter was found to give 5 times higher  $^{20}\text{NeH}$ , and so was not pursued further. This does, however, indicate the importance of adequate gettering of a noble gas ion source.

## References

- [1] M Honda, X Zhang, D Phillips, D Hamilton, M Deerberg, J B Schwieters, Intl Jnl Mass Spectrometry, 387, 1-7 2015  
[2] P Eberhardt, O Eugster, K Marti, Z Naturforsch, 20a, 623-624 (1965) [3] J M Saxton, D J Rousell and S P Edwards, Goldschmidt abstract, 2016 [4] S Valkiers, M Varlam, M Berglund, P Taylor, R Gonfiantini, P De Bievre, Intl Journal of Mass Spectrometry, 269, 71-77 (2008) [5] V S Heber, R Wieler, H Baur, C Olinger, T A Friedmann, D S Burnett, GCA, 73, 7414-7432 (2009).

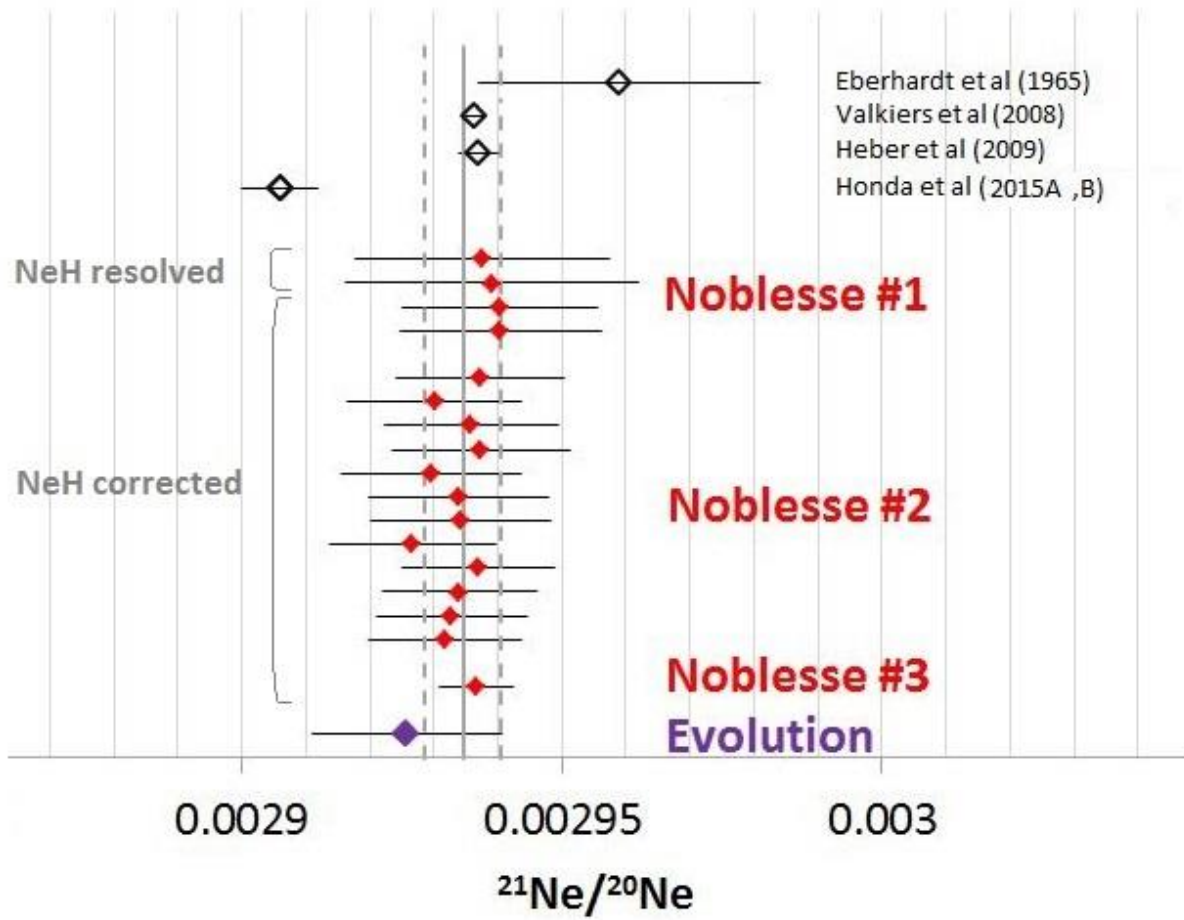


*Figure 1. Summary of results, compared with previously published values. Error bars are 2 s.e.*

# Swift heavy ion induced surface modification of calcite (CaCO<sub>3</sub>) visualized by various techniques

Dedera, S.<sup>(1)</sup>, Glasmacher, U.A.<sup>(1)</sup>, Burchard, M.<sup>(1)</sup>, Trautmann, C.<sup>(2),(3)</sup>

<sup>(1)</sup> University of Heidelberg, <sup>(2)</sup> Technical University Darmstadt, <sup>(3)</sup> GSI Darmstadt,

Natural calcite crystals were irradiated with  $10^6$  <sup>197</sup>Au ions/cm<sup>2</sup> of 11.1 MeV/u at the UNILAC, and with  $10^8$  <sup>238</sup>U ions/cm<sup>2</sup> of 192 MeV/u at SIS18, GSI Darmstadt to create artificial surface and in depth damage. Prior to the experiment the surface of calcite crystals was covered with a hexagonal mask to create irradiated and non-irradiated areas.

Different approaches have been undertaken to visualize the damage caused by swift heavy ions: One possibility are etching techniques at which Na-Ethylenediaminetetraacetic acid (EDTA) + 0.5 - 5% Acetic acid in 1:1 proportion and highly diluted HNO<sub>3</sub> as etching solution turned out to be suitable and reproducible [1]. The resulting etch pits show linear growth and have a size of about 12 μm (±1) after 20 s of etching (EDTA), respectively 15 μm (±2) after 4s of etching (HNO<sub>3</sub>). Etching has the advantages of visibility of the etch pits with an optical microscope and an easy control of size, shape and areal density of the etch pits.

Another approach to investigate surface modifications are spectrographical and advanced imaging methods. Different techniques have been tried out (Raman, IR, AFM, and SEM) of which raman spectroscopy provides the best results. Measured with a new in-situ raman spectroscopy system [2] heavily irradiated areas show new, previously unknown bands correlating with decreasing established bands.

## References

1. *Dedera, S.*, 2015. Visualization of Ion-Induced Tracks in Carbonate Minerals: Dissertation, Heidelberg.
2. *Dedera, S., Burchard, M., Glasmacher, U.A., Schöppner, N., Trautmann, C., Severin, D., Romanenko, A., Hubert, C.*, 2015. On-line Raman spectroscopy of calcite and malachite during irradiation with swift heavy ions. Nuclear Instruments and Methods in Physics Research Section B: Beam Interactions with Materials and Atoms 365, 564–568.

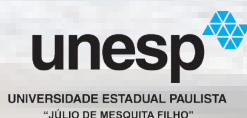
# THERMO2016

15th International Conference on ThermoChronology



September 18-23, 2016 - Maresias, Brazil

Supported by:



## ABSTRACTS

# Late Cretaceous to Cenozoic exhumation of the Fuping Metamorphic Core Complex, Central North China Craton: insights from low-temperature thermochronology

Jian Chang<sup>1,2</sup>, Nansheng Qiu<sup>1,2</sup>, Chang'e Cai<sup>1,2</sup>

1 State Key Laboratory of Petroleum Resources and Prospecting, China University of Petroleum, Beijing, China

2 Basin and Reservoir Research Centre, China University of Petroleum, Beijing, China  
(changjian@cup.edu.cn)

The Fuping Metamorphic Core Complex (FMCC), a typical extensional structure in the Trans-North China Craton and characterized by high-grade tonalitic-trondhjemitic-granodioritic (TTG) gneisses, with minor amounts of mafic granulites, syntectonic granitic rocks and supracrustal rocks<sup>1</sup>, is an ideal location for studying the thinning of North China Craton and Cenozoic rifting of the Bohai Bay Basin. In this study, we firstly studied systematically the chronology and cooling history of the FMCC by integrating with zircon and apatite (U-Th)/He and apatite fission track thermochronology. The weighted mean zircon (U-Th)/He ages range from 70.3 Ma to 79.9 Ma, the apatite fission track ages range from 41.9Ma~51.9 Ma with mean track lengths between  $11.22\pm 2.39$   $\mu\text{m}$  and  $13.31\pm 1.65$   $\mu\text{m}$  and the weighted mean apatite (U-Th)/He ages ranges during 15.1 Ma ~ 43.8 Ma. The joint inverse modeling based on kinds of thermochronological ages, which were gotten from the QTQt software developed by Gallagher<sup>2</sup>, revealed that the FCCC experienced three rapid cooling events at 100 Ma~55 Ma, 46 Ma~40 Ma and since ~25 Ma (Figure 1). The cooling events of 100 Ma~55 Ma and 46 Ma~40 Ma occurred under extension stresses were related to the subduction of the Pacific plate beneath the eastern Asian continent during Late Cretaceous and the mantle upwelling and extensive magmatism during Eocene, respectively. The last cooling was probably related to the eastward upwelling of the asthenosphere that caused by the collision of the Indian to the Eurasian plates and the eastward rollback of the Pacific subduction zone.

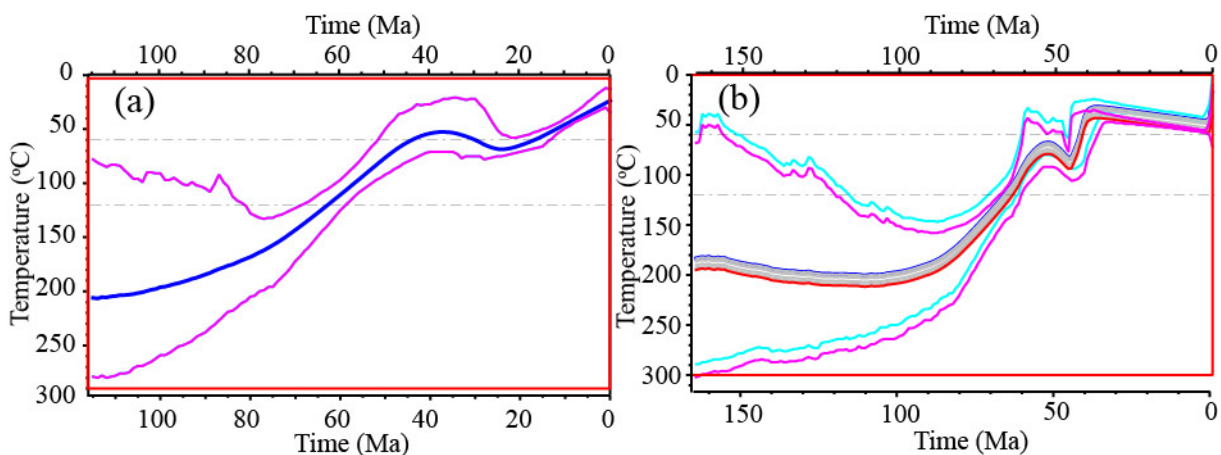


**Figure. 1** (a) the thermal history modeling result of the sample FP-10 in the northern margin of the FMCC; (b) thermal history modeling result for an elevation profile of samples FP-29, FP-30, FP-34, FP-36, FP-43 and FP-44 in the interior of the FMCC.

## References

1. Zhao, G. C., Wilde, S. A., Cawood, P. A. & Lu, L. Z. Petrology and P-T path of the fuping mafic granulites: implications for tectonic evolution of the central zone of the North China Craton. *J. metamorphic Geol.* 18, 375-391 (2000).
2. Gallagher, K. Transdimensional inverse thermal history modeling for quantitative thermochronology. *J. Geophys. Res.* 117, doi:10.1029/2011JB008825 (2012).

# The long-term landscape evolution of Zimbabwe: Insights from a multi-thermochronometer study

Vhairi Mackintosh<sup>1</sup>, Barry Kohn<sup>1</sup>, Andrew Gleadow<sup>1</sup>

1 School of Earth Sciences, University of Melbourne, Victoria, 3010, Australia  
(vmackintosh@student.unimelb.edu.au)

The Zimbabwe Craton and surrounding mobile belts that make up Zimbabwe form the north-eastern part of the southern African plateau. The Phanerozoic evolution of this plateau is of great scientific interest due to its enigmatic gain in elevation (>1000 m) whilst distal from convergent plate boundary processes<sup>1</sup>. However, deciphering the evolution of these cratonic interiors is often difficult using conventional field methods due to the fragmentary nature of their geological record<sup>2</sup>. Low-temperature thermochronology systems are able to record the cooling trajectories of rocks as they ascend the upper crust primarily, in cratonic settings, by denudation. Hence, thermochronology data can be used to constrain the timing and rates of denudation and contribute towards a more thorough understanding of the long-term landscape evolution of continental interiors.

The Phanerozoic record of Zimbabwe is largely unresolved and thermochronology studies are considerably lacking despite their successful, extensive application in neighbouring South Africa in constraining the pattern of denudation across this part of the plateau. The sparse data currently available are spatially limited to mainly the peripheries of Zimbabwe as well as restricted to apatite fission track data<sup>2-4</sup>. In this study, multiple thermochronometers with different temperature sensitivities - apatite (U-Th-Sm)/He (AHe) (~40-80 °C), apatite fission track (AFT) (~60-120 °C) and zircon (U-Th)/He (ZHe) (~130-210 °C) – are employed to unravel a significant portion of the unexplored Phanerozoic history of Zimbabwe.

The data reveal a diachronous, dynamic Phanerozoic thermo-tectonic evolution. Single grain AHe ages range from  $18.8 \pm 1.1$  Ma to  $580.3 \pm 36$  Ma, AFT central ages from  $94.8 \pm 5.9$  Ma to  $433.9 \pm 15.3$  Ma with mean confined track lengths from 11.29 to 13.21  $\mu\text{m}$ , and ZHe single grain ages from  $37.2 \pm 2.3$  Ma to  $636.0 \pm 39.4$  Ma. The oldest AHe, AFT and ZHe ages are located on the low relief, broad topographic high of the Zimbabwe cratonic interior. Thermal history modelling of the interior suggests the region experienced accelerated cooling in the mid-Paleozoic and has since resided at temperatures below the AFT partial annealing zone (PAZ). Most samples from Zimbabwe exhibit large intra-sample ZHe age variation and the effects of radiation damage (negative ZHe date-eU trends). Those samples that do not display a ZHe date-eU trend with moderate eU values have ZHe ages largely between the late Carboniferous – early Jurassic and are spatially associated with localised centres of Karoo rifting<sup>5</sup>. This suggests that this cooling signal is the result of erosion related to this intracratonic rifting. AFT and AHe dates decrease markedly from the cratonic interior towards the northern, eastern and southern margins of Zimbabwe revealing younger Mesozoic-Cenozoic thermal events. All margins record a period of enhanced cooling occurring in the late Jurassic - early Cretaceous coincident, and thus suggestive of a causative link, with Gondwana breakup<sup>1</sup>. Denudation rates were greater in the northern and southern regions illustrated by younger late-Cretaceous AFT and AHe ages (exhumed from depths below the AFT PAZ). In the southern region, the pattern of AFT and AHe dates is dictated by major structural boundaries implying that tectonic reactivation and the associated uplift and erosion is responsible for this cooling. Anomalous Eocene-Miocene AHe dates localized to the Zambezi Escarpment in northern Zimbabwe suggest a period of enhanced exhumation occurred during this time, potentially recording a period of fault reactivation. The use of multiple thermochronometers has provided greater insight into the evolution of the Zimbabwean landscape and suggests that tectonic reactivation of major structures, related to the transmission of stresses from plate boundary reorganisations, has played a key role throughout the Phanerozoic.

## References

1. Tinker, J., de Wit, M. & Brown, R. Mesozoic exhumation of the southern Cape, South Africa, quantified using apatite fission track thermochronology. *Tectonophysics* **455**, 77–93 (2008).
2. Belton, D. X. The low temperature thermochronology of cratonic terranes (Unpublished doctoral dissertation). (2006).
3. Belton, D. X. & Raab, M. J. Cretaceous reactivation and intensified erosion in the Archean–Proterozoic Limpopo Belt, demonstrated by apatite fission track thermochronology. *Tectonophysics* **480**, 99–108 (2010).
4. Noble, W. P. Post Pan African tectonic evolution of eastern Africa: An apatite fission track study (Unpublished doctoral dissertation). (1997).
5. Campbell, S. D. G., Oesterlen, P. M., Blenkinsop, T. G., Pitfield, P. E. J. & Munyanyiwa, H. A provisional 1:2 500 000 scale tectonic map and the tectonic evolution of Zimbabwe. *Ann. Zimbabwe Geol. Surv.* **16**, 31–51 (1991).

# Interplays between the West and the East Antarctica Ice sheets: hints from bedrock and detrital thermochronology and other techniques.

Balestrieri M.L.<sup>1</sup>, Olivetti V.<sup>2</sup>, Pace D.<sup>3</sup>, Rossetti F.<sup>3</sup>, Talarico F.M.<sup>4</sup>, Zattin M.<sup>5</sup>

1 *CNR, Institute of Geosciences and Earth resources, Florence, Italy, balestrieri@igg.cnr.it*

2 *Aix-Marseille Université, CNRS, IRD, CEREGE UM34, Aix en Provence, France*

3 *Department of Sciences, Geological Sciences, University of Roma Tre, Rome, Italy*

4 *Department of Physical, Earth and Environmental Sciences, University of Siena, Italy*

5 *Department of Geosciences, University of Padova, Italy*

Estimate of ice volume during the cyclical earth climate oscillations is a challenging task but crucial to investigate the mechanisms controlling the eustatic sea level changes. The low amplitude/ high frequency component of sea level oscillation is due to astronomically-induced climate changes controlling water retention mainly in the Antarctic Ice sheets<sup>1,2,3</sup>. This short-term component is intensely investigated nowadays for the possible effects on the human activity but how the volume was partitioned between the East and the West Antarctic ice sheets (EAIS, WAIS) in the past and how fast the respective volumes increase remain uncertain. WAIS is smaller than EAIS and contain ice volume equivalent to only 5 m of sea level, but it has been considered capable of ultra-fast melting because of its sensibility to sea temperature<sup>4,5,6</sup>. Recently the capability to produce abrupt collapse and very fast release of huge water volume has been downsize<sup>7</sup>; however, the breath of WAIS in the past remains a key issue to predict its future behavior. The modern Ross Ice Shelf (RIS) is a major component of the WAIS system, and approximately two-thirds of the ice shelf is nourished by ice streams that drain the WAIS, being its western margin fed by EAIS outlet glaciers.

During last glacial maximum (LGM), the RIS thickened and grew into the Ross Ice Sheet (RIS) leading the Ross sea region to be partially or totally occupied by a grounded ice sheet. Evidences for repeated ice sheet volume expansions in the past comes from deep-sea records through the calibration of  $\delta^{18}\text{O}$  to sea-level<sup>2,8,9</sup> although some misfits arise when sites at different latitude are analyzed<sup>10</sup>.

Direct geological evidences of RIS expansions are provided by grounded ice erosive events in the Ross Sea detected through seismic profiles<sup>11,12</sup> or by drill-core records<sup>13</sup> but until now a correlation of local geologic evidences to the global isotopic events has never been attempted.

In the Ross sea region, mountain uplift, basin formation and ice sheet fluctuation left a diagnostic signature within the marine stratigraphic records. Western and Eastern Antarctica have different history and composition resulting in different geo- and thermo-chronology signatures to sediments allowing to trace back their provenance. An extensive study using multiple datings, coupled to petrographic analyses is in progress. The project is divided in an onshore bedrock study in the Northern Victoria Land, devoted to investigate the feed-backs between neotectonics, magmatism and mantle dynamics in the Ross sea region and a detrital study focused on the Quaternary deposits sampled in piston cores from the Ross Sea and to the entire sedimentary record from the Oligocene onward of the numerous drilling projects perform in the Embayment.

## References

1. Hays, J. D., Imbrie, J., & Shackleton, N. J. (1976). Variations in the Earth's orbit: Pacemaker of the ice ages. American Association for the Advancement of Science.
2. Zachos, J.C., Pagani, M., Sloan, L., Thomas, E., Billups, K., 2001. Trends, rhythms and aberrations in global climate 65 Ma to present. *Science* 292, 686– 693.



3. Pälike, Heiko, Richard D. Norris, Jens O. Herrle, Paul A. Wilson, Helen K. Coxall, Caroline H. Lear, Nicholas J. Shackleton, Aradhna K. Tripathi, and Bridget S. Wade, (2006): "The heartbeat of the Oligocene climate system." *Science* 314, no. 5807 1894-1898.
4. Mercer, J.H., 1978. West Antarctic ice sheet and CO<sub>2</sub> greenhouse effect; a threat of disaster. *Nature* 271, 321–325.
5. MacAyeal, D.R., 1992. Irregular oscillations of the West Antarctic ice sheet. *Nature* 359, 29–32.
6. Scherer, R. P., Aldahan, A., Tulaczyk, S., Possnert, G., Engelhardt, H., & Kamb, B. (1998). Pleistocene collapse of the West Antarctic ice sheet. *Science*, 281(5373), 82-85.
7. Pollard, D. and DeConto R. M. Modelling West Antarctic ice sheet growth and collapse through the past five million years. *Nature* 458.7236 (2009): 329-332.
8. Billups, K., Schrag, D.P., 2002. Paleotemperatures and ice volume of the past 27 Myr revisited with paired Mg/Ca and 18O/16O measurements on benthic foraminifera. *Paleoceanography* 17. doi:10.1029/2000PA000567.
9. Pekar, S. F., & DeConto, R. M. (2006). High-resolution ice-volume estimates for the early Miocene: Evidence for a dynamic ice sheet in Antarctica. *Palaeogeography, Palaeoclimatology, Palaeoecology*, 231(1), 101-109.
10. Pekar et al., 2006
11. Cooper, A.K., Barrett, P.J., Hinz, K., Traube, V., Leitchenkov, G., Stagg, H.M.J., 1991. Cenozoic prograding sequences of the Antarctic continental margin: a record of glacio-eustatic and tectonic events. *Marine Geology* 102, 175–213.
12. Bart, P. J. (2003). Were West Antarctic ice sheet grounding events in the Ross Sea a consequence of East Antarctic ice sheet expansion during the middle Miocene?. *Earth and Planetary Science Letters*, 216(1), 93-107.
13. Barrett, P.J., Elston, D.P., Harwood, D.M., McKeley, B.C., Webb, P.N., 1987. Mid-Cenozoic record of glaciation and sea level change on the margin of the Victoria Land Basin, Antarctica. *Geology* 15, 634– 637.
14. Talarico & Sandroni?
15. Zattin, M., Andreucci, B., Thomson, S. N., Reiniers, P. W., & Talarico, F. M. (2012). New constraints on the provenance of the ANDRILL AND-2A succession (western Ross Sea, Antarctica) from apatite triple dating. *Geochemistry, Geophysics, Geosystems*, 13(10).
16. Olivetti V., Balestrieri M.L., Rossetti F., Thomson S., Talarico F.M., Zattin M. (2015). Evidence of a full West Antarctic Ice Sheet back to the early Oligocene: insight from double dating of detrital apatites in Ross Sea sediments. *Terra Nova*, 27, 238–246.

## **Geo-referenced database of Brazilian thermochronological studies**

Silvio Takashi Hiruma<sup>1</sup>, Carlos Henrique Grohmann<sup>2</sup>

*1 Instituto Geológico, Secretaria de Estado do Meio Ambiente de São Paulo, Rua Joaquim Távora, 822, São Paulo, SP, 04015-011, Brazil*

*2 Instituto de Energia e Ambiente, Universidade de São Paulo, São Paulo, SP, 05508-010, Brazil  
(sthiruma@gmail.com)*

In the last decades several thermochronological studies were carried out in Brazilian territory to reconstruct the geological evolution since before the Gondwana breakup. In order to summarize these studies, a geo-referenced database was created in ArcGIS platform based on literature compilation.

The data survey included studies about apatite and zircon fission track and (U-Th)/He dating – the most commonly used methods of low temperature thermochronology – published in indexed journals, thesis, dissertations, books/chapter books, and, eventually, abstract books from scientific events.

The following parameters are recorded for each publication: author, title, year, reference, sample number, geographical coordinates (latitude, longitude), altitude, geological context, type (apatite FT, zircon FT, U-Th/He), method of analysis (population/external detector), mean track length and standard deviation, age, among others. Some publications do not provide a complete and/or systematized information. For example, in some cases the geographical coordinates were extracted from regional-scale illustrations that not permit a precise location of the collected samples. Until now the database includes more than 40 publications (since 1994), with more than 800 records. This database will be updated continuously as additional studies become available.

Spatial distribution of the thermochronological data is highly heterogeneous, with clustering along the northeastern, southeastern and southern Brazil. Zircon fission track and (U-Th)/He data are very scattered, with samples clustered, respectively, in south-southeastern (ages between 65-539.9 Ma) and southeastern Brazil (ages between 50.2-148.5 Ma). Considering the total population of apatite fission track data (ages between 5.9-386.2 Ma), there is a large number of samples with ages between 100 and 60 Ma, which can be related to the continental break-up and subsequent phases of alkaline magmatism and tectonic reactivations from Late Cretaceous to Paleogene. Mean track lengths between 11-13  $\mu\text{m}$  (standard deviations between 1-2  $\mu\text{m}$ ) are predominant, in general associated to slow cooling or more complex thermal histories.

This study was co-funded by FAPESP (2014/01648-7; BIOTA, 2013/50297-0), NSF (DEB 1343578) and NASA.

# The tectonic and geomorphic development of southern Africa as revealed by apatite fission track and apatite (U-Th-Sm)/He thermochronology

Mark Wildman<sup>1</sup>, Roderick Brown<sup>1</sup>, Cristina Persano<sup>1</sup>, Fin Stuart<sup>2</sup>, Romain Beucher<sup>3</sup>

*1 School of Geographical and Earth Sciences, University of Glasgow, UK*

*2 Scottish Universities Environmental Research Centre, East Kilbride, UK*

*3 Department of Earth Science, Faculty of Mathematics and Natural Sciences, University of Bergen, Bergen, Norway*

Low temperature thermochronology techniques are routinely applied to investigate cooling in the upper kilometers of the Earth's crust in response to geological and geodynamic processes. The power of thermochronology lies in being able to provide unique quantitative constraints on the timing and rate of continental denudation over geological timescales in the absence of well-dated onshore stratigraphic information. By obtaining thermochronology data over different length-scales and augmenting outcrop samples with elevation and borehole profiles, robust estimates can be made on the style of denudation over space and time. These estimates provide important insights into the complex interaction between surface uplift, erosion and regional tectonics. Addressing such issues is particularly pertinent for southern Africa where the role of intraplate stresses and dynamic uplift in forming the present day topography of continental margins and the interior plateau has been fiercely debated<sup>1,2,3</sup>.

Over the last thirty years, a concerted effort has been made to use thermochronology to obtain quantitative constraints on the geomorphic evolution of southern Africa, which has led to an extensive thermochronology dataset being available for the region. Apatite fission track (AFT) analysis has, by far, been the most commonly used thermochronometer due to our relatively good understanding of the properties that control fission track annealing and the ability of the technique to constrain cooling of rocks through the upper 2 – 5 km of the Earth's crust. The spatial resolution of this dataset is now sufficiently detailed that distinct patterns of AFT age can be observed at regional and local scales (Figure 1). More recently, in order to achieve more detailed constraints on the timing and magnitude of denudation, apatite (U-Th-Sm)/He (AHe) has been utilised<sup>4,5,6</sup> because of the systems lower theoretical temperature sensitivity than AFT.

Here, we present the AFT and AHe dataset from southern Africa and jointly invert these data using a Bayesian inversion approach<sup>7</sup> to extract time-temperature paths for outcrop samples from the southwest African continental margin and interior plateau. New AFT and AHe data from borehole profiles from South Africa have also been jointly inverted to obtain more robust constraints on the thermal history of the upper crust. Results from joint thermal history models reveal several key features of southern Africa's tectonic and geomorphic evolution:

- (i) Slow cooling of the Kaapvaal craton in the continental interior, indicative of low erosion rates prevailing since the Late Palaeozoic.
- (ii) Onset of off-craton Early Cretaceous cooling linked to the erosion of syn-rift topography.
- (iii) Onset of regional Late Cretaceous cooling triggered by 1 – 4 km of erosion focused at major structural boundaries suggesting local fault reactivation and enhanced by regional mantle driven uplift.
- (iv) Minimal cooling in the Cenozoic driven by low regional erosion rates (c. 5 – 15 m/Myr).

The timing of maximum, structurally controlled, erosion during the Late Cretaceous, predicted by the current thermochronology dataset, is coincident with the timing of maximum sediment accumulation in offshore basins<sup>8</sup> and the timing of major changes in plate velocity and direction<sup>2</sup>

suggesting a causative link between regional tectonic movements, intracontinental deformation and enhanced erosion of southern Africa.

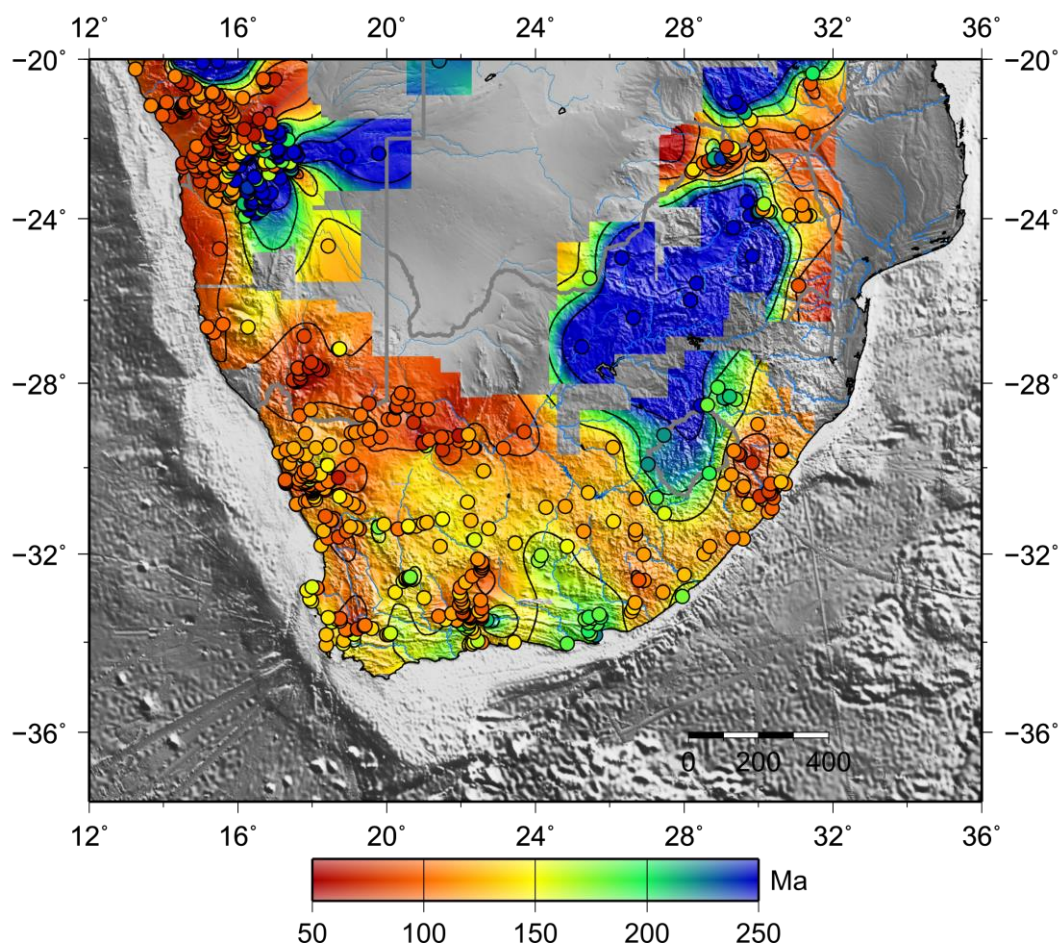


**Figure 1.** Interpolation map of Apatite Fission Track ages from southern Africa.

## References

1. Moore, A., Blenkinsop, T., & Cotterill, F. W. Southern African topography and erosion history: plumes or plate tectonics? *Terra Nova* **21**(4), 310-315 (2009).
2. Colli, L., Stotz, I., Bunge, H.P., Smethurst, M., Clark, S., Iaffaldano, G., Tassara, A., Guillocheau, F. & Bianchi, M.C. Rapid South Atlantic spreading changes and coeval vertical motion in surrounding continents: Evidence for temporal changes of pressure-driven upper mantle flow. *Tectonics*, **33**(7), 1304-1321, (2014).
3. Molnar, P., England, P. C., & Jones, C. H. Mantle dynamics, isostasy, and the support of high terrain. *Journal of Geophysical Research: Solid Earth*, **120**(3), 1932-1957, (2015).
4. Kounov, A., Viola, G., Dunkl, I., & Frimmel, H. E. Southern African perspectives on the long-term morpho-tectonic evolution of cratonic interiors, *Tectonophysics*, **601**, 177-191, (2013).
5. Stanley, J. R., Flowers, R. M., & Bell, D. R. Erosion patterns and mantle sources of topographic change across the southern African Plateau derived from the shallow and deep records of kimberlites. *Geochemistry, Geophysics, Geosystems*, **16**(9), 3235-3256, (2015).
6. Wildman, M., R. Brown, R. Beucher, C. Persano, F. Stuart, K. Gallagher, J. Schwanethal, & A. Carter. The chronology and tectonic style of landscape evolution along the elevated Atlantic continental margin of South Africa resolved by joint apatite fission track and (U-Th-Sm)/He thermochronology, *Tectonics*, **35**, (2016).
7. Gallagher, K. Transdimensional inverse thermal history modeling for quantitative thermochronology. *Journal of Geophysical Research: Solid Earth*, **117**(B2), (2012).
8. Guillocheau, F., Rouby, D., Robin, C., Helm, C., Rolland, N., Le Carlier de Veslud, C., & Braun, J. Quantification and causes of the terrigenous sediment budget at the scale of a continental margin: a new method applied to the Namibia–South Africa margin. *Basin Research*, **24**(1), 3-30, (2012).

# The role of the Büyük Menderes Detachment during Late Cenozoic exhumation of the central Menderes Massif, SW Turkey

Nils-Peter Nilius<sup>1</sup>, Andreas Wölfler<sup>1</sup>, Christoph Glotzbach<sup>2</sup>, Caroline Heineke<sup>3</sup>, Ralf Hetzel<sup>3</sup>,  
Andrea Hampel<sup>1</sup>, Cüneyt Akal<sup>4</sup>, István Dunkl<sup>5</sup>

*1 Institute of Geology, Leibniz University of Hannover, Callinstraße 30, 30167 Germany*

*2 Department of Geosciences, University Tübingen, Wilhelmstraße 56, 72047*

*Tübingen, Germany*

*3 Institute of Geology and Palaeontology, University of Münster, Correnstraße 24, 48149  
Münster, Germany*

*4 Dokuz Eylül University, Engineering Faculty, Department of Geological Engineering,  
Tınaztepe Campus, Buca, 35160 Izmir, Turkey*

*5 Geoscience Centre, University of Göttingen, Goldschmidtstr. 3, 37077 Göttingen,  
Germany*

*(nilius@geowi.uni-hannover.de)*

The western part of the Anatolide belt in SW Turkey experienced a long history of continental extension since the cessation of Alpine nappe stacking in Eocene time<sup>1</sup>. Since the Middle Miocene, a significant fraction of the north-south extension occurred in the central Menderes Massif and was mainly accommodated by the Gediz detachment in the north and the Büyük Menderes detachment in the south<sup>2</sup>. Previous structural and thermochronological studies determined the approximate timing of the middle Miocene-Pliocene exhumation<sup>2,3,4</sup> and proposed a bivergent extension with both detachments being active roughly at the same time. So far, however, only the evolution of the north-dipping Gediz detachment is well constrained, whereas thermochronological and detailed structural investigations from the south-dipping Büyük Menderes detachment are rare.

We present new zircon and apatite (U-Th)/He and fission track ages, which better constrain the cooling and exhumation history of the footwall and hanging wall of the Büyük Menderes detachment. Our thermochronological data indicate a continuous cooling of the footwall rocks since the middle Miocene, with two phases of enhanced cooling and exhumation. The first phase of accelerated exhumation occurred in the Middle Miocene at a rate of ~0.9 km/Ma. As ZFT ages of footwall and hanging wall samples are similar, we infer that the Büyük Menderes detachment was active at less than ~250°C, which is in accordance with the lack of stretching lineations defined by quartz and the absence of dynamic recrystallization features in quartz. The second phase of exhumation proceeded in the Pliocene, when the Büyük Menderes detachment operated at a slip rate of 3.0 (+1.1/-0.6) km/Ma as constrained by AFT data. A Late Oligocene - Early Miocene phase of slow cooling (and exhumation at a rate of ~0.2 km/Ma) is recorded by augen gneiss klippen above the detachment and could be the result of incipient erosion of the Alpine nappe stack. As exhumation in extensional settings is driven by both, tectonic and erosional denudation, we are currently determining erosion rates for the different tectonic units exposed at the Büyük Menderes detachment.

## References

1. Gessner, K., Gallardo, L.A., Markwitz, V., Ring, U., & Thomson, S.N. What caused the denudation of the Menderes Massif: Review of crustal evolution, lithosphere structure and dynamic topography in southwestern Turkey. *Gondwana Research* **24**, 243-274 (2013).
2. Gessner, K., Ring, U., Johnson, C., Hetzel, R., Passchier, C.W. & Güngör, T. An active bivergent rolling-hinge detachment system: Central Menderes metamorphic core complex in western Turkey. *Geology* **29**, 611-614 (2001).
3. Buscher, J. T., Hampel, A., Hetzel, R., Dunkl, I., Glotzbach, C., Struffert, A., Akal, C., & Rätz, M. Quantifying rates of detachment faulting and erosion in the central Menderes Massif (western Turkey) by thermochronology and cosmogenic <sup>10</sup>Be. *Journal of the Geological Society* **170**(4), 669-683 (2013).
4. Hetzel, R., Zwingmann, H., Mulch, A., Gessner, K., Akal, C., Hampel, A., Güngör, T., Petschick, R., Tamas, M., & Wedin, F. Spatiotemporal evolution of brittle normal faulting and fluid infiltration in detachment fault systems: A case study from the Menderes Massif, western Turkey. *Tectonics* **32**, 364-376 (2013).

# **Constraining the extent, thickness and erosional history of the Jurassic continental flood basalts of western Dronning Maud Land, East Antarctica: evidence from low-T thermochronology**

Hallgeir Sirevaag<sup>1</sup>, Joachim Jacobs<sup>1,2</sup>, Anna K. Ksienzyk<sup>1</sup>, István Dunkl<sup>3</sup>

*1 Department of Earth Science, University of Bergen, Allégaten 41, 5007 Bergen, Norway*

*2 Norwegian Polar Institute, Fram Centre, Hjalmar Johansensgate 14, 9296 Tromsø, Norway*

*3 Geoscience Center, University of Göttingen, Goldschmidtstrasse 3, 37077 Göttingen, Germany*

*(hallgeir.sirevaag@uib.no)*

The Dronning Maud Land Mountains (DML), East Antarctica, form an approximately 1500 km long, coast-parallel escarpment, possibly resulting from flexural uplift during the Jurassic rifting between East and West Gondwana. DML is characterized by an alpine topography with a relief of ca. 5500 meters, formed by mountains up to ca. 3500 masl and the major Jutulstraumen-Penckgraben with an incision close to 2000 mbsl. During the Gondwana rifting, significant amounts of continental flood basalts (CFB) associated with the Karoo mantle plume were emplaced at ca. 180 Ma. These basalts are presently widespread in South Africa (i.e. Drakensberg), while on the conjugate margin of East Antarctica, they are only preserved as remnants in wDML. Previous apatite fission track (AFT) studies suggest that Heimefrontfjella was covered by 1.5-2 km of Karoo basalts, while there are no evidences of such thermal event in Gjelsvikfjella further east. Except for these areas, the extent, thickness and the erosional history of these basalts have previously not been accurately constrained. Since DML was one of the nucleation sites for the East Antarctic ice-sheet at 34 Ma, it is important to know whether or not the CFBs contributed to the topography prior to the initiation of the glaciation. By applying a wide range of thermochronological methods (apatite and zircon (U-Th)/He (AHe, ZHe) and AFT), we try to estimate and quantify the extent, thickness and erosional history of the CFBs. A new dataset includes 21 apatite and 8 zircon (U-Th)/He analyses as well as new AFT data.

All ZHe mean ages predate Gondwana break-up. Two samples close to Jutulstraumen-Penckgraben yield Permian mean ages, probably recording initial Permian rifting in the area. The remaining ZHe analyses are derived from the eastern graben shoulder of Jutulstraumen-Penckgraben, an area with no Pan-African overprint. These analyses give scattered ZHe ages up to 650 Ma, indicating that these areas were located at, or close to the surface shortly after the Pan-African orogeny. Since all ZHe ages are pre-break up, the CFBs cannot have exceeded a thickness sufficient for resetting of the ZHe system (i.e. 4 km). Previously published AFT ages from wDML scatter between ca. 80 and 370 Ma, showing that only parts of the AFT system in wDML was reset by the CFBs. While most of the new AFT data give post-break up ages, one sample from western Jutulstraumen-Penckgraben predates the break up, indicative of rapid erosion contemporaneously with CFB emplacement in an active rift setting. AHe analyses give ages from ca. 50 Ma to ca. 150 Ma, while two samples yield AHe ages of ca. 300 Ma and ca. 370 Ma. The latter two are derived from elevated areas close to Jutulstraumen-Penckgraben, indicating that these areas were not affected by the CFBs. The younger AHe ages suggest that the CFBs were covering the entire area with a thickness of at least 1 km. In conclusion, the array of low-T thermochronological methods allows us to constrain the thickness of the CFBs in wDML to 1-4 km, at least until the early Cenozoic.

# Large-scale rift tectonics along the Pacific margin of West Antarctica: Insights from apatite thermochronology

Zundel Maximilian<sup>1</sup>, Spiegel Cornelia<sup>1</sup>, Lisker Frank<sup>1</sup>

*1 University of Bremen, Department 5 Geosciences, Geodynamics of Polar Regions, Klagenfurter Strasse, 28359 Bremen, Germany  
(zundel@uni-bremen.de)*

West Antarctica is a collage of several crustal blocks which were amalgamated in Paleozoic and Mesozoic times forming the Gondwana supercontinent. Subsequent extension since the mid Cretaceous led to continental break-up and the initiation of the West Antarctic Rift System (WARS), one of the largest rift systems on earth. Along this 3000 km long large-scale continental structure within the Antarctic continent several crustal blocks - e.g. Marie Byrd Land, Thurston Island - are being separated again. Due to a perennial ice cover, the precise location, geometry, and tectonic evolution of the WARS are, however, still poorly constrained and understood. Continental break-up was most-likely associated with a period of pronounced erosion and rapid exhumation, hence apatite thermochronology provide an ideal measure to monitor and constrain the shallow crustal tectonic processes active at that time and thus enhance the understanding of the WARS.

Fission-track ages of the Ford Ranges and Edward VII Peninsula in western Marie Byrd Land are ranging between 72 and 97 Ma<sup>1</sup> while apatite (U-Th-Sm)/He ages, obtained during this study, range from 69 to 106 Ma. Nearly identical fission-track and (U-Th-Sm)/He ages, in addition to modelled time-temperature paths, emphasize Late Cretaceous exhumation to a near-surface position. This is in contrast to eastern Marie Byrd Land, where, following the Late Cretaceous rapid exhumation period, an Oligocene rifting period and subsequent uplift of the Marie Byrd Land dome at 20 Ma was derived from thermochronological data<sup>2</sup>. However, such young WARS activity is not observed for the neighbouring crustal block of Thurston Island that is characterized by recently generated fission-track ages ranging between 160 and 92 Ma, showing considerably older ages than those in eastern and western Marie Byrd Land. Considering the large range of fission-track ages and some significantly reduced track lengths, the Thurston Island block might have been exhumed already in the Late Jurassic to early Cretaceous, while parts remained in the Partial Annealing Zone, being subject to track shortening, until final uplift in the Late Cretaceous.

The studied crustal blocks all document a period of rapid exhumation during the Late Cretaceous possibly corresponding with crustal extension as a major event along the Pacific margin of West Antarctica. However, ongoing WARS activity in the Cenozoic seemed to be confined to eastern Marie Byrd Land, not affecting adjacent areas.

## References

1. Lisker, F. & Olesch, M. Multi-Stage Thermal Evolution and Denudation of the Edward VII Peninsula, Marie Byrd Land: Constraints from Apatite Fission-track Thermochronology. *Geol. Jb.*, B95, 33-53p (2003).
2. Spiegel, C., Lindow, J., Kamp, P., Mukasa, S., Lisker, F., Kuhn, G. and Gohl, K. Thermotectonic and geomorphic evolution of Marie Byrd Land and the Pine Island Bay area. XXII International Symposium on Antarctic Earth Sciences, Goa, India, (2015).

# Cenozoic Development of the Central European Eger Rift: First Low-T Thermochronology Results from Basement Borehole Samples

Annika Szameitat<sup>1</sup>, Petra Štěpančíková<sup>1</sup>, Ludwig Zöller<sup>2</sup>, Jonas Kley<sup>3</sup>, István Dunkl<sup>3</sup>

<sup>1</sup> Institute of Rock Structure and Mechanics, Department of Neotectonics and Thermochronology, CAS, Prague, Czech Republic

<sup>2</sup> Universität Bayreuth, Germany

<sup>3</sup> Universität Göttingen, Germany

(szameitat@irms.cas.cz)

As a major part of the European Cenozoic Rift Systems the Eger-Rift and the cross-cutting Mariánské-Lázně Fault (MLF) are important features of the Geology and Geomorphology in the Alpine foreland of the Czech-German border region. The area has experienced significant Cenozoic brittle crustal deformation, basin subsidence and Paleogene to Quaternary intraplate volcanic activity<sup>1-4</sup> and is characterized today by frequent earthquake swarms and CO<sub>2</sub> degassing<sup>5,6</sup>, clearly indicative of active mantle processes. Despite intense investigations into the structural and tectonic history of this area, the exact Cenozoic tectonic development of the region remains debated. For this reason a new international multidisciplinary project utilizing structural geology, geomorphology, paleoseismology, low-temperature thermochronology, applied geophysics and modern seismology commenced earlier this year, aiming to investigate the late Cenozoic to present tectonic activity of the western Eger Rift.

As part of this large-scale interdisciplinary project we investigate the low-temperature thermochronology of the Eger-Rift and Mariánské-Lázně Fault shoulders as well as the subsidence and thermal structure of the adjacent Cheb Basin. Here we present a first dataset of low-temperature thermochronology ages from this area, including a vertical depth profile from an almost 2 km deep borehole penetrating the granitic basement of the nearby Fichtelgebirge (Germany). These low-T data help constraining the subsidence history and geothermal state of the western side of MLF, including the Cheb Basin. These samples were analyzed with both apatite and zircon (U-Th)/He method in the newly opened Helium Laboratory at the Institute of Rock Structure and Mechanics in Prague using our new ASI Alphachron<sup>TM</sup> extraction line and compared to the existing data from Red Thermoluminescence analysis in the same borehole<sup>7</sup> and from fission track and ZHe dating in the nearby KTB borehole<sup>8,9</sup>.

## References

1. Malkovsky M. The Mesozoic and Tertiary basins of the Bohemian Massif and their evolution. *Tectonophysics* 137; 31-42 (1987).
2. Prodehl C., Mueller S., Haak V. The European Cenozoic rift system. In: Olsen KH (ed) Continental Rifts: Evolution, Structure, *Tectonics. Develop in Geotect* 25, Elsevier, 133-212 (1995).
3. Dèzes P, Schmid S, Ziegler PA. Evolution of the European Cenozoic Rift System: Interaction of the Alpine and Pyrenean orogens with their foreland lithosphere. *Tectonophysics* 389, 1-33 (2004).
4. Ulrych J., Dostal J., Adamovič J., Jelínek E., Špaček P., Hegner E., Balogh K. Recurrent Cenozoic volcanic activity in the Bohemian Massif (Czech Republic). *Lithos* 123;133–144 (2011).
5. Geissler, W.H., Kämpf, H., Kind, R., Bräuer, K., Klinge, K., Plenefisch, T., Horálek, J., Zedník, J., and Nehybka, V. Seismic structure and location of a CO<sub>2</sub> source in the upper mantle of the western Eger (Ohře) Rift, central Europe. *Tectonics* 24, TC5001 (2005).
6. Fischer, T., Horálek, J., Hrubcová, P., Vavryčuk, V., Bräuer, K., Kämpf, H. Intra-continental earthquake swarms in West-Bohemia and Vogtland: A review. *Tectonophysics* 611, 1-27. (2014).
7. Schmidt, C., et al., Thermochronometry using red TL of quartz? e Numerical simulation and observations from in-situ drill-hole samples, *Radiation Measurements*, <http://dx.doi.org/10.1016/j.radmeas.2015.04.004> (2015)
8. Coyle, D. A., G. A. Wagner, E. Hejl, R. Brown, and P. Van den Haute The Cretaceous and younger thermal history of the KTB site (Germany): Apatite fission-track data from the Vorbohrung, *Geol. Rundsch.*, 86, 203–209, doi:10.1007/s005310050132. (1997).
9. Wolfe, M. and Stockli, D. Zircon (U–Th)/He thermochronometry in the KTB drill hole, Germany, and its implications for bulk He diffusion kinetics in zircon, *Earth and Planetary Science Letters*, 295, 69–82 (2010).



## **Thermochronology and Geodynamics of continental extension associated with the Turkana Depression in East Africa**

Andrew Gleadow<sup>1</sup>, Samuel C Boone<sup>1</sup>, Barry Kohn<sup>1</sup>, Christian Seiler<sup>1</sup> and David Foster<sup>2</sup>

<sup>1</sup>*University of Melbourne, Australia*

<sup>2</sup>*University of Florida, USA*  
(gleadow@unimelb.edu.au)

One of the most obvious features of the East Africa Rift System (EARS) is that rifting is localized within two separate, much more extensive regions of major crustal uplift and volcanic construction centred on the Ethiopian Dome in the north and East African Dome, or Plateau, in the south. The Ethiopian Dome is traversed by a single major rift zone, whereas rifting in the East African Dome is divided into two branches, the western and eastern rifts, with the eastern branch traversing the volcanically-active Kenyan Dome. These major domal uplifts reach typical elevations of around 3,000 m and 2,500 m respectively with even higher volcanic peaks.

Defining the gap between the two major domes, and cutting across the ~N-S trend of the modern Neogene rift, is the Turkana Depression (TD), a broad ~200 km wide belt of relatively subdued topography and average elevations of only ~500 m. This depression is partly underlain by older rift structures that extend discontinuously from the Kenyan coast to South Sudan and east to the Central Africa Rift system. These older rifts contain substantial thicknesses of Late Cretaceous to Paleogene sedimentary fill and hydrocarbon resources. Lake Turkana in northern Kenya occurs where the modern (Miocene-Recent) rift system crosses the trend of the older rifts, and is approximately mid-way between the two topographic highs of the Ethiopian and Kenyan domes. The topographic segmentation of the EARS into discrete domes, and the occurrence of broad uplifts elsewhere in Africa, led to the idea that these were the surface manifestation of upwelling mantle plumes. Seismic tomography beneath East Africa, however, has been ambiguous, with various studies suggesting that the region is underlain either by two discrete upwelling mantle plumes corresponding to the domal uplifts, or alternatively by a single N-S elongated upwelling beneath the whole region.

Apatite fission track analysis within the Proterozoic Mozambique Belt from northern Tanzania to NW Kenya shows apparent ages ranging from <40 Ma to >200 Ma. Thermal history modelling shows that this area is dominated by a single, regionally-extensive cooling event of Late Cretaceous to Paleogene age, corresponding to the main phase of sedimentary fill in the adjacent older rift systems. This major cooling event occurs across an approximately 200 km wide, NW-SE trending belt of basement rocks adjacent to the TD that we attribute to surface denudation of 3-4 km along the formerly uplifted shoulders of the older rifts. This denudation contributed to extensional thinning of the crust across not only the older (Cretaceous) rift basins beneath the TD, but also across an even wider zone of uplifted basement bordering this area.

The major extensional event revealed by the older rifts and the thermochronology of the adjacent basement substantially modified the lithospheric structure along the trend of the TD. The broad mantle upwelling associated with Neogene rifting has acted differentially across the continental lithosphere previously modified by Cretaceous extension, to segment uplift into the discrete domes. Thus the present-day morphology of East Africa results from regional uplift over an extensive zone of upwelling mantle divided by lower elevations within the previously thinned lithosphere of the Turkana Depression.

# Paleocene-Early Eocene uplift of the Altyn Tagh Mountain: Evidence from detrital zircon fission track analysis and seismic sections in the northwestern Qaidam basin

Yadong Wang<sup>1</sup>, Jianjing Zheng<sup>1</sup>, Youwei Zheng<sup>1</sup>, Xingwang Liu<sup>1</sup>  
 1 No 382 Donggang Western Road, Lanzhou, China  
 (wangyd2015@lzb.ac.cn)

Most existing tectonic models suggest that the deformation and uplift of the northern Tibetan Plateau is the latest crustal response to the collision of the India Plate and Eurasian Plate. The tectonic evolution of Altyn Tagh Mountain (hereafter called simply the “Altyn Tagh”), on the northern margin of the Tibetan Plateau, has attracted considerable scientific attention. In this study, we use fission track age dates of detrital zircons from the northwestern Qaidam basin together with sedimentary observations to understand more fully the Cenozoic tectonic uplift of the Altyn Tagh. Detrital zircons from five borehole samples distributed in different folds in the northwestern Qaidam basin yielded ages mainly ranging from 88.5 to 49.2 Ma, older than their sedimentary deposition ages (43.8–22 Ma). The binomial distribution in grain age fitted peaks was generally dominated by one young peak, P1, which varied from 73.6 to 47.2 Ma (Fig. 1). A thinning of the Cenozoic Lulehe Formation (53.5–43.8 Ma) stretched from the inner Qaidam basin to the slopes of the Altyn Tagh in the seismic sections of the northwestern Qaidam basin. Based on magnetostratigraphic dating, there was a hiatus in sedimentation in the Qaidam basin between 65 Ma and 54 Ma; this was confirmed by seismic profiles and borehole data, which show an unconformity between the Mesozoic Quanyagou Formation and the Lulehe Formation. Combined with an analysis of provenance, the detrital zircon young peak age and the sedimentary record revealed that the most significant regional uplift of the Altyn Tagh occurred during the Paleogene-Early Eocene, almost coinciding with the collision of the Indian and Eurasian plates between 65 Ma and 44 Ma.

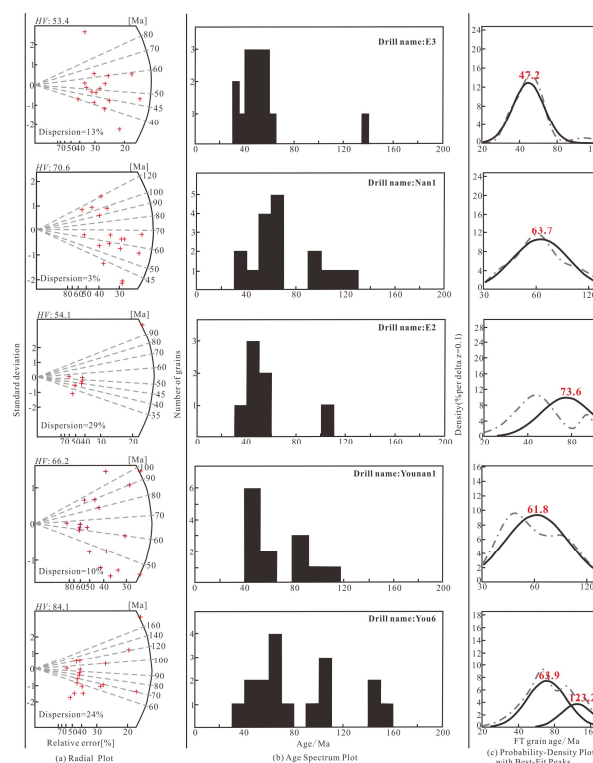


**Figure 1.** Detrital zircon fission track radial plots and single-grain age and decomposed age distributions for the northwestern Qaidam basin. The black crosses represent single-grain ages, gray dashed lines are the curves of observed grain age distributions, and bold lines are the curves of binomial best fit peaks. Peak fitting follows Galbraith and Green [1990] and Brandon [1996] using BINOMFIT [from Brandon, 1992].

# Denudation history of the SE Brazil margin from combined low temperature thermochronology and $^{40}\text{Ar}/^{39}\text{Ar}$ weathering geochronology: Implications for landscape evolution

B. P. Kohn<sup>1</sup>, I. O. Carmo<sup>2</sup> and P. M. Vasconcelos<sup>3</sup>

*1 School of Earth Sciences, University of Melbourne, Victoria, 3010, Australia*

*2 PETROBRAS/CENPES/PDEXP/GEOTEC, Rio de Janeiro, RJ, Brazil*

*3 School of Earth Sciences, University of Queensland, Brisbane, Qld 4072, Australia  
(b.kohn@unimelb.edu.au)*

Continental rifting resulting in the formation of the South Atlantic passive margin occurred ~130 Ma. The SE Brazilian margin is characterized by a pair of mountain ranges (Serra do Mar and Serra da Mantiqueira) formed parallel to a low elevation coastal plain. Further inland the Doce Valley separates the Serra da Mantiqueira from an elevated hinterland plateau. Thermochronology studies indicate pronounced Late Cretaceous–Paleocene cooling/denudation occurring many Myr following continental breakup<sup>1-5</sup>. The mechanism or controls on present physiography and their relationship to thermochronology data have been the subject of considerable discussion<sup>1-5</sup>.

We present apatite fission track (AFT), apatite (U-Th-Sm)/He and zircon (U-Th)/He thermochronology results from basement samples along a series of transects up to ~500 km from the SE Brazilian rifted continental margin, between 19°–23°S. These include data from vertical profiles up to elevation differences of ~2000 m across some of the most prominent topographic features. We also combine regional  $^{40}\text{Ar}/^{39}\text{Ar}$  weathering geochronology data<sup>6-7</sup> related to some of our samples, which provide minimum ages for sample residence within ~100m from the Earth's surface and serve as a powerful independent constraint on thermal history models.

ZHe data show a strong negative correlation between age and [eU] primarily reflecting a radiation damage effect, with the older ages related to cooling post late Precambrian Brasiliano orogeny. AFT data show a general systematic increase of age from ~50 Ma (coastal plain area) up to ~178 Ma (hinterland plateau), but exceptionally older results, up to ~250 Ma, occur at highest elevations of the Serra do Mar. AHe data show some age dispersion, but in general follow the AFT age trend. Thermal history modelling of all thermochronology data from vertical profiles show pronounced Late Cretaceous–Paleocene cooling, but when samples from the higher elevation profiles are included a possible Early Cretaceous cooling episode is also apparent. Unconstrained thermal history models from hinterland plateau samples show monotonic cooling to present day. However, when an  $^{40}\text{Ar}/^{39}\text{Ar}$  weathering constraint (65±5 Ma) is imposed, models show cooling from Late Jurassic–Early Cretaceous time, and minimal post-65 Ma denudation, which is estimated at ~2m/Ma<sup>8</sup>. This is in marked contrast to unconstrained thermal history models indicating ~1–1.25 km of denudation.

Our findings support the notion that the evolution of the SE Brazil margin was shaped by two cooling episodes: slow cooling from the Jurassic to Early Cretaceous and a more pronounced cooling episode during Late Cretaceous–Paleogene time long after Early Cretaceous Gondwana break-up. Our results also suggest greater post-break up denudation in coastal areas (>2.5 km) compared to the interior (<1 km). Denudation related to the later event supplied large volumes of sediment to hydrocarbon-rich adjacent offshore basins<sup>9</sup>. Possible models to explain the onset of post-rift cooling include: (i) localized Campanian–Paleocene alkaline magmatism, commonly attributed to a mantle plume mechanism, (ii) Late Cretaceous uplift driven by tectonic reactivation<sup>10-11</sup> possibly related to mechanical constriction of the South America plate resulting from slow relative motion between this plate and the African and the Nazca plates<sup>12-13</sup> or (iii) climatically driven erosional effects operating on an elevated margin<sup>14</sup>.

## References

1. Gallagher, K., Hawkesworth, C.J. & Mantovani, M. The denudation history of the onshore continental margin of SE Brazil inferred from apatite fission track data. *Journal of Geophysical Research* **99**, 18117-18145 (1994).
2. Cogné, N., Gallagher, K. & Cobbold, P.R. Post-rift reactivation of the onshore margin of southeast Brazil: evidence from apatite (U-Th)/He and fission track data. *Earth and Planetary Science Letters* **309**, 118-130 (2011).
3. Karl, M., Glasmacher, U.A., Kollenz, S., Franco-Magalhaes, A.O.B., Stockli, D.F. & Hackspacher, P.C. Evolution of the South Atlantic passive continental margin in southern Brazil derived from zircon and apatite (U-Th-Sm)/He and fission-track data. *Tectonophysics* **604**, 224-244 (2013).
4. Jelinek, A.R., Chemale Jr, F. van der Beek, P.A., Guadagnin, F., Cupertino, J.A. & Viana, A. Denudation history and landscape evolution of the northern East-Brazilian continental margin from apatite fission track thermochronology. *Journal of South American Earth Sciences* **54**, 158-181 (2014).
5. Green, P.F., Lidmar-Bergström, K., Japsen, P., Bonow, J.M. & Chalmers, J.A. (2013). Stratigraphic landscape analysis, thermochronology and the episodic development of elevated, passive continental margins. *Geological Survey of Greenland Bulletin* **30**, 150 p. (2013).
6. Carmo, I., Vasconcelos, P.M.  $^{40}\text{Ar}/^{39}\text{Ar}$  geochronology of weathering profiles in southeastern Brazil. IV South American Symposium on Isotope Geology (Short Papers), Salvador, p. 49-52 (2003).
7. Carmo, I.O., Vasconcelos, P. Geological evidence for pervasive Miocene weathering, Minas Gerais, Brazil. *Earth Surface Processes and Landforms* **29**, 1303-1320 (2004).
8. Vasconcelos, P. & Carmo, I.O. Calibrating denudation chronology through  $^{40}\text{Ar}/^{39}\text{Ar}$  weathering geochronology. *Earth Science Reviews* (submitted).
9. Fetter M., De Ros, L.F. & Bruhn, C.H.L. Petrographic and seismic evidence for the depositional setting of giant turbidite reservoirs and the paleogeographic evolution of Campos Basin, offshore Brazil. *Marine and Petroleum Geology* **26**, 824-853 (2009).
10. Cobbold P.R., Meisling, K.E. & Mount, V.S. Reactivation of an obliquely rifted margin, Campos and Santos basins, southeastern Brazil. *AAPG Bulletin* **85**, 1925-1944 (2001).
11. Lima, C. Ongoing compression across South American plate: observations, numerical modelling and some implications for petroleum geology. *Geological Soc. London, Special Publications* **209**, 87-100 (2003).
12. Pardo-Casas F. & Molnar P. Relative motion of the Nazca (Farallon) and South American plates since Late Cretaceous time. *Tectonics*, **6**, 233-248 (1987).
13. Nürnberg D., Müller R.D. The tectonic evolution of the South Atlantic from Late Jurassic to present. *Tectonophysics*. **191**, 27-53 (1991).
14. Sacek, V., Carmo, I.O., Kohn, B.P. & Vasconcelos, P.M. Numerical modeling and quantification of surface and tectonic processes combined with low temperature thermochronology data in southeastern Brazil. 14<sup>th</sup> International Thermochronology Conference (Abstract) – Chamonix (2014).

# **Controls of denudation in continental margin of southeast Brazil deduced by analysis of *in situ* produced $^{10}\text{Be}$ concentration in river sediments**

De Souza. D. H.<sup>1</sup>, Hackspacher. P. C<sup>2</sup>, Stuart. F.<sup>3</sup>, Pupim. F. N.<sup>4</sup>

*1 Geosciences and Environmental graduate program – São Paulo State University, Brazil*

*2 Institute of Earth and Exact Sciences – São Paulo State University, Brazil*

*3 Scottish Universities Environmental Research Centre, United Kingdom*

*4 Institute of Geosciences – University of São Paulo - Brazil*

*danieudani@yahoo.com.br*

Post-rift reactivation in the southeast region of Brazil created passive margin topography that is characterized by two coast-parallel mountain ranges (Serra do Mar and Serra da Mantiqueira) separated by Tertiary sedimentary basins<sup>1</sup>. The absence of significant earthquakes<sup>2</sup> suggest relative tectonic stability at least during the Late Quaternary. This topography in a tectonically stable environment allows some assessments: 1. To check whether the landscape is in steady state, with low and spatially homogeneous erosion rates; 2. Assess the relative role of climate in the landscape evolution, since the topographical diversity has generated a large difference in average annual rainfall, from 2800 mm (ocean side) to 1300 mm (continent).

We present new catchment-averaged denudation rates using *in situ*-produced  $^{10}\text{Be}$  from 21 river (3 from literature<sup>3</sup>) on the continental margin of southeast Brazil (Fig.1). Denudation rates were correlated with local relief extract by SRTM image and mean annual precipitation (1977 to 2006). The catchment-averaged denudation rates range from 5 m/Ma to 56 m/Ma (Fig. 1). Two patterns are clear: 1. Escarpment basins have higher rates than highland basins in all compartments. This is verified by the positive correlation between denudation rates and local relief (Fig.1). 2. The Serra do Mar compartment erodes 2-3 times faster than Serra da Matiqueira.

Despite relief (or slope) being an important control of denudation, it cannot explain alone the change in magnitude. The logarithmic curve in the correlation denudation x relief suggests a threshold when denudation rate increases without a change of the Serra do Mar relief. That is similar to tectonically active sites where the slope threshold has been reported as a key issue in the control of erosion rates considered the point where the landslides become the main erosional process<sup>5</sup>. The lack of earthquakes and fast uplift appears to be the reason for low erosion rates in this region, but the extreme rainfall events trigger the landslides in Serra do Mar. The correlation between denudation and rainfall is positive, but this correlation is strong and deletes the “slope threshold” when we link rainfall by relief (Fig. 1).

Thus, different catchments erode at different rates, in which the amount of precipitation drives the denudation rates according to a defined topography (relief and slope values), so that the erosion is mainly concentrated in escarpment zones. That's reported also for other wet passive margins<sup>6</sup>, and differs from passive margins under arid climate where escarpments zones and highlands have both very low rates<sup>7</sup>. Therefore, we conclude that landscape is not in steady-state and the climate has a significant role in the landscape changing.

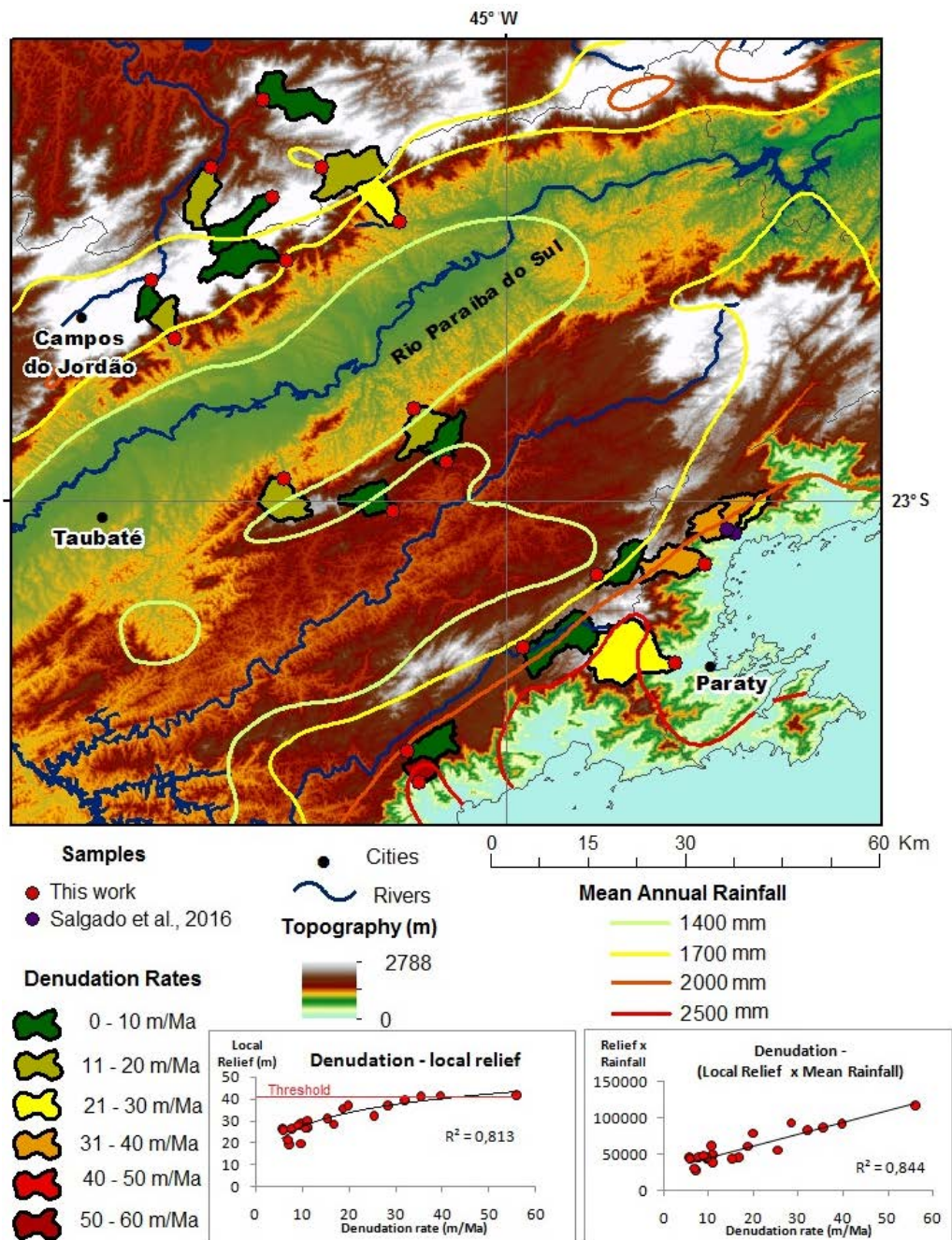


**Figure 1.** Study area map. Plots show the correlation between denudation rate, local relief and mean rainfall.

## References

1. Cobbold, P.R., Meisling, K.E., Mount, V.S., Reactivation of an obliquely rifted margin, Campos and Santos Basins, Southeastern Brazil. *AAPG Bulletin* 85, 1925–1944. (2001).
2. Assumpção, M. Seismicity and stresses in the Brazilian passive margin, *Bull. Seismol. Soc. Am.*, 88, 160–169.3. (1998).
3. Salgado, A.A.R., Rezende, E.d.A., Bourlès, D., Braucher, R., Silva, J.R.d., Garcia, R.A., Relief evolution of the Continental Rift of Southeast Brazil revealed by *in situ*-produced  $^{10}\text{Be}$  concentrations in river-borne sediments, *Journal of South American Earth Sciences* (2016), doi: 10.1016/j.jsames.2016.02.002.
4. Granger D.E., Kirchner J.W., Finkel R., 1996. Spatially averaged long-term erosion rates measured from in-situ-produced cosmogenic nuclides in alluvial sediment. *The journal of Geology*, 104, 249-257.
5. Montgomery, D.R., Brandon, M.T., 2002. Topographic controls on erosion rates in tectonically active mountain ranges. *Earth Planet. Sci. Lett.* 201, 481–489.
6. Vanacker, V., von Blanckenburg, F., Hewawasam, T., Kubik, P.W., 2007. Constraining landscape development of the Sri Lankan escarpment with cosmogenic nuclides in river sediment. *Earth Planet. Sci. Lett.* 253, 402–414.
7. Bierman, P.R., Caffee, M., 2001. Slow rates of rock surface erosion and sediment production across the Namib Desert and escarpment, southern Africa. *Am. J. Sci.* 301, 326–358.

# Long-term evolution of the western South Atlantic passive continental margin in a key area of SE Brazil revealed by thermokinematic numerical modeling

Christian Stippich<sup>1</sup>, Florian Krob<sup>1</sup>, Ulrich A. Glasmacher<sup>1</sup>, Peter C. Hackspacher<sup>2</sup>  
1 *Institute of Earth Sciences, Heidelberg University, Im Neuenheimer Feld 234, 69120 Heidelberg, Germany,*  
2 *Instituto de Geociências e Ciências Exatas da Universidade Estadual Paulista - IGCE/UNESP, Rio Claro, Brasil*  
(christian.stippich@geow.uni-heidelberg.de)

The aim of the research is to quantify the long-term evolution of the western South Atlantic passive continental margin (SAPCM) in SE-Brazil. Excellent onshore outcrop conditions and extensive pre-rift to post-rift archives between São Paulo and Laguna allow a high precision quantification of exhumation, and rock uplift rates, influencing physical parameters, long-term acting forces, and process-response systems. Research will integrate published<sup>1</sup> and partly published thermochronological data from Brazil, and test lately published new concepts on causes of long-term landscape and lithospheric evolution in southern Brazil. Six distinct lithospheric blocks (Laguna, Florianópolis, Curitiba, Ilha Comprida, Peruipe and Santos), which are separated by fracture zones<sup>1</sup> are characterized by individual thermochronological age spectra. Furthermore, the thermal evolution derived by numerical modeling indicates variable post-rift exhumation histories of these blocks. In this context, we will provide information on the causes for the complex exhumation history of the Florianópolis, and adjacent blocks.

The climate-continental margin-mantle coupled process-response system is caused by the interaction between endogenous and exogenous forces, which are related to the mantle-process driven rift – drift – passive continental margin evolution of the South Atlantic, and the climate change since the Early/Late Cretaceous climate maximum. Special emphasis will be given to the influence of long-living transform faults such as the Florianópolis Fracture Zone (FFZ) on the long-term topography evolution of the SAPCM's. A long-term landscape evolution model with process rates will be achieved by thermo-kinematic 3-D modeling (software code PECUBE<sup>2,3</sup> and FastScape<sup>4</sup>). Testing model solutions obtained for a multidimensional parameter space against the real thermochronological and geomorphological data set, the most likely combinations of parameter rates, and values can be constrained. The data and models will allow separating the exogenous and endogenous forces and their process rates.

## References

1. Karl, M., Glasmacher, U.A., Kollenz, S., Franco-Magalhaes, A.O.B., Stockli, D.F., Hackspacher, P., 2013. Evolution of the South Atlantic passive continental margin in southern Brazil derived from zircon and apatite (U-Th-Sm)/He and fission-track data. *Tectonophysics*, Volume 604, Pages 224-244.
2. Braun, J., 2003. Pecube: A new finite element code to solve the 3D heat transport equation including the effects of a time-varying, finite amplitude surface topography. *Computers and Geosciences*, v.29, pp.787-794.
3. Braun, J., van der Beek, P., Valla, P., Robert, X., Herman, F., Goltzbacj, C., Pedersen, V., Perry, C., Simon-Labric, T., Prigent, C. 2012. Quantifying rates of landscape evolution and tectonic processes by thermochronology and numerical modeling of crustal heat transport using PECUBE. *Tectonophysics*, v.524-525, pp.1-28.
4. Braun, J. and Willett, S.D., 2013. A very efficient, O(n), implicit and parallel method to solve the basic stream power law equation governing fluvial incision and landscape evolution. *Geomorphology*, v.180-181, 170-179.

# The evolution of Baffin Island: an integrated apatite fission track and apatite (U-Th)/He study

Scott Jess<sup>1</sup>, Randell Stephenson<sup>1</sup>, Roderick Brown<sup>2</sup>

*1 School of Geosciences, University of Aberdeen, Aberdeen, AB24 3UE, UK.*

*2 School of Geographical and Earth Sciences, University of Glasgow, Glasgow, G12 8QQ, UK.*

*(r01sj14@abdn.ac.uk)*

The passive margins of the North Atlantic continue to be an area of great geological and geomorphological debate, as the timing of major tectonic events, in various locations, remains undefined. The West Greenland margin, on the eastern flank of Baffin Bay, is believed to have experienced tectonic uplift throughout the Neogene in three major pulses (36-30Ma, 11-10Ma & 7-2Ma)<sup>1</sup>. However, Baffin Island, on the western flank, is considered to have undergone a slow protracted cooling history and little tectonic activity since the Mesozoic<sup>2</sup>.

The present work investigates the thermal evolution of Baffin Island in greater detail through the expansion of a published apatite fission track (AFT) study, from the Cumberland Peninsula, with the addition of a suite of apatite (U-Th)/He (AHe) ages. Increasing the available thermochronological data from the region is anticipated to improve the understanding of the recent geological history and will apply the 'Broken Crystals' technique<sup>3</sup> in the expectation of obtaining greater constraints on thermal modelling in an area dominated by AHe dispersion. Apatites from the previous study are all sourced from Archaean aged rocks that present high levels of dispersion and create great difficulty in establishing effective thermal histories. This novel approach is believed to aid the modelling of dispersed AHe data by utilising fragments of grains that have been broken along their weak basal cleavage.

Results from this work will contribute to a greater understanding of Baffin Island's shallow crust, the timing of cooling events and the extent of its erosion. The region records major tectonic activity offshore in the early Palaeocene and further afield in the North Atlantic which could play a pivotal role in the margin's development. Understanding how these major tectonic controls interact with the Canadian passive margin could help in interpreting post-rift histories for other North Atlantic margins.

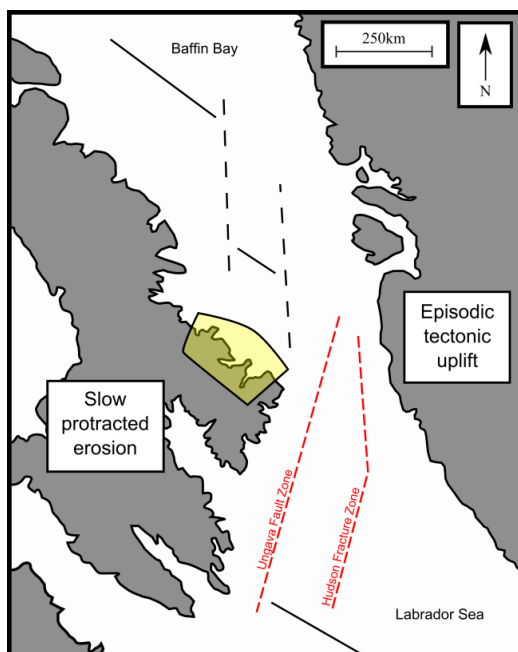


**Figure 1.** Map of study area with location of previous AFT work highlighted in yellow. The two margins of Baffin Bay are separated by a region of structural importance with two major fault zones (the Ungava and Hudson) connecting spreading in the Labrador Sea and Baffin Bay.



## References

1. Japsen, P., Bonow, J.M., Green, P.F., Chalmers, J.A. & Lidmar-Bergstrom, K. 2006, "Elevated, passive continental margins: Long-term highs or neogene uplifts? New evidence from West Greenland", *Earth and Planetary Science Letters*, vol. 248, no. 1-2, pp. 330-339.
2. McGregor, E.D., Nielsen, S.B., Stephenson, R.A., Petersen, K.D. & MacDonald, D.I.M. 2013, "Long-term exhumation of a Palaeoproterozoic orogen and the role of pre-existing heterogeneous thermal crustal properties: a fission-track study of SE Baffin Island", *Journal of the Geological Society*, vol. 170, no. 6, pp. 877-891.
3. Brown, R.W., Beucher, R., Roper, S., Persano, C., Stuart, F. & Fitzgerald, P. 2013, "Natural age dispersion arising from the analysis of broken crystals. Part I: Theoretical basis and implications for the apatite (U-Th)/He thermochronometer", *Geochimica et Cosmochimica Acta*, vol. 122, pp. 478-497.

## **Quantifying uplift and denudation of a heterogeneous crust; a detailed multi-thermochronometric study of central west Britain**

Katarzyna Łuszczak<sup>1</sup>, Cristina Persano<sup>1</sup>, Finlay M. Stuart<sup>2</sup>

*1 School of Geographical and Earth Sciences, University of Glasgow, Glasgow, UK*

*2 Isotope Geosciences Unit, SUERC, East Kilbride, UK*

*(k.luszczak.1@research.gla.ac.uk)*

Quantifying the amount, timing and rate of rock uplift and denudation is crucial for unravelling the interplay between deep and surface process. Thermochronometry can be used to determine cooling histories of rocks, but quantifying the amount of denudation requires estimation of the geothermal gradient. Although efforts have been made to predict the effect of changes in the basal heat flow and fluid circulation on the upper crust geothermal gradient, little attention has been paid to the role of the crustal heat production and the thermal conductivity of the rocks that are being denuded. Also overlooked is the influence of density variation on the isostatic response of the crust to denudation and, therefore, total rock uplift.

The amount of early Palaeogene denudation of Britain is controversial<sup>1-4</sup>. Apatite fission track (AFT) data show that rocks now exposed in the English Lake District were at  $>110^{\circ}\text{C}$  in the early Palaeogene<sup>1,2</sup>, which requires  $>3$  km of denudation for a geothermal gradient of  $30^{\circ}\text{C}/\text{km}$ . These estimates are at odds with stratigraphic reconstructions<sup>5</sup> and modelling of thickness of magmatic underplating<sup>4</sup>. New AFT, and apatite and zircon (U-Th-Sm)/He ages extend the resolution of the thermal histories, and the spatial coverage, embracing the English Lake District, southern Scotland and northern Wales. AFT ages have a 'U-shape' profile with the youngest, 48–75 Ma, in the Lake District increasing to  $>200$  Ma in Scotland and Wales. Combined with the zircon and apatite He ages, this pattern requires early Palaeogene temperatures of  $110$ – $130^{\circ}\text{C}$  in the Lake District decreasing to  $\sim 60^{\circ}\text{C}$  north and south. We have used a numerical model to constrain the thermal effect of heat producing granite batholith in the Lake District beneath blanketing layers of low thermal conductivity sedimentary rocks. Denudation varies from 1.5 to 2.2 km on the south coast of Scotland and in the Lake District to less than 1.5 km in southern Scotland and northern Wales (Fig. 1). This pattern mirrors the spatial variation in thickness of magmatic underplating<sup>6,7</sup> (Fig. 1). The amount of denudation driven by permanent uplift due to underplating has been computed taking the density of the uplifted rocks and the palaeo-topography into consideration; in every location, these estimates are lower than those derived from the thermochronometric data. The difference between the two estimates is constant across the region, and translates into  $355 \pm 115$  m of tectonic uplift. The magnitude and long-wavelength character of this uplift component suggest that it was produced by transient, thermal and/or dynamic support from the mantle plume. The combination of thermal and underplating-derived uplift can explain the amount of denudation predicted by the thermochronometric data (Fig. 1), without invoking any other mechanism, such as intra-plate stresses, which has been suggested in the past as a main cause of the Cenozoic denudation<sup>8</sup>. The suggestion that the uplift is solely of mantle plume origin is also supported by the spatial distribution of denudation, which resembles a dome, with gentle changes across the landscape, without an evident reactivation of pre-existing structures.

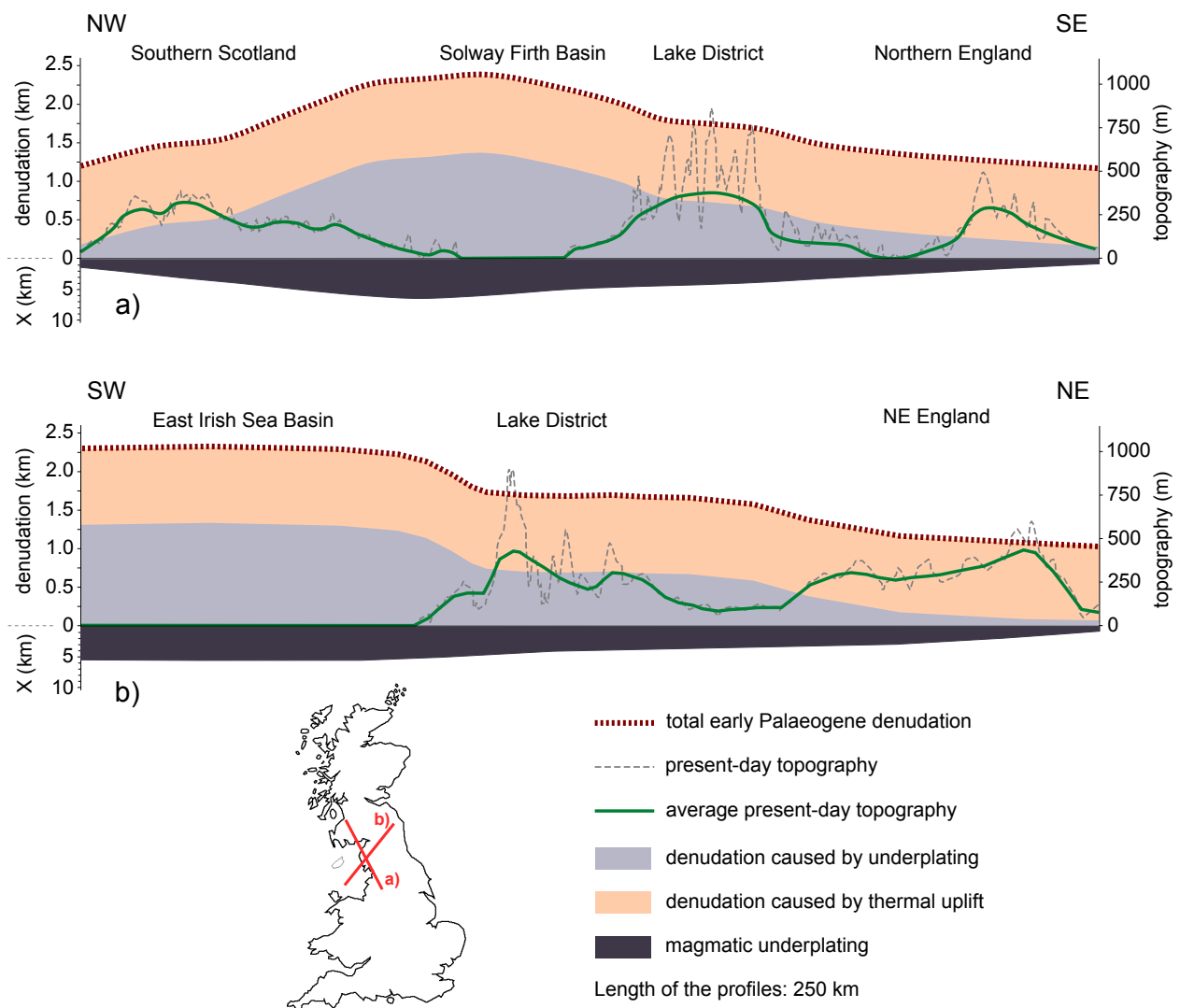


**Figure 1.** Two cross sections, NW-SE and SW-NE, showing the amount of early Palaeogene denudation juxtaposed to the present-day topography (after GoogleEarth data) and thickness of magmatic underplating (after the underplating map of Tomlinson et al.<sup>7</sup>). The map below shows the locations of the cross section lines.

## References

- Green, P. F. On the thermo-tectonic evolution of northern England: evidence from fission track analysis. *Geological Magazine* **123**, 493–506 (1986).
- Lewis, C. L. E., Green, P. F., Carter, A. & Hurford, A. J. Elevated K/T palaeotemperatures throughout northwest England: three kilometres of Tertiary erosion? *Earth and Planetary Science Letters* **112**, 131–145 (1992).
- Green, P. F. Early Tertiary paleo-thermal effects in northern England: reconciling results from apatite fission track analysis with geological evidence. *Tectonophysics* **349**, 131–144 (2002).
- Tiley, R., White, N. & Al-Kindi, S. Linking Paleogene denudation and magmatic underplating beneath the British Isles. *Geological Magazine* **141**, 345–351 (2004).
- Holliday, D. W. Mesozoic cover over northern England: interpretation of apatite fission track data. *Journal of the Geological Society* **150**, 657–660 (1993).
- Al-Kindi, S., White, N., Sinha, M., England, R. & Tiley, R. (2003), ‘Crustal trace of a hot convective sheet. *Geology* **31**, 207–210 (2003).
- Tomlinson, J. P., Denton, P., Maguire, P. K. H. & Booth, D. C. Analysis of the crustal velocity structure of the British Isles using teleseismic receiver functions. *Geophysical Journal International* **167**, 223–237 (2006).
- Holford, S. P., Green, P. F., Duddy, I. R., Turner, J. P., Hillis, R. R. & Stoker, M. S. Regional intraplate exhumation episodes related to plate-boundary deformation. *Geological Society of America Bulletin* **121**, 1611–1628 (2009).

## **Preliminary Apatite Fission Track Ages from NW-Mozambique Precambrian Shield, Africa**

Marcos Müller Bicca<sup>1</sup>, Andrea Ritter Jelinek<sup>2</sup>, Ruy Paulo Philipp<sup>3</sup>

*1 Instituto de Geociências – Universidade Federal do Rio Grande do Sul, Campus do Vale. Av. Bento Gonçalves, 9500, Porto Alegre, Rio Grande do Sul, CEP 91509-900, Brazil*

*2 Instituto de Geociências – Universidade Federal do Rio Grande do Sul, Campus do Vale. Av. Bento Gonçalves, 9500, Porto Alegre, Rio Grande do Sul, CEP 91509-900, Brazil*

*3 Instituto de Geociências – Universidade Federal do Rio Grande do Sul, Campus do Vale. Av. Bento Gonçalves, 9500, Porto Alegre, Rio Grande do Sul, CEP 91509-900, Brazil*

*(marcos.mb83@gmail.com)*

The study of exhumation and landscape evolution of Precambrian belts and platforms using low temperature thermochronological methods has become a robust tool for the improvement of regional tectonic models. This study was developed in northwest Mozambique which is formed by a complex Precambrian belt of dominantly Mesoproterozoic and Neoproterozoic ages, that record important moments of the tectonic evolution of Rodinia and Gondwana supercontinents, from its early stages during assemblage until their breakup. This belt is segmented by a series of ductile crustal scale E-W, N-S, NW-SE structures, reactivated in a brittle regime during the Phanerozoic, caused by far compressive stress fields in the south-southwestern margin of Gondwana. These reactivations led to block subsidence and development of grabens and half-grabens that hosts the volcano-sedimentary sequences assigned to the Karoo Supergroup and younger deposits, which comprise magmatic and sedimentary associations of the Great East African Rift System.

The aim of this study was to identify distinct tectonic reactivation episodes by determining the thermal ages and denudation rates of these Precambrian rocks, which contributed to the sedimentation basins intracratonic housed in grabens oriented E-W and NW-SE and associate it with regional tectonic processes. Therefore, we collected 17 rock samples from Mozambican shield, distributed in a NW-SE and NE-SW oriented transects, in order to comprise the main regional structures.

Preliminary data allowed the identification of thermal ages from Middle Triassic ( $239 \pm 15$  Ma) to Upper Cretaceous ( $85 \pm 9$  Ma), correlated to important regional and local tectonic activity. The mean confined track lengths obtained from 12 samples range from  $7.11 \pm 0.31 \mu\text{m}$  a  $12.28 \pm 0.19 \mu\text{m}$  with standard deviation of  $2.57 \mu\text{m}$  and  $1.95 \mu\text{m}$ , respectively. Overall, the ages are much younger than the stratigraphic age of the rocks sampled indicating that intense exhumation processes affected the region during the Mesozoic Era. The confined track length distributions indicate that the samples register a long residence time within the partial annealing zone. The older ages are situated close to the latter stages of the Cape Fold Belt tectonic activity, which was related to the subduction of the Panthalassa seafloor, and may represent cooling episodes caused by erosion and denudation associated with tectonic reactivations induced by a far stress field crustal propagation. During Lower Jurassic the region was affected by the thermal activity of the Karoo magmatism in the early stages of Gondwana breakup and may represent punctual thermal changes associated with thermal uplift and intrusion of contemporaneous dykes. The youngest ones represent exhumation processes related to rift flanks uplift in response to Gondwana breakup which affected the East African margin and also by early extensional stages of the Great East African Rift System.

# Plateau erosion and ridge preservation: differential erosion or tectonic reactivation in the Mantiqueira Range, SE Brazil.

Leandro Duque<sup>1</sup>, Miguel Tupinambá<sup>1</sup>

1 Tektos - Geotectonic research group, Faculty of Geology, Rio de Janeiro State University, Brazil  
(ledoliveira@yahoo.com.br)

Based on fission tracks age (Gallagher et al, 1995; Hackspacher et. al., 2007; Cogné et al, 2011; Jelinek et al., 2014) it is safe to say that the Mantiqueira Range had at least four phases of thermal cooling that began in the Early Cretaceous rift in the context of the supercontinent Gondwana, followed by a thermal cooling in the Late Cretaceous and Paleogene in another. AHE samples (Cogné, 2011) show a new uplift in the Neogene.

However, all these phases of thermal cooling were felt in different way in southern and northern Mantiqueira Range. While the first was raised to ever higher altitudes, reaching 2700m, the second suffered a setback erosive leveling it to between 1000 and 1200 m of altitude and distancing it from its original escarpment. The serrano alignment of Mantiqueira Range extends from São Paulo State to the border with the Espírito Santo State. Between São Paulo and the Massif Itatiaia, the mountain is characterized by a predominant direction of fault line scarp N60E. The massif on the escarpment gives way to a staggered relief, whose lower level is the high Pomba River depression, with a story that still needs to be better positioned within the Cenozoic evolution of southeastern Brazil.

Ages  $^{39}\text{Ar}/^{40}\text{Ar}$  in weathering profiles (Carmo, 2005) positioned the depression in the Miocene, 5 My and one Fission Track age (Carmo, 2005) in the Late Cretaceous, 96Ma. Younger age by Luminescence (Oliveira et al, 2014) pointed Holocene ages for the older sedimentation, 11.7 My. So there is a gap between the upper Cretaceous and Miocene that needs to be filled.

Inside the depression there are compartments that indicate it is a stabilized environment and evolved from morphogenetic point of view, with gentle topography, developed soil profiles, extensive river plains and the absence of current scars of mass movements. On the other hand, it shows compartment indicating a still active erosion. The valleys are closed with steep topography and signs of recent mass movements. The physiography of compartments indicates not only link with erosion, but also indicates subordination to tectonic events, with the landscape following the regional structures of the Boa Vista ridge, higher orographic feature and highlighted on a regional scale. The continuity of Mantiqueira Range that was segmented by Pomba River.

To try to clarify the origin of Pomba River depression five samples were collected for Apatite Fission Track, making a vertical profile in the Boa Vista ridge and five samples AHE in same points to clarify events that have happened after the Late Cretaceous, possibly in the Neogene. To date, samples for Fission Track were undated, are awaiting the etched attack. And the apatite samples (U-Th)/He still need to be concentrated.

## References

1. Carmo, I.O. Geocronologia do intemperismo cenozoico no Sudeste do Brasil. *Tese de doutorado*. Universidade Federal do Rio de Janeiro. Departamento de Geologia, 2004.
2. Cogné, N; Gallagher, K; Cobbold, P.R. Post-rift reactivation of the onshore margin of southeast Brazil: Evidence from apatite (U-Th)/He and fission-track data. *Earth and Planetary Science Letters*, v. 309, n. 1, p. 118-130, 2011.
3. Gallagher, Kerry. Evolving temperature histories from apatite fission-track data. *Earth and Planetary Science Letters*, v. 136, n. 3, p. 421-435, 1995.
4. Hackspacher, P. C., de Godoy, D. F., Ribeiro, L. F. B., Neto, J. C. H., & Franco, A. O. B. (2007). Modelagem térmica e geomorfologia da borda sul do Cráton do São Francisco: termocronologia por traços de fissão em apatita. *Brazilian Journal of Geology*, 37(4), 76-86.

5. Oliveira, L.A.F.; Magalhaes, J.A.P.; Lima, F.B.S.; Carvalho, A. 2014. Fatores condicionantes da configuração de fundos de vale colmatados no Alto-Médio Rio Pomba, leste de Minas Gerais. *Revista Brasileira de Geomorfologia*, v.15(4).

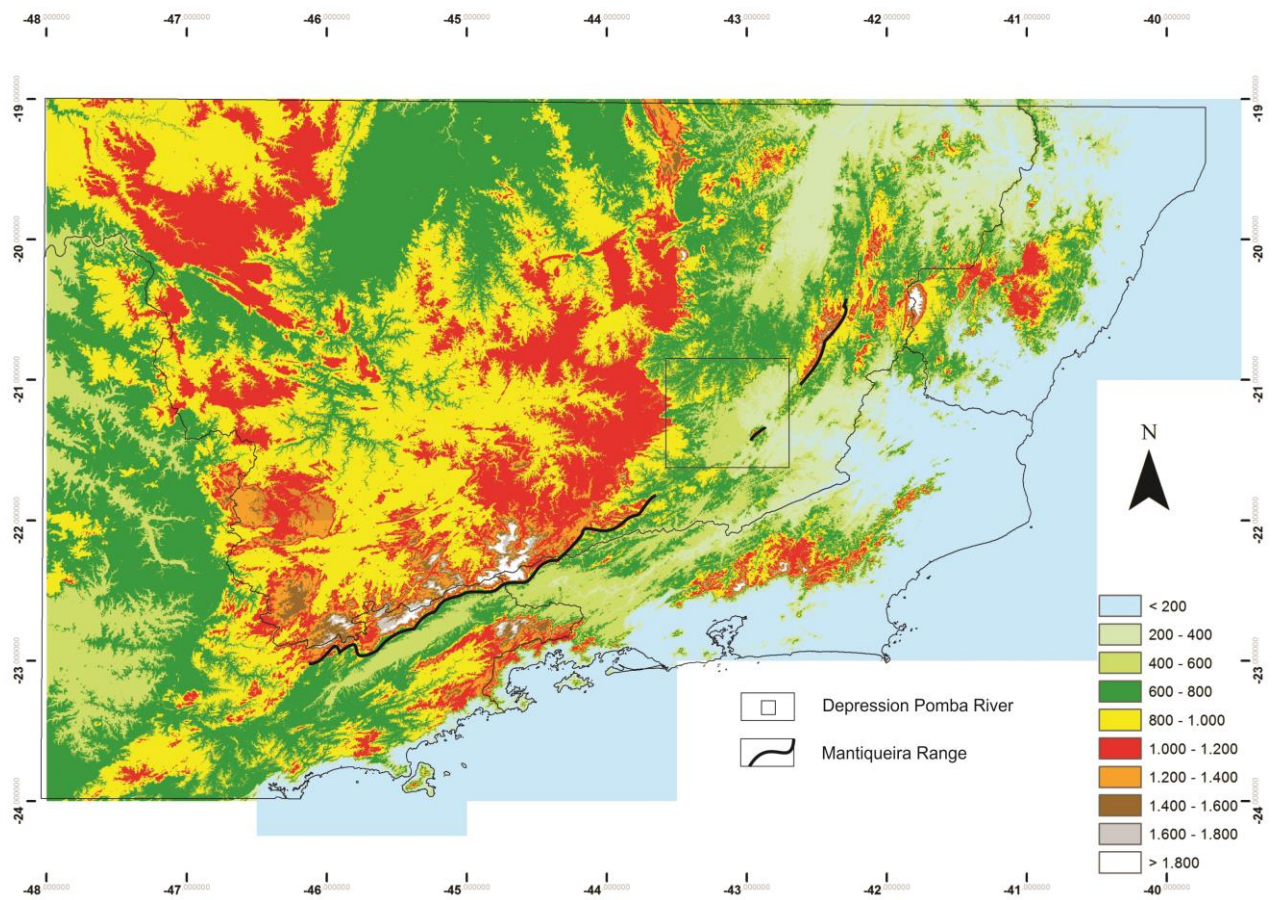


Figure 1 Hypsometry of southeastern Brazil highlighting the Mantiqueira Range and study area.

# Evaluating post-rift vertical displacements of southeastern Brazil passive margin using granophyric diabase dykes as depth indicator

S Miguel Tupinambá<sup>1</sup>, Monica Heilbron<sup>1</sup>

1 Tektos - Geotectonic research group, Faculty of Geology, Rio de Janeiro State University, Brazil  
(tupi@uerj.br)

In a first attempt to estimate crustal post-rift vertical displacements at the southeastern Brazil continental margin<sup>1</sup>, F. F. Almeida, an outstanding Brazilian geocientist, noticed a topographic difference of 11 km between the Santos Basin basement and the peaks of the Serra do Mar. He also suspected that post-Cretaceous erosion and uplift could have wiped out flood basalts from the coastal area<sup>2</sup>. In this paper we test Almeida's values of vertical displacement using Cretaceous granophyric diabase dykes as depth indicators.

The occurrence of granophyres or granophyric intergrowths in basalt magma is constrained by a low-pressure crystallization condition (1 bar)<sup>3</sup>, and is only possible in near surface environments. Therefore, granophyric diabase dykes can be used as reliable paleosurface markers.

In SE Brazil onshore continental margin, granophyric Cretaceous basalt dykes were described in different topographic situations. The highest ones (600m a.s.l.) belong to a NE trending dike swarm near the city of Carmo (Rio de Janeiro State) where granophyric rocks were described<sup>4</sup>. The dikes have thickness of tens of meters and are composed by medium to coarse grained dolerites and gabbros with clinopyroxene and plagioclase (labradorite) in an interstitial texture. Granophyric intergrowths were observed within intergranular spaces of plagioclase laths. A K/Ar determination made on a thin dolerite gives an age of 126 +/- 2 Ma<sup>5</sup>. Coarse grained facies of the dikes yield a plagioclase K/Ar age of 132 +/- 6 Ma<sup>6</sup>. The lowest ones (sea level) are located at the São Paulo State Coast, in Ubatuba. The Toninhas diabase dyke<sup>7</sup>, with 30 m thick, has a core with granophyre and thin bands of granophyric diabase. Its K/Ar age is 135 +/- 6 Ma<sup>8</sup>.

In the offshore portion of the margin, the lowest segment of the Campos Marginal Basin, the São João da Barra Low, reaches a depth of 9000 m<sup>9</sup>. The economic basement of the Campos Basin is represented by basalts with clear volcanic structures and textures<sup>10</sup>, with a K/Ar age of 126 +/- 2 Ma<sup>11</sup>.

Therefore, during the Lower Cretaceous basaltic shallow intrusive dykes and volcanics were in similar crustal level. At the Present, their onshore erosional and covered offshore remnants are vertically displaced by 9600 meters. The horizontal distance between the highest and lowest markers is almost 300 km.

## References

- 
- <sup>1</sup> Almeida, F.F.M. De - 1976 - The system of continental rifts bordering the Santos Basin, Brazil. *Anais Acad. Bras. Cienc.* **48** (supl.): 15-26.
  - <sup>2</sup> Almeida, F.F.M. De - 1983 - Relações tectônicas das rochas alcalinas mesozóicas da região meridional da Plataforma Sul-Americana. *Rev. Bras. Geoc.* **13** (3): 139-158.
  - <sup>3</sup> Bellieni, G.; Comin-Chiaramonti, P.; Marques, L.S.; Melfi, A. J.; Piccirillo, E.M. & Stofa, D. - 1984 - Low-pressure evolution of basalt sills from bore-holes in the Paraná Basin (Brazil). *TMPM*, **33**, 25-47
  - <sup>4</sup> Conceição, J.R. De; Zalan, P.V. & Wolff, S. - 1988 - Mecanismo, evolução e cronologia do rift sul atlântico. *Bol Geoc. Petrobrás*, **2** (2/4): 255-265.
  - <sup>5</sup> Asmus, H.E. - 1975 - Controle estrutural da deposição meso-cenozóica nas bacias de margem continental brasileira. *Rev. Bras. Geoc.* **5** (3): 160-175.

- 
- <sup>6</sup> Nurnberg, D. & Muller, R.D. - 1991 - The tectonic evolution of the South Atlantic from late Jurassic to present. *Tectonophysics* 191: 27-53.
- <sup>7</sup> Gomes, C.B. & Berenholc, M. - 1980 - Some geochemical features of the Toninhas dike, Ubatuba, State of Sao Paulo, Brazil. *An. Acad. Bras. Cienc.* **52** (2):339-346.
- <sup>8</sup> Damasceno, E.C. - 1966 - Estudo preliminar dos diques de rochas básicas e ultrabásicas da região de Ubatuba, Estado de São Paulo. *An. Acad. Bras. Cienc.* 38 (2): 293-304.
- <sup>9</sup> Dias, J.L.; Guazelli, W.; Catto, A.J. & Vieira, J.C. - 1987 - Integração do arcabouço estrutural da bacia de Campos com o embasamento Pré-Cambriano adjacente. in SIMPOSIO DE GEOLOGIA REGIONAL RJ-ES, 1, Rio de Janeiro. *Anais... SGB/RJ/ES*: 189-197
- <sup>10</sup> Mizusaki, A.M.; Thomaz Filho, A. & Valença, J. - 1988 - Volcano sedimentary sequence of neocomian age in Campos Basin (Brazil). *Rev. Bras. Geoc.* **18** (3): 247-251.
- <sup>11</sup> Misuzaki, A.M.P.; Petrini, R.; Bellieni, G.; Comin-Chiaramonti, P.; Dias, S.J.; De Min, A. & Piccirillo, E. - 1992 - Basalt magmatism along the passive continental margin of SE Brazil (Campos Basin). *Contr. Mineral Petrol.* 111: 143-160.
- Bellieni, G.; Comin-Chiaramonti, P.; Marques, L.S.; Melfi, A.J.; Piccirillo, E.M. & Stolfa, D. - 1984 - Low-pressure evolution of basalt sills from bore-holes in the Paraná Basin (Brazil). *TMPM*, 33, 25-47.



## Low-Temperature Thermochronology in Alkaline Intrusions Areas Brazilian Southeast.

Carolina Doranti-Tiritan<sup>1</sup>, Peter C. Hackspacher<sup>1</sup>, Marli Carina S. Ribeiro<sup>1</sup>, Ulrich A. Glasmacher<sup>2</sup>

<sup>1</sup>*Institute of Geosciences and Exact Sciences (IGCE), São Paulo State University, Rio Claro-SP Brazil*

<sup>2</sup>*Institute of Earth Sciences, Heidelberg University, Im Neuenheimer Feld 234, 69120 Heidelberg, Germany  
(cadoranti@gmail.com)*

The Late Cretaceous is recognized as the most important period for the emplacement of alkaline complexes in South America, and thermochronological study of these complexes, together with other geological data, is fundamental to understand their role in the evolution of the South American Platform. Alkaline intrusions are distributed from the southeast Brazilian coast to the interior of the territory. The landscape evolution is associated with several distinct exhumation events at the South American passive continental margin<sup>1</sup>. The present study sets out to better understand the configuration of the long-term landscape evolution of the southeast Brazilian highlands, providing insights on the behaviour of the coupled magmatic tectonic-erosional system, comparing thermochronological data from two alkaline intrusions, Poços de Caldas Alkaline Massif (PCAM), São Sebastião Island (SSI), the Passa Quatro Alkaline Complex (PQAC) and Itatiaia alkaline complex (ITAC).

The PCAM is the biggest alkaline structure located in the interior of the continent, 300km from the coastline (Rio de Janeiro). The structure is formed as a caldera, covering over 800km<sup>2</sup>, intruding Precambrian basement around 83Ma<sup>2</sup>. The author described intermediate rocks as nepheline syenites, phonolites and tinguaites intruded in a continuous and rapid sequence lasting between 1 to 2 Ma. Meanwhile, the SSI (236km<sup>2</sup>) is located at the coast, 200 km southeast of the city of São Paulo and is characterized by an intrusion in Precambrian granitic-gnaissic rocks affected by the Panafrican/Brazilian Orogen. This crystalline basement is intruded by Early Cretaceous subalkaline basic and acid dykes, as well as by Late Cretaceous alkaline stocks (syenites) and dykes (basanite to phonolite). The Early and Late Cretaceous magmatic activities occurred, respectively, before and after the Africa-South America continental break-up and formation of the ocean crust<sup>3</sup>.

The ITAC is 220 km<sup>2</sup> and is located on the boundary between the states of Rio de Janeiro and Minas Gerais. This also intrudes into the Precambrian basement, which is represented by the Juiz de Fora metamorphic complex<sup>4</sup>. The ITAC is structurally linked to the SE Brazilian continental rift, which developed in an ENE to EW trending transcurrent system by the end of the Brasiliano-Pan African Cycle and which was reactivated during the breakup of Gondwana<sup>5</sup>. The alkaline complex is composed of syenites, foyaites, pulaskites, quartz syenites, magmatic breccias and alkaline granite<sup>6</sup>. The mean K-Ar age obtained on ten biotites from the Itatiaia rocks is 70.5 ± 3.3 Ma<sup>7</sup>. Although, PQAC is 148 km<sup>2</sup>, is close to the ITAC. The K-Ar age obtained on only one sample of amphibole separated from a nepheline syenite is 67 ± 3 Ma<sup>8</sup>. The Rb-Sr age (whole rock) determined was 70.4 ± 0.5 Ma<sup>9</sup>. Several factors, such as geomorphology, similar age and petrology, and the close relative location, suggest that the Passa Quatro and the Itatiaia complexes are comagmatic<sup>8</sup>.

The Apatite Fission-Track ages for PCAM range from 333.3±27.6 to 94.0±13.7 Ma at the surrounded metamorphic basement area, and 76.8±10.9 to 48.7±10.7 Ma in the alkaline Massif. The older ages, are concentrated on the lower topography region (700 until 1200m) in the north side alkaline massif. In the SSI area 7 apatite fission track results are available, two from the crystalline basement (121.1±11.5 Ma and 49.4±4.8) and 5 from the alkaline stocks (112.5±13; 91.1±11.2Ma; 89.4±13.4 88.2±8.5; 71.3±7.9). Only 3 samples from PCAM has enough length measurements for

numerical modelling and 2 samples from SSI. The results show that the main difference between the areas is that PCAM region register older history then the coastal area of SSI, where thermal history starts register cooling event after the South Atlantic rifting process, while in the PCAM area register a previous history, since Carboniferous. The short mean track lengths in PCAM compared with the longer mean track lengths of SSI, confirm this thermal history evolution differences between both areas. Ages from PQAC and IAC are from the Eocene (ranging from  $42\pm 3$  to  $51.6\pm 8,4$ ), being very similar with the PCAM alkaline region. The age-elevation relationship shows that the ages decrease systematically with increasing elevation with a break-in-slope near the 150Ma, 80Ma and around 50Ma, which means that the landscape evolution can be associated with several distinct exhumation events at the South American passive continental margin, which include the Gondwana break-up, the Late Cretaceous alkaline magmatism, and the Cenozoic evolution of a N-S trending continental graben system.

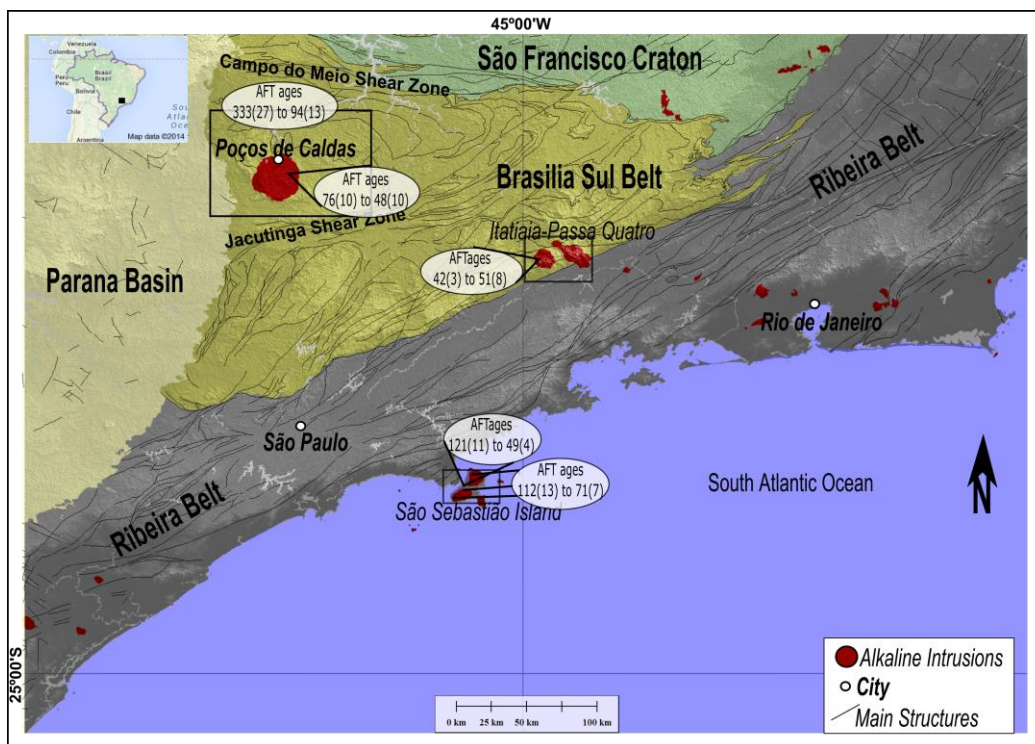


**Figure 1.** Regional geological map with Fission Track Ages distribution on the studied Alkaline Complexes

## References

- <sup>1</sup>Hackspacher P.C., Ribeiro L.F.B., Ribeiro M.C.S., Fetter, A.H., Hadler Neto J.C., S. Tello Saenz, C.A. & Dantas E.L. 2004. Consolidation and break -up of the South American platform in Southeastern Brazil: tectonothermal and denudation histories. *Gondwana Res.*, 7:91101
- <sup>2</sup>Ulbrich, H.H.G.J., Vlach, S.R.F., Ulbrich, M.N.C. and Kawashita, K. (2002) Penecontemporaneous Syenitic-Phonolitic and Basic-Ultrabasic-Carbonatitic Rocks at the Poços de Caldas Alkaline Massif, SE Brazil: Geological and Geochronological Evidence. *Revista Brasileira de Geociências*, 32, 15-26
- <sup>3</sup>G. Bellieni, C.R. Montes-Lauar, A. De Min, E.M. Piccirillo, G. Cavazzini, A.J. Melfi and LG. Pacca, Early and Late Cretaceous magmatism from SBo Sebastib Island (SE Brazil): Geochemistry and petrology, *Geochim. Bras.* 4(1), 59-83, 1990. [ M.J.G. Fonseca, Z.C.G. Silva, D.A. Campos and P. Torsatto, Texto explicativo. Carta geoldgica do Brasil ao Milionsimo. Folhas Rio de Janeiro, Vitdria e Iguape (SF 23/SF 24 e SG 231, DNPM, 1979.
- <sup>4</sup>F.F.M. Almeida and Y. Hasui, 0 Pre-Cambrian0 do Brasil, Bliicher, 1984
- <sup>5</sup>E. Ribeiro Filho, Geologia e petrografia dos' maciqs alcali- nos do Itatiaia e Passa Quatro, *Bol. 302 FFCL-USP* 22, 9-93, 1967.
- <sup>6</sup>G. Amaral, J. Bushee, U.G. Cordani, K. Kawashita and J.H Reynolds, Potassium-argon ages of alkaline rocks from Southern Brazil, *Geochim. Cosmochim. Acta* 31, 117-142, 1967.
- <sup>7</sup>E. Ribeiro Filho and U.G. Cordani, Contemporaneidade das intrudes de rochas sieniticas do Itatiaia, Passa Quatro e Morro Redondo, *Ann. XX Congr. Bras. Geol. (Vitbrial, 1, pp. 62-63, 1966.*
- <sup>8</sup> Montes Lauar C.R., Pacca I.G., Melfi A.J., Kawashita K. 1995. Late Cretaceous alkaline complexes, southeastern Brazil: paleomagnetism and geochronology. *Ear. Planet. Sci. Lett.*, 134:425-440
- <sup>9</sup>F. Penalva, Geologia e tectbnica da regib do Itatiaia, *Bol. 302 FFCL-USP* 22,99-196, 1967.

# Timing and Petrogenesis of the Mesozoic granitoids at Duerji areas, Inner Mongolia and its tectonic implications

SU ZHOU<sup>1</sup>, Ruizhao QIU<sup>2</sup>, Guoqin ZHANG<sup>1</sup> and Cui LIU<sup>1</sup>

*1 China University of Geosciences of Beijing, Beijing, 100083, China*

*2 Development and Research Center, China Geological Survey, Beijing, 100037, China*

*(E-mail of the corresponding author ZHOUSU62@SINA.COM)*

LA-MC-ICP-MS zircon U-Pb dating and geochemical data are reported for three granitoids at Duerji areas in Ulanhot, Inner Mongolia, China, in order to constrain its formation time, petrogenesis and the regional tectonic setting. Located in the south section of the Great Xing'an Range, which is superimposed on the location of ancient Asian and the west coast of the Pacific tectonic domain, Duerji intrusive bodies occur as batholith-like, and consist of monzogranite, granite, alkalic feldspar granite, granite-porphyr, plagioclase-granite, biotite-bearing monzogranites, and biotite-bearing granite, whose main rock type is flesh pink monzogranite. The zircons from the intrusive rocks were dated by the LA-MC-ICP-MS. Three reliable weighted mean ages of <sup>206</sup>Pb/<sup>238</sup>U (131.3±0.25 Ma, MSWD=0.3; 130.5±0.45 Ma, MSWD=3.3 and 213.0±0.7 Ma, MSWD=0.4) respectively were obtained for monzogranite, alkalic feldspar granite and alkalic feldspar granite in various parts of Duerji pluton. Furthermore, two older age information in the two latter samples were also gained, there are (150.2±0.37) Ma, MSWD=0.96 and (238.1±1.8)Ma, MSWD=1.7. Combining with the data of biotite K-feldspar granites (154.5±0.5Ma, U-Pb method, Sihong Jiang et al., 2011), we speculate that Duerji granitoid intrusive body is a composite batholith formed by polyphasic intrusion and three times of magmatic activities at least might have occurred during the Mesozoic era in the district. The Duerji granitoids are characterized by high silic, high alkali, peraluminous and low calcium with SiO<sub>2</sub> of 73.09%~77.26%, Na<sub>2</sub>O+ K<sub>2</sub>O of 7.78%~8.74%, CaO of 0.37%~0.89%. They are K-rich calc alkaline series and peraluminous, enriched in light rare earth elements (LREEs) and large ion lithophile elements (LILEs), but depleted in heavy rare earth elements (HREEs) and high field strength elements (HFSEs). Their values of ε<sub>Hf</sub>(t) from zircon of the Duerji lithological units are about +7.8 for Early Cretaceous rocks and +10 for Triassic rocks, indicating that their primary magmas were derived from partial melting of the juvenile lower crust magma and a diminished fraction of mantle over time.

Acknowledgements: Research supported by the international Science & Technology cooperation Program of China (ISTCP) (2011DFA22460) and China Geological Survey 1212010811066 and 12120113086400).

## References

1. JIANG Si-hong, NIE Feng-Jun, LIU Yi-fei, HOU Wan-rong, BAI Da-ming, LIU Yan, LIANG Qing-ling. Geochronology of intrusive rocks occurring in and around the Mengentaolegai silver-polymetallic deposit. 2011. Inner Mongolia. Journal of Jilin University (Earth Science Edition) (in Chinese with English abstract). 41(6): 1755-1769



**THERMO2016**

**SESSION 8**

**OROGENESIS & LONG-TERM  
LANDSCAPE EVOLUTION**

## (U-Th)/He thermochronometric mapping of NE Japan Arc: Preliminary results

Shigeru Sueoka<sup>1</sup>, Takahiro Tagami<sup>2</sup>, Barry P. Kohn<sup>3</sup>, Shoma Fukuda<sup>2</sup>  
1 Japan Atomic Energy Agency, Fukui 919-1279, Japan  
2 Kyoto University, Kyoto 606-8502, Japan  
3 University of Melbourne, Victoria 3010, Australia  
([sueoka.shigeru@jaea.go.jp](mailto:sueoka.shigeru@jaea.go.jp))

A paradox of deformation in NE Japan Arc is that the short-term deformation observed by geodetic techniques and the long-term deformation estimated from geomorphic and geologic evidence is different in rate and/or direction<sup>1</sup>. Deformation observed by geodetic research consists of elastic deformation released during earthquake cycles and inelastic deformation expended in developing landforms. To separate the two components, the use of geomorphic/geologic techniques is a practical approach to estimate inelastic deformation<sup>2</sup>. We performed apatite and zircon (U-Th)/He (AHe and ZHe) thermochronometric analyses from Cretaceous or early Paleogene granitic rocks along two profiles across NE Japan Arc (Fig. 1) for estimating long-term vertical deformation rates. The northern profile (N-profile) ranges across the Kitakami Mountains, Ou Backbone Range (OBR), and Taihe-Shirakami Mountains, while the southern profile (S-profile) includes the Abukuma Mountains, OBR, and Iide-Asahi Mountains. To date, AHe and ZHe ages of the S-profile and AHe ages of the N-profile have been obtained. AHe ages on the fore-arc side, i.e., Kitakami and Abukuma Mountains, are  $> \sim 50$  Ma, implying a stable tectonic/geologic setting over the Cenozoic. On the other hand, young AHe ages of  $< 10$  Ma were obtained in OBR and the back-arc side, namely Taihe-Shirakami and Iide-Asahi Mountains; the youngest ages are  $\sim 1$  Ma in OBR. These AHe ages can be grouped into three populations of  $\sim 10$  Ma,  $\sim 5$  Ma, and  $< 3$  Ma, which are consistent with different uplift stages of the mountains estimated from provenance analysis of the adjacent basins<sup>3-4</sup>. In addition, sample localities are generally at some distance from high geothermal gradient zones around volcanic centers. Therefore, the AHe ages acquired are interpreted as reflecting a record of uplift and denudation over the last ten million years. On the back-arc side, AHe ages are generally estimated at  $\sim 10$  Ma in the Iide-Asahi Mountains to the south, but at  $\sim 5$  Ma in the Taihe-Shirakami Mountains to the north. Taking into account that uplift of the Asahi Mountains is older than that of the Dewa Hills to the north at  $\sim 5$  Ma<sup>4</sup>, the AHe ages around 10 Ma may indicate the time of initiation of uplift of the Iide-Asahi Mountains. In the OBR and back-arc side, both AHe and ZHe ages tend to yield younger ages from mountain bases to ridges. This observation is in contrast with the case of the Kiso Range<sup>5</sup> and northern Akaishi Range<sup>6</sup>, reverse fault block mountains in SW Japan Arc, where thermochronometric ages young from ridges to the marginal faults. This difference might arise from the existence of the volcanic arc, i.e., horizontal heterogeneity of the thermal structure and/or domal isostatic uplift derived from magmatic intrusions, but this is still debatable. For more detailed constraints on the thermal histories, it is planned to apply other thermochronometers, such as the apatite/zircon fission-track and zircon U-Pb methods, and to conduct additional AHe and ZHe age determinations.

### References

1. Ikeda, Y. Implications of active fault study for the present-day tectonics of the Japan arc. *Active Fault Research* **15**, 93-99 (1996) in Japanese with English abstract.
2. Ikeda, Y. Strain buildup in the Northeast Japan orogen with implications for gigantic subduction earthquakes. *Episodes* **37**, 234-245 (2014).
3. Nakajima, T., Danahra, T., Iwano, H. & Chinzei, K. Uplift of the Ou Backbone Range in Northeast Japan at around 10 Ma and its implication for the tectonic evolution of the eastern margin of Asia. *Palaeogeography, Palaeoclimatology, Palaeoecology* **241**, 28-48 (2006).
4. Moriya, S., Chinzei, K., Nakajima, T. & Danhara, T. Uplift of the Dewa Hills recorded in the Pliocene paleogeographic change of the western Shinjo Basin, Yamagata Prefecture. *Journal of the Geological Society of Japan* **114**, 389-404 (2008) in Japanese with English abstract.

5. Sueoka, S., Kohn, B.P., Tagami, T., Tsutsumi, H., Hasebe, N., Tamura, A. & Arai, S. Denudation history of the Kiso Range, central Japan, and its tectonic implications: Constraints from low-temperature thermochronology. *Island Arc* **21**, 32-52 (2012).
6. Sueoka, S., Kohn, B.P., Ikeda, Y., Kano, K., Tsutsumi, H. & Tagami, T. Uplift and denudation history of the Akaishi Range based on low-temperature thermochronologic methods. *Journal of Geography (Chigaku Zasshi)* **120**, 1003-1012 (2011) in Japanese with English abstract.

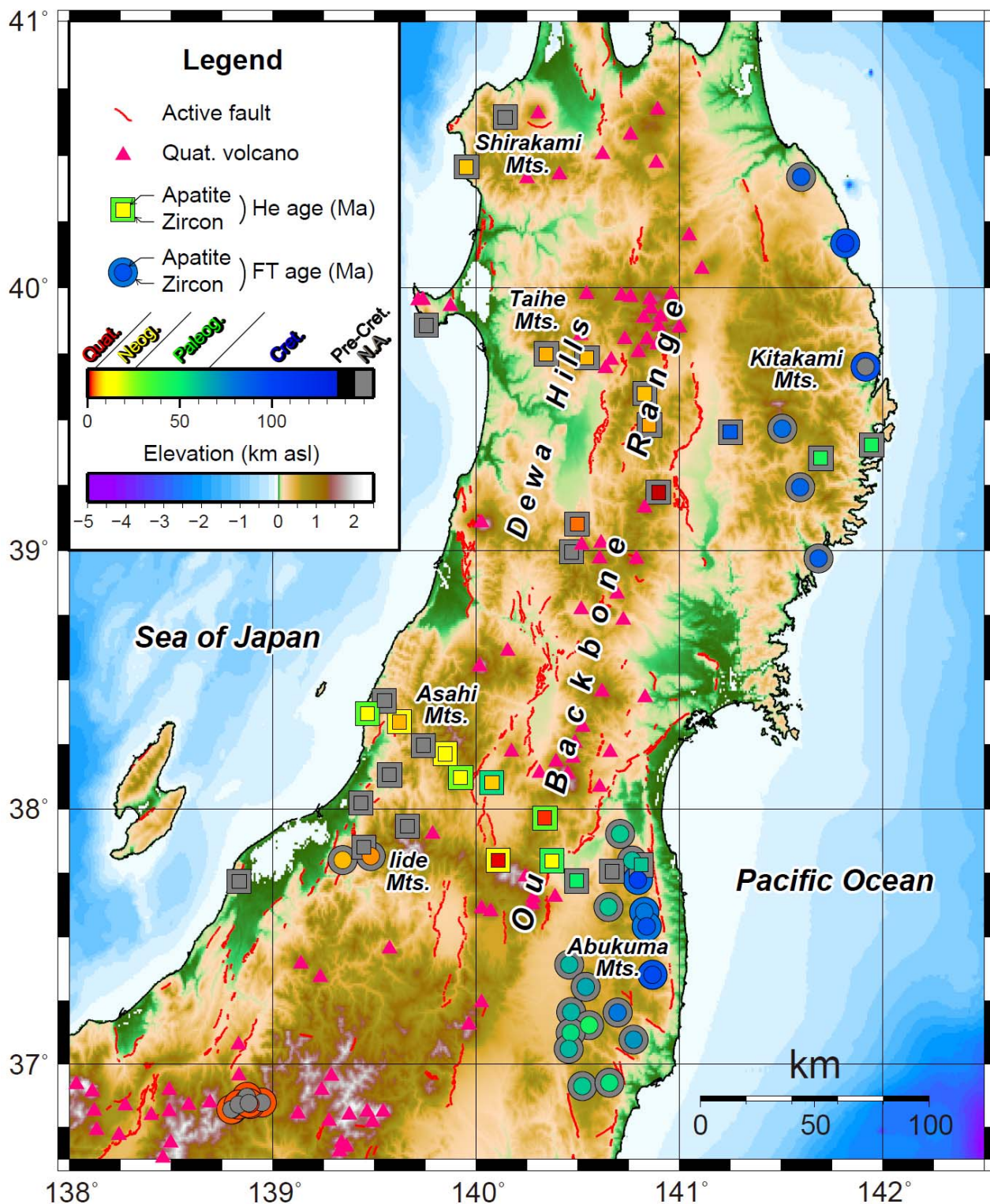


**Figure 1.** Thermochronometric ages of bedrock in the NE Japan Arc. (U-Th)/He ages obtained in this study, whereas fission-track ages were compiled from previous studies.

# Cooling and exhumation history of the Tianfozhishan, Yanji Area, NE China, revealed by fission-track thermochronology

Xiaoming Li, Chuanjun Wu

*Key Laboratory of Mineralogy and Metallogeny, Guangzhou Institute of Geochemistry,  
Chinese Academy of Sciences, Guangzhou, China  
(lixm@gig.ac.cn)*

The Yanji area, northeastern (NE) China, is located at the border of China, Russia and Korea, and was considered as a part of the orogenic collage between North China craton in the south and the Jiamusi-Khanka Massifs in the northeast<sup>1-3</sup> (Fig.1a). The Tianfozhishan is a hill in the Yanji area (Fig.1b), over 1200m above sea level, composed of granite with zircon U-Pb age of  $196 \pm 7$  Ma by LA-ICP-MS method<sup>2</sup>.

In this study, we carried out apatite and zircon fission-track (FT) analyses, to reveal the cooling, and inferred exhumation history of the Tianfozhishan. The measured apatite and zircon FT ages are markedly younger than the formation ages of the host-rocks, representing the cooling ages of the samples during the uplift and denudation processes because of their negligible effects from magmatic or tectonic activities since the Late Cretaceous<sup>1</sup>, and roughly increase with elevation, respectively (Fig.1c). The cooling rate is  $\sim 5^\circ \text{C/Ma}$  in the late Cretaceous by using zircon and apatite “mineral pair” FT ages vs. their closure temperatures. The exhumation rate is  $\sim 0.16 \text{mm/a}$  during  $\sim 100\text{--}96$  Ma, and  $\sim 0.1 \text{mm/a}$  during  $\sim 83\text{--}76$  Ma by using zircon and apatite FT ages vs. difference in elevation, respectively.

All of apatite FT distributions are unimodal with a mean length of  $11.8\text{--}12.9 \mu\text{m}$  and a standard deviation of ca.  $1.7 \mu\text{m}$ , and the mean Dpar values of apatite FT vary from  $(1.5 \pm 0.2) \mu\text{m}$  to  $(2.0 \pm 0.3) \mu\text{m}$ . The modeling time-temperature cooling curves exhibit multi-stages or episodic patterns, including two rapid and one slow cooling since the Late Mesozoic, and are similar to those from Li et al. (2010). However, the exhumation rates of  $\sim 0.16 \text{mm/a}$  during  $\sim 100\text{--}96$  Ma, and of  $\sim 0.1 \text{mm/a}$  during  $\sim 83\text{--}76$  Ma, by using zircon and apatite FT ages vs. difference in elevation, respectively, were less than of  $\sim 0.19 \text{mm/a}$  during  $\sim 95\text{--}80$  Ma, by calculating with the modeling cooling curve and assuming the steady-state geothermal gradient of  $35^\circ \text{C/km}$ . Thus, the paleogeothermal gradient of the Tianfozhishan, even of the Yanji Area, was possibly greater than  $35^\circ \text{C/km}$  in the late Cretaceous.

This work was financially supported by the National Natural Science Foundation of China (Grant Nos. 41072158 and 41372227).

## References

1. Jilin Bureau of Geology and Mineral Resources (JBGMR). *Regional Geology of Jilin Province* (Geological Publishing House, Beijing, 1988) (in Chinese with English summary).
2. Wu, F.Y., Sun, D.Y., Ge, W.C., Zhang, Y.B., Grant, M.L., Wilde, S.A., Jahn, B.M. Geochronology

of the Phanerozoic granitoids in northeastern China. *Journal of Asian Earth Sciences* **41**, 1–30 (2011).

- Li, X.M., Gong, G.L., Yang, X.Y., Zeng Q.S. Late Cretaceous-Cenozoic exhumation of the Yanji area, NE China: Constraints from fission track thermochronology. *Island Arc* **19**, 120–133(2010).

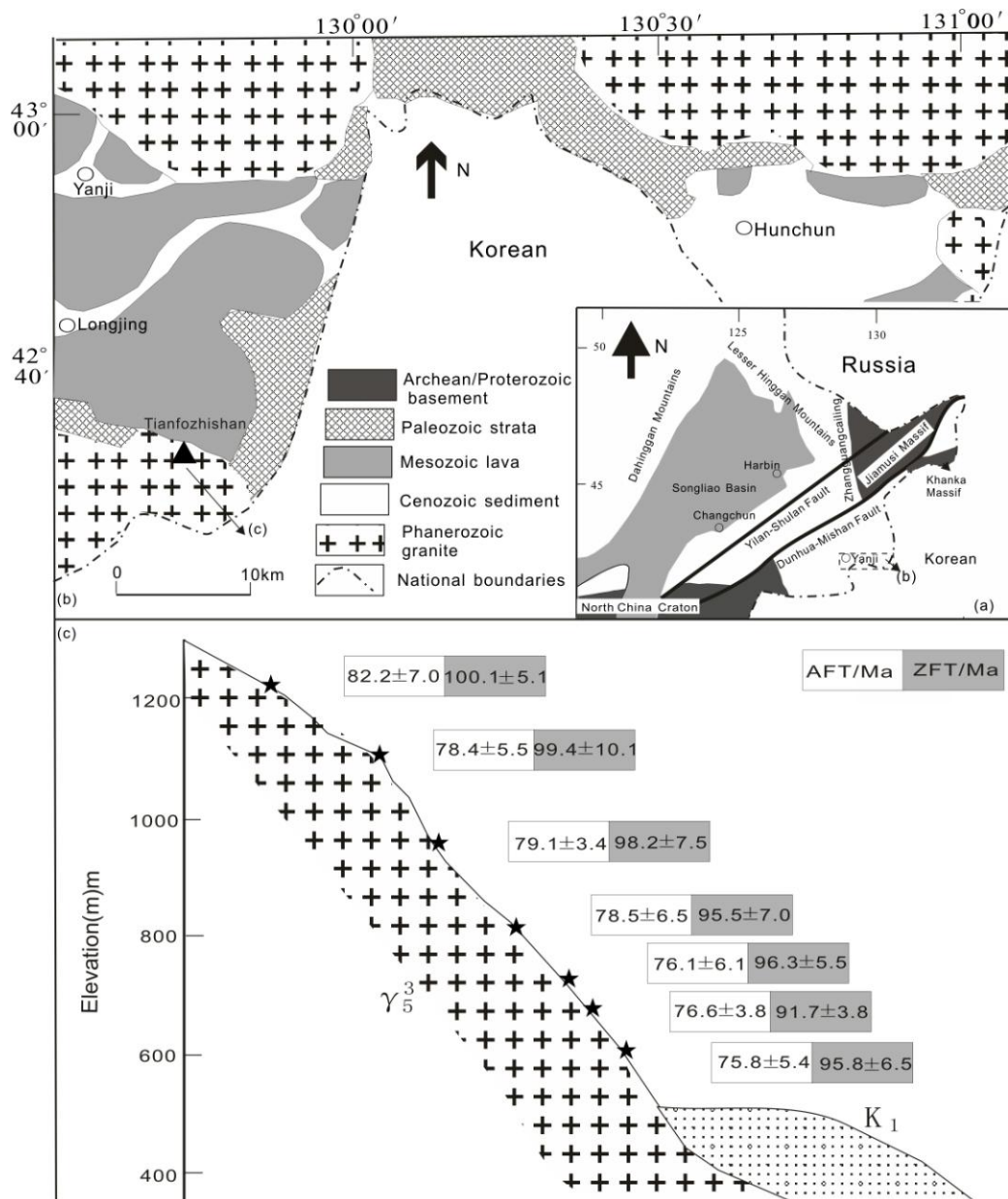


**Figure 1.** (a) Tectonic divisions of NE China; (b) Geological sketch of the Yanji area, showing the Tianfozhishan; (c) The map of the granite sample locations, elevations, and the apatite and zircon fission-track ages of the Tianfozhishan.



# The application of low-temperature thermochronology to an active low-angle normal fault, the Mai'iu Fault in Papua New Guinea

J. Oesterle<sup>1</sup>, D. Seward<sup>1</sup>, T. Little<sup>1</sup>, K. Norton<sup>1</sup>, D. Stockli<sup>2</sup>

*1 Victoria University of Wellington, Cotton Building, PO Box 600, Wellington, New Zealand*

*2 The University of Texas at Austin, 1 University Station C1100, Austin, TX 78712, USA  
(juergen.oesterle@vuw.ac.nz)*

Low-angle normal faults (LANFs) exhume rocks at angles  $<30^\circ$ . Their apparent non-Andersonian behavior has been long debated and still remains a conundrum. Here, we present the first low-temperature ages from the Suckling-Dayman metamorphic core complex (SDMCC) in SE Papua New Guinea. The SDMCC consists of two contrasting domal structures, the Dayman Dome (smooth broad landform) and the Suckling Dome (well incised relief). Both are bounded to the north by one of the best-exposed and fastest slipping active LANFs, the Mai'iu Fault, with geodetic data suggesting a horizontal slip rate of  $>7-9$  mm/yr<sup>1</sup>. The application of low-temperature thermochronology will contribute to a growing body of information about LANFs. Exhumation of the SDMCC can be linked to extension in the Woodlark Rift (Fig. 1), one of the few places on Earth that spans the transition from seafloor spreading to continental extension<sup>2</sup>. Two models have been proposed to predict the low-angle geometry of such faults. The first proposes that the fault was initially formed in a low-angle geometry<sup>3</sup>, the second (rolling hinge model) predicts that normal faults are deformed into a dome shape due to progressive unloading and isostatic rebound<sup>4-6</sup>. Here, we apply various geo- and thermochronologic methodologies, especially the FT and (U-Th)/He techniques, to determine the cooling history of the SDMCC and deduce the slip history of the Mai'iu Fault. The data set will be supported by Raman spectroscopy analyses on carbonaceous material in order to map contours of maximum paleo-temperatures on the footwall. Information of the thermal architecture of the SDMCC will allow us to determine the original fault geometry of the Mai'iu Fault and therefore distinguish between an original LANF and a rolling hinge model. Biotite and hornblende from intrusive bodies (Mai'iu Monzonite, Suckling Granite) within the footwall of the SDMCC yield Late Miocene-Pliocene K/Ar ages<sup>7</sup>. New, provisional ZFT central ages obtained from the Suckling Granite and Mai'iu Monzonite indicate cooling to below  $\sim 300^\circ\text{C}$  at less than 3 Ma. Moreover, provisional AFT central ages from the same rocks yield less than 2 Ma for the Suckling Granite and the Mai'iu Monzonite and suggest emplacement to upper crustal levels at that time. The pristine geomorphic preservation of the Dayman Dome implies little erosion. Hence, the contribution of erosion to exhumation is estimated to be insignificant and exhumation is mainly attributed to tectonic unroofing associated with slip on the Mai'iu Fault.

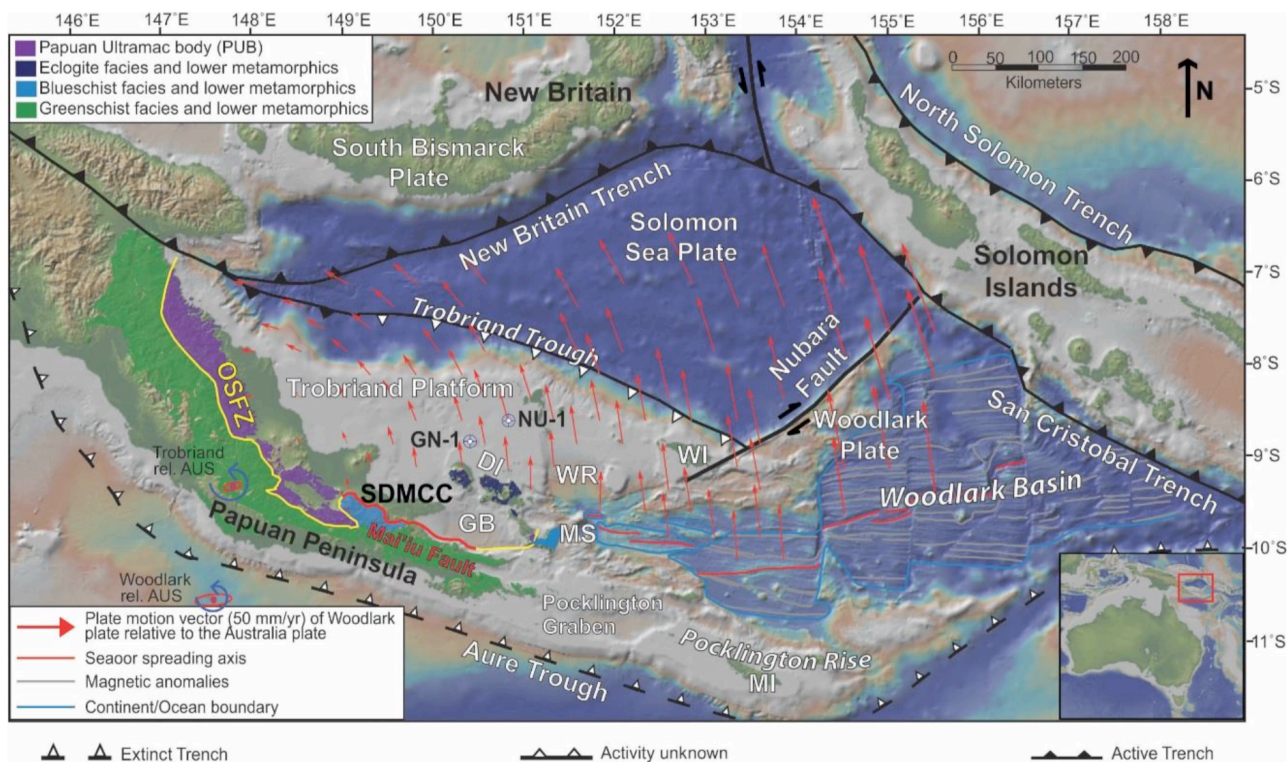


**Figure 1.** Tectonic setting of the Woodlark Rift. Basemap modified from Fitz and Mann (2013). Red vectors show rotation of the Woodlark and Trobriand microplates about poles of rotation (labelled Trobriand rel. AUS and Woodlark rel. AUS). DEI = D'Entrecasteaux Islands, WI = Woodlark Island, WR = Woodlark Rise, GB = Goodenough Bay, MI = Misima Island, OSFZ = Owen Stanley Fault Zone, MS = Moresby Seamount, SDMCC = Suckling-Dayman metamorphic core complex. GN-1 = Goodenough 1 drill site, NB-1 = Nubiam 1 drill site. Modified from Wallace et al. (2014).

## References

1. Wallace, L. M., Ellis, S., Little, T., Tregoning, P., Palmer, N., Rosa, R., Stanaway, R., Oa, J., Nidkomu, E., & Kwazi, J. Continental breakup and UHP rock exhumation in action: GPS results from the Woodlark Rift, Papua New Guinea. *Geochem. Geophys. Geosyst.* **15**, 4267–4290, doi:10.1002/2014GC005458 (2014).
2. Abers, G. A., Eilon, Z., Gaherty, J. B., Jin, G., Kim, Y. H., Obrebski, M. & Dieck, C. Southeast Papuan crustal tectonics: Imaging extension and buoyancy of an active rift. *J. Geophys. Res. Solid Earth* **121**, doi:10.1002/2015JB012621 (2015).
3. Lister, G.S. & Davis, G.A. The origin of metamorphic core complexes and detachment faults formed during Tertiary continental extension in the northern Colorado River region, U.S.A. *Journal of Structural Geology* **11**, 65-94 (1989).
4. Buck, W.R. Flexural rotation of normal faults. *Tectonics* **7**, 959–974 (1988).
5. Hamilton, W. in *Geologic and hydrologic investigations of a potential nuclear waste disposal site at Yucca Mountain, southern Nevada* (eds Carr, M. D. & Yount, J. C.) 51-85 (US Geological Survey, Denver, 1988).
6. Wernicke, B. & Axen, G. J. On the role of isostasy in the evolution of normal fault systems. *Geology* **16**, 848-851 (1988).
7. Davies, H. L. & Smith, I. E. Tufi-Cape Nelson. 1:250 000 Geological Series, Explanatory Notes, *Bureau of Mineral Resources, Geology and Geophysics Australia* **165**, SC/55-8, SC/55-4 (1974).
8. Baldwin, S. L., Lister, G. S., Hill, E. J., Foster, D. A. & McDougall, I. Thermochronologic constraints on the tectonic evolution of active metamorphic core complexes, D'Entrecasteaux Islands, Papua New Guinea, *Tectonics* **12**, 611–628, doi:10.1029/93TC00235 (1993).

# Apatite (U-Th)/He thermochronometry in the northern Patagonian Andes: new insights into the exhumation history of the thrust belt-foreland sector

Elisa Savignano<sup>1</sup>, Massimiliano Zattin<sup>1</sup>, Stefano Mazzoli<sup>2</sup>, Marta Franchini<sup>3</sup>, Cécile Gautheron<sup>4</sup>.

<sup>1</sup> Department of Geosciences, University of Padua, Via Gradenigo, 6, Padua (PD) - Italy

<sup>2</sup> DiSTAR, University of Naples Federico II, Largo San Marcellino, 10, Naples (NA) - Italy

<sup>3</sup> CONICET - Centro Patagónico de Estudios Metalogenéticos, Universidad Nacional Del Comahue – Argentina

<sup>4</sup> Université Paris Sud, UMR GEOPS-CNRS 8148, 91405 Orsay - France.

(elisa.savignano@studenti.unipd.it)

The Patagonian Andes represent a unique natural laboratory to study the relationships between surface deformation and slab dynamics. In fact, building of the southern Andes has been interpreted to have been controlled by alternating stages of flat- and steep-slab subduction, which produced alternating shortening and upper plate extension episodes<sup>1,2,3,4</sup>, respectively. This evolution can be recognized in the adjacent thrust belt-foreland system, in which progressive and non-steady-state processes acting in several pulses during Late Cretaceous, Late Eocene and Late Miocene times have been detected. Deformation in the Andean retro-wedge sector varied not only in time (i.e. with major ‘cycles’ of mountain building and orogenic collapse, respectively), but also in space, due to the variable transmission of horizontal compressive stress away from the orogen.

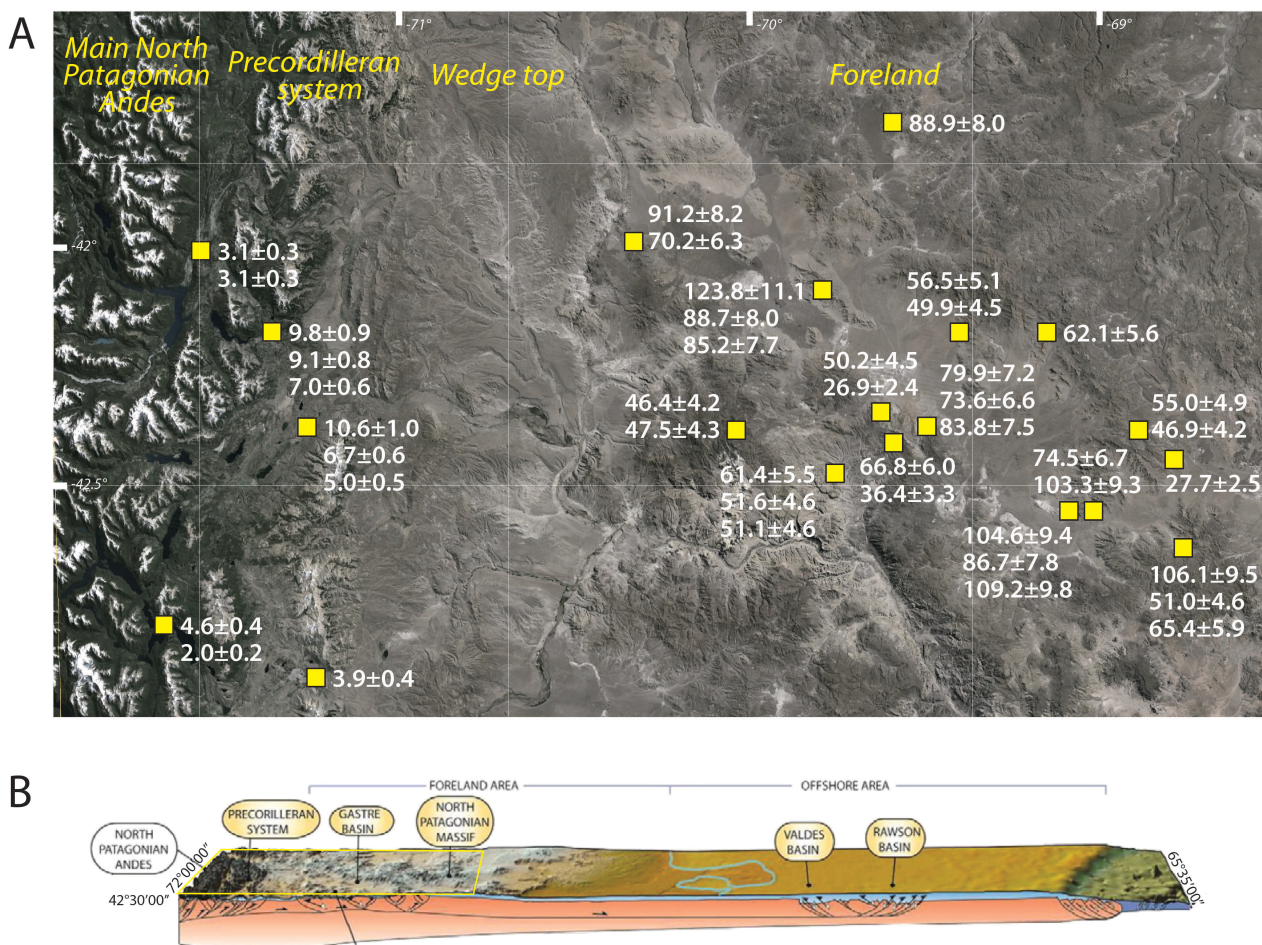


**Figure 1.** (A) Landsat image of the study area showing sampled sites and obtained AHe ages; morphostructural domains defined according to Orts et al. (2012). (B) Schematic structural profile

of the onshore and offshore areas across the northern Patagonia sector considered in this research and location of figure A (after Gianni et al., 2015).

The result is a present day complex structural architecture due to heterogeneous deformation. In this study, we integrate field structural observations with apatite (U-Th)/He (AHe) thermochronology in the Esquel-Gastre area (located at latitudes 41.30–43.00°S) in order to analyse and compare the exhumation patterns from the frontal part of the orogen and from the adjacent foreland sector. These data provide new insights into the timing and modes of coupling vs. uncoupling of the deformation between the northern Patagonian fold and thrust belt and its foreland. The collected samples span through different morpho-structural domains, from the variably deformed foreland to the eastern slope of the Main North Patagonian Andes. Analyzed samples mainly belong to basement lithologies (see Fig. 1 for the sample location). The resultant AHe ages can be grouped into two major populations: (i) a first group characterized by Miocene–Pliocene ages (10.6 to 2.0 Ma) belonging to the Precordillera area, and (ii) a second group of samples with Upper Cretaceous to Eocene ages (26.9 to 123.8 Ma) distributed in the foreland zone. Our study suggests that configurations of flat-slab vs. steep-slab subduction may exert an important role in controlling the coupling vs. uncoupling of the deformation between the thrust belt and its foreland in the Patagonian Andes. Late Miocene to Pliocene AHe ages from the frontal part of the northern Patagonian Andes correlate well with a shortening and exhumation stage documented to have occurred in the thrust belt during steep subduction characterized by high convergence rates (> 4 cm/a). On the other hand, AHe ages obtained for the ‘broken foreland’ unravelled final exhumation at near-surface conditions during Late Cretaceous to Paleogene times.

## References

1. Ramos, V. A., & Folguera, A. Andean flat-slab subduction through time. *Geological Society, London, Special Publications*, **327(1)**, 31-54 (2009).
2. Folguera, A., & Ramos, V. A. Repeated eastward shifts of arc magmatism in the Southern Andes: a revision to the long-term pattern of Andean uplift and magmatism. *Journal of South American Earth Sciences*, **32(4)**, 531-546 (2011).
3. Orts, D. L., Folguera, A., Encinas, A., Ramos, M., Tobal, J., & Ramos, V. A. (2012). Tectonic development of the North Patagonian Andes and their related Miocene foreland basin (41° 30'-43° S). *Tectonics*, **31(3)** (2012).
4. Orts, D. L., Folguera, A., Giménez, M., Ruiz, F., Vera, E. A. R., & Klinger, F. L. Cenozoic building and deformational processes in the North Patagonian Andes. *Journal of Geodynamics*, 86, 26-41 (2015).
4. Gianni, G., Navarrete, C., Orts, D., Tobal, J., Folguera, A., & Giménez, M. Patagonian broken foreland and related synorogenic rifting: The origin of the Chubut Group Basin. *Tectonophysics*, **649**, 81-99. (2015).

# Thermochronologic Perspectives for the Crustal Dynamics of the Japan Arc

Takahiro Tagami<sup>1</sup>

*1 Div. of Earth and Planetary Sciences, Kyoto University, Kyoto 606-8502, Japan  
(tagami@kueps.kyoto-u.ac.jp)*

The Crustal Dynamics Project, an interdisciplinary project to study the dynamics of island arc deformation, was initiated in 2014 to better understand the geodynamic background and framework that generated the 2011.3.11 Mega-earthquake and Tsunami disaster. In this project, our thermochronology research unit is a part of the “Deformation Group” that aims at understanding crustal deformation of the Japanese islands in various spatio-temporal scales. Towards this goal, a series of geodetic, geomorphological and geological data are currently being compiled and integrated in target areas to figure out both the elastic and non-elastic strains that have been accumulated at a variety of timescales (~1y to ~1my). In particular, both geomorphological and geological approaches are useful to better constrain the non-elastic strain, which is a key to unravel long-term crustal deformation and landscape development of island arcs. Thermochronology is one of such useful approaches and offers a unique tool to quantitatively reconstruct the vertical component of crustal movements of km scales.

Recent progress of low-temperature thermochronology, e.g., developments of (U-Th-Sm)/He method and fission-track inversion modeling, enables to analyze uplift-denudation-cooling histories of the island-arc mountains with good confidence. This is particularly fruitful for studying the topographic evolution of Japan Arc, because many of the Japanese mountains are started to uplift in recent time (e.g., late Pliocene to Quaternary) after an extended period of relative tectonic quiescence, and hence the resultant smaller amount of total uplift is only resolvable by low-temperature thermochronology. This was first demonstrated by elucidating the uplift-denudation-cooling process of the Kiso Mountain, in which average topographic changes of the tilted mountain block were quantitatively reconstructed<sup>1-2</sup>.

In this presentation, I give an overview of the tectonic and thermochronologic background and then highlight some of the ongoing thermochronological researches in the Crustal Dynamics Project. The current research targets are:

- (1) Compilation of previously reported thermochronological data from the Japan Arc, to search for research targets and strategy,
- (2) (U-Th-Sm)/He and fission-track analyses of the NE Japan Arc (Tohoku area), which is a main subaerial part of the overriding plate of the Mega-earthquake epicenter,
- (3) (U-Th-Sm)/He, fission-track and U-Pb analyses of the Hida Mountain, which is a part of central mountain ranges that are formed by recent collisional convergence between the NE and SW Japan Arcs, and may have suffered an overspread deformation with great strain rates, as deduced from the exposure of youngest granites on the Earth<sup>3</sup>.

## References

1. Sueoka, S. et al. Denudation history of the Kiso Range, central Japan, and its tectonic implications: Constraints from low-temperature thermochronology. *Island Arc* **21**, 32-52 (2012).
2. Sueoka, S., Tsutsumi, H. & Tagami, T. New approach to resolve the amount of Quaternary uplift and associated denudation of the mountain ranges in the Japanese Islands, *Geoscience Frontiers*, **7**, 197-210 (2016).
3. Ito, H. et al. Earth's youngest exposed granite and its tectonic implications: the 10–0.8 Ma Kurobegawa Granite *Scientific Reports* **3**, 1306 (2013).

# Low temperature thermochronometry reveals early Cenozoic differential exhumation in the southern Rocky Mountains, Colorado

Alyssa Abbey, Nathan Niemi

University of Michigan 1100 N University Ave, Ann Arbor, MI, USA

alabbey@umich.edu

The Cenozoic evolution of the Southern Rocky Mountains remains a controversial issue in terms of timing and mechanistic causes of rejuvenation, surface uplift and exhumation. Proposed mechanisms for uplift and relief generation in the southern Rockies span a variety of mechanisms and timescales, including Laramide to early Cenozoic uplift driven by either de-eclogitization through crustal hydration during mountain building<sup>1</sup>, or regional scale surface rebound from the removal of the Shatsky rise and subsequent mantle upwelling<sup>5</sup>. Mid- to late-Miocene uplift is also proposed, potentially driven by mantle convection and long-wavelength dynamic topography<sup>2</sup>, or Rio Grande Rift (RGR) propagation, tilting, erosion and associated isostatic rebound.<sup>6,7</sup> RGR propagation, erosion and isostasy are also invoked by others who propose Pleistocene to Present uplift<sup>4</sup> followed by increased river incision and relief generation, although recent relief production driven by Pleistocene climate change and the enhancement of alpine glaciation has also been suggested.<sup>8</sup> Thus, there is no consensus on the driving mechanisms that led to present Rocky Mountain topography, and there is no agreement on the timing of when elevation gain or relief production began. To discriminate between proposed driving mechanisms we will need a clear understanding of the timing and rates of elevation gain and relief production in the southern Rocky Mountains.

We use apatite helium (AHe) low-temperature thermochronometry to examine timing and rates of exhumation in the lower Arkansas River canyon in central Colorado (Fig1A). Our helium data do not record a young (no ages <15Ma) pulse of exhumation driving river incision and instead suggest the majority of exhumation in the region was Laramide driven, occurring from late Cretaceous to Eocene time. This region of the southern Rockies is characterized by a low relief erosion surface capped by relatively undeformed Oligocene-Miocene (36.7-19.9Ma) volcanic rocks. The Arkansas River cuts a 1-1.5km deep canyon through these volcanic rocks into the Precambrian basement providing exposure for vertical transect sampling. AHe and previously published AFT<sup>3</sup> ages reveal differential cooling from east to west—late Cretaceous cooling in AFT and AHe samples closer to Canon City, CO and Paleocene-Eocene cooling ages farther west towards Salida, CO (Fig1A and B). These results do not support a late Miocene pulse of regional exhumation and suggest little burial and re-exhumation occurred after erosion surface formation and volcanic deposition. Additionally, we are able to better constrain the timing of the erosion surface to between ~54 Ma and 37 Ma and that around 1.5km of material was removed in the process (Fig1C).

## References

1. Jones, C. H. Mahan, K. H. Butcher, L. A. Levandowski, W. B. & Farmer, G. L. Continental uplift through crustal hydration. *Geology*, **43**(4), 355–358 (2015).
2. Karlstrom, K. E. Coblenz, D., Dueker, K. Ouimet, W. Kirby, E. Van Wijk, J. et al. Mantle-driven dynamic uplift of the Rocky Mountains and Colorado Plateau and its surface response: Toward a unified hypothesis. *Lithosphere*, **4**(1), 3–22 (2012).
3. Kelley, S.A. & Chapin, C.E. Denudation history and internal structure of the Front Range and Wet Mountains, Colorado, in Cather, S.M., et al., eds., Tectonics, geochronology, and volcanism, in the southern Rocky Mountains and Rio Grande rift: New Mexico Bureau of Geology and Mineral Resources Bulletin **160**, 41–78 (2004).
4. Leonard, E. M. Geomorphic and tectonic forcing of late Cenozoic warping of the Colorado piedmont. *Geology*, **30**(7), 595–598 (2002).
5. Liu, L. Gurnis, M. Seton, M. Saleeby, J. Müller, R. D. & Jackson, J. M. The role of oceanic plateau subduction in the Laramide orogeny. *Nature Geoscience*, **3**(5), 353–357 (2010).
6. McMillan, M. E. Angevine, C. L. & Heller, P. L. Postdepositional tilt of the Miocene-Pliocene Ogallala Group on the western Great Plains: Evidence of late Cenozoic uplift of the Rocky Mountains. *Geology*, **30**(1), 63–66 (2002).

7. McMillan, M. E. Heller, P. L. & Wing, S. L. History and causes of post-Laramide relief in the Rocky Mountain orogenic plateau. *Geological Society of America Bulletin*, **118(3-4)**, 393–405 (2006).
8. Small, E. E. & Anderson, R. S. Pleistocene relief production in Laramide mountain ranges, western United States. *Geology*, **26(2)**, 123 (1998).

**Figure 1:**

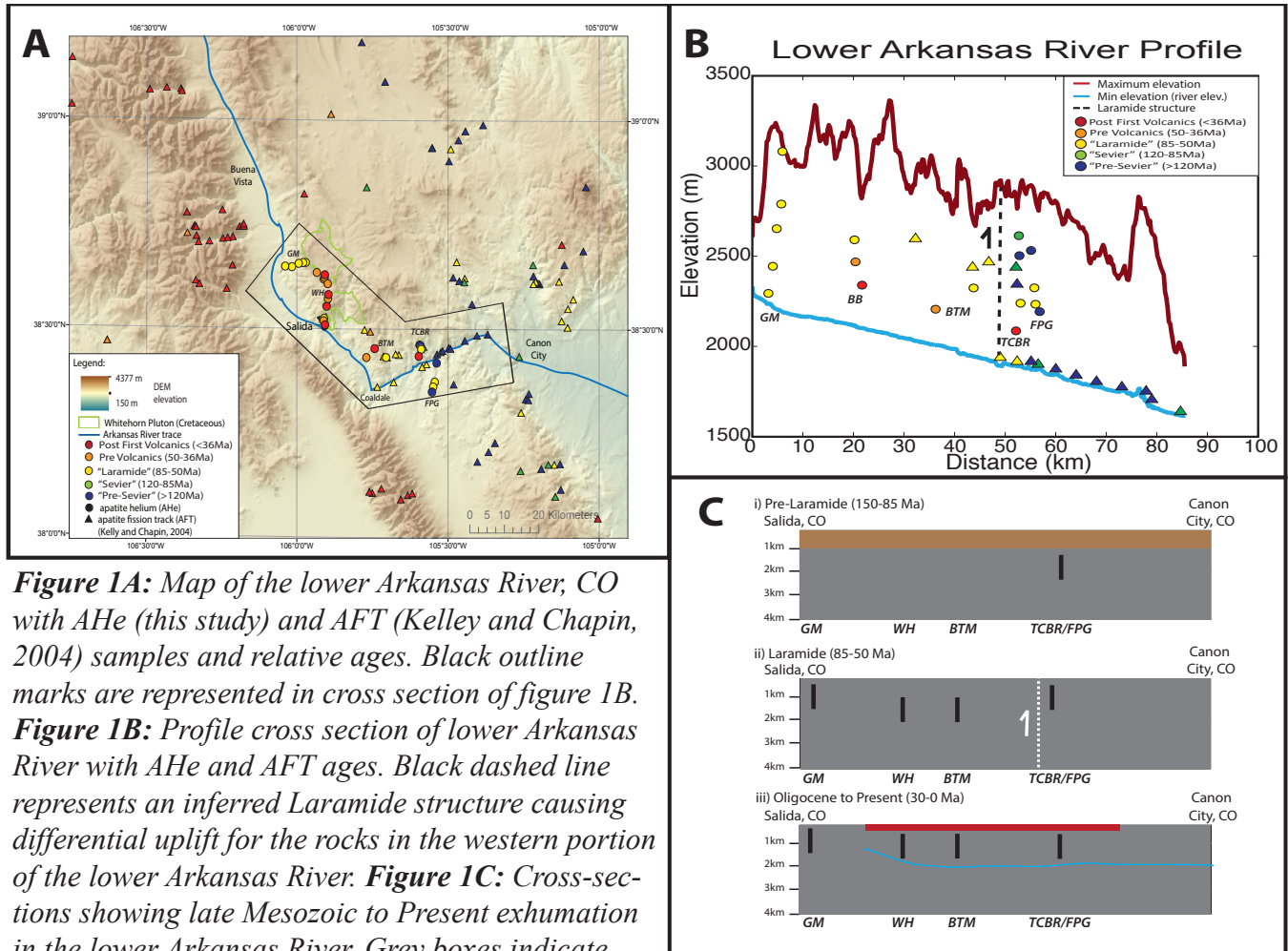


**Figure 1A:** Map of the lower Arkansas River, CO with AHe (this study) and AFT (Kelley and Chapin, 2004) samples and relative ages. Black outline marks are represented in cross section of figure 1B. **Figure 1B:** Profile cross section of lower Arkansas River with AHe and AFT ages. Black dashed line represents an inferred Laramide structure causing differential uplift for the rocks in the western portion of the lower Arkansas River. **Figure 1C:** Cross-sections showing late Mesozoic to Present exhumation in the lower Arkansas River. Grey boxes indicate crystalline basement rock, brown box indicates sedimentary rock and red box shows volcanic deposits. Thick vertical black lines mark AHe transects. i) Pre-Laramide: what is now CO was at low elevations experiencing sedimentary deposition (terrestrial until ~98Ma followed by marine sediments when the region was covered by an interior seaway). These sediments could have been a minimum of 300m to 1600m thick based on present day sedimentary packages found in the western Great Plains. AFT and AHe ages from samples in the eastern section of the lower AR indicate surface temperatures (<~40°C) during this time. ii) Laramide: compression and mountain building reaches CO during the Laramide Orogeny causing uplift disappearance of the seaway by ~72Ma. Erosion of the sedimentary deposits drives high rates of exhumation. Differential uplift between the east and west (white dashed line) is inferred from differences in thermochronometry ages of samples at similar elevations (Fig1B). By the end of the Laramide almost all samples are at surface temperatures and development of the regional erosion surface is underway. iii) Post-volcanic deposition: active volcanism and deposit of blanketing flows begins ~37Ma and continues to ~20Ma. Thickness of the volcanics is not enough to cause significant burial of the basement below and the final pulse of exhumation, seen in the AHe data, occurs by the early Miocene, potentially driven by river incision of a paleo-Arkansas River (blue line).

# Rapid Plio-Pleistocene erosion of the central Colorado Plateau documented by apatite thermochronology from the Henry Mountains

Kendra E Murray<sup>1,2</sup>, Peter W Reiners<sup>1</sup>, Stuart N Thomson<sup>1</sup>

<sup>1</sup>Department of Geosciences, University of Arizona, USA

<sup>2</sup>Department of Earth and Environmental Sciences, University of Michigan, USA  
(kemurray@email.arizona.edu)

Apatite thermochronology is, in principle, uniquely suited to document the Cenozoic exhumation of the Colorado Plateau (southwest USA) and reveal the region's cryptic history of epeirogenic uplift and erosion. However, results from the region have pushed the current limits of these methods, stimulating substantial advances like the RDAAM<sup>1,2</sup> and renewing the debate over the age of the Grand Canyon, Colorado River integration, and the evolution of the Plateau's southwestern margin<sup>3-7</sup>. In large part, this is because the region's bedrock resided at <120 °C (<4-5 km) for much of the Phanerozoic, so the temperature sensitivity of the apatite thermochronometers during Cenozoic exhumation is a convoluted function of apatite grain composition and thermal history<sup>6,8</sup>. This complication is amplified in the region's iconic Permian-Mesozoic sandstones, which have diverse detrital apatite populations variably reset by Mesozoic-Cenozoic burial in both radiation damage and radiogenic daughter content.

In the central Colorado Plateau, we overcome this challenge by sampling these sandstones in the Oligocene Henry Mountains intrusive complex<sup>9</sup>, where heating around shallow plutons overprinted their convoluted thermal history and primed them to document only post-Oligocene rock cooling. Using zircon U/Pb geochronology to confirm the timing of magmatic heating and AFT analyses to determine the extent of Oligocene resetting in the country rocks, we identify and interpret a robust apatite He archive of the late Cenozoic erosion of the Plateau interior. These sandstones have <26 Ma apatite He ages with positive-slope age-eU trends (3-25 Ma, 5-180 ppm eU) that require a distinctive late Cenozoic thermal history that we constrain using the RDAAM<sup>2,10</sup> in HeFTy<sup>11</sup>. Model results require sample residence at apatite He partial-retention temperatures until 10-8 Ma; good-fit *t-T* paths (n=100 per sample modeled) require cooling <40 °C no earlier than 5 Ma (most 3-2 Ma). This Plio-Pleistocene cooling reflects 1.5-2 km of rapid exhumation at time-averaged rates of ~250-700 m/Ma. This result<sup>12</sup> refines and improves upon previous apatite He results from the central Colorado Plateau, which suffered from substantial age variability but suggested regional erosion started <10 Ma, perhaps as young as 5 Ma<sup>13</sup>.

In the latest Miocene, integration of the modern Colorado River through the western Grand Canyon (ca. 5.6 to 5.3 Ma<sup>14</sup>), >500 km downstream of the Henry Mountains, lowered regional base-level. Multiple lines of evidence suggest this drove significant erosion of the Plateau interior. Rapid and variable late Pleistocene incision rates (up to ~500 m/Ma) from cosmogenic nuclide age determinations of strath terraces along the main stem of the Colorado River and its tributaries in the Henry Mountains region<sup>15-17</sup> agree with the erosion rates we infer from apatite He data, and together with modern channel profiles suggest this region is transiently responding to regional baselevel fall<sup>15</sup>, perhaps enhanced by localized feedback between unroofing and isostatic rebound<sup>17</sup> or dynamic uplift<sup>18</sup>. Thermochronology from high-relief, high-elevation Henry Mountains landscape is also likely documenting increased mountain snowpack and seasonal runoff in the Pleistocene, which could have cooled the groundwater flowing downslope through these sandstones from the highest elevations<sup>19</sup> and likely accelerated local bedrock erosion<sup>20,21</sup>.

## References

1. Flowers, R. M., Shuster, D. L., Wernicke, B. P. & Farley, K. A. Radiation damage control on apatite (U-Th)/He dates from the Grand Canyon region, Colorado Plateau. *Geology* **35**, 447-450 (2007).
2. Flowers, R. M., Ketcham, R. A., Shuster, D. L. & Farley, K. A. Apatite (U-Th)/He thermochronometry using a radiation damage accumulation and annealing model. *Geochimica et Cosmochimica Acta* **73**, 2347-2365



- (2009).
3. Flowers, R., Wernicke, B. P. & Farley, K. A. Unroofing, incision, and uplift history of the southwestern Colorado Plateau from apatite (U-Th)/He thermochronometry. *Geological Society of America Bulletin Part I* **120**, 571–587 (2008).
  4. Wernicke, B. The California River and its role in carving Grand Canyon. *GSA Bulletin* **123**, 1288–1316 (2011).
  5. Lee, J. P. *et al.* New thermochronometric constraints on the Tertiary landscape evolution of the central and eastern Grand Canyon, Arizona. *Geosphere* **9**, 216–228 (2013).
  6. Fox, M. & Shuster, D. L. The influence of burial heating on the (U–Th)/He system in apatite: Grand Canyon case study. *Earth and Planetary Science Letters* **397**, 174–183 (2014).
  7. Flowers, R. M., Farley, K. A. & Ketcham, R. A. A reporting protocol for thermochronologic modeling illustrated with data from the Grand Canyon. *Earth and Planetary Science Letters* **432**, 425–435 (2015).
  8. Carter, A. & Gallagher, K. Characterizing the significance of provenance on the inference of thermal history models from apatite fission-track data—A synthetic data study. *Geological Society of America Special Papers* **378**, 7–23 (2004).
  9. Gilbert, G. K. *Report on the Geology of the Henry Mountains*. (Government Printing Office, 1877).
  10. Gautheron, C., Tassan-Got, L., Barbarand, J. & Pagel, M. Effect of alpha-damage annealing on apatite (U–Th)/He thermochronology. *Chemical Geology* **266**, 157–170 (2009).
  11. Ketcham, R. A. Forward and inverse modeling of low-temperature thermochronometry data. *Reviews in Mineralogy and Geochemistry* **58**, 275–314 (2005).
  12. Murray, K. E., Reiners, P. W. & Thomson, S. N. Rapid Plio-Pleistocene erosion of the central Colorado Plateau documented by apatite thermochronology from the Henry Mountains. *Geology* (accepted).
  13. Hoffman, M. D., Stockli, D. F., Kelley, S. A., Pederson, J. L. & Lee, J. in *CRevolution 2—Origin and Evolution of the Colorado River System, Workshop Abstracts* (eds. Beard, L. S., Karlstrom, K. E., Young, R. A. & Billingsley, G. H.) 132–136 (2011).
  14. House, P. K., Pearthree, P. A. & Perkins, M. E. in *Special Paper 439: Late Cenozoic Drainage History of the Southwestern Great Basin and Lower Colorado River Region: Geologic and Biotic Perspectives* **439**, 335–353 (Geological Society of America, 2008).
  15. Cook, K. L., Whipple, K. X., Heimsath, A. M. & Hanks, T. C. Rapid incision of the Colorado River in Glen Canyon - insights from channel profiles, local incision rates, and modeling of lithologic controls. *Earth Surf. Process. Landforms* (2009). doi:10.1002/esp.1790
  16. Darling, A. L. *et al.* New incision rates along the Colorado River system based on cosmogenic burial dating of terraces: Implications for regional controls on Quaternary incision. *Geosphere* **8**, 1020–1041 (2012).
  17. Pederson, J. L., Cragun, W. S., Hidy, A. J., Rittenour, T. M. & Gosse, J. C. Colorado River chronostratigraphy at Lee’s Ferry, Arizona, and the Colorado Plateau bull’s-eye of incision. *Geology* **41**, 427–430 (2013).
  18. Karlstrom, K. E. *et al.* Mantle-driven dynamic uplift of the Rocky Mountains and Colorado Plateau and its surface response: Toward a unified hypothesis. *Lithosphere* **4**, 3–22 (2012).
  19. Whipp, D. M. & Ehlers, T. A. Influence of groundwater flow on thermochronometer-derived exhumation rates in the central Nepalese Himalaya. *Geology* **35**, 851–4 (2007).
  20. Pelletier, J. D. The impact of snowmelt on the late Cenozoic landscape of the southern Rocky Mountains, USA. *GSA Today* **19**, 4–11 (2009).
  21. Johnson, J. P. L., Whipple, K. X. & Sklar, L. S. Contrasting bedrock incision rates from snowmelt and flash floods in the Henry Mountains, Utah. *GSA Bulletin* **122**, 1600–1615 (2010).

# Thermochronological Constraints on the Cenozoic Accretion and Deformation in Western Colombia

León, S.<sup>1</sup>, Parra, M.<sup>2</sup>, Cardona, A.<sup>3</sup>

1. *Institute of Geosciences, University of Sao Paulo, Brazil*

2. *Institute of Energy and Environment, University of Sao Paulo, Brazil*

3. *Department of Processes and Energy, National University, Colombia*  
([sleonva@usp.br](mailto:sleonva@usp.br))

The Cenozoic evolution of the NW South-American continental margin was shaped by two major tectonic events associated to the interaction with the Caribbean Plate during its motion northeastwards<sup>1</sup>: (1) the collision of an island arc-oceanic plateau system in the Late Cretaceous-Paleocene<sup>2,3</sup>, and (2) the collision of the Panama Arc in the Middle Miocene<sup>4,5</sup> (*Figure 1*). Tectono-stratigraphic analysis in eastern Colombia have been used to describe various orogenic episodes in the time span between these two major collisional events, although their trigger mechanisms have been mostly related with the changing velocity of the South-American plate and tectonic inheritance<sup>6-8</sup>. However, the combined effects of collisional episodes in the west and the easterly triggered tectonism in central Colombia remain unclear.

In this contribution, we present results of provenance analysis carried out on sedimentary sequences exposed along the northern Western Cordillera of Colombia. Sandstone petrography, U-Pb geochronology and heavy minerals analysis, suggest that Late Cretaceous-Paleocene sedimentary units contain material derived from the South-American continental margin and are probably related with a trench or forearc setting. Conversely, in Eocene-Early Miocene sequences this South-American signature is absent. Accordingly, the latter units should have been deposited in an allochthonous position farther to the west, possibly associated with the Panama Arc. Overlying both units, a post Middle Miocene thick conglomeratic sequence contains detrital material derived from the continental margin, revealing that the Panama Arc was already docked to the South-American margin before Late Miocene.

Ongoing low-temperature thermochronology analysis in pre and syn to post-collisional units will allow us to identify periods with rapid exhumation linked with the tectonic evolution of the South-America Caribbean interaction during Cenozoic. Additionally, cooling ages obtained from rocks directly involved in the suture zone will be compared with temporal constraints of previous tectono-stratigraphic studies carried out in the hinterland and foreland, aiming at reconstructing and unified model of tectonic evolution in NW South America

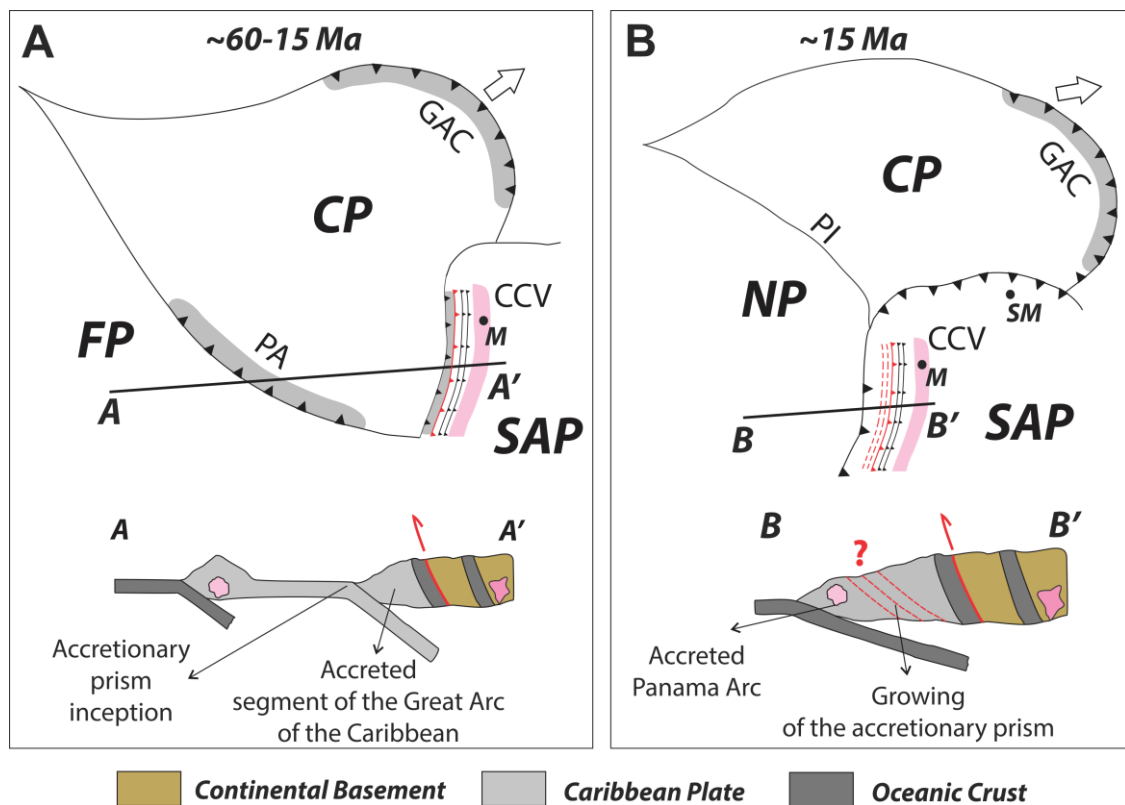


**Figure 1.** Cenozoic paleogeography of NW South-America. FP: Farallon Plate; NP: Nazca Plate; PA: Panama Arc; PI: Panama Isthmus; CP: Caribbean Plate; GAC: Great Arc of the Caribbean; CCV: Central Cordillera Volcanic Arc; M: Approximated location of Medellin city for spatial reference; SM: Approximated location of Santa Marta city for spatial reference; SAP: South-American Plate. Modified after <sup>9</sup>.

## References

1. Pindell, J. & Kennan, L. in *The geology and evolution of the region between North and South America, Geological Society of London, Special Publication* (eds. James, K., Lorente, M. A. & Pindell, J.) 1–60 (2009).
2. Kerr, A. C. *et al.* Cretaceous Basaltic Terranes in Western Colombia : Elemental , Chronological and Sr – Nd Isotopic Constraints on Petrogenesis. *J. Petrol.* **38**, 677–702 (1997).
3. Villagómez, D. & Spikings, R. Thermochronology and tectonics of the Central and Western Cordilleras of Colombia: Early Cretaceous–Tertiary evolution of the Northern Andes. *Lithos* **160-161**, 228–249 (2013).
4. Duque-Caro, H. The Choco Block in the northwestern corner of South America : Structural, tectonostratigraphic, and paleogeographic implications. *J. South Am. Earth Sci.* **3**, 71–84 (1990).
5. Montes, C. *et al.* Middle Miocene closure of the Central American Seaway. *Science (80-. )*. **348**, 226–229 (2015).
6. Parra, M., Mora, A., López, C., Rojas, L. E. & Horton, B. K. Detecting earliest shortening and deformation advance in thrust-belt hinterlands: Example from the Colombian Andes. *Geology* **40**, 171–174 (2012).
7. Mora, A. *et al.* in *Thick-Skin-Dominated Orogens: From Initial Inversion to Full Accretion* (eds. Nemčok, M., Mora, A. & Cosgrove, J. W.) 411–442 (Geological Society of London, Special Publication, 377, 2013). doi:10.1144/SP377.6
8. Reyes-Harker, A. *et al.* Cenozoic paleogeography of the Andean foreland and retroarc hinterland of Colombia. *Am. Assoc. Pet. Geol. Bull.* **99**, 1407–1453 (2015).
9. Pindell, J. L. in *Caribbean Geology: An Introduction* 13–39 (U.W.I. Publishers Association, Kingston, 1994).

# Constraints on the magnitude and longevity of geothermal and meteoric fluid flow from (U-Th)/He thermochronometry

Daniel F. Stockli<sup>1</sup>, Daniel Arnost<sup>1</sup>, Alison MacNamee<sup>1</sup>

*1 Dept. of Geological Sciences, University of Texas at Austin, USA  
(stockli@jsg.utexas.edu)*

Crustal fluid flow plays a fundamental role in tectonic and thermal processes, and the potential importance of meteoric fluid infiltration in determining shallow subsurface and upper-crustal isotherms and geothermal gradients has been established in recent studies<sup>1</sup>. In zones of deep meteoric fluid infiltration or geothermal fluid advection, subsurface temperature isotherms can be significantly depressed or elevated, causing marked deflections in (U-Th)/He partial retention zones. Age patterns associated and correlated with these isotherm deflections can be used to examine the role of paleohydrologic or geothermal systems. Here we present two case studies, employing apatite (AHe) and zircon (ZHe) (U-Th)/He thermochronometry, that explore the effects of (1) infiltration of cold meteoric fluid into the subsurface, leading to marked depression of isotherms in the new Gotthard Base Tunnel in the Alps of Switzerland and (2) fault-controlled advection of hot, geothermal fluids in an extensional setting in Dixie Valley, Nevada.

The 58 km long Gotthard Base Tunnel through the backbone of the Swiss Central Alps provides a unique window into the subsurface thermal evolution of the Swiss Alps. The tunnel temperatures reach up to 42°C with positive and negative anomalies mimicking the topography. However, the temperature profile exhibits a marked -15°C temperature anomaly below Piora syncline where a karstified dolomite zone funnels meteoric water deep into the massif, cooling the syncline and adjacent bedrock. While ZHe ages in the tunnel and surface are invariant across the syncline, (8.0-10.0 Ma), high-density AHe samples show reproducible ages of ~2.5 Ma that dramatically increase to ~5.5 Ma around the Piora Zone, recording isotherm depression due to meteoric fluid infiltration. Thermal modeling quantifies both the Alpine exhumation and the thermal history of the Piora Zone and shows that the anomaly is long lived, with an age of ~5-8 Ma, and clearly predates the onset of Alpine glaciation - likely driven by latest Miocene uplift and relief generation in the External Massifs.

A detailed study of geothermal fluid flow from the geothermal field of Dixie Valley in Nevada demonstrates the effects of hot fluid advection on AHe ages. The valley is bound to the west by high-angle normal faults along which the adjacent Stillwater Range formed, and is characterized by dilatational fault corners that show elevated near-surface geothermal gradients (geothermal anomalies). While three elevation transects record advective cooling of the footwall due to exhumation onset at ~4 Ma, samples from the range front in the vicinity of the dilatational corners show ages as young as 200 ka. In map view, these young ages define “hot spots” where AHe ages were hydrothermally reset, demonstrating the ability to resolve conductive cooling ages from overprinted, fluid-reheated ages. Interpolation of AHe ages shows that the youngest ages correspond with remarkable accuracy to the spatial extents of previously mapped geothermal anomalies, suggesting AHe dating as a cost-effective tool in the exploration of blind geothermal resources.

These case studies demonstrate that high-density low-temperature thermochronometry is a powerful tool in reconstructing paleo-fluid flow in response to meteoric fluid infiltration and geothermal fluid circulation.

## References

1. Whipp, D.M., and Ehlers, T.A., 2007, Influence of groundwater flow on thermochronometer-derived exhumation rates in the central Nepalese Himalaya: *Geology*, v. 35, no. 9, p. 851–854, doi: 10.1130/G23788A.1.

## **Post-incaic phase supergene copper enrichment and pediplanation, Northern Chile, Centinela District.**

Caroline Sanchez<sup>1,2</sup>, Stéphanie Brichau<sup>2</sup>, Rodrigo Riquelme<sup>1</sup>, Sébastien Carretier<sup>2</sup>, Christopher Lopez<sup>1</sup>, Eduardo Campos<sup>1</sup>, Vincent Regard<sup>2</sup>, Gérard Hérail<sup>2</sup>, Carlos Marquardt<sup>3</sup>, Constantino Mpodozis<sup>4</sup>

1 *Universidad Católica del Norte, Chile.*

2 *Géosciences Environnement Toulouse, OMP, UPS, CNRS, IRD, Université Toulouse, France*

3 *Pontificia Universidad Católica de Chile, Chile*

4 *Antofagasta Minerals S.A., Chile.*

[csanchez@get.obs-mip.fr](mailto:csanchez@get.obs-mip.fr)

Supergene copper enrichment occurs during porphyry unroofing<sup>1,2</sup>. However, there are very few geological data documenting when this mineralization occurs, whether at the moment of the tectonic uplift responsible for the unroofing, or much later during relief waning and pedimentation. Here, we present new low-temperature thermochronologic data of the Late Cretaceous to Eocene porphyries from the Centinela mining district in the Atacama Desert. The modeling of 6 fission tracks and 10 (U-Th)/He ages on apatite and U-Pb dating on zircon (including 3 new ones) indicate a significant phase of cooling associated to denudation between 45 and 30 Ma, a longer time period for the Incaic deformation phase than previously reported<sup>3</sup>. Comparing those results with the 22-14 Ma<sup>4</sup> supergene and exotic mineralization ages in the district indicates that enrichment took place during the flattening phase of the relief. It also suggests a ~10 Ma response time gap between the main phase of denudation and the supergene mineralization. Those results have a direct impact on mining prospection strategy.

### **References**

1. Sillitoe, Richard H. "Supergene oxidized and enriched porphyry copper and related deposits." *Economic Geology 100th Anniversary Volume 29* (2005): 723-768.
2. Hartley, A.J., Rice, C.M. Controls on supergene enrichment of porphyry copper deposits in the Central Andes: a review and discussion. *Mineralium Deposita* 40 (2005), 515–525.
3. Charrier, Reynaldo, Marcelo Farías, and Víctor Makshev. "Evolución tectónica, paleogeográfica y metalogénica durante el Cenozoico en los Andes de Chile norte y central e implicaciones para las regiones adyacentes de Bolivia y Argentina." *Revista de la Asociación Geológica Argentina* 65.1 (2009): 05-35.
4. Sedimentological constraints on geomorphologic and palaeoclimate conditions for supergene and exotic-Cu mineralization: the mid Eocene-Miocene Centinela Basin, Atacama Desert." *Basin Research*, submitted.

# Linking Late Miocene magmatism and exhumation of the Pamir-West Kunlun Mountains to lithospheric thinning

Kai Cao<sup>1, 2\*</sup>, Guocan Wang<sup>1, 2</sup>, Zhongcheng Zeng<sup>3</sup>, Anne Replumaz<sup>4</sup>,

<sup>1</sup> State Key Laboratory of Geological Processes and Mineral Resources, School of Earth Sciences, China University of Geosciences, Wuhan 430074, China

<sup>2</sup> Center for Global Tectonics, China University of Geosciences, Wuhan 430074, China

<sup>3</sup> Shaanxi Center of Geological Survey, Xi'an 710068, China

<sup>4</sup> Institut des Sciences de la Terre, Université Grenoble, BP 53, Grenoble 38041, France  
(\* [kai.cao@cug.edu.cn](mailto:kai.cao@cug.edu.cn))

A growing number of tectonic, climatic and ecologic evidences suggest that the Tibetan Plateau has likely developed outward and upward since the Late Miocene<sup>1</sup>. In northern Tibet, the ribbon-like occurrence of magmas and volcanic rocks seems to dictate the possible link between the plateau growth to lithospheric deformation. Three end-member models are proposed to account for Neogene magmatism and crustal deformation in northern Tibet, including 1) southward subduction of the Tarim lithosphere mantle<sup>2-3</sup>, 2) convective removal of lower lithosphere<sup>4-6</sup>, and 3) penetration of molten crust into Kunlun terrane<sup>7-8</sup>. Distinguishing these competing models is critical to understand the intracontinent orogenesis in central Asia, in which the lithospheric processes have led to upper crust deformation.

In this study, we report newly-discovered potassic plutons emplaced at ~11 Ma in the SE Pamir. Together with recently-reported volcanism at ~12 Ma in the West Kunlun Mts.<sup>9</sup>, it can be inferred that Late Miocene magmas extend from the north-central Tibet to the central Pamir. Furthermore, our new apatite fission-track analysis in the SE Pamir-West Kunlun Mountains present uniform ages clustering at ~11-6 Ma. Forward and inverse modeling indicate Late Miocene (~11-6 Ma) rapid exhumation of the SE Pamir-West Kunlun Mountains, concurrent with accelerated exhumation of the Shakh dara dome<sup>10</sup>, initial doming of the Muztagata massif<sup>11-13</sup>, and thrusting of the West Kunlun Mts. front faults<sup>11</sup>. The simultaneous doming and potassic magmatism imply stress relaxation of the upper crust at that time, which was likely related to the thinning of lower lithosphere of the northern Tibet, as imaged by geophysical observations<sup>3, 14</sup>. We propose that detachment of lower lithosphere, triggering lithosphere thinning, seems a more plausible mechanism responsible for Neogene magmatism, rock exhumation and plateau growth in northwestern Tibet.

## References

1. Molnar, P. & Rajagopalan, B., Late Miocene upward and outward growth of eastern Tibet and decreasing monsoon rainfall over the northwestern Indian subcontinent since ~10 Ma. *Geophys. Res. Lett.* **39**, L9702 (2012).
2. Matte, P. *et al.*, Tectonics of western Tibet, between the Tarim and the Indus. *Earth Planet. Sc. Lett.* **142**, 311 (1996).
3. Wittlinger, G. *et al.*, Teleseismic imaging of subducting lithosphere and Moho offsets beneath western Tibet. *Earth Planet. Sc. Lett.* **221**, 117 (2004).
4. Turner, S. *et al.*, Timing of Tibetan uplift constrained by analysis of volcanic rocks. *Nature* **364**, 50 (1993).
5. Turner, S. *et al.*, Post-collision, shoshonitic volcanism on the Tibetan Plateau: Implications for convective thinning of the lithosphere and the source of ocean island basalts. *J. Petrol.* **37**, 45 (1996).
6. Molnar, P., England, P. & Martinod, J., Mantle dynamics, uplift of the Tibetan Plateau, and the Indian monsoon. *Rev. Geophys.* **31**, 357 (1993).
7. Le Pape, *et al.*, Penetration of crustal melt beyond the Kunlun Fault into northern Tibet. *Nat. Geosci.* **5**, 330 (2012).
8. Wang, Q. *et al.*, Crustal Melting and Flow beneath Northern Tibet: Evidence from Mid-Miocene to Quaternary Strongly Peraluminous Rhyolites in the Southern Kunlun Range. *J. Petrol.* **53**, 2523 (2012).
9. Cao, K., *et al.*, Exhumation history of the West Kunlun Mountains, northwestern Tibet: Evidence for a long-lived, rejuvenated orogen. *Earth Planet. Sc. Lett.* **432**, 391 (2015).
10. Stübner, K. *et al.*, The giant Shakh dara migmatitic gneiss dome, Pamir, India-Asia collision zone: 2. Timing of dome formation. *Tectonics* **32**, 1404 (2013).
11. Cao, K., *et al.*, Cenozoic thermo-tectonic evolution of the northeastern Pamir revealed by zircon and apatite fission-track thermochronology. *Tectonophysics* **589**, 17 (2013).
12. Robinson, A. C. *et al.*, Cenozoic evolution of the eastern Pamir: Implications for strain-accommodation mechanisms at the western end of the Himalayan-Tibetan orogen. *Geol. Soc. Am. Bull.* **119**, 882 (2007).
13. Sobel, E. R. *et al.*, Late Miocene-Pliocene deceleration of dextral slip between Pamir and Tarim: Implications for Pamir orogenesis. *Earth Planet. Sc. Lett.* **304**, 369 (2011).
14. Zhang, Z. *et al.*, The Moho beneath western Tibet: Shear zones and eclogitization in the lower crust. *Earth Planet. Sc. Lett.* **408**, 370 (2014).

## Multi-stage cooling events of the Gangdese terrane during the Cenozoic: Implications for the high plateau forming in south Tibet

Guocan Wang<sup>1,2</sup>, Tianyi Shen<sup>1,2</sup>, Peter van der Beek<sup>3</sup>, Matthias Bernet<sup>3</sup>,  
An Wang<sup>1,2</sup>, Kexin Zhang<sup>1</sup>

1 *Center for Global Tectonics, School of Earth Sciences, China University of Geosciences, Wuhan, China*

2 *State Key Laboratory of Geological Processes and Mineral Resources (GPMR), China University of Geosciences, Wuhan, China*

3 *Institut des Sciences de la Terre (ISTerre), Université Grenoble Alpes, Grenoble, France (wgcan@cug.edu.cn)*

Constrain the uplift and exhumation history of the Gangdese terrane is critical for understanding the complex geodynamic evolution of the Tibetan Plateau. We present new fission track (FT) analysis of 8 detrital zircon and 1 detrital apatite samples from sandstones, and 6 detrital zircon samples from modern sediments in Mt. Kailas area, western Tibet. The sandstone samples were collected along three stratigraphic sections in the Late Oligocene-Early Miocene Kailas Formation. In addition, eight bedrock samples for both zircon and apatite FT age dating were collected from the Gangdese batholith at the eastern Mt. Kailas area.

The detrital zircon FT ages of the sandstones show high peaks at  $52.4\pm 6.9$  and  $31.2\pm 5.2$  Ma (Fig. 1A). The detrital zircon FT ages of the modern sediments exhibit a strong peak at  $\sim 35$ - $26$  Ma from all samples and two younger peak ages at  $\sim 15$  Ma from samples near the south of the Lunggar rift and at  $\sim 10$  Ma from samples in the Karakorum shear zone (Fig. 1B). The detrital apatite FT sample from the Kailas Formation has been fully reset after deposition and yields two peak ages at  $13.7\pm 2.0$  and  $8.0\pm 2.9$  Ma. The zircon FT ages from Gangdese batholith concentrate in 21-19 Ma, whereas the apatite FT ages range from  $16.3\pm 1.9$  to  $6.7\pm 1.4$  Ma. The HeFTy thermal modeling combined the zircon and apatite FT ages and apatite FT lengths illustrate a rapid cooling between 20-15 Ma at a rate of 30-24 °C/Ma (Fig. 1C). Thermal modeling of the sample at south of Lunggar rift also shows a rapid cooling at  $\sim 11$  Ma (Fig. 1C).

The detrital zircon FT data shows that the source of the Kailas Formation experienced rapid cooling at the Early Cenozoic probably due to the exhumation driven by the India-Asia collision and the subsequent volcanic activities. The Oligocene peak age is possibly related to the movement along the north-dipping Gangdese thrust between  $\sim 30$ - $24$  Ma, which caused extensive denudation of the Gangdese batholith in its hanging wall<sup>1</sup>. This result does not support the opinion that the Gangdese batholith transitioned to an inactive status between the Middle Eocene and Early Miocene. The rapid cooling started in the Early Miocene was observed not only at the Gangdese batholith, but also in the Kailas Formation<sup>2,3</sup> and Himalaya region<sup>4</sup>, which could be attributed to the uplift resulting from slab break off of the subducted Indian lithosphere during 20-15 Ma<sup>5,6</sup>. The south Gangdese terrane margin should obtain its high altitude after this phase of uplift. The rock cooling after the Middle Miocene is mostly close to the active faults, which are associated with the Karakorum fault or N-S normal faults.

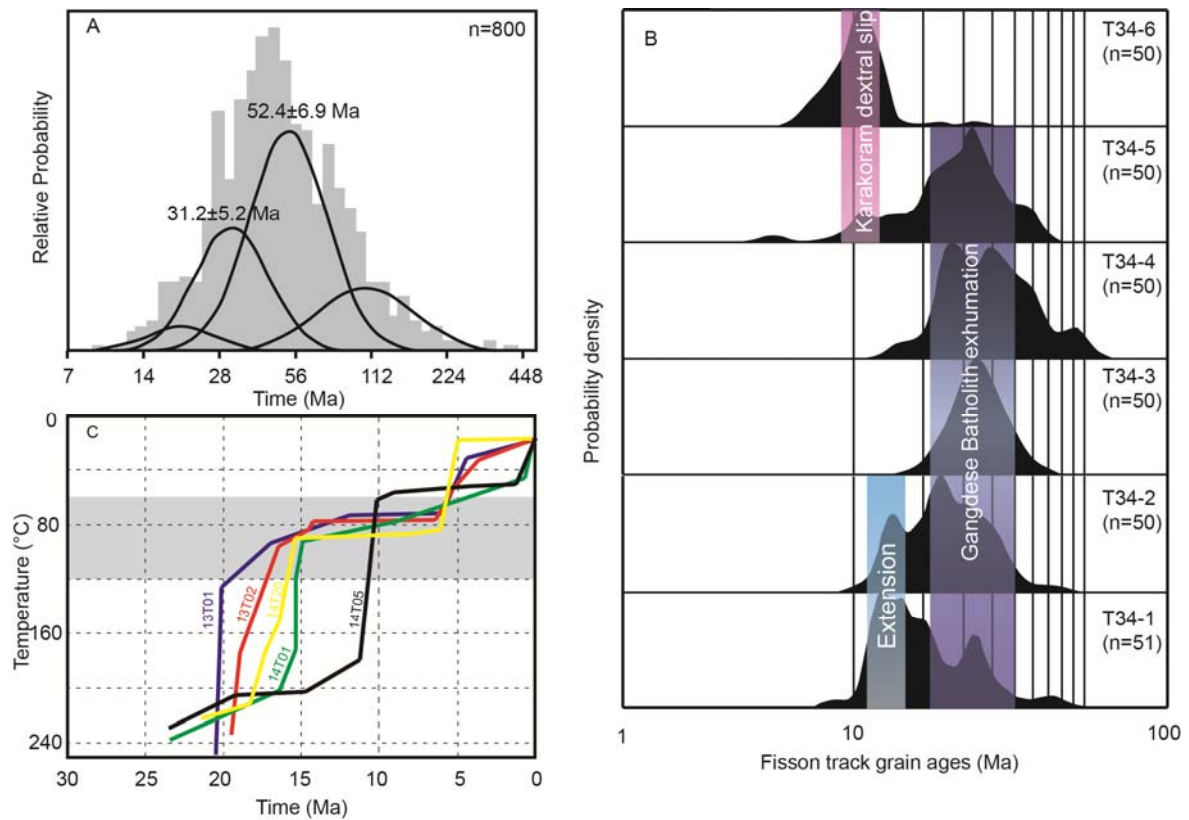


**Figure 1.** A. Probability density plot of detrital zircon fission track ages of the Kailas Formation in western Tibet. B. Probability density plot of detrital zircon fission track ages of the modern river sediments in Mt. Kailas area. C. HeFTy program modeling results showing best fits for five samples from Gangdese batholith.  $n$  in A and B is the number of counted grains.

## References

1. Yin, A., Harrison, T.M., Ryerson, F.J., Chen, W., Kidd, W.S.F. & Copeland, P. Tertiary structural evolution of the Gangdese thrust system, southeastern Tibet. *J. Geophys. Res.* 99, 18175-18201 (1994).
2. Sanchez, V.I., Murphy, M.A., Robinson, A.C., Lapen, T.J. & Heizler, M.T. Tectonic evolution of the India-Asia suture zone since Middle Eocene time, Lopukangri area, south-central Tibet. *J. Asian Earth Sci.* 62, 205-220 (2013).
3. Carrapa, B., Orme, D.A., DeCelles, P.G., Kapp, P., Cosca, M.A. & Waldrip, R. Miocene burial and exhumation of the India-Asia collision zone in southern Tibet: response to slab dynamics and erosion. *Geology* 42, 443-446 (2014).
4. Bernet, M., van der Beek, P., Pik, R., Huyghe, P., Mugnier, J., Labrin, E. & Szulc, A. Miocene to Recent exhumation of the central Himalaya determined from combined detrital zircon fission-track and U/Pb analysis of Siwalik sediments, western Nepal. *Basin Res.* 18, 393-412 (2006).
5. Husson, L., Bernet, M., Guillot, S., Huyghe, P., Replumaz, A., Robert, X. & van der Beek, P. Dynamic ups and downs of the Himalaya. *Geology* 42, 839-842 (2014).
6. Replumaz, A., Capitanio, F.A., Guillot, S., Negredo, A.M. & Villasenor, A. The coupling of Indian subduction and Asian continental tectonics. *Gondwana Res.* 26, 608-626 (2014).



## **Constraining Uplift and Erosion in the Western Himalayan Syntaxis. A Multiple Thermochronometric Study from the Neelum River Region, NW Himalayas, Pakistan**

Syed Ali Turab<sup>1,2</sup>, Kurt Stüwe<sup>1</sup>, Finlay M. Stuart<sup>3</sup>, David M. Chew<sup>4</sup>, Nathan Cogne<sup>4</sup>  
*1 Institut für Erdwissenschaften, Universität Graz, Universitätsplatz 2, 8010 Graz, Austria.*  
*2 National Centre of Excellence in Geology, University of Peshawar, Peshawar-25120,  
Khyber Pakhtunkhwa, Pakistan.*  
*3 Isotope Geosciences Unit, Scottish Universities Environmental Research Centre, East  
Kilbride G75 0QF, UK.*  
*4 Department of Geology, School of Natural Sciences, Trinity College Dublin, Dublin 2,  
Ireland.*  
(syed.ali-turab@edu.uni-graz.at)

Tectonics and erosion have been suggested as alternative driving mechanisms for rapid exhumation of the western Himalayan syntaxis. The geometry of the region showing rapid exhumation holds this key information. Main agent of rapid exhumation could thus be nominated by understanding whether the exhumation follows the major structures (tectonics) or the drainage pattern (erosion) (Fig. 1A). In order to resolve this debate we combine (U-Th-Sm)/He, fission track and U-Pb dating of apatite with (U-Th)/He dating of zircon and stream power analysis from the Neelum valley region of Azad Jammu and Kashmir, Pakistan (Fig. 1B). Pooled fission track ages show a range of  $2.2 \pm 0.4$  to  $7.0 \pm 0.4$  Ma ( $1\sigma$ ) while apatite He ages range from  $2.0 \pm 0.1$  to  $8.7 \pm 0.5$  Ma. Zircon He ages show a range from  $6.1 \pm 0.1$  to  $14.6 \pm 0.3$  Ma and apatite U-Pb ages are Proterozoic to as young as 17.0 Ma and can be separated into three groups depending on the degree they have been affected by Himalayan tectonics. Stream power analysis of the Neelum river catchment indicates high steepness index of  $K_{sn} > 500 \text{ m}^{0.9}$  along the major river and lower  $K_{sn}$  in the headwaters. The boundary between samples with unaffected and affected U-Pb ages, as well as transition from high  $K_{sn}$  to lower  $K_{sn}$  values along the main Neelum river, fit well with the mapped trace of the Main Central Thrust (which has been a topic of controversy), thus corroborating the presence of the thrust in the southeastern parts of our study area. Thermal history modeling indicates accelerated exhumation at  $\sim 10$  Ma in the uppermost 5-6 km of the crust that might represent the onset of movement along Main Boundary Thrust. In combination with published cooling ages, our data indicate that exhumation contours run more or less parallel to the major structures in the region and fission track ages are younger close to the main faults supporting the contention that tectonics is the main driving mechanism for exhumation at the western syntaxis of the Himalayas (Fig. 1C).

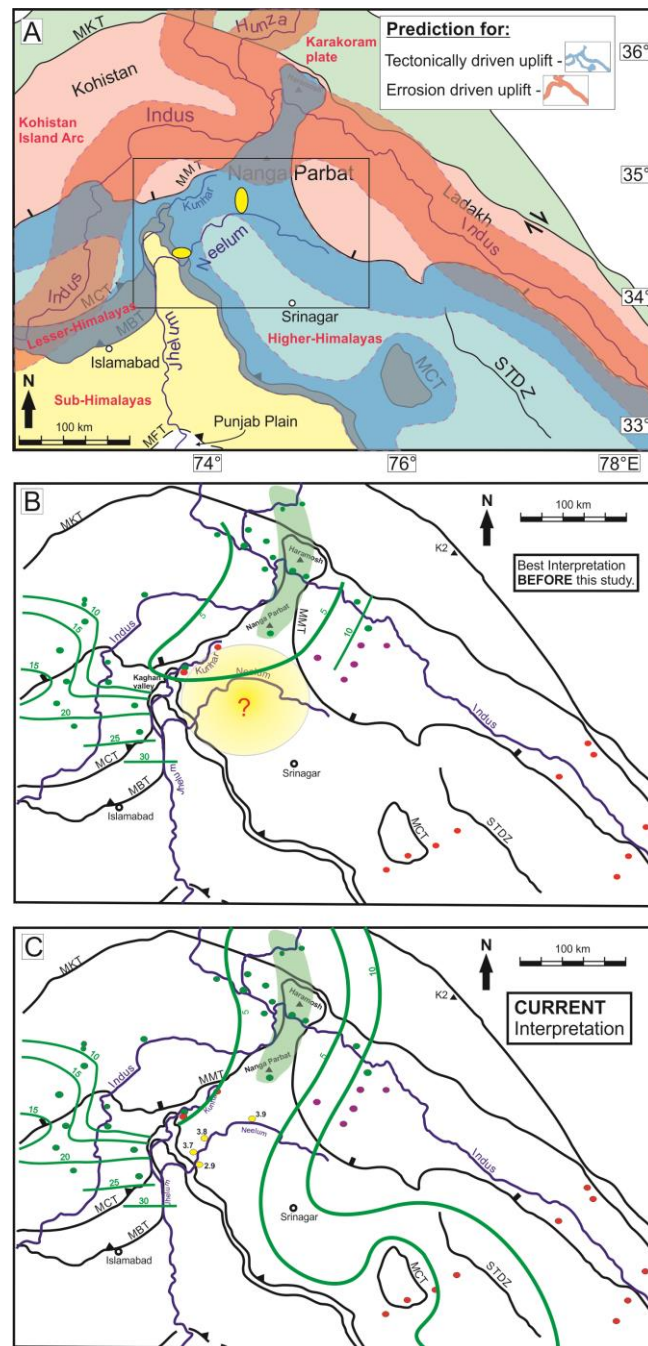


**Figure 1.** Geological map (A) showing predictions for areas with high exhumation rates. Red text highlights different rock units (after Wilke et al., 2012). Yellow ellipses show the location of two profiles sampled; (B) map of the same area as (A), showing regional scale faults and rivers along with published apatite fission track ages. Green dots and contours = after Zeitler (1985) also showing region of high exhumation rates (green area). Red dots = after Wilke et al. (2012) and references therein. Purple = van der Beek et al. (2009). Yellow transparent ellipse highlights a region without data and hence tackled herein this study; (C) Same map as (B) with the addition of new apatite fission track data from this study and re-interpretation of exhumation age-contours.

## References

1. Van der Beek, P., Van Melle, J., Guillot, S., Pêcher, A., Reiners, P. W., Nicolescu, S. & Latif, M. Eocene Tibetan plateau remnants preserved in the northwest Himalaya. *Nature Geoscience* **2**, 364-368 (2009).
2. Wilke, F. D. H., Sobel, E. R., O'Brien, P. J. & Stockli, D. F. Apatite fission track and (U-Th)/He ages from the Higher Himalayan Crystallines, Kaghan Valley Pakistan: Implications for an Eocene Plateau and Oligocene to Pliocene exhumation. *Journal of Asian Earth Sciences* **59**, 14-23 (2012).
3. Zeitler, P. K. Cooling history of the NW Himalaya, Pakistan. *Tectonics* **4** (1), 127-151 (1985).

# Provenance and exhumation history of the Sierra Nevada de Santa Marta, Colombian Caribbean: The relationship between orogenic pulses and the Caribbean - South America tectonic during the Cenozoic

Sebastian Echeverri<sup>1</sup>, Mauricio Parra<sup>2</sup>

1 Institute of Geosciences – University of Sao Paulo, Brazil

2 Institute of Energy and Environment – University of Sao Paulo, Brazil

juansebasecheverri@gmail.com

A still poorly understood interaction among the Caribbean (CA), Nazca (NP) and South American (SA) plates, which includes alternating episodes of subduction and arc-continent collision, has given rise to the northwestern Andes in northern Colombia. Dextral migration and oblique subduction of the CP along a pre-strained South American margin since ~70 Ma have resulted in the formation of transpressional and transtensional domains, the displacement and rotation of massifs, and the formation of sedimentary basins<sup>1-2</sup>. One of these massifs, the up to 5.8 km-high Sierra Nevada de Santa Marta (SNSM) is the highest coastal range on Earth and consists of a collage of igneous and metamorphic rocks with ages ranging from from Proterozoic to Eocene<sup>3</sup>.

Paleocene-Eocene calc-alkaline granitoids (~56-45Ma) exposed in the northern SNSM are the relict of a magmatic arc associated with the subduction of the Caribbean plate<sup>4</sup>. From Eocene onwards, initial magmatic quiescence and subsequent pulses of exhumation are associated with the dextral lateral translation of the Caribbean plate, and triggered the opening of Oligocene to recent extensional and strike-slip related basins around the SNSM, straddling the Oca and Santa Marta-Bucaramanga fault systems

Sedimentary facies, new paleocurrent, conglomerate and sandstone petrography, and heavy mineral analyses in such alluvial Oligocene-Pliocene strata surrounding the SNSM, and in their modern analogues, suggest proximal source areas located in the Sierra Nevada. The dominant presence of arkose, lithic arkose and feldspathic litharenites with angular grains and clayey matrix, as well as the abundance and preservation unstable heavy minerals (*e.g.* biotite, amphibole) suggest little transport and rapid sedimentation from nearby source areas.

Such local provenance is further illustrated by new apatite fission track and (U-Th) He data obtained in one bedrock age-elevation profile and 5 detrital samples collected in modern sand samples from rivers draining the the NW range's sector, as well as sparse published data. Episodic orogenesis is characterized by two stages of rapid exhumation during the early to middle Eocene (55-41Ma) and the late Oligocene-middle Miocene (~25-11 Ma) followed by stages of much slower exhumation. Bedrock and detrital ages typify a northwestward increase in long-term exhumation rates, in agreement with the development of a structural syntaxis.

The lack of AHe cooling ages younger than 7 Ma in a high-relief, deeply incised range with a pronounced gravity anomaly, suggests a present-day stage of denudational immaturity in which recent uplift has caused less than ~2 km of exhumation, so that erosion has not yet exhumed ages associated to this very last tectonic pulse. Ongoing investigations on quaternary denudation rates based on cosmogenic radio nuclides and sediment discharge data will help bridge the gap between short-term and long-term denudation and provide insights on the geodynamic mechanisms responsible for the uplift of this exotic range.

## References

1. Pindell, J., Kennan, L., Maresch, W.V., Stanek, K.-P., Draper, G., Higgs, R. Plate-kinematics and crustal dynamics of circum-Caribbean arc-continent interactions: Tectonic controls on basin development in Proto-Caribbean margins. *Geol. Soc. Am. Spec. Pap.* **394**, 7–52 (2005).

2. Montes, C., Guzman, G., Bayona, G., Cardona, A., Valencia, V., and Jaramillo, C. Clockwise rotation of the Santa Marta massif and simultaneous Paleogene to Neogene deformation of the Plato-San Jorge and Cesar-Ranchería basins: *Journal of South American Earth Sciences* **29**, 832-848 (2010).
3. Tschanz, C. M., Jimeno, A., and Vesga, C. Geology of the Sierra Nevada de Santa Marta area (Colombia): Ingeominas, Bogotá (1969).
4. Cardona, A., Weber, M., Valencia, V., Bustamante, C., Montes, C., Cordani, U., Muñoz, C.M. Geochronology and geochemistry of the Parashi granitoid, NE Colombia: Tectonic implication of short-lived Early Eocene plutonism along the SE Caribbean margin. *J. South Am. Earth Sci.* **50**, 75–92 (2014).
5. Villagómez, D., Spikings, R., Mora, A., Guzmán, G., Ojeda, G., Cortés, E., Van der Lelij, R. Vertical tectonics at a continental crust-oceanic plateau plate boundary zone: Fission track thermochronology of the Sierra Nevada de Santa Marta, Colombia: *Tectonics* **30**, 1-18 (2011).
6. Cardona, A., Valencia, V., Weber, M., Duque, J., Montes, C., Ojeda, G. Y., Reiners, P., Domanik, K., Nicolescu, S., and Villagomez, D. Transient Cenozoic stages in the southern margin of the Caribbean plate: U-Th/He thermochronological constraints from Eocene plutonic rocks in the Santa Marta massif and Serrania de Jarará, northern Colombia: *Geologica Acta* **9**, 3-4, 445-466 (2011).

## Unravelling the late Miocene exhumation in the West-Central Pyrenees

Charlotte Fillon<sup>1</sup>, Raphael Pik<sup>2</sup>, Frédéric Mouthereau<sup>1</sup>, Nicolas Bellahsen<sup>3</sup>, C. Gautheron<sup>4</sup>, Sylvain Calassou<sup>5</sup>, Emmanuel Masini<sup>5</sup>

*1 GET, Université Paul Sabatier, Toulouse, France*

*2 CRPG, Université de Lorraine, Nancy, France*

*3 ISTEP, Université Pierre et Marie Curie, Paris, France*

*4 GEOPS, Université Paris Sud, Orsay, France*

*5 Total, Pau, France*

*(charlotte.fillon@get.omp.eu)*

The Pyrenean range is a classical doubly-vergent orogenic wedge, flanked by two foreland basins. During the last decade, the Pyrenees have been extensively studied for understanding various geodynamic processes, from hyper-extension to post-orogenic evolution of foreland basins. In this framework, numerous low-T thermochronological studies (300 ages across the range) have been published, documenting the different phases of pre-, syn-, and post-orogenic exhumation. The orogen climax is dated to late Eocene, with rates of 2.8 mm/yr, as revealed by AFT/AHe vertical profiles performed in the cristalline massifs of the central Axial Zone<sup>1,2</sup>. The latest compressional features in the southern Pyrenean foreland are dated of late Oligocene and the orogen is supposed to be mainly inactive since then.

Nevertheless, there is growing evidence from independent methods that a late Miocene (around 10 Ma) uplift occurred in the south central and western Pyrenees, as well as to the north-east. To the South, we linked the post-orogenic exhumation to the excavation of the foreland valleys caused by the opening of the endorheic Ebro basin towards the Mediterranean Sea. To the West, the tectonic out-of-sequence reactivation of the Gavarnie thrust has been invoked<sup>3</sup> to explain the late Miocene AHe ages in the Bielsa massif.

In this study, we present time-Temperature paths from a new dataset of AHe, AFT and ZHe ages from three different massifs in the western/central part of the Axial Zone. The thermal modeling was conducted using QTQt<sup>4,5</sup> and consists of inversions of 3 age/elevation profiles (AHe, ZHe and AFT) from 10 samples in the Bielsa massif, 4 in the Bordères-Louron massif and 9 in the Neouvielle massif.

From these paths, we precisely position the signal of 10 Myr-exhumation in the central cristalline massif (Neouville pluton). The other massifs to the East and South do not seem to have recorded this exhumation. Moreover, the time-Temperature paths recently published<sup>6</sup>, show a similar phase of exhumation in westernmost massifs of "Cauterets".

This study thus summarizes all evidences for the post-orogenic phase and attempt to provide preliminary explanation for it: is exhumation linked to the Aquitaine foreland basin evolution? Does it reflect a tectonic reactivation of the Pyrenees? or is the signature of a regional/global climate change conditions ?

## References

1. Fitzgerald, P. G., Muñoz, J. A., Coney, P. J., & Baldwin, S. L. (1999). Asymmetric exhumation across the Pyrenean orogen: implications for the tectonic evolution of a collisional orogen. *Earth and Planetary Science Letters*, 173(3), 157-170.
2. Fillon, C., & van der Beek, P. (2012). Post-orogenic evolution of the southern Pyrenees: constraints from inverse thermo-kinematic modelling of low-temperature thermochronology data. *Basin Research*, 24(4), 418-436.
3. Jolivet, M., Labaume, P., Monié, P., Brunel, M., Arnaud, N., & Campani, M. (2007). Thermochronology constraints for the propagation sequence of the south Pyrenean basement thrust system (France-Spain). *Tectonics*, 26(5).
4. Gallagher, K. (2012). Transdimensional inverse thermal history modeling for quantitative thermochronology. *Journal of Geophysical Research: Solid Earth*, 117(B2).
5. Gallagher, K., Charvin, K., Nielsen, S., Sambridge, M., & Stephenson, J. (2009). Markov chain Monte Carlo (MCMC) sampling methods to determine optimal models, model resolution and model choice for Earth Science problems. *Marine and Petroleum Geology*, 26(4), 525-535.
6. Bosch, G. V., Teixell, A., Jolivet, M., Labaume, P., Stockli, D., Domènech, M., & Monié, P. (2016). Timing of Eocene–Miocene thrust activity in the Western Axial Zone and Chaînons Béarnais (west-central Pyrenees) revealed by multi-method thermochronology. *Comptes Rendus Geoscience*.



**THERMO2016**

**SESSION 9**

**BASIN EVOLUTION AND THERMAL HISTORIES**

# Detrital zircon (U-Th)/He and fission track data of natural deep borehole samples and its geological significance

Qiu Nansheng, Cai Change

*State Key Laboratory of Petroleum Resource and Prospecting, China University of Petroleum,*

*Beijing 102249, China*

*(Corresponding author: qiunsh@cup.edu.cn)*

**Abstract:** The zircon (U-Th)/He and fission track (FT) thermochronometry has been used as a thermal indicator to study thermal history of the deep sedimentary basin at high temperature. The closure temperature of helium and annealing temperature of FT are important parameters for the zircon (U-Th)/He thermochronometry. In this paper, the zircon He closure temperature and FT annealing temperature were studied by establishing the evolutionary pattern between zircon He and FT ages and zircon burial depth based on the data of natural borehole samples obtained from the Cenozoic strata in the Bohai Bay and Tarim basins, which have different thermal settings. The results show that the zircon He closure temperature of natural samples in the sedimentary basin is approximately 195°C, higher than the temperature obtained from the thermal simulation experiments (183°C). The high He closure temperature resulted from long term radiation damage accumulation and sufficient grain radius. In addition, two zircon FT age profiles from different thermal background show that there exist different annealing temperatures. The ZFT annealing temperature is about 160°C in the deep borehole of Tarim basin with low thermal background. However, the ZFT annealing temperature is about 210°C in the deep borehole of the Bohai Bay basin with high thermal background. We also point out that effective uranium concentration and radiogenic <sup>4</sup>He concentration have apparent influence on the zircon He and FT ages. This study is a reevaluation of the conventional zircon He closure temperature and annealing temperature. Thus, properly understanding the ZHe/ZFT ages, closure/annealing temperatures, and their influence factors, ZHe/ZFT dating can provide the true explanation of the testing zircon He/FT ages, and has a great guiding significance in the studying of the evolution of source rocks and the process of hydrocarbon accumulation in the deep sedimentary basin.

**Key words:** Zircon He age; Zircon fission track; Closure temperature; Annealing temperature; Radiation damage; Sedimentary basin



## Thermal history of the Campos Basin from apatite fission track thermochronology in borehole samples

Christie Helouise Engelmann de Oliveira<sup>1</sup>, Andréa Ritter Jelinek<sup>1</sup>, Farid Chemale Jr.<sup>2</sup>,  
Matthias Bernet<sup>3</sup>

*1 Universidade Federal do Rio Grande do Sul, Brazil*

*2 Universidade de Brasília, Brazil*

*3 Université Joseph Fourier, France  
(christie.oliveira10@gmail.com)*

The Campos Basin is the largest offshore sedimentary basin in the southeastern Brazilian margin and originated by breakup of West Gondwana in the Early Cretaceous. We carried out a thermochronological study by apatite fission track analysis from deep-water borehole samples of the Campos Basin in order to define thermal events during basin evolution. Apatite fission track central ages and single grain ages vary from  $116 \pm 12$  Ma to  $285 \pm 19$  Ma and from 44 to 499 Ma, respectively, and do not show a correlation with depth. All apatite fission track central ages are older than the stratigraphic age and their single grain ages suggest they have not undergone substantial post-depositional annealing and are therefore representative of their provenance. The apatite fission track age distribution includes three age components: a) a Permian component (ca. 270 Ma; 41%), b) a Late Jurassic component (ca. 160 Ma; 40%) and c) a Cretaceous component (ca. 95 Ma; 19%). The thermal history model derived from the borehole samples suggest rapid reheating during the Pleistocene to the present-day temperatures, and is probably linked to an eustatic fall. The youngest apatite fission track ages of 44 Ma are not well resolved but possibly represent apatite grains that have been completely reset and correspond to the youngest volcanic event in the region at ca. 43 Ma (Winter et al., 2007).

### References

1. Winter, W. R., Jahnert, R. J., França, A. B. Bacia de campos. *Boletim de Geociências da Petrobras* **15**, 511-529 (2007).

## **A tectonically uplifted Xichang basin at the southeastern Tibetan plateau, as revealed by structural geology and thermochronology data**

Bin DENG<sup>1\*</sup>, Shugen LIU<sup>1</sup>, Zhiwu LI<sup>1</sup>, Gaoping ZHAO<sup>1</sup>, Lei JIANG<sup>1</sup>, and Luba JANSKA<sup>2</sup>  
Author<sup>3</sup>

1- *State Key Laboratory of Oil and Gas Reservoir Geology and Exploitation/Chengdu University of Technology, Chengdu, China, 610059*

2-*Geological Survey of Canada-Atlantic, Dartmouth, N.S. Canada  
(dengbin13@main.cdut.edu.cn)*

The Xichang basin, an uplifted terrestrial basin in southeastern Tibet, provides key information about formation and processes at the eastern Tibetan plateau. To determine when and how the uplifted basin developed, we conducted detailed structural observations and obtained thermochronology data from the Xichang basin and its periphery. The Xichang basin is characterized by gentle deformation of terrestrial strata, segmented by E-vergent thrusting boundary faults in the Daliang Mts. for example the Shimian-Qiaojia fault and Ganluo-Zhaojue fault, to separate the southwestern Sichuan basins. Two stages of deformation, strike-slipping and following E-W oriented shortening resulted in an oblique shortening between the southeastern Tibetan Plateau and the Sichuan basin. Restored balanced transects of post-late-Triassic strata along ~250 km long traverse indicate ~10 % east-west shortening strain (i.e., ~20-30 km) at the southeastern Tibetan plateau during Cenozoic time.

New apatite fission track data interpreted in the light of (U-Th)/He data confirmed the two-stage post-Late Mesozoic evolution history across the Xichang basin and its periphery. A subsidence and burial episode of the Xichang basin was dominated by terrestrial deposition prior to early Cenozoic time, followed by a mountain building process with two-step accelerated cooling and exhumation processes at ~40-30 Ma and ~10-5 Ma, with rates of ~2.0 °C/Myr and ~8 °C/Myr, respectively. It suggests that the Xichang basin has experienced ~2.5-5 km of exhumation, which is much larger than that of the adjacent southwestern Sichuan basin, where it is ~1-2 km. This demonstrates an uplift of the Xichang basin when compared to the Sichuan basin.

Our structural transects and thermochronology data show a high degree of consistency between the Xichang basin and the southwestern Sichuan basin. It indicates similar tectonic evolution in pre-Cenozoic time at the western margin of the South China block, which at this time was represented by a Palaeo-Yangtze terrestrial basin. Subsequently, the Daliang Mts. dissected the basin into an uplifted Xichang basin and the Sichuan basin. Furthermore, one-dimensional modelling of crustal thickening with erosion supports a tectonic shortening mechanism to account for the uplift of the Xichang basin, situated in the southeastern Tibetan plateau.

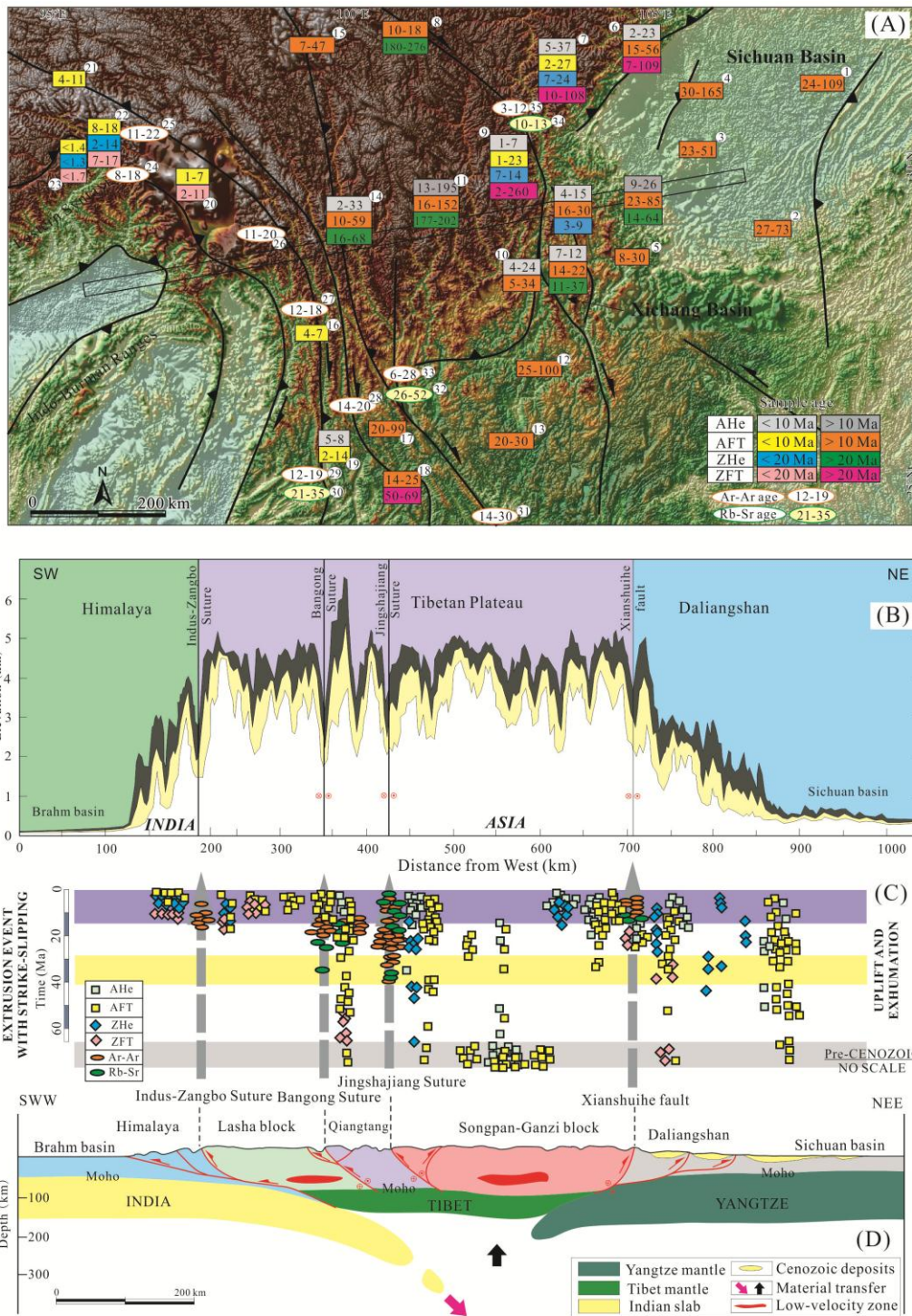


**Figure 1.** (a) General structural features in the eastern Himalayan syntaxis, southeastern Tibetan plateau to the Sichuan basin. The grey, yellow, blue, pink and red etc. rectangles and ellipses along boundary faults represent the correlation between cooling age measured in the Xichang basin and cooling ages across the continental collision zone in eastern Tibet. (b) Swath profile across eastern Tibet to the Sichuan basin, indicating significant difference in elevation across the region and an uplifted Xichang basin in comparison with the Sichuan basin; both of them show consistency in terrestrial strata deposition and two-step enhanced cooling processes during the Cenozoic. (c) Geo- and thermo-chronology data profiles show a close relationship between cooling and exhumation ages across the eastern Tibetan plateau. (d) Regional interpretive geologic transect from the eastern Himalayan syntaxis to the Sichuan basin.

## **The tectonic and denudation history of East Greenland: insights from apatite FT and He data**

A.G. Szulc<sup>1</sup>, T. Bernard<sup>2</sup>, P. Steer<sup>2</sup>, K. Gallagher<sup>2</sup>, A. Carter<sup>3</sup>, T. Kinnaird<sup>4</sup>, A.G. Whitham<sup>1</sup>, C. Johnson<sup>1</sup>

*1 CASP, Cambridge, UK*

*2 Géosciences Rennes, France*

*3 Earth and Planetary Sciences, Birkbeck, University of London, UK*

*4 Scottish Universities Environmental Research Centre (SUERC), UK*

*(adam.szulc@casp.cam.ac.uk)*

Excellent exposures of Mesozoic sediments in East Greenland are direct analogues for offshore petroleum reservoirs on the Mid-Norway and NE Greenland continental shelves. East Greenland is also considered to have been a source for some of the sediment that comprises these reservoirs. As such, a greater understanding of the tectonic and denudation history of East Greenland will have important implications for both academia and industry. Since the late 1990's CASP has been accumulating apatite fission track data from across East Greenland between 68°N and 75°N. The majority of these data come from a number of vertical profiles through the Caledonian basement and the oldest post-Caledonian sediments. More recently, apatite helium dating was conducted on samples from three of the vertical profiles. Inverse modelling of the vertical profile data provides thermal history constraints that correlate closely with structural and sedimentological field observations. Emerging from this exercise is a better picture of the tectonic and denudation history of East Greenland. For example, the start of rifting is now considered to have been much younger than the Devonian age that is widely reported in the literature. The results also have implications for the importance and timing of regional unconformity surfaces and suggest that an important phase of denudation occurred during the Late Triassic-Early Jurassic. The denuded sediment volume during this time period exceeded the accommodation space of the East Greenland margin. Along with provenance data, this confirms that East Greenland supplied a large proportion of the sediments that now comprise the petroleum basins of the Mid-Norway continental shelf. The data also provide insights into the late stage thermal evolution of the East Greenland continental crust. A heating phase at  $55\pm 5$  Ma, which relates to burial beneath basaltic lava flows is followed by a cooling phase at  $30\pm 5$  Ma. Fault offset estimates can at best explain only ~20% of this cooling. We therefore suggest that the most viable cooling mechanism is enhanced erosion as a result of the onset of glaciation. East Greenland has traditionally been thought to have been free of ice until the last 10 Myr. Our results imply that ice was present 4x earlier at the Eocene-Oligocene boundary. This coincides with a world-wide fall in surface temperature and the onset of Antarctica glaciation, indicating a climatic coupling of the northern and southern hemispheres.

## **Tracking low temperature tectonism of the St. Lawrence Platform (Canada) through apatite and zircon (U-Th)/He thermochronology**

David Schneider<sup>1</sup>, Rebecca Hardie<sup>1</sup>, Justin Emberley<sup>1</sup>, Jeremy Powell<sup>1</sup>

*1 Department of Earth & Environmental Sciences, University of Ottawa, Canada  
(david.schneider@uottawa.ca)*

The St. Lawrence Platform of eastern Canada lies within an intracratonic rift system and has historically been explored as a potential hydrocarbon reservoir. Previous and extensive vitrinite reflectance studies on the basin resolved the degree of thermal maturation yet the timing of the thermal maximum is not well understood. Determining the timing of such low temperature events can allow for a better understanding of the shallow crustal processes that may have allowed for the generation and entrapment of oil and gas. We have employed apatite (AHe) and zircon (ZHe) (U-Th)/He thermochronology across a network of late Cambrian to late Ordovician siliciclastic and Mesoproterozoic Grenvillian crystalline basement samples in order to resolve the history within a ~200-40°C window. Single crystal dates from individual samples show age dispersion by as much as 300 m.y. with a strong positive to negative correlation with increasing eU concentration. A similar positive correlation can be observed when significant intra-sample grain size variation is present. Raman spectroscopy results indicate that zircon varies from very crystalline to a transitional state, and exhibit both positive and negative age-damage trends, as a consequence of the progressive impact of radiation damage on He diffusion. AHe and ZHe dating of the crystalline rocks from ~1000 m elevations into the platform sediments (65 m) was conducted to evaluate the temperature-time history of the rift flank. Our data resolve Neoproterozoic post-Grenvillian 1-2°C/m.y. cooling and exhumation of the basement before rifting, and subsequent slow (0.3-0.1°C/m.y.) and protracted cooling to present. The crystalline basement has not experienced sufficient heating (>200°C) to reset the He systematics, including effects of the Cretaceous Great Meteor hotspot. Within the western corner of the platform, AHe and ZHe thermochronology for the Ottawa Embayment show trends of heating to temperatures that exceed those expected for the 1-2 km of estimated burial during the Devonian, yet remain cooler than the ZHe partial retention zone. To the east, near Montréal, thermal maxima of up to 200°C occurred during the middle Ordovician into the Devonian. Middle Paleozoic heating of the platform sediments is synchronous with the Taconic and Acadian orogenies occurring along the margin of Laurentia. Maximum heating is followed by a protracted cooling through the ZHe partial retention zone into the late Jurassic and early Cretaceous, when the cooling rate increases by an order of magnitude through the AHe partial retention zone until ca. 100 Ma. Increased Cretaceous cooling slightly precedes the alkaline intrusions that are likely related to the passage of the hot spot across the platform. From Anticosti Island, in the eastern platform, crystalline basement (at 1700 m depth) yield Oligocene AHe ages whereas the Ordovician units (1520 m depth) record Paleocene-Eocene AHe ages. Increased recognition of these low temperature events has augmented our understanding of the evolution of the platform and the rift, and consequently reduces the risks associated with oil and gas exploration.

# Low-temperature thermochronology of the Turkana Depression, East African Rift System: Insight into the lithospheric response to rift superposition

Samuel C Boone<sup>1</sup>, Andrew Gleadow<sup>1</sup>, Barry Kohn<sup>1</sup>, Christian Seiler<sup>1</sup> and Ling Chung<sup>1</sup>  
<sup>1</sup>University of Melbourne, Australia  
(samcboone@gmail.com)

The Turkana Depression (TD), with its subdued topography, wide region of extension (~150 km) and thinned continental crust (~20 km), contrasts strongly with the rest of the East African Rift System (EARS) south of the Afar triple junction. Elsewhere, the EARS is comprised of narrow rift trends (~50 km) traversing the uplifted, thicker crust (~35-40 km) of the Ethiopian and East African Domes. The Turkana region also hosts the oldest rift-related volcanics and extensional basins in the EARS, making it a critical region for understanding the geodynamic evolution of rifting in East Africa. Its location at the intersection of the failed Cretaceous-Paleogene South Sudanese-Anza Rifts and Paleogene-Recent EARS makes it an ideal region to investigate if, and how, the crustal architecture inherited from earlier rifting affected the lithospheric response to later extension. However to date, no thermochronological data exists to constrain the timing of rift inception, degree of rift-related denudation and subsidence histories of basins in the TD.

Here we present apatite fission track (AFT) and (U-Th)/He (AHe), and zircon (U-Th)/He (ZHe) data from Precambrian basement and Late Cretaceous-Eocene sedimentary rocks in the TD. ZHe results from basement rocks record rapid Early Cretaceous cooling likely representing deep-seated exhumation associated with South Sudanese-Anza rifting. Detrital zircon grains from overlying Late Cretaceous-Eocene sandstones yield a range of older ZHe ages, consisting of a predominant Silurian-Early Devonian population and secondary group of Permian-Middle Jurassic ages. The older age population is interpreted to represent early Paleozoic denudational cooling that affected the source provenance(s) associated with regional post-Pan African exhumation that affected East Africa at that time. By comparison, Permian-Middle Jurassic single grain ZHe ages may represent cooling associated with Permian-Early Jurassic Karoo rifting that affected eastern Kenya, although the negative correlation to effective uranium (eU) content suggests these younger ages may, instead, be associated with radiation damage effects.

AFT results from basement rocks in southern Turkana indicate continued cooling into the early Paleogene, and are interpreted as representing denudation associated with flexural uplift of Anza Rift shoulders. In the axis of the Anza Rift, the northern TD underwent a period of subsidence ending in the Miocene, which accumulated a ~4 km thick sequence of sedimentary and volcanic deposits that fully rejuvenated AFT and AHe ages. Major basin-bounding faults associated with the EARS record a transition into a period of rapid cooling due to the initiation of extension in the latest Eocene-Oligocene. From there, rifting propagated eastward over time, with extension in the Omo-Turkana Basin beginning in the mid-Miocene as documented by rapid cooling of AFT and AHe ages in eastern Turkana. Thermal history models indicate that the margins of the TD experienced up to 4 km of denudation in response to extension, ~2-3 times greater than reported for the Kenyan Rift. We propose that the very low effective elastic thickness of the Turkana lithosphere, at least in part a consequence of its inherited Cretaceous-Paleogene rifting history, resulted in significantly increased isostatic uplift in response to EARS-related extension.

# Distinguishing thermal rift-related inheritance from subsequent orogenic exhumation in the Pyrenees

Arnaud Vacherat<sup>1</sup>, Frédéric Mouthereau<sup>1</sup>, Raphaël Pik<sup>2</sup>

<sup>1</sup> *Geoscience Environnement Toulouse (GET), Université de Toulouse, UPS, Univ. Paul Sabatier, CNRS, IRD, 14 av. Edouard Belin, F-31400 Toulouse, France  
(arnaud.vacherat@get.omp.eu)*

<sup>2</sup> *CRPG, UMR 7358 CNRS-Université de Lorraine, BP20, 15 rue Notre-Dame des Pauvres, 54500 Vandœuvre-lès-Nancy, France*

Collisional orogenic belts result from the shortening of previously thinned continental margins. If the last episode of collision-related cooling is generally well recorded from low-temperature thermochronology, the earliest cooling stages related to incipient continental accretion are generally much more difficult to resolve. There are however keys for dating the onset of cooling and therefore to better evaluate shortening and plate reconstructions. Here, we constrain the long-term cooling history of the Pyrenees by distinguishing the onset of collision thermal conditions from rift-related processes from subsequent orogenic evolution.

Kinematic reconstructions of the Iberian and European plates motions indicate that during Lower Cretaceous, extension in the Pyrenees resulted in a wider domain of extremely thinned crust between the central and western parts of the belt. Here, we first focus on the Mauléon basin (north-western Pyrenees) using detrital zircons (U-Th-Sm)/He and fission track analyses. To capture the role of rift-related processes in collision we inverse modeled our thermochronological data using relationships between zircon (U-Th-Sm)/He ages and Uranium content combined with thermo-kinematic models from rifting to collision. We show that the basin recorded a significant rift-related heating event at about 100 Ma characterized by high geothermal gradients (~80°C/km). After inversion started at ca. 84 Ma, these high temperatures lasted 30 Myr until collision occurred in relation with onset of orogenic exhumation at ca. 50 Ma.

In the Central Pyrenees, we performed in-situ apatite and zircon fission track and (U-Th-Sm)/He analyses on granitic bedrock samples of the Ariège massifs (Trois-Seigneurs and Arize). Our data show cooling from mid-crustal level in the Late Cretaceous and fast cooling at ca. 50 Ma. Although, these data show remarkably consistent cooling event between the Western and Central Pyrenees at 50 Ma indicating coeval exhumation in the Ariège and Mauléon region, detailed analyses of the earlier stages show some significant differences.

Thermal constraints from the Ariège region are compared with RSCM temperatures obtained from the surrounding folded Mesozoic units. A significant gap is found between maximum temperatures reached in the massifs and the adjacent sedimentary cover. This suggests a distinctive tectonic history between the crystalline basement and the basins, providing clues on how plate convergence was accommodated within the northern Pyrenean domain.

# **Burial and exhumation history of the Mackenzie Plain, NWT, Canada: integration of apatite (U-Th)/He and fission track thermochronometry**

Jeremy Powell<sup>1</sup>, David Schneider<sup>1</sup>, Dale Issler<sup>2</sup>, Daniel Stockli<sup>3</sup>

*1 Department of Earth & Environmental Sciences, University of Ottawa, Canada*

*2 Geological Survey of Canada, Calgary Office, Canada*

*3 Jackson School of Geoscience, University of Texas at Austin, USA  
(jpowe068@uottawa.ca)*

Sedimentary strata from the Mackenzie Plain, currently in the foreland of the Mackenzie Mountains of the northern Canadian Cordillera, record a dynamic geologic history from the Paleozoic through to the Paleogene. Whereas Late Cretaceous to Paleogene foreland basin strata presently cover the Plain, unconformities throughout the sedimentary succession indicate that episodic burial and exhumation are a common theme through deep time. Knowledge of the timing and magnitude of these events is especially critical for understanding potential hydrocarbon systems, as the timing of maturation for the Devonian source rock is a major uncertainty for oil and gas exploration. However, quantitative thermochronology studies for the region are sparse, and limited to Neoproterozoic strata from the Mackenzie Mountains<sup>1</sup> and a single well in the Mackenzie Plain<sup>2</sup>. To better understand the tectonic and thermal evolution of the study area, samples were collected for apatite (U-Th)/He (AHe) and fission track (AFT) thermochronometry. Strategic sampling followed a transect along the deformation front and across the Plain. We targeted outcrops of the Devonian Imperial Formation and the Late Cretaceous Slater River Formation. These formations straddle a significant regional unconformity, and ultimately help to quantify the magnitude of the late Paleozoic to early Mesozoic thermal history in comparison with the Late Cretaceous to Paleocene thermal event related to foreland basin development.

We report 61 single-grain AHe dates from seven samples. AHe dates vary from  $225 \pm 14$  Ma to  $3 \pm 0.2$  Ma, with the majority of dates recording cooling between the Late Cretaceous to Miocene. Whereas several samples exhibit correlations between AHe date and parameters such as radiation damage (eU) and grain size, all samples demonstrate varying degrees of intra-sample date dispersion. All five samples chosen for AFT thermochronology display an even greater degree of variation, with AFT dates scattered between the Cambrian and Miocene throughout our dataset. Although no correlations exist between DPAR and AFT age or track length distribution, we note a strong relationship between grain chemistry and ages. We use the parameter  $r_{mr0}$ <sup>3</sup> to distinguish up to four discrete kinetic populations per sample, with consistent Triassic, Cretaceous and Miocene pooled ages. Inverse thermal history modeling of AFT and AHe samples reveals that the Devonian strata likely reached maximum burial temperatures ( $130^{\circ}\text{C}$ – $180^{\circ}\text{C}$ ) prior to Triassic unroofing. Strata were reheated to lower temperatures in the Cretaceous to Paleogene ( $90^{\circ}\text{C}$ – $120^{\circ}\text{C}$ ), and have a dog-legged Cenozoic cooling history, with an initial Paleocene phase related to Cordilleran deformation and a final Miocene phase. This t-T information is used to assess 1D burial histories of local wells and the hydrocarbon potential of regional Devonian and Cretaceous source rocks.

Ultimately, these data reflect the complications, and possibilities, of low-temperature thermochronology in sedimentary rocks where detrital variance results in a broad chemistry range in the apatite population. We use chemistry-dependent fission track annealing kinetics to explain dispersion in both our AFT and AHe datasets and detail the thermal history of strata that have experienced a protracted cooling history through the uppermost crust.



## References

1. Powell, J., Schneider, D., Stockli, D., & Fallas, K. Zircon (U-Th)/He thermochronology of Neoproterozoic strata from the Mackenzie Mountains, Canada: Implications for the Phanerozoic exhumation and deformation history of the Northern Canadian Cordillera. *Tectonics* **35**, (2016).
2. Issler, D.R., Grist, A.M., & Stasiuk, L.D. Post-Devonian thermal constraints on hydrocarbon source rock maturation in the Keele Tectonic Zone, Tulita area, NWT, Canada, from multi-kinetic apatite fission track thermochronology, vitrinite reflectance and shale compaction. *Bulletin of Canadian Petroleum Geology* **53**, 405-431 (2005).
3. Ketcham, R.A., Donelick, R.A., & Carlson, W.D. Variability of apatite fission-track annealing kinetics: III. Extrapolation to geologic timescales. *American Mineralogist* **84**, 1235-1255 (1999).

# Late Cenozoic exhumation of the Southern Patagonian Andes (47°S) constrained by low-temperature thermochronology and inverse numerical modeling

Viktoria Georgieva<sup>1</sup>, Edward R. Sobel<sup>1</sup>, Artur Sobczyk<sup>2</sup>, Kerry Gallagher<sup>3</sup>, Taylor Schildgen<sup>1,4</sup>, Todd A. Ehlers<sup>5</sup>, Manfred R. Strecker<sup>1</sup>

*1 University of Potsdam, Institute of Earth and Environmental Science, Karl-Liebknecht-Str. 24-25, 14476 Potsdam-Golm, Germany*

*2 University of Wrocław, Institute of Geological Sciences, Cybulskiego 32 50-205 Wrocław, Poland*

*3 University of Rennes1, Géosciences Rennes UMR 6118, 35042 Rennes Cedex, France*

*4 Helmholtz-Zentrum Potsdam, Deutsches GeoForschungsZentrum GFZ, Telegrafenberg, 14473 Potsdam, Germany*

*5 University of Tübingen, Department of Geosciences, Wilhelmstr. 56, 72074 Tübingen, Germany*

*(viktorija@geo.uni-potsdam.de)*

The present study combines new and published apatite (U-Th)/He and apatite fission track data from three elevation transects in the region of the Northern Patagonian Icefield to constrain the late Cenozoic thermal history of the Southern Patagonian Andes at these latitudes. The Northern Patagonian Icefield is hosted by a high mountain massif in the Southern Andes located inland of the Chile Triple Junction, where the Chile Rise collides with the South American continent. Ridge collision started 16 Ma ago at the southernmost end of South America ( $\sim 54^\circ\text{S}$ )<sup>1</sup>; since then, oblique collision of subsequent ridge segments has resulted in a stepwise northward migration of the triple junction and associated northward opening of an asthenosphere slab window below Patagonia. We focus on the effects of the closely spaced most recent collision of three short ridge segments at the latitudes of the Northern Patagonian Icefield.

In a previous study we proposed a neotectonic model for this region, which links the effects of oblique ridge collision with enhanced strain partitioning on the structural evolution of the upper plate<sup>2</sup>. Here we present new thermochronological data that further supports our neotectonic model and, together with published apatite (U-Th/He) and fission track data from a nearby elevation transect<sup>3,4</sup>, perform inverse thermal modelling with HeFTy<sup>5</sup> and QTQt<sup>6</sup> to constrain the late Cenozoic thermal history and exhumation and thereby re-evaluate the previous hypotheses.

The inverse thermal modelling is performed on selected single samples (HeFTy and QTQt) and multiple samples (QTQt) for each elevation transect. QTQt and HeFTy are two widely used modeling programs which have, fundamentally different functionalities<sup>7</sup>. Their complimentary application is aimed to combine the strengths of both algorithms and provide more robust constraints on the information stored in the thermochronological data and its significance in the regional geological context.

Previous studies have focused their conclusions on far-reaching thermal effects of the approaching ridge collision and slab window recognized in patterns of Late Miocene reheating in modelled thermal histories<sup>3,4</sup>. Our results show that the data can be explained with a simpler thermal history than previously proposed models; we will discuss differences in the model setup that likely lead to the varying results. The ensemble of modelled thermal histories presented here reproduces the observed data well and includes a Late Miocene protracted passage and/or residence in the partial annealing zone of apatite fission track and well-constrained Pliocene-to-recent stepwise exhumation. These findings are in good agreement with the geological record of this region which indicates an Early Miocene phase of active mountain building associated with surface uplift and an active fold-and-thrust belt<sup>3,8</sup> followed by a period of stagnation of deformation, peneplanation and lack of synorogenic deposition<sup>9</sup>. The subsequent period of stepwise exhumation likely resulted from a combination of pulsed glacial erosion<sup>10</sup> and concurrent neotectonic activity<sup>2</sup>.

## References

- 1 Breitsprecher, K. & Thorkelson, D. J. Neogene kinematic history of Nazca-Antarctic-Phoenix slab windows beneath Patagonia and the Antarctic Peninsula. *Tectonophysics* **464**, 10--20, doi:doi:10.1016/j.tecto.2008.02.013 (2009).
- 2 Georgieva, V. *et al.* Tectonic control on rock uplift, exhumation and topography above an oceanic-ridge collision – Southern Patagonian Andes (47°S), Chile. *Tectonics*, doi:10.1002/2016TC004120 (2016).
- 3 Blisniuk, P. M., Stern, L. A., Chamberlain, C. P., Idleman, B. & Zeitler, P. K. Climatic and ecologic changes during Miocene surface uplift in the Southern Patagonian Andes. *Earth and Planetary Science Letters* **230**, 125-142, doi:10.1016/j.epsl.2004.11.015 (2005).
- 4 Guillaume, B. *et al.* Dynamic topography control on Patagonian relief evolution as inferred from low temperature thermochronology. *Earth and Planetary Science Letters* **364**, 157-167, doi:10.1016/j.epsl.2012.12.036 (2013).
- 5 Ketcham, R. A. Forward and inverse modeling of low-temperature thermochronometry data. *Reviews in mineralogy and geochemistry* **58**, 275-314, doi:10.2138/rmg.2005.58.11 (2005).
- 6 Gallagher, K. Transdimensional inverse thermal history modeling for quantitative thermochronology. *Journal of Geophysical Research: Solid Earth* **117**, doi:10.1029/2011JB008825 (2012).
- 7 Vermeesch, P. & Tian, Y. Thermal history modelling: HeFTy vs. QTQt. *Earth-Science Reviews* **139**, 279-290, doi:10.1016/j.earscirev.2014.09.010 (2014).
- 8 Suarez, M., de la Cruz, R. & Bell, C. M. Timing and origin of deformation along the Patagonian fold and thrust belt. *Geological Magazine* **137**, 345-353, doi:10.1017/S0016756800004192 (2000).
- 9 Scalabrino, B. *et al.* A morphotectonic analysis of central Patagonian Cordillera: Negative inversion of the Andean belt over a buried spreading center? *Tectonics* **29** (2010).
- 10 Lagabrielle, Y., Scalabrino, B., Suarez, M. & Ritz, J. F. Mio-Pliocene glaciations of Central Patagonia: New evidence and tectonic implications. *Andean Geology* **37**, 276-299 (2010).

# **Evolution of the South Atlantic passive continental margin and lithosphere dynamic movement in Southern Brazil derived from zircon and apatite (U-Th- Sm)/He and fission-track data**

Krob, F.C.<sup>1</sup>, Stippich, C.<sup>1</sup>, Glasmacher, U.A.<sup>1</sup>, Hackspacher, P.C.<sup>2</sup>

(1) Institute of Earth Sciences, Research Group Thermochronology and Archaeometry, Heidelberg University, INF 234, 69120, Heidelberg, Germany

(2) Instituto de Geociências e Ciências Exatas, Universidade Estadual Paulista, Av. 24-A, 1515, Rio Claro, SP, 13506-900, Brazil

florian\_krob@web.de

Passive continental margins are important gearchives related to mantle dynamics, the breakup of continents, lithospheric dynamics, and other processes. The main concern yields the quantifying long-term lithospheric evolution of the continental margin between São Paulo and Laguna in southeastern Brazil since the Neoproterozoic. We put special emphasis on the reactivation of old fracture zones running into the continent and their constrains on the landscape evolution. In this contribution, we represent already consisting thermochronological data attained by fission-track and (U-Th-Sm)/He analysis on apatites and zircons. The zircon fission-track ages range between 108.4 (15.0) and 539.9 (68.4) Ma, the zircon (U-Th-Sm)/He ages between 72.9 (5.8) and 427.6 (1.8) Ma whereas the apatite fission-track ages range between 40.0 (5.3) and 134.7 (8.0) Ma, and the apatite (U-Th-Sm)/He ages between 32.1 (1.52) and 92.0 (1.86) Ma. These thermochronological ages from metamorphic, sedimentary and intrusive rocks show six distinct blocks (Laguna, Florianópolis, Curitiba, Ilha Comprida, Peruibe and Santos) with different evolution cut by old fracture zones. Furthermore, models of time-temperature evolution illustrate the differences in Pre- to post-rift exhumation histories of these blocks. The presented data will provide an insight into the complex exhumation history of the continental margin based on the existing literature data on the evolution of the Paraná basin in Brazil and the latest thermochronological data. We used the geological model of the Paraná basin supersequences (Rio Ivaí, Paraná, Gondwana I-III and Bauru) to remodel the subsidence and exhumation history of our consisting thermochronological sample data. First indications include a fast exhumation during the early Paleozoic, a slow shallow (northern blocks) to fast and deep (Laguna block) subduction from middle Paleozoic to Mesozoic time and a extremely fast exhumation during the opening of the South Atlantic (Cretaceous time). This enables a possible interpretation of the southeastern Brazilian margin being an outer part of the Paraná basin and even the possible source area for the Ordovician to Carboniferous sediments. Further on, we try to research the newly gained exhumation history models for indications on the evolution and movement of the lithosphere of the southeastern Brazilian mantle.

# The influence of inherited extensional structures on the growth of basement-cored ranges and their foreland basins.

Sebastián Zapata<sup>1\*</sup>, Edward Sobel<sup>1</sup>, Cecilia del Papa<sup>2</sup>

- 1) University of Potsdam, Institute of Earth and Environmental Sciences.
- 2) Universidad de Cordoba, Facultad de Ciencias Exactas, Físicas y Naturales.  
\*szapata@uni-potsdam.de

The region east of the 6000 m high Puna plateau and the Eastern Cordillera of NW Argentina is characterized by a wedge-shaped ~250-km-wide fold-and-thrust belt, which defines the eastern border of the orogen and transitions into the unrestricted Chaco-Paraná foredeep. The spatial extent of the fold-and-thrust belt correlates with thick Paleozoic units that provide the basal decollement of the wedge. South of 24°S, however, these mechanically weak layers thin out and disappear, and the thin skinned style of deformation terminates. The reactivated, inherited anisotropies have produced discrete ranges that occur both along the eastern flank of the plateau and far to the east within the otherwise undeformed foreland. The reactivation of pre-existing normal faults during subsequent contractile deformation can exert a profound influence on both exhumation of ranges and sedimentary basin formation. This topic has been addressed in the well-exposed, arid intermontane basins and ranges of NW Argentina as well as more humid sectors of the broken foreland farther east. However, the more humid eastern flank of the Sierras Pampeanas has been less well-studied, despite its simpler structural history. In the Tucumán and Choromoro basins, structures that deform the foreland basins as well as their sedimentary thicknesses have been well analyzed using industry seismic reflection data. However, to date, a quantitative source-to-sink approach has not been applied in this area. Therefore, we will integrate thermochronology, structural data, and provenance and basin analysis to test whether Cretaceous normal faults exert a first-order control on the pattern and magnitude of Cenozoic contractile deformation in basement-cored ranges as well as subsidence patterns in the adjacent foreland basins. The ages of the largely continental foreland-basin fill remain imprecisely constrained, with the exception of the strata corresponding to the Middle Miocene Paraná marine transgression, reflecting both the difficulty of dating non-marine sequences and the poor outcrop quality. In this work we will present the different scientific question, the methodology, the hypothesis and the results of the first field campaign.

## Key Words

Inherited structures, Central Andes, Sierras Pampeanas; thermochronology, Provenance.



**THERMO2016**

**SESSION 10**

**MINERALIZATIONS**

# Post-batholith Mo(W) metallogenesis following super large magma activity in Xiao Hinggan Mountains, Northeast China

Liu C<sup>1</sup>, Luo Z.H<sup>1</sup>, Deng J.F<sup>1</sup>, Zhang Y<sup>2</sup>, Duan P.X<sup>1</sup>, Zhao H.D<sup>2</sup>, Tian S.P<sup>2</sup>, Zhang L.L<sup>1</sup>

1. *China University of Geosciences, Beijing, 100083, China*

2. *Heilongjiang Province Institute of Regional Geology Survey, Haerbin, Heilongjiang Province, 150080, China*  
(502625368@qq.com)

Many (super)-large Mo(W) deposits were founded in recently 15 years in Xiao Hinggan Mountains, northeast China, including Luming, Huojihe, Cuihongshan, Cuiling (super)-large-middle Mo(W) deposits. In these ore districts, multi-stage granitic rocks were developed. So it was the key that which granitic rocks were the ore-forming intrusive bodies of Mo (W). For Luming Mo Deposit, the dating shows the Luming Granite Porphyry (LGP) was formed at  $174.0 \pm 2 \text{ Ma}$  (MSWD=3.2). The five molybdenite samples from Luming Deposit yield a Re-Os isochron age of  $177.8 \pm 2.3 \text{ Ma}$  (MSWD=0.078) and a Re-Os weighted average age of  $177.5 \pm 1.2 \text{ Ma}$  (MSWD=0.058); The the isochron age of  $^{40}\text{Ar}/^{39}\text{Ar}$  dating of biotite of the Luming Granite (LG, coarse-middle grained texture) is  $176.0 \pm 2.0 \text{ Ma}$  (MSWD=1.9). Considering field geology, petrography, and former achievements, the authors suggest that the batholith of LG (176Ma) was formed slightly earlier than LGP (174Ma). The metallogenesis of molybdenite is coeval or slightly later than LGP. Thus, the ore-forming intrusive body of Luming metallogenesis of molybdenite is the LGP, but not the batholiths of LG (Liu C. et al., 2014)<sup>1</sup>. In Huojihe Mo Deposit, the authors got the similar results with Luming Deposit. The  $^{40}\text{Ar}-^{39}\text{Ar}$  plateau age of biotite monzogranite (BM, coarse-middle grained texture) is  $175.95 \pm 0.86 \text{ Ma}$  and the model ages of the molybdenite are determined to be  $180.7 \pm 2.5 \text{ Ma} \sim 181.3 \pm 2.6 \text{ Ma}$  (Zhang L.L et al., 2014)<sup>2</sup>. Which are consistent with the dating of biotite monzogranite (BM) by LA ICP-MS zircon U-Pb method ( $186 \pm 1.7 \text{ Ma}$ ) (Yang Y.C et al., 2012)<sup>3</sup>. So, the BM is just the wall rock, but not the ore-forming intrusive body of Mo. Such situation are developed in Cuihongshan and Cuiling Mo (W) deposits. The LG in Luming, BM in Huojihe, coarse-middle grained monzogranites in Cuihongshan and in Cuiling belong to one big batholith ( $>>100 \text{ km}^2$ ), and are probably products of the same one super large magma activity in early Jurassic from area geology research. These coarse-middle grained granites are not the ore-forming intrusive bodies of the Mo (W) ores. But they probably provide the conduit and driving force for fluid carrying the Mo (W) material when the batholith uplifts. At the same time, the batholith acts as a restricting control for Mo (W) ore bodies. So, this paper suggests the deposits were formed following the large granitic magma activity, we name this as "Post-batholith Mo (W) metallogenesis".

## References

1. Liu C, Deng J.F, Luo Z.H, Tian S.P., Zhang Y, Zhong C.T, Zhao H.D, Kong W.Q and Duan P.X. 2014. Post-batholith metallogenesis: Evidence from Luming super large molybdenite deposit in Xiaoxingan'ling Range. *Acta Petrologica Sinica*, 30(11): 3400-3418 (in Chinese with English abstract)
2. Zhang LL, Liu C, Zhou S, Sun K, Qiu RZ and Feng Y. 2014. Characteristics of ore-bearing granites and

- ore-forming age of the Huojihe molybdenum deposit in Lesser Xing' an Range. *Acta Petrologica Sinica*, 30(11): 3419-3431 (in Chinese with English abstract)
3. Yang Y.C, Han S.J, Sun D.Y, Guo J and Zhang S.J. 2012. Geological and geochemical features and geochronology of porphyry molybdenum deposits in the Lesser Xing' an Range-Zhangguangcai Range metallogenic belt. *Acta Petrologica Sinica*. 28(2): 0379-0390 (in Chinese with English abstract)



## AUTHOR INDEX

### A

A. Carter – 137  
A.G. Whitham – 137  
Adam G. Szulc – 137  
Agustín Cardona – 119  
Alan Greig – 62  
Alfredo Camacho – 40  
Alice Recanati – 6  
Alison MacNamee – 121  
Alka Tripathy-Lang – 7  
Alyssa Abbey – 115  
An Wang – 124  
Andrea Hampel – 82  
Andrea Ritter Jelinek – 97, 134  
Andreas Klügel – 34  
Andreas Wölfler – 82  
Andrés Mora – 13  
Andrew Gleadow – 22, 62, 75, 86, 139  
Andrew Smye – 68  
Anette von der Handt – 24  
Anna K. Ksienzyk – 83  
Anne-Magali Seydoux-Guillaume – 6  
Anne Replumaz – 123  
Annika Szameitat – 85  
Antonio C. Galindo – 18  
Arnaldo Luis Lixandrão Filho – 44, 48  
Arnaud Vacherat – 140  
Artur Sobczyk – 143

### B

B.I.A. McInnes – 57  
B.J. McDonald – 57  
Barry P. Kohn – 22, 62, 75, 86, 88, 106, 139  
Bernard Guest – 66  
Bin Deng – 135  
Blair Schoene – 60  
Brett Hamilton – 66

### C

C.L. Kirkland – 57  
C. Johnson – 137  
C. Trautmann – 72  
Cai Change – 133  
Camilla Maya Wilksinson - 17  
Carlos Alberto Tello Sáenz – 26  
Carlos Henrique Grohmann – 79  
Carlos Marquardt - 122  
Carolina Doranti-Tiritan – 102  
Caroline Heineke – 82  
Caroline Sanchez – 122  
Cécile Gautheron – 6, 24, 30, 112, 130  
Cecilia del Papa - 146  
Chang'e Cai – 74  
Charlotte Fillon – 130  
Chelsea D. Willett – 39  
Chloé Gerin – 6  
Chris Sykes – 66  
Christian Seiler – 22, 86, 139  
Christian De Capitani – 24  
Christian Stippich – 92, 145  
Christie Helouise Engelmann de Oliveira – 134  
Christoph Glotzbach – 82  
Chuanjun Wu – 108  
Constantino Mpodozis - 122  
Cornelia Spiegel – 32, 34, 84  
Cristina Persano – 4, 80, 95  
Cristopher Lopez - 122  
Cui Liu – 104, 148  
Cüneyt Akal – 82  
Cyril Bachelet – 6

### D

D. Seward – 110  
Dale Issler – 141  
Daniel Arnost – 121  
Daniel F Stockli – 13, 46, 68, 110, 121, 141

Daniel Henrique de Souza – 90  
Danieli Fernanda Canaver Marin – 36  
David Foster – 86  
David L. Shuster – 7, 31, 39  
David M. Chew – 126  
David M. Webster – 51  
David Rousell – 70  
David S. Thiede - 18  
David Schneider – 138, 141  
Deng J.F. – 148  
Donato Pace – 77  
Duan P.X. – 148  
Duval Mbongo-Djimbi – 6

## **E**

Eduardo Campos - 122  
Edward R. Sobel – 143, 146  
Elisa Savignano – 112  
Elton Luiz Dantas – 26  
Emmanuel Masini – 130

## **F**

Fabiano do Nascimento Pupim – 90  
Fabrice Brunet – 30  
Farid Chemale Jr. – 134  
Federico Galster – 46  
Federico Rossetti – 77  
Fernando A.P. L. Lins - 18  
Fernando C. Alves da Silva - 18  
Finlay M. Stuart – 4, 36, 80, 90, 95, 126  
Florian Krob – 92, 145  
Franco Maria Talarico – 77  
Frank Lisker – 84  
Frédéric Mouthereau – 140, 130  
Frédérico Garrido – 6

## **G**

Gaoping Zhao – 135  
Gérard Hérail - 122  
Guocan Wang – 123, 124  
Guoqin Zhang – 104

## **H**

Hallgeir Sirevaag – 83  
Hugh O'Neill – 62

## **I**

Iain H. C. Henderson 17  
Isabela O. Carmo – 88  
István Dunkl – 82, 83, 85

## **J**

James Douglas Walker – 53  
James K. W. Lee – 40  
Jaziel M. Sá - 18  
Jeremy Powell – 138,141  
Jérôme Roques – 6  
Jian Chang – 74  
Jiangping He – 2  
Jianjing Zheng – 87  
Joachim Jacobs – 83  
John Saxton – 70  
Jonas Kley – 85  
Juergen Erwin Oesterle – 110  
Julia Pickering – 66  
Julio Cesar Hadler Neto – 44, 48  
Justin Emberley – 138

## **K**

K. Norton – 110  
Kai Cao – 123  
Kalin McDannell – 60  
Katarzyna Łuszczak – 4, 95  
Kendra E Murray – 117  
Kerry Gallagher – 6, 43, 51, 137, 143  
Kexin Zhang – 124  
Kurt Stüwe – 126

## **L**

Laurent Tassan-Got – 6  
Leander Franz – 24  
Leandro Duque – 98  
Lei Jiang – 135

Ling Chung – 62, 139  
Lisa D. Stockli – 68  
Luba Jansa – 135  
Ludwig Zöller – 85  
Luo Z.H. – 148

## **M**

M. Burchard – 72  
Ma Yan – 21  
Manfred R. Strecker – 143  
Manuel Moreira – 30  
Marcos Müller Bicca – 97  
Maria Laura Balestrieri – 77  
Mark Harrison – 60  
Mark Wildman – 80  
Marli Carina Siqueira-Ribeiro – 36, 102  
Marta Franchini – 112  
Martin Danišik – 57  
Massimiliano Zattin – 77, 112  
Matthias Bernet – 54, 124, 134  
Matthew Fox – 7, 39  
Mauricio A Bermúdez Cella – 11  
Mauricio Parra – 13, 119, 128  
Maximilian Zundel – 84  
Meinert Rahn – 24  
Miguel Tupinambá – 98, 100  
Mohammad S. Sohi - 32  
Monica Heilbron – 100  
Morgan Ganerød - 17  
Murat T. Tamer – 27

## **N**

N.J. Evans – 57  
Nansheng Qiu – 74  
Nathan Cogne - 126  
Nathan Evenson – 31  
Nathan Niemi – 64, 115  
Nicolas Bellahsen – 130  
Nikki Seymour – 68  
Nils-Peter Nilius – 82  
Noah M. McLean – 53

## **P**

P. Steer – 137  
Pang Jianzhang – 21  
Patrick Boyd – 46, 68  
Patrick Monien – 34  
Paulo M. Vasconcelos - 18, 88  
Peter Christian Hackspacher – 8, 36, 90, 92, 102, 145  
Peter van der Beek – 124, 54  
Peter W Reiners – 31, 117  
Peter Zeitler – 60  
Petra Štěpančíková– 85  
Pieter Vermeesch – 2, 22

## **Q**

Qingyang Li – 22  
Qiu Nansheng – 133

## **R**

Ralf Hetzel – 82  
Ramon Schmid – 24  
Randell Stephenson – 93  
Raphaël Pik – 140, 130  
Ravi Kumar – 59  
Ray Donelick – 59  
Raymond Jonckheere – 27  
Rebecca Hardie – 138  
Richard Armstrong – 40  
Richard A. Ketcham – 13, 27, 54  
Robert A. Creaser – 40  
Roderick W. Brown – 4, 51, 80, 93  
Rodney C. Ewing – 56  
Rodrigo Riquelme – 122  
Romain Beucher – 51, 80  
Rosana Silveira Resende – 26  
Rosella Pinna-Jamme – 6, 30  
Ruben Rosenkranz – 32  
Ruizhao Qiu – 104  
Ruy Paulo Philipp – 97

## **S**

Samuel C Boone – 86, 139

Sandro Guedes – 44, 48  
Santiago León – 119  
Sebastian Dederer – 72  
Sebastian Echeverri – 128  
Sebastián Zapata - 146  
Sébastien Carretier – 122  
Scott Jess – 93  
Shengbiao Hu – 50  
Shigeru Sueoka – 106  
Shoma Fukuda – 106  
Shugen Liu – 135  
Silvio Takashi Hiruma – 79  
Stefano Mazzoli – 112  
Stéphane Schwartz - 30  
Stéphanie Brichau – 122  
Steven Edwards – 70  
Stuart N Thomson – 117  
Su Zhou – 104  
Syed Ali Turab – 126  
Sylvain Calassou – 130

## **T**

T. Becker – 57  
T. Bernard – 137  
T. Little – 110  
T. Kinnaird – 137  
Takahiro Tagami – 106, 114  
Taylor Schildgen – 143  
Tian S.P. – 148  
Tianyi Shen – 124  
Tim Redfield - 17  
Todd A. Ehlers – 143

## **U**

Ulrich Anton Glasmacher – 8, 72, 92, 102, 145

## **V**

Valerio Olivetti – 77  
Vhairi Mackintosh – 75  
Viktoria Georgieva – 143

Vincent Regard - 122  
Vera Kolb – 34

## **W**

Wang Ying – 21  
Wanming Yuan – 15  
William Matthews – 66  
Wu Ying – 21  
Wang Yizhou – 21  
Weixing Li – 56

## **X**

Xiaoming Li – 108  
Xiaoyin Tang – 50  
Xingwang Liu – 87

## **Y**

Yadong Wang – 87  
Yasir A. Abdu – 40  
Youwei Zheng – 87

## **Z**

Zheng Dewen – 21  
Zhiwu Li – 135  
Zhang L.L. – 148  
Zhang Y. – 148  
Zhao H.D. – 148  
Zhongcheng Zeng – 123

## SPONSORS:

### Gold Level Sponsors:



**GeoSep Services**  
Quality Mineral Separations and Analytical Services

## INSTITUTIONAL SPONSORS:



### Institutional Support:



UNIVERSITÄT  
HEIDELBERG  
ZUKUNFT  
SEIT 1386

